



University
of Glasgow

Quin, Caroline (2010) *Novel chemical tools for the study of oxidative stress and ageing*. PhD thesis.

<http://theses.gla.ac.uk/1576/>

Copyright and moral rights for this thesis are retained by the author

A copy can be downloaded for personal non-commercial research or study, without prior permission or charge

This thesis cannot be reproduced or quoted extensively from without first obtaining permission in writing from the Author

The content must not be changed in any way or sold commercially in any format or medium without the formal permission of the Author

When referring to this work, full bibliographic details including the author, title, awarding institution and date of the thesis must be given

Novel chemical tools for the study of oxidative stress and ageing

A thesis submitted in part fulfilment for the degree of Doctor of Philosophy

Caroline Quin

Department of Chemistry

University of Glasgow



February 2010

Table of Contents

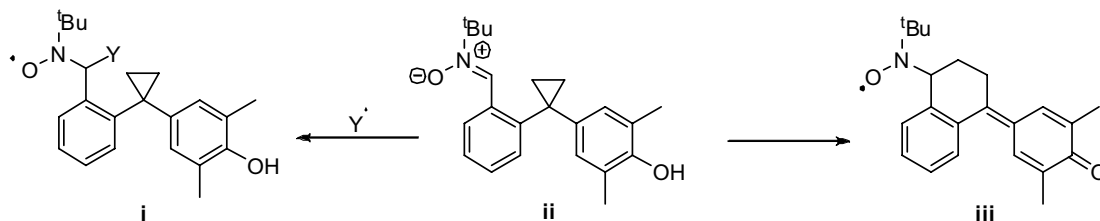
1	Oxidative stress and Ageing	1
1.1	Ageing and today's society	1
1.2	Free Radical Theory of ageing	2
1.3	Reactive Oxygen Species	3
1.4	Production of superoxide in the mitochondria	5
1.5	Reaction of the hydroxyl radical with DNA	9
1.6	Reaction of radicals with lipids.....	11
1.7	Reaction of the radicals with proteins	12
2	Antioxidant Defences	14
2.1	Introduction to antioxidant defences	14
2.2	Antioxidant Enzymes	14
2.3	Endogenous Antioxidants	15
2.4	Exogenous Antioxidants.....	16
3	Methods for investigation of oxidative stress and reactive oxygen species..	19
3.1	Chemiluminescent Probes.	19
3.2	Fluorescent Probes	21
3.3	Spin trapping and electron paramagnetic resonance spectroscopy.	22
4	Nitron spin traps	27
5	Nitrones as therapeutics	32
6	Evaluation of a Dual Sensor Spin-Trap	35
6.1	Synthesis	36
6.2	EPR spectroscopy	37
7	Synthesis and Evaluation of a Mitochondrial Targeted Spin	42

7.1	Background	42
7.2	Synthesis	48
7.3	Uptake in Mitochondria	60
7.4	Spin trapping of superoxide radicals	61
7.5	Spin trapping of hydroxyl radicals	62
7.6	Analysis by HPLC and ESI-MS	64
8	MS probe for H ₂ O ₂	67
8.1	Background	67
8.2	Synthesis of MitoB	70
9	Mitochondrial moderators.....	73
9.1	Background	73
9.2	Synthesis of Type A compound	77
9.3	Reaction of type A moderator with radicals.....	79
9.4	Synthesis of Type B - hydrogen peroxide stimulated selective uncoupling molecule.....	84
9.5	Reaction of Boronate with Hydrogen Peroxide	86
9.6	Attempts to synthesize a Mitochondrial targeted version.....	90
9.7	Synthesis of a TEMPO derivative.	92
9.8	Reaction of the TEMPO derivative with Hydrogen Peroxide	94
10	Mitochondria-targeted, light-activated uncoupler.....	96
10.1	Background.....	96
10.2	Synthesis of the light-activated uncoupler.....	98
11	Conclusions and future work	101
11.1	Conclusions.....	101
11.2	Future Work	102

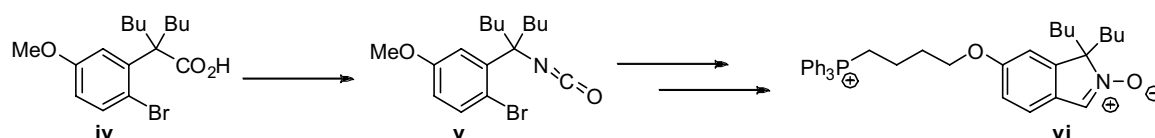
12 Experimental..... 103

Abstract

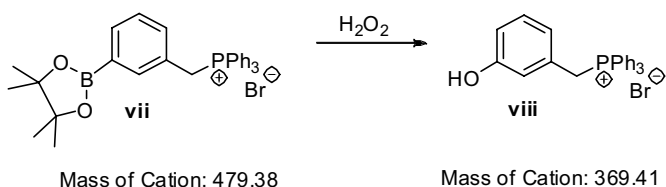
Oxidative stress is implicated in the ageing process and age-related diseases. A dual sensor spin trap **i** was used with electron paramagnetic resonance (EPR) spectroscopy to detect and distinguish between oxygen-centred radicals, carbon-centred radicals and redox active metal ions, all of which contribute to oxidative stress.



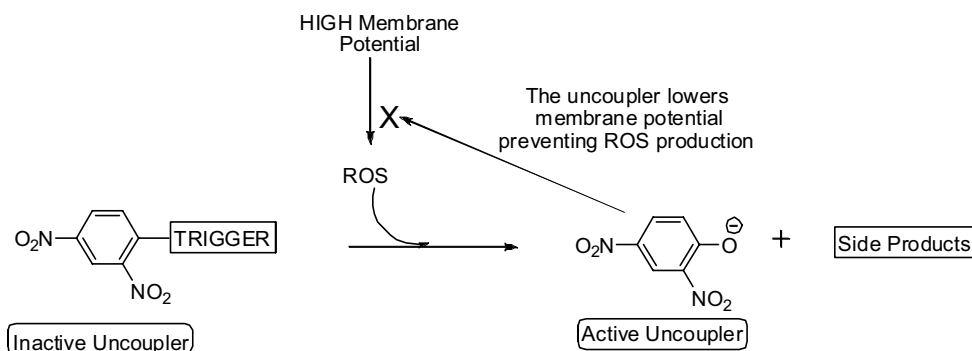
A novel mitochondria-targeted nitron spin trap MitoSpin **vi** has been prepared for the detection and amelioration of oxidative stress. The synthesis utilises a novel Parham-type cyclization of aryl bromide **iv** to afford the isoindolone core **vi** in good yield. MitoSpin **vi** accumulates in mitochondria in the presence of a membrane potential and affords a unique EPR signal and electrospray ionisation mass spectrometry (ESI-MS) detectable oxidation product on reaction with hydroxyl radicals.



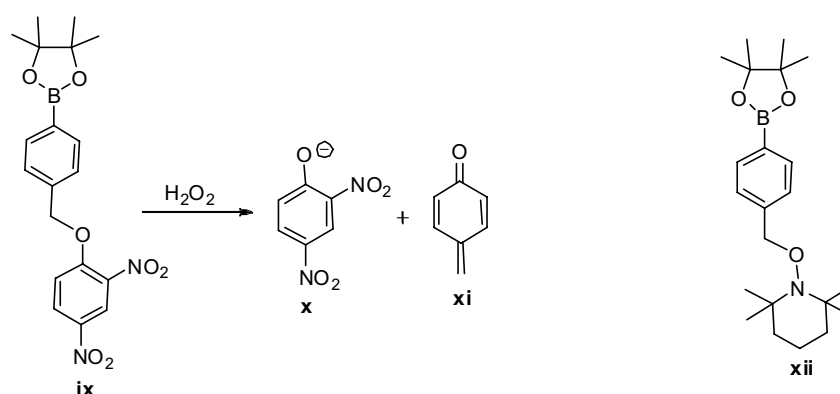
A hydrogen peroxide-sensitive, mitochondria-targeted probe **vii** has been prepared. It utilises the reactivity of the boronate moiety with hydrogen peroxide to afford an oxidation product. This process is easy to detect by ESI-MS.



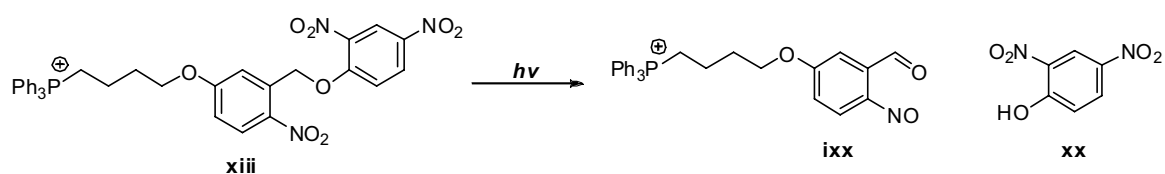
Mitochondrial moderators were synthesised, which are designed to react with to release an uncoupler (proton trans locator). If released *in vivo* the uncoupler would lower the mitochondrial membrane potential inhibiting further ROS production.



Moderator **ix** released dinitrophenoxyl anions (DNP^-) **x** upon reaction with hydrogen peroxide with a second order rate constant of approximately $11 \text{ M}^{-1}\text{s}^{-1}$. A responsive antioxidant molecule **xii** was also prepared and released the spin probe TEMPO upon reaction with hydrogen peroxide.



Finally a mitochondria-targeted, light-activated probe **xiii** which releases uncoupler dinitrophenol **xx** on irradiation has been synthesised. The probe has now been shown by a collaborator to uncouple individual mitochondria in smooth muscle cells upon UV irradiation.



Acknowledgements

With any accomplishment you make in life there are always plenty of people who helped you along the way. Therefore there are a lot of people I would like to thank for helping and supporting me during my PhD. First of all I would like to thank my supervisor Dr Richard Hartley for giving me the opportunity to undertake this PhD, for putting up with all my questions and my messy bench. I would also like to thank all those who I have collaborated with over the course of my PhD. David Collinson, Eric McInnes and Ruth Edge, at the EPR centre in Manchester, Mike Murphy and Jan Trnka in Cambridge for their work on the mitochondrial targeted compounds and for letting me play with mitochondria, as well as Prof. Nick Cannon and Dr Susan Chalmers at the University of Strathclyde who tested the light activated probe. Additionally, I'd like to thank the technical staff at the University of Glasgow; David Adam for NMR, Jim Tweedie for MS, Kim Wilson for IR, Ted Easton for Stores.

Furthermore, I wish to thank all the members of the lab (Henderson and Loudon) past and present for all the fun, tea and biscuits. A special mention to Stuart Caldwell for all his help in figuring out EPR and special thanks to those who kept me sane, Calver (despite your extreme tidiness), Ching, Claire P, Claire Mac, Linsey, Louise and Nicola. I'd also like to thank my long suffering friend and flatmate Kristina for pretending to be interested in chemistry and for cooking my dinner in stressful times. And thanks to Gavin for putting up with my extreme grumpiness whilst writing up. And as always there are the people who support me in all that I do, my family-especially my extraordinary Mum who provides endless love and support.

Author's Declaration

This thesis represents the original work of Caroline Quin unless explicitly stated in the text. The research upon which it is based was carried out at the University of Glasgow during the period of October 05 and September 2008, under the supervision of Dr Richard Hartley.

Abbreviations

Ac - Acetyl	DIBAL - Diisobutylaluminium hydride
Aq - Aqueous	DMAP - 4-(Dimethylamino)pyridine
Ar - Aromatic Ring	D - Doublet
Asc - Ascorbate	DMF - 1,1-Dimethylformaldehyde
ATP - Adenosine TriPhosphate	DMSO - Dimethylsulfoxide
ATR - Attenuated total reflection	DMPO - 5,5-Dimethyl-1-pyrroline-N-oxide
Bn- Benzyl	DNA - Deoxyribonucleic acid
Bu - Butyl	DNP - Dinitrophenol
^t Bu - <i>tert</i> -Butyl	DPPA - Diphenylphosphorylazide
°C - Degrees Celsius	EDPO - 5-ethoxycarbonyl-3,5-dimethyl-pyrroline N-oxide
cat. - Catalytic	EI - Electron ionisation
CI - Chemical ionisation	EMPO - 5-ethoxycarbonyl-5-methyl-1-pyrroline <i>N</i> -oxide
ChEPMPO - 5-(Cholesteryloxyethoxy phosphoryl)-5-methylpyrrolineN-oxide	EPPN - <i>N</i> -2-(2-ethoxycarbonyl-propyl)- α -phenylnitrone
cm. - Centimetres	EPR - Electron Paramagnetic Resonance
conc. - Concentration	Eq. - Equivalent
CoQ - Co-enzyme Q	Et - Ethyl
CytC - Cytochrome C	ETC - Electron transport chain
DBU - 1,8-Diazabicyclo[5.4.0]undec-7-ene	EWG - Electron Withdrawing Group
DCE - Dichloroethane	FAB - Fast atom bombardment
DCM - dichloromethane	FAD- Flavin adenine dinucleotide
DEPMPO - 5-Diethoxyphosphoryl-5-methyl-1-pyrroline- <i>N</i> -oxide	FCCP - Carbonyl cyanide- <i>p</i> -(trifluoromethoxy) phenylhydrazone
DHF - Dihydrofuran	GS - Glutathione
DIAD - Diisopropyl azo dicarboxylate	h - Hours

HOMO - Highest occupied molecular orbital	PUFA - Polyunsaturated Fatty Acid
HPLC - High through put liquid chromatography	Py - Pyridine
HRMS - High resolution mass spectrometry	q - quartet
Hz - Hertz	RNA -
IR - Infrared spectrometry	ROS - Reactive oxygen species
J = Coupling constant	RT - Room temperature
LDA - Lithium Diisopropyl Amine	s - singlet
LUMO - Lowest unoccupied molecular orbital	SOD - Superoxide dismutase
m - multiplet	SOMO - Singly occupied molecular orbital
Me - methyl	STAZN - Stilbazulenyl nitron
Min - minutes	t - triplet
Mp - melting point	TBAF - <i>tert</i> -Butyl ammonium fluoride
MOM - methoxymethyl ether	TBS - <i>tert</i> -Butyldimethylsilane
MS - Mass spectrometry	TEMPO - 2,2,6,6-tetramethylpiperidine-1-oxyl
Mw - microwave	THF - Tetrahydrofuran
NAD - Nicotinamide adenine dinucleotide	TMINO - 1,1,3-trimethylisoindole <i>N</i> -oxide
NBS - <i>N</i> -Bromosuccinamide	Tol - Toluene
NMR - Nuclear magnetic Resonance	TPAP - Tetrapropylammonium perruthenate
NOBA - 3-nitrobenzyl alcohol	TPP - Triphenylphosphine
PBN - α -phenyl- <i>tert</i> -butylnitron	Ts - Tosyl
Ph - Phenyl	UV - Ultraviolet
PhMe - Toluene	

1 Oxidative stress and Ageing

1.1 Ageing and today's society

Ageing and the deterioration our bodies face as our years advance is a topic that most people know about and in some case even worry about. Whether it is an elderly relative or our own hearing and eyesight declining it is a fact we all have to face - an issue we all have in common.

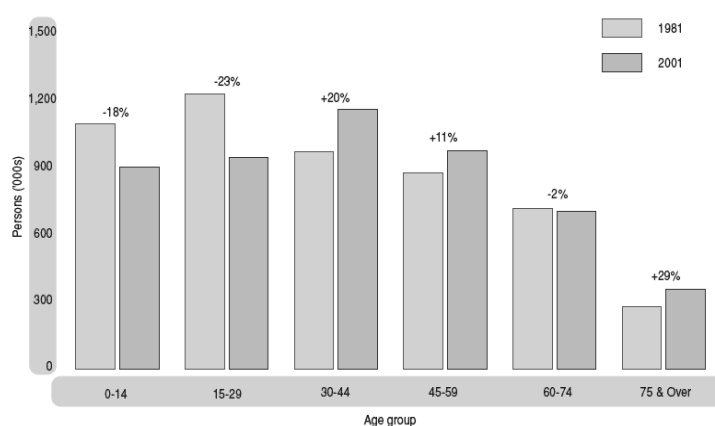


Figure 1

Recent figures show today there are approximately 6 million people over the age of 65 living in the UK¹, with current trends suggesting that by 2025 this number would increase to 14 million¹. The 2001 census in Scotland showed the over 75 years age group had increased 29% since 1981², Figure 1. In today's society the NHS currently spends 43 % of the annual budget³, on the health and social care for the elderly. It is currently estimated that on average older men and women will live 6.8 and 9.1 years of their lives, respectively with a debilitating condition⁴. These conditions include dementia, stroke, Alzheimer's disease, heart disease and age-related macular degradation³. It is feared that with the current spend by 2025 with the estimated increase in elderly population the NHS will not have sufficient funds to treat the elderly.

Although a lot is known about the consequences of ageing and the diseases attributed to it the actual process by which we age is not fully understood. Therefore there is a demand for better research tools and techniques to help

better understand this process so that we can one day prevent the deterioration and hopefully have a better quality of life.

1.2 Free Radical Theory of ageing

The main theory to why and how we age is the free radical theory of ageing which was postulated by Denman Harman in the mid 1950s⁵. His theory states that our body ages as a result of accumulative damage to our cells due to repeated oxidative stress. Oxidative stress is defined as the point at which the level of pro-oxidant activity is higher than the antioxidant activity *in vivo*. When this occurs the concentration of reactive oxygen species (ROS), which are generally free radicals, is increased. Free radicals react with biomolecules such as DNA, proteins and lipids. Reaction with biomolecules can cause irreversible damage leading to cell dysfunction and ultimately apoptosis. As Harman's later research focused on the mitochondria,⁶ its dysfunction and its relation to ageing and disease the free radical theory of ageing is often linked to the mitochondrial theory of ageing, which specifically links mitochondrial damage caused by oxidative stress to ageing and disease. Oxidative stress has been linked to a number of age-related diseases due to observations of biomarkers⁷.

There have been many experiments carried out which further substantiate the free radical theory of ageing. Experiments have shown that there is an inverse relationship between basal metabolic rates of animals and their life-spans⁸. In most cases smaller animals have shorter life spans. They consume more O₂ per body mass unit than larger animals⁸. One piece of evidence for the relationship between high metabolic rate and lifespan is the fact that Queen Bees live longer than the more active worker bees whose O₂ consumption would be much higher⁹. When worker bees were prevented from flying they too showed increased longevity. When species have similar metabolic rates but very different life spans e.g. pigeons and rats which have a 35 year and 3 year lifespan respectively their mitochondria are found to produce different levels of ROS, with 0.9 nmol H₂O₂ per min per mg of protein in the rat, and only 0.6 nmol of H₂O₂ per min per mg of protein in the pigeon¹⁰. These results are further supported by calorie restriction experiments, which show decrease in calorie intake leads to increased lifespan¹¹. It has also been shown that mitochondria isolated from aged tissues produce more ROS which may be a result of previous damage¹². Furthermore, increased levels of the products of radical reactions with radicals

have been observed in studies of age-related diseases.⁷ The symptoms of these diseases also have links to mitochondrial dysfunction¹³. Although it cannot be concluded from the evidence of these experiments that free radicals are solely responsible for ageing and the deterioration experience as we age, it clearly shows that ROS and oxidative stress do play an important role.

1.3 Reactive Oxygen Species

There are a number of ROS (Figure 2) with a variety of reactivities.

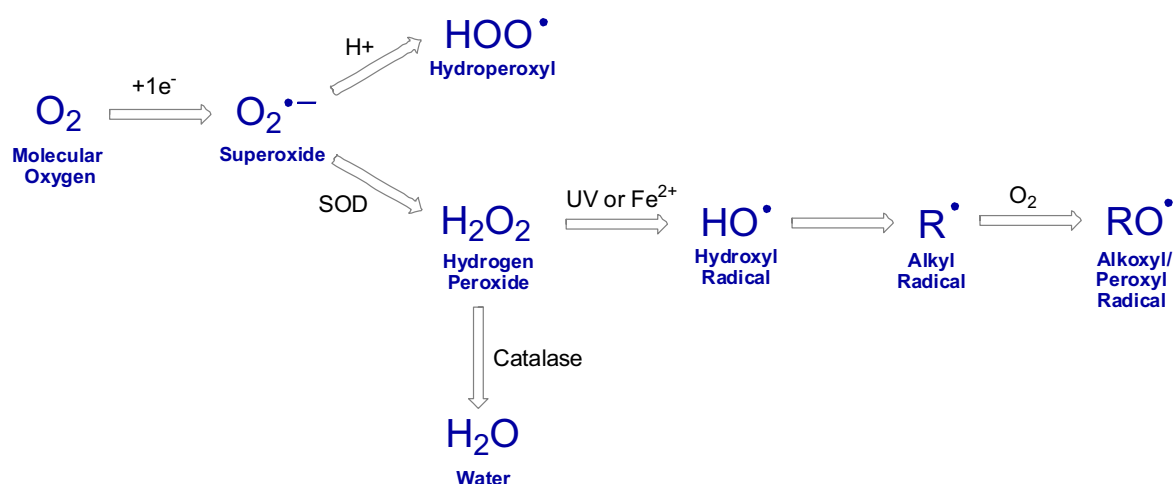


Figure 2: Reactive oxygen species

All of the ROS can be traced back to oxygen. Oxygen itself is a mild oxidant and can exist in more than one state, i.e. a triplet ground state or singlet activated states¹⁴. Ground state dimolecular oxygen is itself a diradical with two unpaired electrons within different π^* anti-bonding orbitals (Figure 3).

Although it has a radical ground state molecular oxygen is not highly reactive and this is due to the unpaired electrons having the same spin quantum number. This necessitates that if oxygen oxidises another molecule by accepting two electrons, these electrons must also have parallel spins. This means that there is a limit to the oxidations oxygen can carry out and results in oxygen accepting one electron at a time restricting its reactivity and decreasing reaction rates. However, after an input of energy the spin of one of the electrons in molecular oxygen can flip producing singlet oxygen. There are two forms of singlet oxygen, $^1\Delta_g$ singlet oxygen which has a longer lifetime and has the electrons of anti-

parallel spin occupying the same orbital; this species has no unpaired electrons and therefore is not a radical. The second form is $^1\Sigma_g$ singlet oxygen, which is more reactive as it has two unpaired electrons of opposite spin. This species has a very short lifetime and usually decays rapidly to $^1\Delta_g$ singlet oxygen. The spin restriction of ground state oxygen is alleviated in these activated species and therefore the oxidant activity is greater¹⁵.

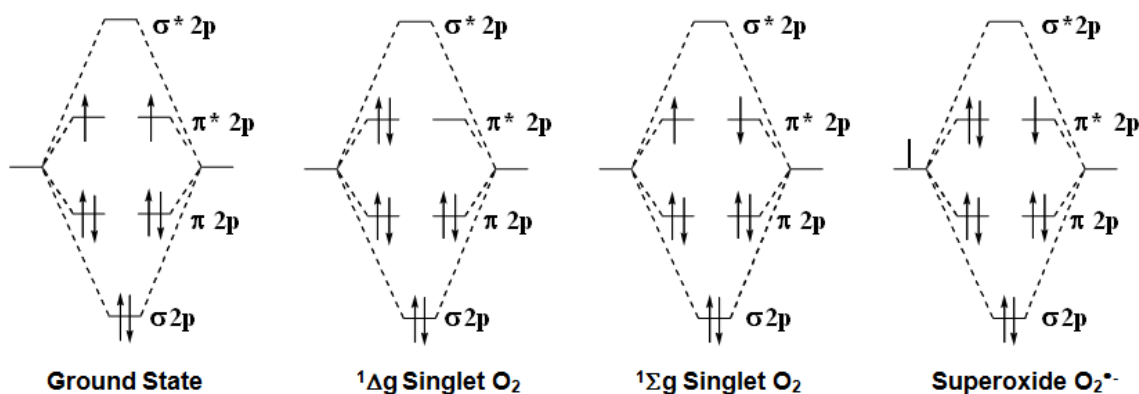


Figure 3: Electron arrangement of oxygen

Oxygen can undergo a one electron reduction to form a superoxide anion. The extra electron enters the anti-bonding π^* orbital leaving only one unpaired electron, (Figure 3). Superoxide is made naturally *in vivo* in a variety of ways. In fact 2-6 % of all oxygen consumed leads to the production of superoxide giving a yield of 3×10^7 molecules per person on a daily basis¹⁴. The main sources of free radical production are the mitochondria. The mitochondria are the cell organelles mainly responsible for energy metabolism. Mitochondria contain two distinct chambers: the inner matrix, surrounded by the inner membrane, and the intermembrane space, between the inner and outer membranes. The electron transport chain which carries out the third and final phase of respiration is situated within the inner membrane and is believed to be the main source of superoxide production. It is thought that ROS are formed due to the leakage of electrons from the electron transport chain (ETC), Figure 4.

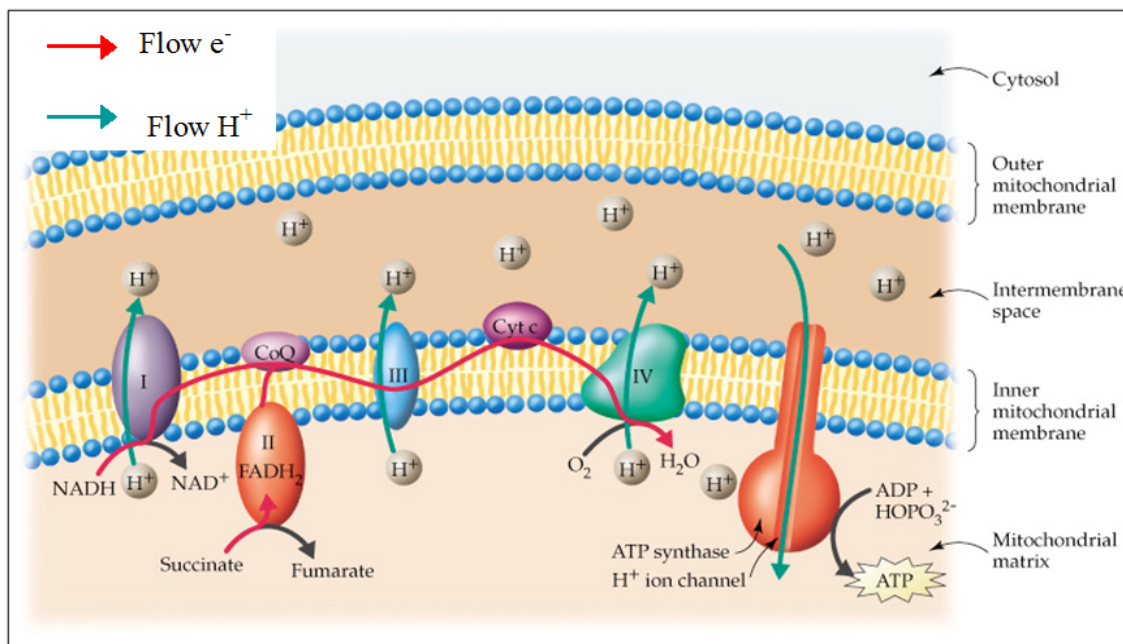
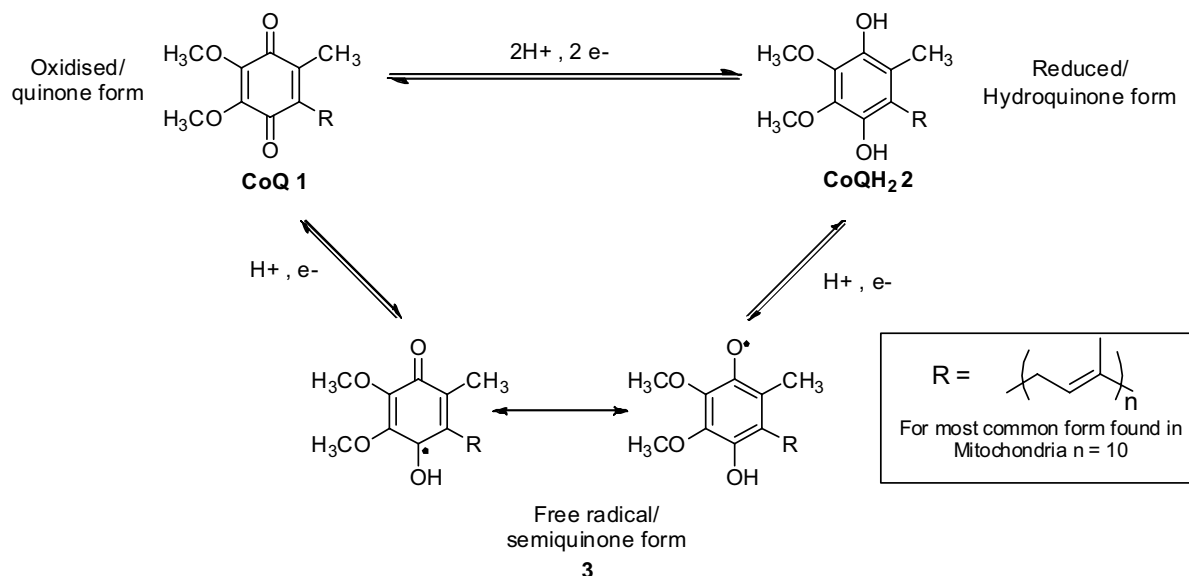


Figure 4: The electron transport chain¹⁶

The ETC utilises the reduced forms of the coenzymes nicotinamide dinucleotide NAD^+ and flavin adenosine dinucleotide FAD, produced during glycolysis and the citric acid cycle, the first two stages of respiration. These molecules are oxidised by transferring an electron onto the metal complexes I-IV. These electrons are passed along a chain of electron carriers, such as ferryl and cytochrome complexes, through a series of redox reactions ultimately resulting in the reduction of atmospheric oxygen to water with the production of adenosine triphosphate (ATP). Throughout this process protons are transported from the inner mitochondrial matrix into the intermembrane space. This proton gradient means that there is both a large membrane potential ($\Delta\psi$) across the inner membrane, -150 to -170 mV, and a difference in pH, with matrix 1.4 units lower than the cytosol.¹⁷ The protons flow through ATP synthase down this gradient driving the formation of adenosine triphosphate (ATP).

1.4 Production of superoxide in the mitochondria

Originally it was thought the main source of superoxide in mitochondria was from complex III¹¹. It was thought that the large membrane potential may encourage the leakage of electrons through the Q cycle, labelled as CoQ in Figure 4.

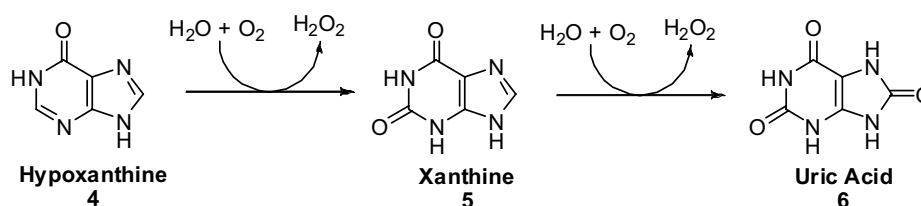


The Q cycle, Scheme 1, involves the reduction of Co-enzyme Q (CoQ) 1, a quinone, to a hydroquinone CoQH₂ 2. CoQ is reduced twice during this process and therefore the reaction proceeds via a free radical intermediate. The partially reduced semiquinone form 3 of the carrier molecule (ubisemiquinone) is thought to be responsible for electron leakage and generation of ROS at high protonmotive force¹⁸. However, recent evidence suggests that superoxide production from complex III, although it does occur, is relatively low.

The main source of superoxide is now thought to be complex I¹⁹. The exact mechanism of production is not fully understood it is thought it may occur due to a number of factors. It has been observed that when there is a high NADH/NAD⁺ ratio in the mitochondrial matrix there is increased production of superoxide²⁰. Another method of production is thought to be reverse electron transfer (RET) which occurs when the mitochondria are not making ATP and consequently have a high Δp (protonmotive force) and a reduced CoQ (coenzyme Q) pool. This causes the back transfer of electrons from CoQH₂ to complex I which can sometimes lead to reduction of oxygen to afford superoxide²⁰ Therefore the generation of O₂•⁻ within the mitochondrial matrix is not just dependent on the local O₂ concentration but also on the Δp as well as the NADH/NAD⁺ and CoQH₂/CoQ ratios.

There are also other ways in which superoxide can be formed *in vivo* for example ‘respiratory burst’ in phagocytic cells where the enzyme NADPH oxidase transfers electrons from NADPH across cell membranes to molecular oxygen producing superoxide in order to kill foreign micro-organisms as part of our body’s immune defence²¹.

Other enzymes are also sources of superoxide production. Xanthine oxidase, part of the molybdenum iron-sulfur flavin hydroxylase and catalase family, (an enzyme found in the liver) produces superoxide and hydrogen peroxide when carrying out the metabolism of hypoxanthine²².



Scheme 2: Production of superoxide by xanthine oxidase

The enzyme catalyses oxidation of hypoxanthine **4**, a naturally occurring purine derivative, to xanthine **5** and then from xanthine to uric acid **6** for excretion. In both steps the substrate is oxidised, the oxygen atom originates from the water molecule, and oxygen reduced to hydrogen peroxide. Molecular oxygen is reduced to hydrogen peroxide in two steps where superoxide is the intermediate. Approximately 20% of electron flux results in the production of superoxide²³, for this reason Xanthine oxidase is often used to produce superoxide *in vitro* for spin trapping experiments.

<u>Couple (Oxidant / Antioxidant)</u>	<u>E° / mV</u>	
$HO^{\cdot}, H^{+} / H_2O$	2310	<div style="display: flex; align-items: center; justify-content: center;"> <div style="width: 10px; height: 100px; border-left: 1px solid black; margin-right: 5px;"></div> <div style="text-align: center;"> <p>Highly oxidising</p> <p>↓</p> <p>Highly reducing</p> </div> </div>
$RO^{\cdot}, H^{+} / ROH$	1600	
$HOO^{\cdot}, H^{+} / H_2O_2$	1150	
ROO^{\cdot}, H^{+} (lipid peroxy radical) / $ROOH$	1060	
$O_2^{\cdot-}, 2H^{+}$ (superoxide anion) / H_2O_2	940	
$PUFA^{\cdot}, H^{+} / PUFA-H$ (polyunsaturated fatty acid)	600	
\cdot -tocopheryl, H^{+} / \cdot -tocopherol (Vit E)	500	
Ascorbate \cdot , $H^{+} /$ ascorbate		
monoanoin (Vit C)	282	

Figure 5: One electron reduction potential of common ROS²⁴

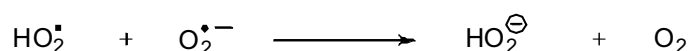
The superoxide radical has a one electron reduction potential of 0.94 V meaning it is only moderately oxidising and does not react easily with biomolecules. When superoxide is in its protonated form, the hydroperoxyl radical, it is more reactive with a one electron reduction potential of 1.06 V. Neither superoxide nor hydroperoxyl radicals are thought to be the main cause of free radical damage to our cells. Although, it is not the reactions of superoxide with cells that cause oxidative stress, reactions in which it is involved leads to the production of more reactive ROS so that superoxide is the precursor to all subsequent reactive species.

The first ROS that superoxide generates is hydrogen peroxide. Hydrogen peroxide is formed via dismutation (disproportionation) which can occur with or without an enzyme²⁵.



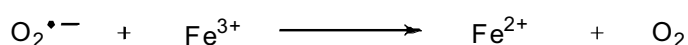
Scheme 3: Superoxide dismutation

Dismutation is the reaction of 2 molecules of superoxide, one of which is reduced and the other oxidised to afford hydrogen peroxide and oxygen, respectively. The probability of disproportionation occurring as illustrated in the above equation is low as this would require a tetramolecular reaction and the rate constant for this reaction is close to zero.



Scheme 4: Superoxide dismutation

There is a much higher probability that one of the superoxide molecules would be protonated before reacting with the secondary superoxide molecule, Scheme 4, which, has a rate constant $9.7 \times 10^7 \text{M}^{-1}\text{s}^{-1}$.¹⁴ Superoxide will reduce the high oxidation state ions of transition metals, most commonly Fe(III) and Cu(II), Scheme 5.



Scheme 5: Reaction of superoxide with Iron(III) ions

It reduces the Fe(III) of the haem protein cytochrome C, converting it to free Fe(II), as well as the Cu(II) found in plastocyanin converting it to Cu(I).¹⁴ These ions can then reduce hydrogen peroxide to produce the more damaging hydroxyl radical by the Fenton reaction, Scheme 6.

Hydrogen peroxide has no unpaired electrons and is therefore not a radical. It is a mild oxidising and reducing agent and although not particularly harmful itself, it easily diffuses across membranes, and it can move far from the source of production to generate hydroxyl radicals through the Fenton reaction with free iron(II) ions.²⁶



Scheme 6: Fenton reaction of hydrogen peroxide with Iron(II) ions

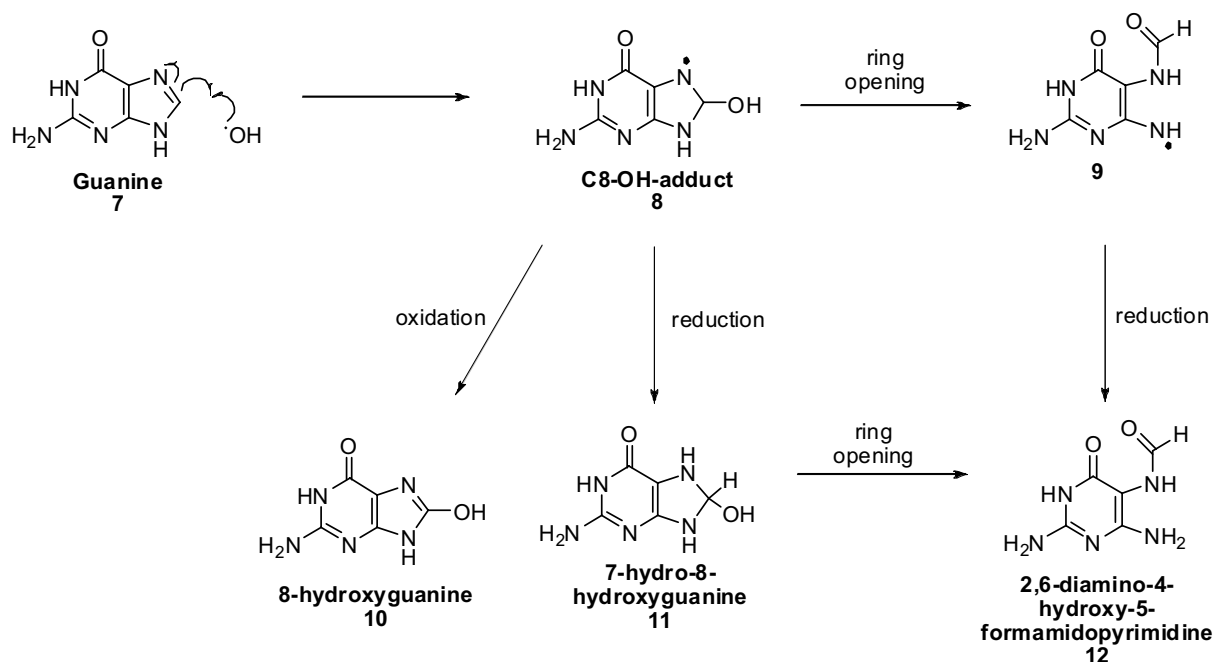
The iron(II) ion comes from iron containing complexes within the body such as haem. The iron(II) ions are released from the complexes by superoxide as discussed previously. The combined reactions of superoxide with Fe(III) and hydrogen peroxide with Fe(II) are called the Haber-Weiss process. Hydroxyl radicals can also be generated by catalysis from the ions of other transition metals such as copper, cobalt or chromium¹⁴. Formation of the hydroxyl radical from homolytic fission of hydrogen peroxide can also be achieved with heat, UV exposure or by ionising radiation. The damaging effects of radiation occur as a result of the production of hydroxyl radicals via the homolytic fission of water.

The hydroxyl radical is the most reactive of all the ROS and its reactions with biomolecules occur with rate constants very close to the ideal rate constant of diffusion controlled processes. As a result it has a very short half-life of nanoseconds and a reaction radius of only 30 Å²⁷. The hydroxyl radical can react with all of the cells biomolecules such as DNA, proteins and lipids affording a variety of carbon-centred and alkoxy and peroxy radicals. It is therefore postulated to be the main source of oxidative damage to cells.

1.5 Reaction of the hydroxyl radical with DNA

The highly reactive hydroxyl radical causes modification at multiple positions within the DNA strand reacting at the both sugar groups and the DNA bases. Any

position in the sugar is vulnerable to attack by the hydroxyl radical and attack leads to cleavage of the DNA strand²⁸. The reaction of sugars is further encouraged by the weak iron-binding properties of deoxyribose²⁸. All of the bases as with the sugars are susceptible to attack by the hydroxyl radical at a range of positions and a variety of products can be formed. For example, reaction with guanine and adenine can occur at the C5, C4 or C8 positions.²⁹ Reaction at the C-8 position is thought to be the predominant reaction and leads to the production of distinctive products, 10 -12 (Scheme 7), which can be used as oxidative stress indicators.³⁰ The reaction between guanine and the hydroxyl radical forms the radical adduct **8** which can then react in two ways, if the adduct is reduced it forms FAPy-guanine **12** and if it is oxidised **8**-hydroxyguanine **10** is produced.



Scheme 7: Reaction of hydroxyl radicals at the C-8 position^{29, 30}

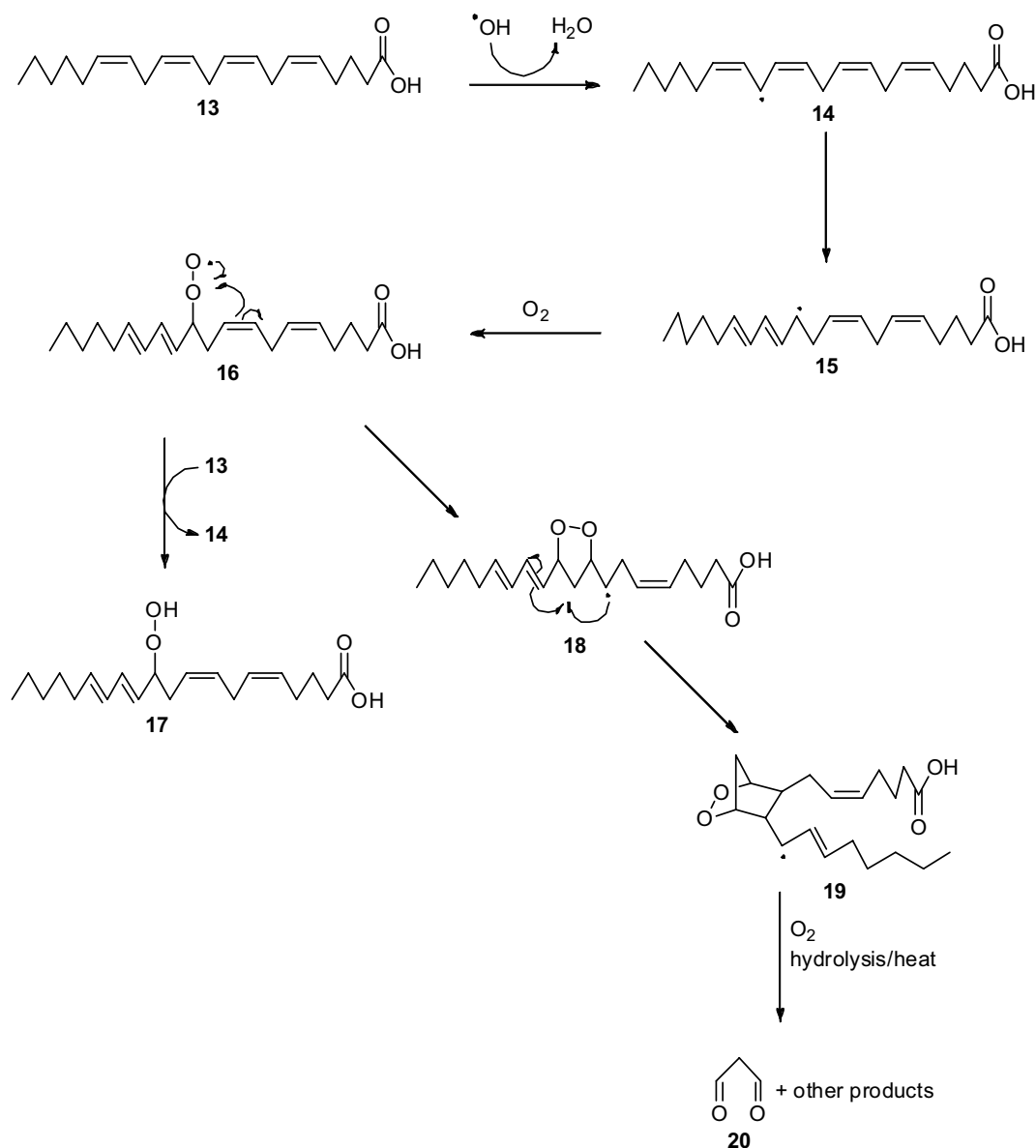
The reaction with bases leads to alteration in the base structure and causes weakening of the H-bonding between the two stands of DNA, changing the helical structure. Both reaction at the sugar and the base can lead to disruption to the DNA replication which can lead to cell dysfunction. When hydroxyl radical production is low damage to the DNA can be repaired very easily, however during oxidative stress the increased level of damage often prevents complete repair and increases the chance of radical damage causing cellular

dysfunction. The increased oxidative products of DNA have been reported in a plethora of age-related diseases.

1.6 Reaction of radicals with lipids

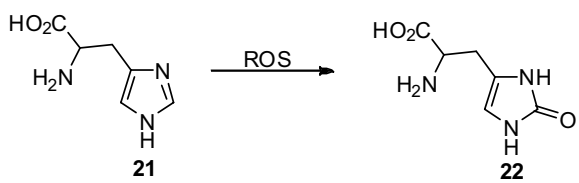
Cell membrane phospholipids and other polyunsaturated fatty acids (PUFAs) are susceptible to oxidation and are regular targets of free radical attack resulting in cell damage via a chain reaction known as lipid peroxidation³¹, Scheme 8. The reduction potential of PUFA[•]/PUFA is approximately 0.6 V which means it should be thermodynamically possible from HO[•], HO₂[•] And RO[•] to oxidise PUFAs, however hydroxyl radicals will do this most readily provided they do not react with other molecules within the membrane first³¹.

Lipid peroxidation is the reaction of polyunsaturated fatty acids via a number of reactive radical intermediates. The process is initiated by the hydroxyl radical when it abstracts a hydrogen atom from the methylene unit of a fatty acid **13** yielding water and a bisallylic carbon-centred radical **14**. The fatty acid radical then carries out a stabilizing molecular rearrangement producing a conjugated diene **15**, with isomerisation of the alkene. The carbon-centred radical could react with another carbon-centred radical or other reactive cell components causing crosslinks to other membrane molecules such as proteins and cholesterol, and damage to other biomolecules. However, under aerobic conditions the carbon-centred radical **15** reacts with molecular dioxygen yielding a peroxy radical **16**. Peroxy radicals can abstract a hydrogen atom from another molecule of fatty acid **13** to give a lipid peroxide **17** and a further radical **14** propagating the chain reaction. The peroxy radical **16** can alternatively carry out an intramolecular reaction forming a cyclic peroxide **18** which degrades via an endocyclic peroxide **19** to give the highly reactive malondialdehyde **20** and other products. The formation of lipid peroxides and rearrangements cause disturbance to the membranes that can lead to membrane rupture, leakage and ultimately cell death. Furthermore the malondialdehyde **20** is a toxic side product that can react with the DNA bases guanine, adenosine and cytosine damaging DNA³².

Scheme 8: Lipid peroxidation³¹

1.7 Reaction of the radicals with proteins

As with DNA, ROS can react at many sites within proteins mainly reacting with sulfur containing or unsaturated amino acids, e.g. the oxidation of histidine 21 illustrated in Scheme 9. Due to migration of the radical caused by the close proximity of amino acids within proteins the product observed does not necessarily indicate the first site of reaction¹⁴. Radical reactions can lead to cross-linking and structural change, however, in most cases unless the amino acids in or around the active site are damaged there is no impairment to the function of the protein.³³



Scheme 9: Oxidation of histidine by ROS³⁴

2 Antioxidant Defences

2.1 Introduction to antioxidant defences

In order to prevent the damage to our cells and biomolecules caused by ROS, as discussed in the previous chapter, our bodies have a wide range of antioxidants which quench radicals or prevent their formation ameliorating oxidative stress. Antioxidants come in an assortment of sizes, shapes and types. They can be enzymes, molecules made *in vivo* or molecules consumed in our diet. These antioxidant defences will be the main focus of this chapter.

2.2 Antioxidant Enzymes

There are three main classes of enzymatic antioxidants, superoxide dismutases, catalases and glutathione peroxidises. Superoxide dismutase (SOD) is a class of enzyme which converts two molecules of superoxide into hydrogen peroxide and oxygen. There are two forms of SOD, a manganese containing version found in the mitochondria and a copper/zinc version found in the cytosol³⁵. The active sites contain, histidine and aspartate residues³⁶, Figure 6.

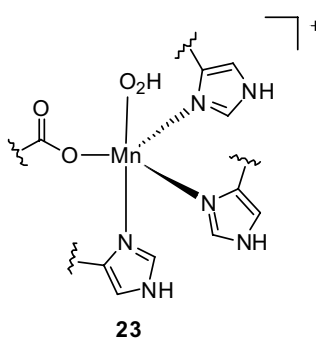
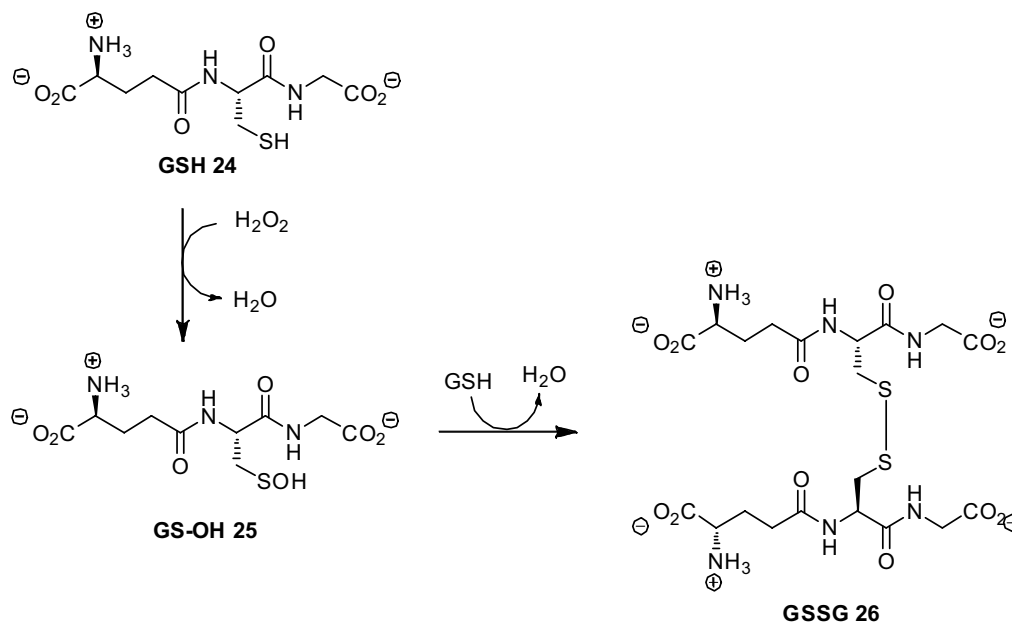


Figure 6: Active site superoxide dismutase

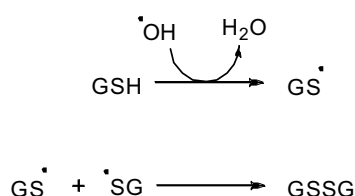
The hydrogen peroxide produced by SOD can then go on to react with catalase enzymes which convert the peroxide into water and oxygen. Glutathione peroxidase also converts hydrogen peroxide into water. The enzyme reduces hydrogen peroxide via the oxidation of the small tripeptide glutathione (GSH) **24** to a glutathione dimer (GSSG) **26**¹⁴, Scheme 10.



Scheme 10: Formation of the glutathione dimer

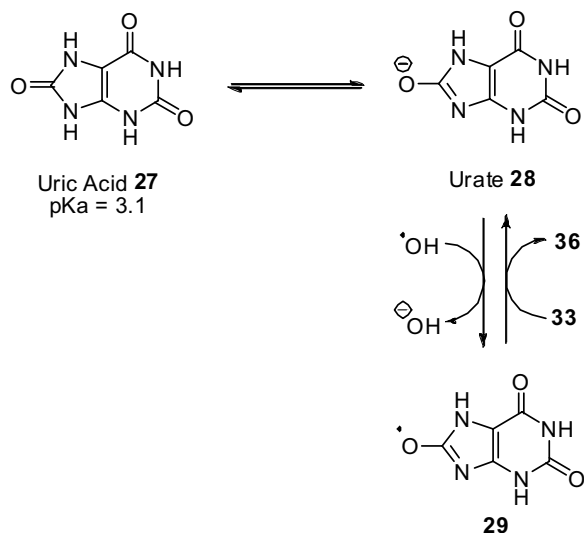
2.3 Endogenous Antioxidants

Glutathione can also react directly with radicals non-enzymatically. The radical species, e.g. hydroxyl radicals, would react with glutathione by hydrogen abstraction to form the thiyl radical which disproportionate to afford the dimer, similarly to the enzymatic process.



Scheme 11: Non-enzymatic reaction of glutathione with hydroxyl radicals

Another naturally occurring antioxidant is uric acid **27**, which exists as the negatively charged urate **28** at physiological pH, reacts with strong oxidants, such as hydroxyl radicals, forming a secondary radical **29** stabilised by delocalisation around the purine ring. The stabilised radical will then be quenched with either glutathione or ascorbic acid, Scheme 12.

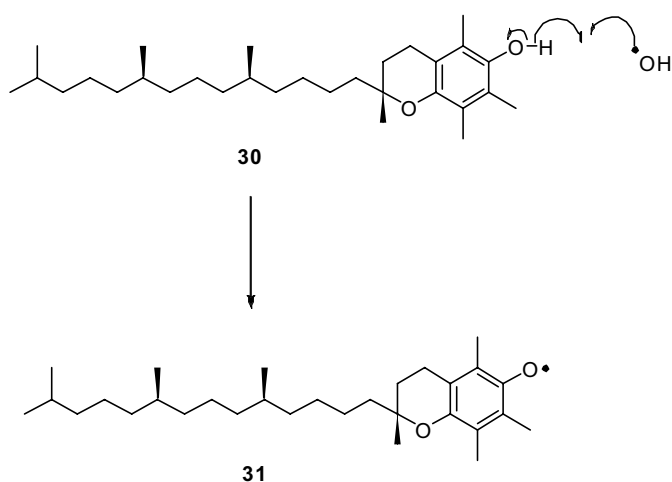


Scheme 12: Reaction of Uric acid with hydroxyl radicals

Other molecules include, coenzyme Q lipoic acid³⁷ and some phenolic sex hormones e.g. oestrone.³⁸

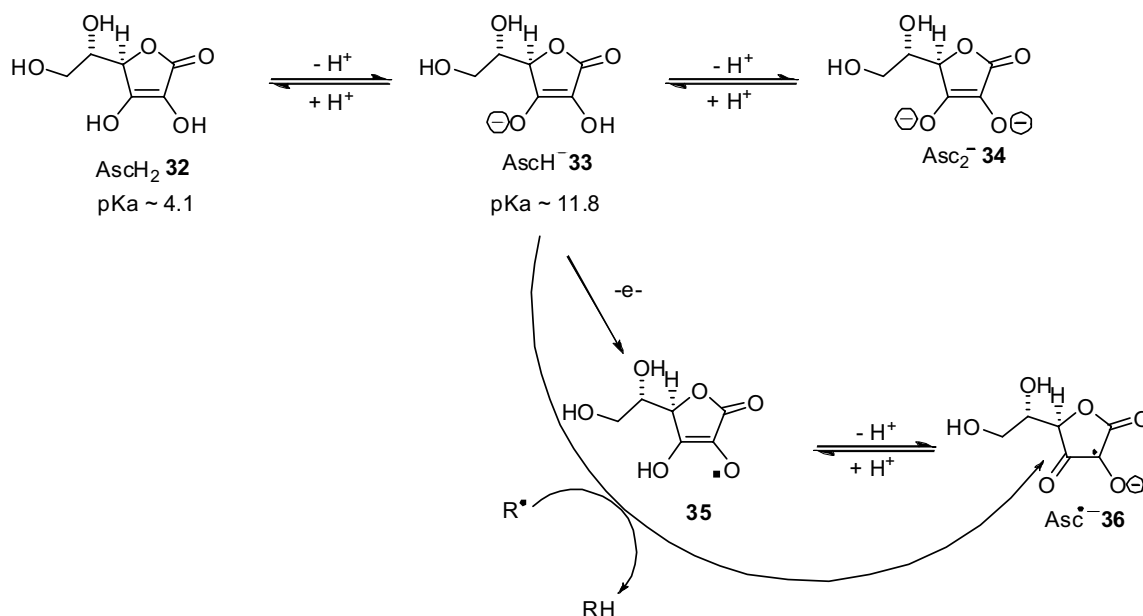
2.4 Exogenous Antioxidants

The two most well known exogenous antioxidants are *d*- α -tocopheryl **30** (the main component of vitamin E) and ascorbic acid **32** (vitamin C). Vitamin E is a group of tocopherol compounds where *d*- α -tocopheryl **30** is the main compound. It is a scavenger of peroxy radicals, terminating the chain reaction of lipid peroxidation. The reaction proceeds with the donation of a hydrogen atom to the peroxy radical affording the more stabilized tocopheryl radical **31** which is then quenched with either glutathione or ascorbic acid¹⁴.



Scheme 13: Reaction of *d*- α -tocopheryl with hydroxyl radical

Vitamin C, (Ascorbic acid) **32** is the water-soluble antioxidant partner for lipid soluble vitamin E and reacts with the tocopheryl radical **31** to regenerate the vitamin **30**.



Scheme 14: Reaction of ascorbic acid with radicals¹⁴

Ascorbic acid (AsCH₂) **32** has 2 ionisable hydroxyl groups. At physiological pH it exists mainly as the monoanion form AsCH⁻ **33**. AsCH⁻ reacts with a radical via the donation of a hydrogen atom to produce Asc^{•-} **36** a stable unreactive radical semihydroascorbate. This reaction is thought to terminate the chain reaction.

Many other exogenous antioxidants are of plant origin; some examples are the polyphenols quercetin **37**, catechin**38** and the carotenoid beta-carotene **39**, Figure 7. The compounds may act as food preservatives due to their ability to quench radicals. Although all the compounds reduce radical species *in vitro* there is evidence to suggest that many of the polyphenols are not absorbed after consumption and are therefore not as good at reducing radicals *in vivo*. Indeed quercetin 4'-glucoside has been shown to be highly metabolized in the guts of rats.³⁹

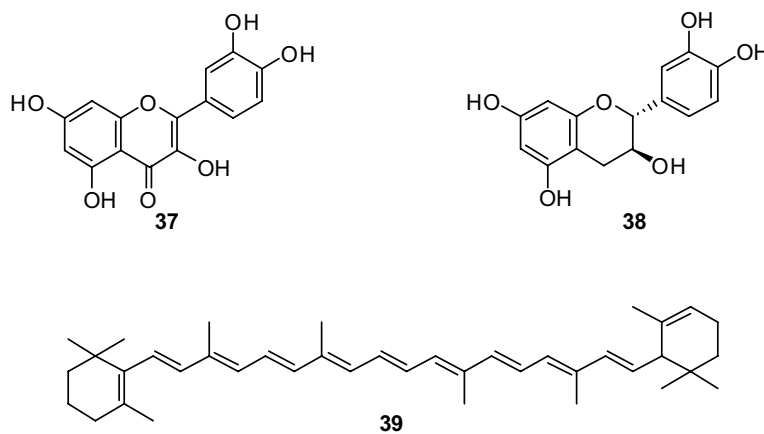


Figure 7: Antioxidants from plants

On the other hand the carotenoids are absorbed and some play a critical role in converting singlet oxygen back to triplet oxygen in the eye, where UV irradiation is high. Their role as radical scavengers though is a matter of some debate as the products of the reactions with ROS are themselves harmful and β -carotene supplementation increases mortality in smokers.⁴⁰

3 Methods for investigation of oxidative stress and reactive oxygen species.

All of the information discussed in the first two chapters was uncovered utilising the many techniques employed for the investigation of ROS and oxidative stress. ROS are so short-lived *in vivo*, Figure 8, as they either react with biomolecules, produce secondary radical species or are metabolised. For this reason they cannot be detected directly and therefore a number of different techniques are employed to investigate them.

Reactive Oxygen Species	Half-life
Superoxide	10^{-5} s
Hydrogen Peroxide	1 min
Hydroxyl	10^{-9} s

Figure 8: Approximate half-lives of ROS species in biological systems⁴¹

The main techniques employed to study ROS are chemical based and use small synthetic molecules which react with ROS allowing reporting, quantification identification and amelioration of oxidative stress and ROS. Synthesis and evaluation of molecules of this type will be the main focus of this thesis. The main methods are outlined below.

3.1 Chemiluminescent Probes.

The study of ROS using chemiluminescence employs light-emitting probes. Chemiluminescence is the emission of light by a substance as a result of it undergoing a chemical reaction. When studying oxidative stress the reaction is with ROS allowing oxidative stress to be observed and ROS quantified by measuring the light emitted.

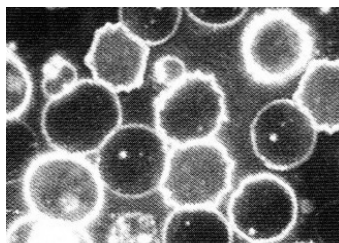
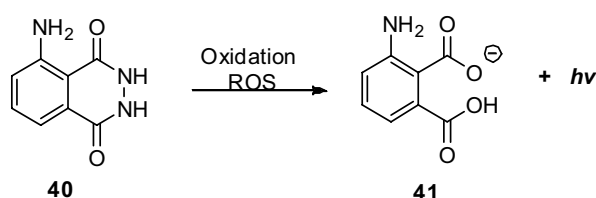


Figure 9: Oxidative stress in red blood cells detected by chemiluminescence

Some examples of commonly used chemiluminescent probes are described below.

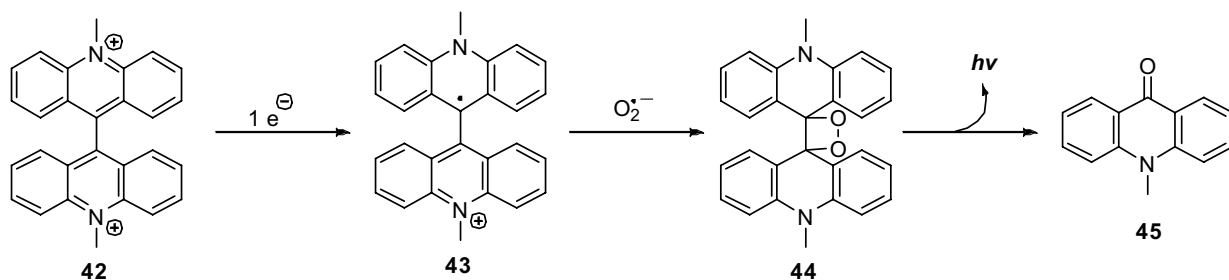
Luminol **40** is a probe and has been used to study ROS production in phagocytes and neutrophils⁴². When luminol undergoes oxidation to afford carboxylate **41** light is emitted, Scheme 15.



Scheme 15: Luminol

Luminol is not selective for individual ROS so therefore can indicate oxidative stress and can quantify ROS as a whole but does not allow for differentiation between ROS. Furthermore, as the transformation step from non-light-emitting to light-emitting is generally oxidation, other oxidants within the cell can lead to the light emitting product which gives erroneous results⁴³.

Some chemiluminescent probes have shown slight selectivity for individual ROS; for example lucigenin **42**, Scheme 16, is a commonly used chemiluminescent probe which has shown some selectivity for superoxide⁴⁴.

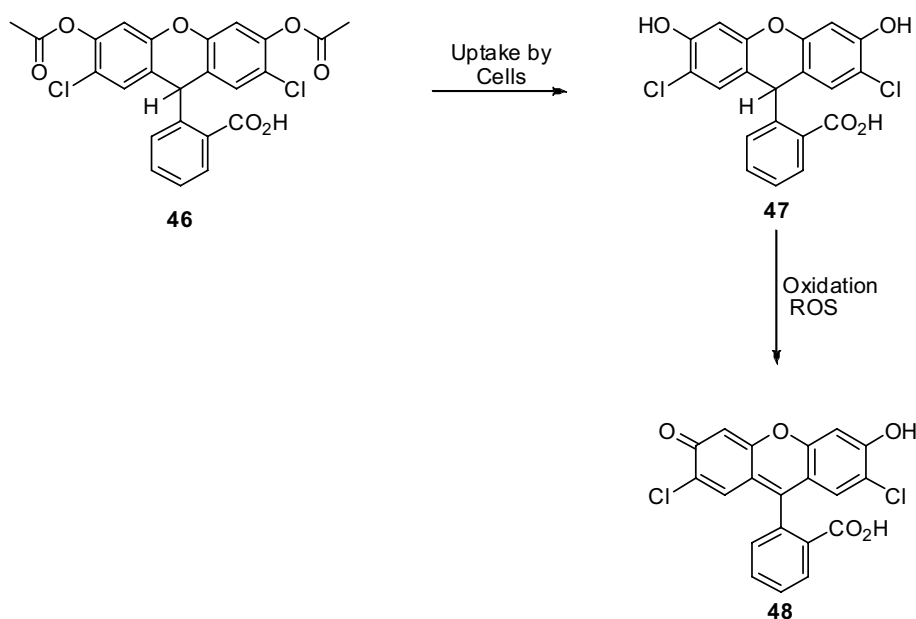


Scheme 16: Reaction of lucigenin with superoxide

Lucigenin under goes a one electron reduction to produce the carbon centred radical **43** which reacts with superoxide as shown in Scheme 16. However, Lucigenin can still lead to erroneous results as the carbon-centred radical **43** can reduce O_2 to $O_2^{\cdot-}$ to generate the unstable endoperoxide **44** whose decomposition to **45** generates light.

3.2 Fluorescent Probes

Dichlorofluorescein diacetate was first described in 1965 as a way to measure hydrogen peroxide⁴⁵, Scheme 17.



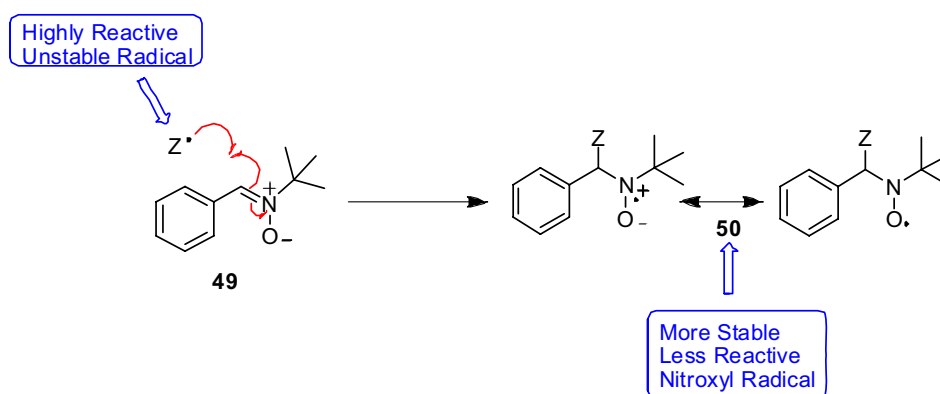
Scheme 17: Reaction of dichlorofluorescein with ROS

Dichlorofluorescein **46** is non-fluorescent upon uptake into cells and tissues it is deacetylated to afford 2,7-dichlorofluorescein **47**. The phenolic is oxidised by ROS forming the fluorescent product, 2,7-dichlorofluorescein **48**.

Similarly to the chemiluminescent probe luminol, dichlorofluorescein is non-selective for ROS and can be easily oxidised within the cell. However, there have been some recent reports of caged fluorescent probes which show selectivity towards hydrogen peroxide. As these probes are relevant to parts of this thesis they are reviewed extensively in Chapter 8 pg 76. Detection of ROS by fluorescent probes is a rapidly expanding field; Soh has published a comprehensive review of these probes⁴³.

3.3 Spin trapping and electron paramagnetic resonance spectroscopy.

Spin traps react with ROS to afford detectable products. They work essentially by catching the highly reactive radicals such as peroxy, hydroxyl, and methyl radicals forming more stable radical adducts, Scheme 18 that can be detected using electron paramagnetic resonance (EPR) spectroscopy. The main chemical family of spin trap is the nitron family, radicals react with the nitrones to form the stabilized nitroxyl radical as shown for the nitron PBN **49** giving a nitroxide **50** which is termed the spin adduct. As the nitroxyl radicals have unpaired electrons they can be detected by electron paramagnetic resonance spectrometry.



Scheme 18: General reaction of nitrones with radicals

EPR spectroscopy can only detect unpaired electrons which gives spin-trapping an advantage over chemluminescence and activated fluorescence as there are less erroneous results as generally the nitron has to react with a radical species in order to produce a signal. EPR spectroscopy can detect unpaired electrons within transition metals such as iron, manganese and those within metal complexes as well as a wide variety of organic radicals. EPR spectroscopy works due to a principle called the Zeeman Effect²⁵. Electrons have spin and when subjected to a static magnetic field the electrons can either orientate themselves spin aligned or spin against the magnetic field. This causes the electrons to split between two different energy levels, which vary in energy, dependent on the magnetic field applied²⁵ (Figure10).

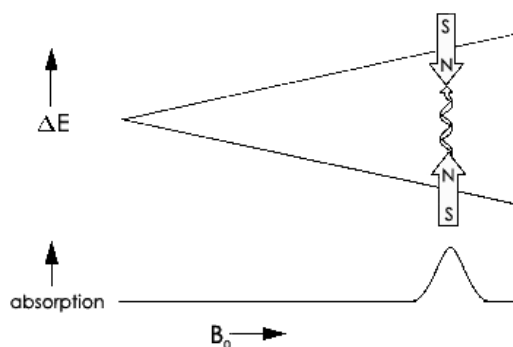


Figure 10

When radiation is applied to the electron within the magnetic field at the correct energy the electron will move from the lower level to the higher level. Thus an absorption spectrum is obtained. The lifetime of electron spin states is much shorter than nuclear spin states, so EPR absorptions are much broader than NMR signals. To improve the signal to noise ratio EPR spectra are reported in the first derivative i.e. the rate of change of absorption rather than absorption is reported. When neighbouring atomic nuclei have spin, such as hydrogen nuclei and nitrogen nuclei, the magnetic moment of the nucleus leads further splitting of energy levels and more complex signals, Figure 11.

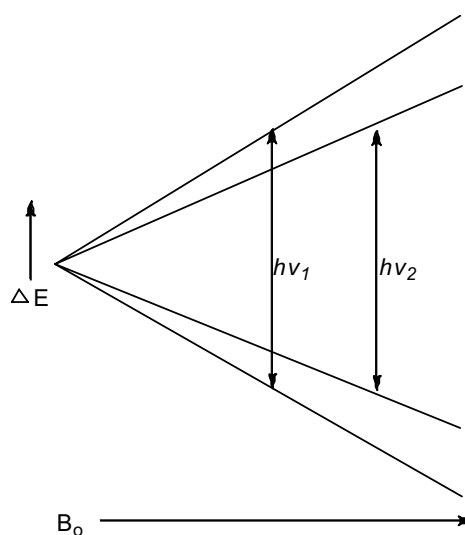


Figure 11: Splitting caused by neighbouring nuclei

The nuclei are like mini magnets to which the unpaired electron can either be spin with or spin against. For the hydrogen which is spin $\frac{1}{2}$ this affords a doublet resulting from the transition shown. For nitrogen which is spin 1 a triplet is observed.

The oxygen-centred, nitroxyl radicals have a neighbouring nitrogen and often a beta hydrogen atom which contribute to hyperfine splitting, Figure 12. This leads to a triplet of doublets. In some cases, such as the spectrum for the hydroxyl adduct of DMPO, Figure 13, where the nitrogen and hydrogen couplings are equivalent, quartets are observed⁴⁶.

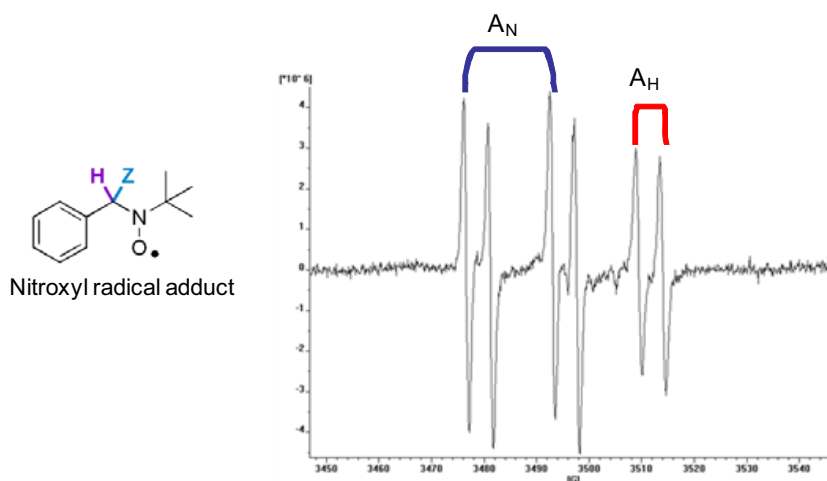


Figure 12: Hyperfine splitting of a nitroxyl radical adduct

.The size of the hyperfine splitting is determined by the probability that the unpaired electron will occupy the orbital surrounding the nuclei²⁵. Essentially the higher the probability of the radical occupying the orbitals surrounding the nuclei, the higher the splitting observed. Therefore, in the spectra for nitroxyl radicals the nitrogen is normally the largest splitting. However, the size of the hyperfine splitting in the spin adduct is determined by both the nature of the spin trap and the nature of the reacting radical and can vary greatly.

For example an electronegative atom will pull electron density away from the nitrogen and hydrogen lowering both the hyperfine splitting. In some examples the EWG leads to more pronounced coupling to the γ/δ hydrogens. This can be seen with the hyperfine splitting for DMPO adducts⁴⁶, formed from trapping superoxide (Figure 13).

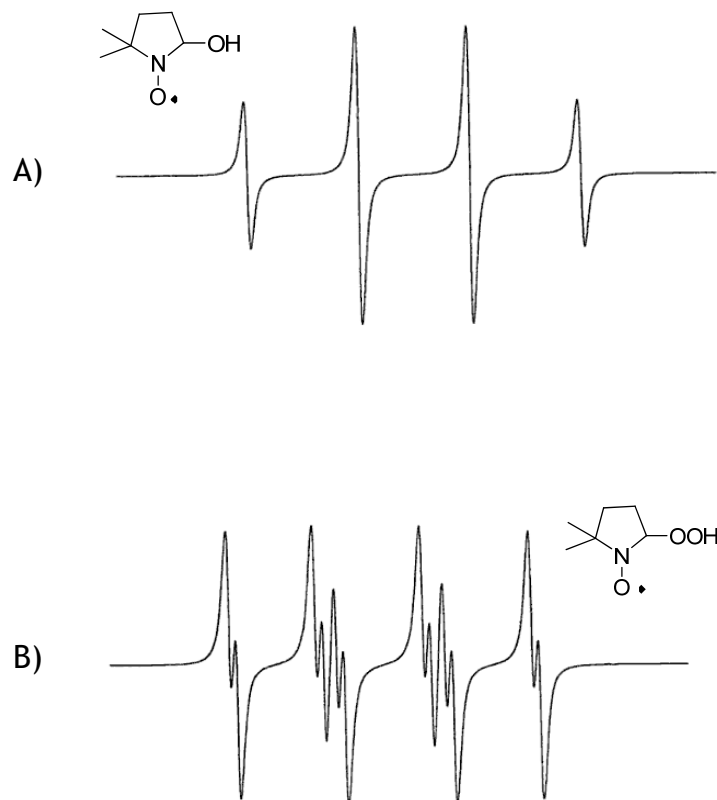


Figure 13: **A:** EPR spectrum for DMPO hydroxyl adduct. Hyperfine = $A_N = 14.9$ (t), $A_H^\beta = 14.9$ G (d); **B:** EPR spectrum for DMPO hydroperoxyl adduct. Hyperfine = $A_N = 14.3$ (t), $A_H^\beta = 11.4$ G (d); $A_H^\gamma = 1.3$ G

Smaller nitrogen and hydrogen hyperfine splittings are also observed when an electron withdrawing group (EWG) is included at other positions of the spin trap, Figure 14. Thus generally the superoxide adducts have smaller hyperfine splitting than the hydroxyl adducts which are smaller than the methyl adducts and the presence of an ester or aryl group in close proximity also reduces the hyperfine.

Spin Trap	Methyl adduct	Hydroxyl adduct	Superoxide adduct
DMPO 51⁴⁶ 	$A_N = 16.2$ $A_H = 23.0$	$A_N = 15.10$ $A_H = 15.10$	$A_N = 14.30$ $A_H = 11.40$
EMPO 52⁴⁷ 	$A_N = 15.42$ $A_H = 22.30$	$A_N = 14.00$ $A_H = 15.00$	$A_N = 13.28$ $A_H = 9.67$

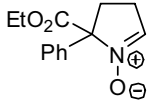
EPhPO 53⁴⁸			
	$A_N = 14.90$	$A_N = 13.43$	$A_N = 13.05$
	$A_H = 21.63$	$A_H = 14.70$	$A_H = 9.00$

Figure 14: Influence of EWG on hyperfine splittings

As well as the hyperfine splittings an EPR spectrum is also identified by the g-factor. The g factor is a dimensionless number which is specific to the spectrum observed. It is related to the size of the energy gap (ΔE) and the magnetic field (H)²⁵, Figure 15.

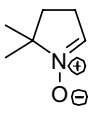
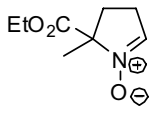
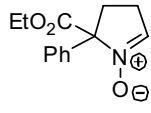
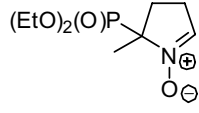
$$\Delta E = g\beta H$$

Figure 15

The g-factor for the free electron is 2.00232 and most organic radicals have a g-factor close to this. There are many different frequencies of radiation which are used to excite unpaired electrons from low frequency S Band (2-4 GHz) and Q band (35 GHz) to the very high W band (100 GHz). EPR spectrometry is normally measured at X band frequency, 9-10 GHz. Spectra can also be taken in different media: they can be in solution phase or solid phase resulting in isotropic and anisotropic spectra respectively. Solid phase experiments can either be run on a frozen solution or on a crystal. These types of experiment are generally run when investigating inorganic radical and are used not just to detect a radical but to learn about the radical's environment electron density patterns in the radical's environment. In solution phase EPR spectroscopy molecules are constantly tumbling leading to an isotropic signal which is an average of all the possible conformations. A symmetrical spectrum is therefore observed. When organic radicals are large or are encapsulated it can lead to decreased tumbling which can affect the signal decreasing the symmetry⁴⁹. In some cases the signal can become completely anisotropic.

4 Nitron spin traps

Nitrones have evolved since the discovery of PBN **49** and DMPO **51**. Much work has been carried out to form derivatives which have improved radical trapping properties and increased longevity of radical adducts. Early research focused on synthesizing and designing nitron spin traps which have elongated half lives radical adducts or increasing the reactivity of nitrones towards superoxide radicals. There have been a large number of DMPO and PBN analogues synthesized⁵⁰, Figure 16. Studies show there is a link between substituents at the C-5 position of DMPO and the tert-butyl group on PBN which can significantly affect the half life of the subsequent adducts formed, with electron withdrawing groups leading to the longer lived radical species.

Spin Trap	T ^{1/2} Superoxide adduct
DMPO 51 ⁴⁶ 	< 1 min
EMPO 52 ⁵¹ 	10-20 min
EPhPO 53 ⁴⁸ 	16 min
DEPMPO 54 ⁵⁰ 	~14 min

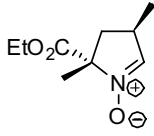
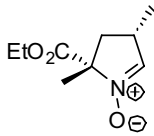
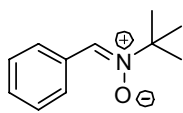
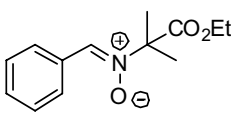
3,5-anti-EDPO 50 ⁵² 	11.5 min
3,5- syn-EDPO 55 ⁵² 	47 min
PBN 49 ⁵⁰ 	< 1 min
EPPN 57 ⁵³ 	5.9 min

Figure 16: Half-lives of selected spin-traps

As the presence of the cyclic system also increased longevity of adducts there have been a range of various ring shapes and sizes incorporated in spin-traps⁵⁴. A further factor which has been shown to make a difference to the half life of adducts is the relative conformation of substituents on the ring of cyclic spin traps, e.g. 3,5-syn-EDPO **56**,⁵² which has the carboxy and methyl groups on the same side, has a longer lifetime than 3,5-anti-EDPO **55**.

In more recent years research has been focused on improving physical properties for reactions *in vivo*. Durand has synthesised a series of amphiphilic spin traps for increased solubility in biological systems⁵⁵, Figure 17.

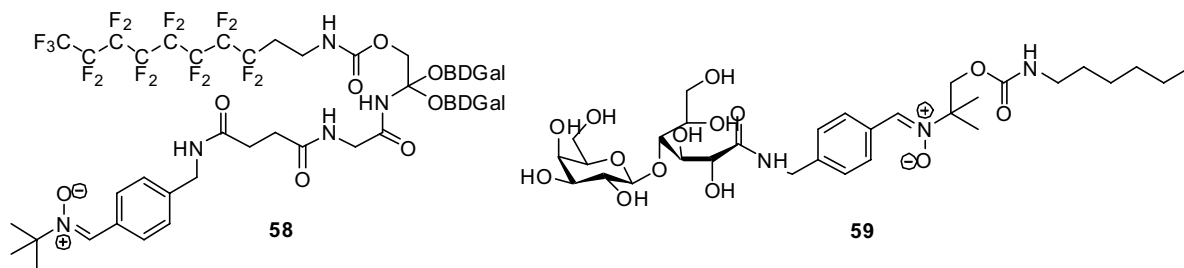
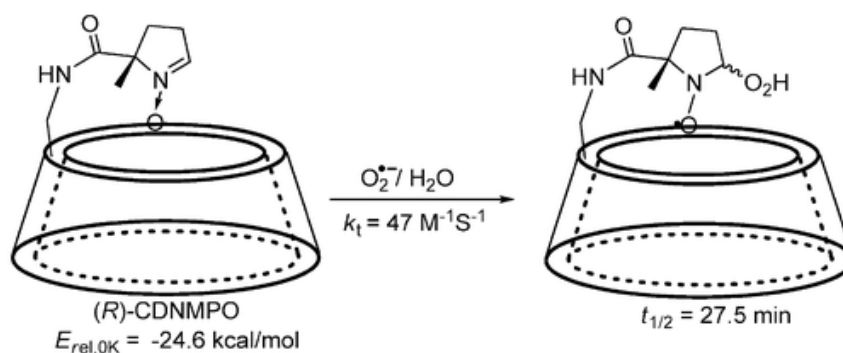


Figure 17: Amphiphilic spin traps

The half-life of spin adducts formed during trapping of superoxide radicals with either DMPO or PBN are significantly increased with the addition of cyclodextrin as the spin trap forms an inclusion complex with the nitroxyl radical shielding it. As a result of this research Villemena has formed a DMPO derivative with a cyclodextrin attached **60** in order to increase the longevity of the radical adduct *in vivo*⁵⁶ because radical adducts are readily reduced to the EPR silent hydroxylamine *in vivo* by glutathione or ascorbic acid. The cyclodextrin encapsulates the nitroxyl radical formed **61** preventing reduction and increasing the half life, Scheme 19 .



Scheme 19: Nitroxyl cyclodextrin inclusion complex⁵⁶

There have also been targeted spin traps synthesized. Villemena has more recently synthesized a membrane-targeted cyclodextrin conjugate⁵⁷, Figure 18.

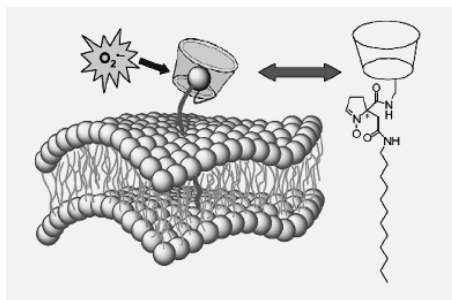
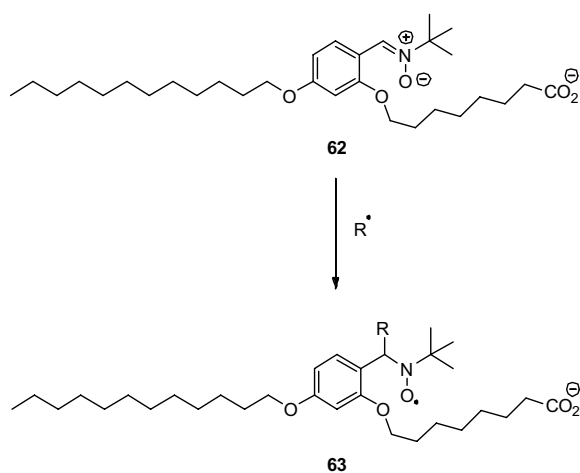


Figure 18: Membrane targeted cyclodextrin conjugate⁵⁷

There have been a number of other nitrones targeted to membranes for the investigation of lipid peroxidation. Tordo has synthesised a cholesterol conjugate, 5-(cholesteryloxyethoxyphosphoryl)-5-methylpyrroline-*N*-oxide (5-ChEPMPO)⁵⁸. There have also been a number of membrane-targeted nitrones synthesised within the Hartley group. Incorporation into the membrane can be detected by EPR spectroscopy as the spectrum of the nitroxide adduct formed in liposomes is anisotropic^{49,59} Figure 19. Spin traps have also been targeted to sulfhydryl containing enzymes⁶⁰ and mitochondria⁶¹.

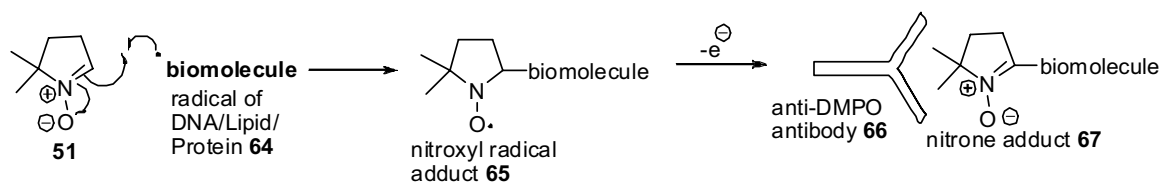


Scheme 20: Reaction of membrane targeted nitron with radicals



Figure 19 Anisotropic EPR spectrum of adduct immobilised in membrane

Immuno spin trapping⁶² is another interesting development into the study of oxidative stress by spin trapping. The main focus of immuno spin trapping is to trap DNA and protein radical species.



Scheme 21: Immuno-spin trapping⁶²

The technique utilises DMPO which was selected due to its solubility in aqueous solutions and its safety and pharmacokinetic profile and a DMPO antibody. When a cell is under stress radicals are produced, these radicals react with DNA and proteins producing secondary radicals **64** which react with DMPO **51** to afford the radical adduct **65**. The radical adduct **65** will undergo oxidation to **67** and can then be isolated from the cell using the DMPO specific antibody **66**. The trapped biomolecules can then be studied in order to identify biological targets for oxidative stress and potential biomarkers for oxidative stress, Scheme 21.

5 Nitrones as therapeutics

Nitrones as mentioned above were discovered over 40 years ago and as chapter 4 illustrates a lot of work has been carried out involving their spin trapping properties. However, two decades after their discovery scientists began to notice they also have significant biological activity and demonstrated their potential to protect biological systems against oxidative stress⁶³. PBN **49**, and NXY-059 **68**, Figure 20, have shown promise as therapeutics.

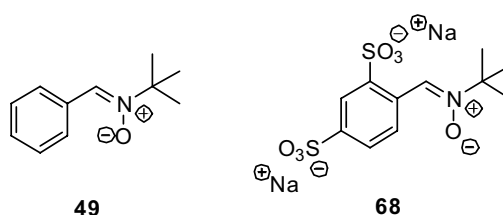


Figure 20: PBN and NXY-059

The first reports of PBN **49** being tested as a therapeutic dates back to 1980 when scientists observed lowered brain damage on the administration of PBN **49** shortly after brain ischemia in gerbils⁶⁴. Since then nitrones have been investigated as potential therapeutics for a number of neural and systematic functions such as atherosclerosis⁶⁵, septicaemia, cancer⁶⁶ and hearing loss⁶⁷ as well as stroke⁶⁸.

The most significant research into use of nitrones as therapeutics is for the treatment of stroke and brain ischemia. In fact NXY-059 **68** had entered clinical trials and had shown positive results in both Phase I and Phase II clinical trials, showing significant improvement to the level of brain damage in induced ischemia in rats as well as a good safety profile in healthy volunteers. However, the nitrone failed the phase III clinical trials when treating stroke patients⁶⁹.

Since the discovery of NXY-059 **68** a number of other nitrones have been synthesized as potential therapeutics for the treatment of stroke. Stilbazulenyl dinitrone, STAZN **69**, Figure 21, contains two nitrone functional groups attached by an alkene. It shows increased ability to cross the blood brain barrier versus PBN **49** and NXY-059 **68** and this results in therapeutic doses being 300-600 fold lower than PBN and NXY-059⁷⁰.

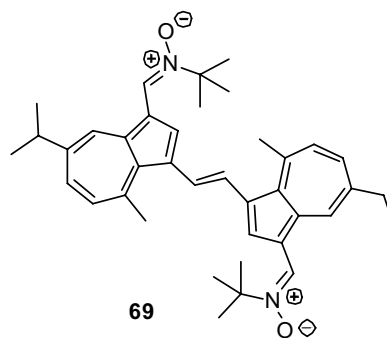


Figure 21: STAZN

Another nitronium specifically synthesized to treat cerebral ischemia is 2-[[[(1,1-dimethylethyl)oxidoimino]methyl]-3,5,6-trimethylpyrazine (TBN) **71**, which contains a nitronium moiety conjugated to a tetramethylpyrazine (TMP) molecule **70**. TMP is traditionally used to treat stroke by encouraging blood flow within the brain and preventing clots. This should mean that the TMP nitronium **71** will treat stroke in two ways, via the nitronium preventing damage and via TMP increasing the blood flow improving recovery of the tissue providing better treatment for the recovery of stroke patients⁷¹. Furthermore nitroniums have also shown promise for the treatment of myocardial ischemia/reperfusion, with reports DMPO and its derivative showing therapeutic properties⁷²

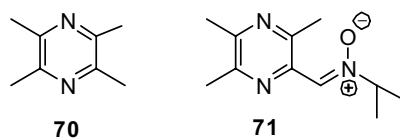


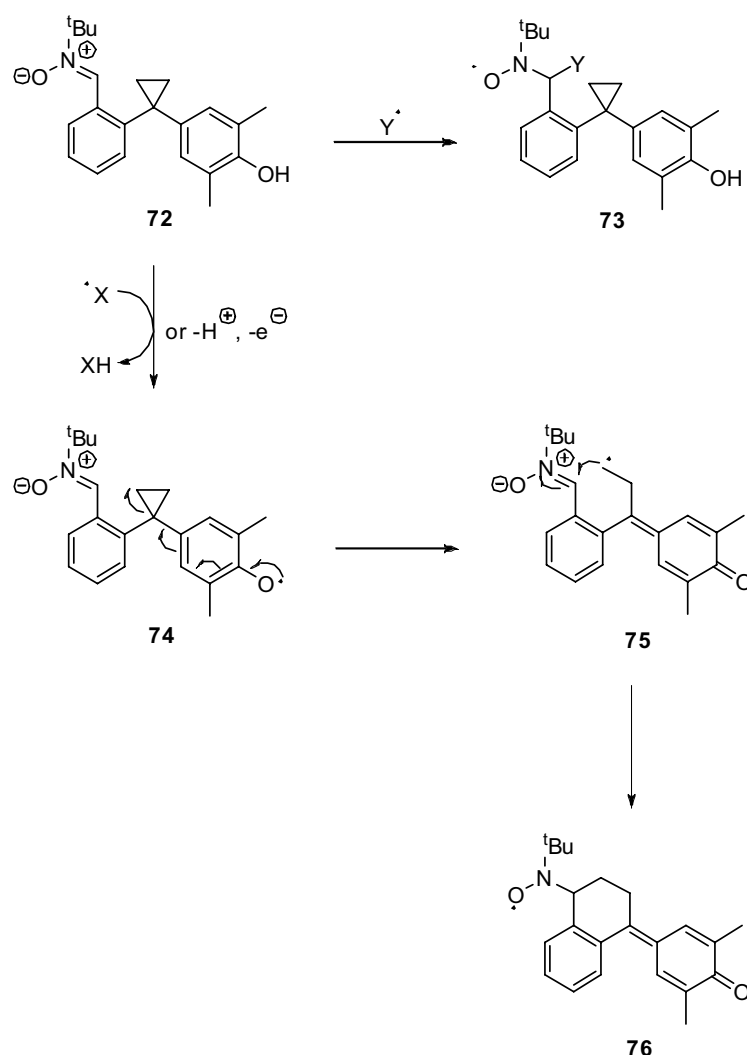
Figure 22: TMP and TPN

The mechanism of the biological activity of nitroniums is not known, although it is mainly attributed to their antioxidant properties which are well known due to their use as spin-traps and is further substantiated by literature which reports the use of other antioxidants as therapeutics⁷³. However, *in vitro* results suggest that the concentration of PBN and other nitroniums must be mM to be effective antioxidants and *in vivo* studies show that the tissue concentration of PBN only reaches μM levels⁸⁵. There is some evidence to show affinity of nitroniums to

enzymes which mean the nitronone may accumulate where they are required leading to biological activity⁵⁷. In light of this other potential mechanisms have been proposed. It is thought the nitrones either interact with enzymes or elicit a biological response due to their anti-inflammatory properties⁷⁴.

Evaluation of a Dual Sensor Spin-Trap

As previously discussed in the introduction, one of the main problems with the current methods for the detection of ROS and chemical contributors to oxidative stress is the ability to distinguish between different radicals. Spin-trapping with nitrones currently offers the best method for distinguishing between ROS as the stable radical adducts afford characteristic spectra. However, most nitroxyl spin adducts produce an EPR spectrum consisting of a triplet of doublets which means in some cases simulation and calculation of hyperfine splitting and g-value have to be carried out before the radical adduct can be identified.



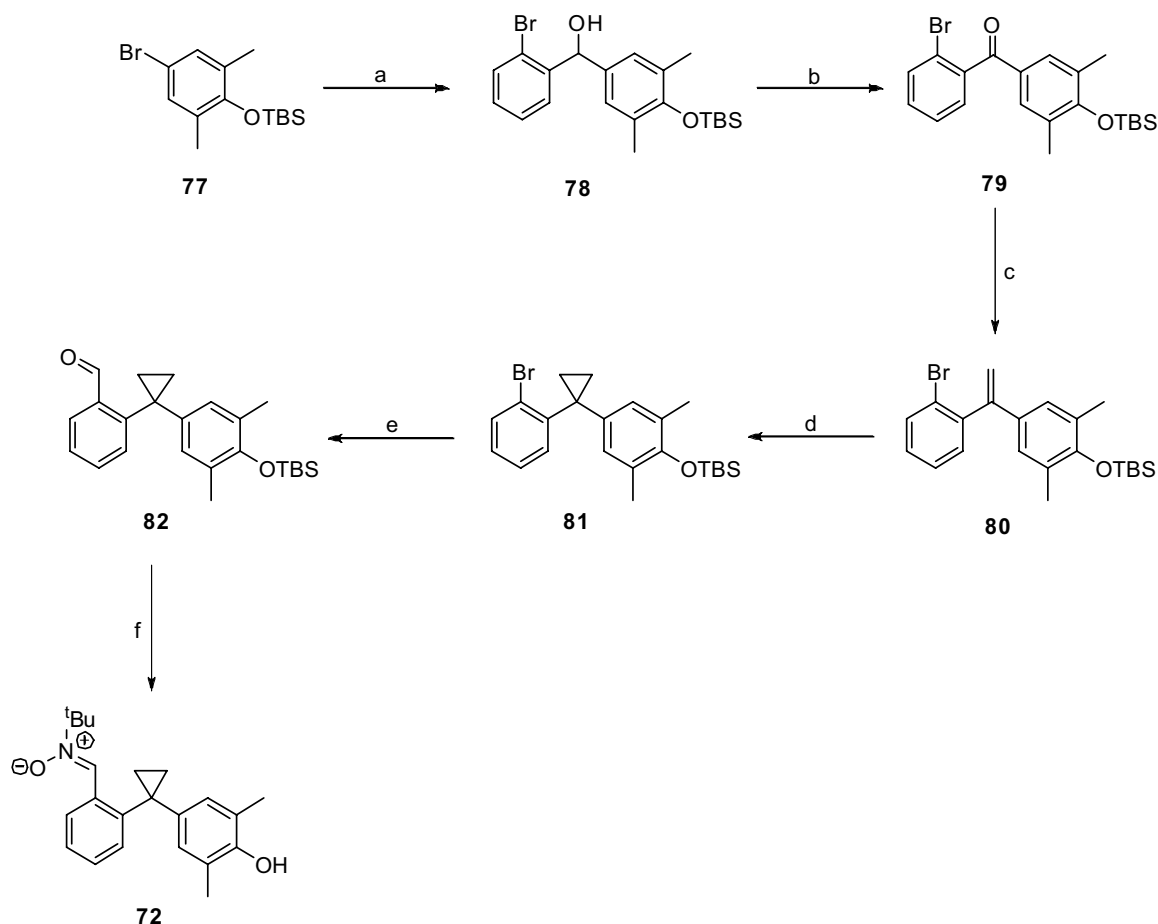
Scheme 22: Reaction of the dual sensor with radical species

Thus, a nitron probe was designed and synthesised within the Hartley group with two reactive sites which should react with different ROS resulting in unique spectra providing even clearer distinction in spectra allowing for clearer differentiation between radical adducts. The dual sensor probe **72** consists of two separate aromatic rings, which are bridged by a cyclopropane, with nitron and phenolic functional groups which would react with radical species by two separate mechanisms, Scheme 22.

Very reactive hydroxyl radicals $\cdot\text{OH}$ and electron rich carbon centred radicals ($\text{Y}\cdot$) would be expected to react at the nitron functionality forming a stable nitroxyl radical adduct **73**. Electron-poor radicals ($\text{X}\cdot$) which do not react well with nitrones might be expected to react at the phenolic moiety via hydrogen atom abstraction or by proton loss and electron transfer affording the phenoxyl radical **74**. The cyclopropane should then open rapidly to give an unstable primary carbon-centred radical **75** which should react with the nitron forming a tricyclic nitroxyl radical **76**. The two distinctive nitroxide adducts **73** and **76** should give dissimilar EPR spectra allowing for the differentiation between radicals $\text{Y}\cdot$ and $\text{X}\cdot$

5.1 Synthesis

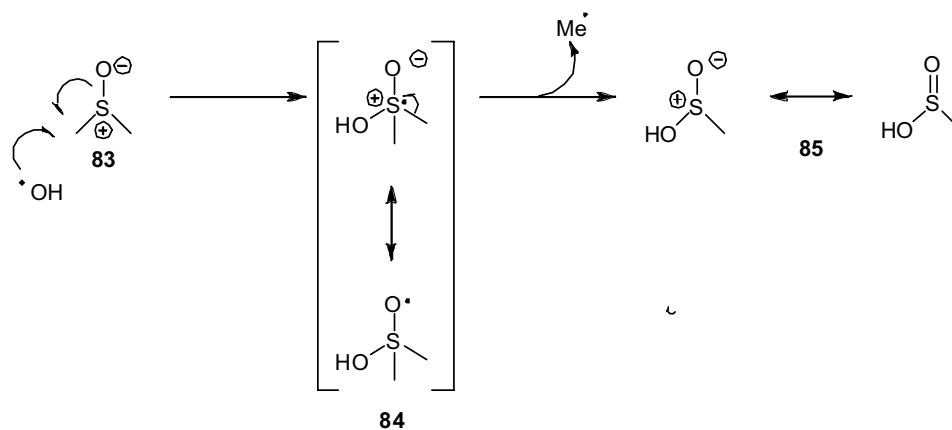
The dual sensor was synthesized by another member of the Hartley group as outlined in Scheme 23. The bromide **77** was treated with BuLi to form the lithiated species and reacted with the benzaldehyde to form the alcohol **78**, introducing the second aromatic ring. The alcohol **78** was then oxidised using manganese oxide to form the ketone **79** which was converted to the terminal alkene **80** via a Wittig reaction this was followed by the modified Simons-Smith reaction which produced the cyclopropane **81**. Lithium-bromine exchange followed by reaction with DMF gave the aldehyde **82** followed by condensation with *tert*-butyl hydroxylamine acetate produced the target nitron **72**.



Scheme 23: Reagents and conditions: a) i) 1 eq. BuLi, THF, -78°C ii) 1 eq. 2-bromobenzaldehyde, 69%; b) MnO_2 , DCM, reflux, 100% ; c) 2 eq. $\text{Ph}_3\text{P}=\text{CH}_2$, THF, 0°C , 94%; d) 10 eq. CH_2I_2 , 5 eq. Et_2Zn , DCM, Reflux, 76%; e) i) 1.1 eq. BuLi, ii) DMF; f) i) 1.5 eq. $^t\text{BuNHOH}\cdot\text{AcOH}$, 1.5 eq. NaHCO_3 , EtOH, reflux, ii) Bu_4NF , THF, 16 % over 2 steps.

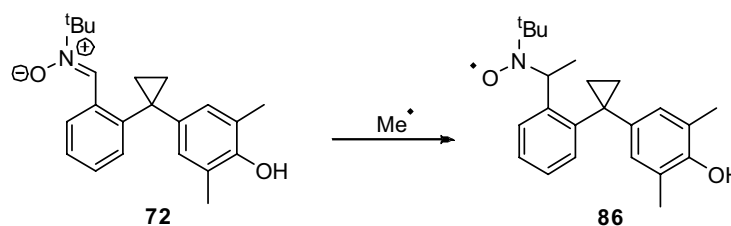
5.2 EPR spectroscopy

The nitron was then reacted with radical species and the EPR spectra obtained. The methyl radical was produced using Fenton conditions in DMSO. Iron (II) ions reduce hydrogen peroxide to generate hydroxyl radicals and water (Scheme 6). The hydroxyl radicals react with DMSO **83** to give the resonance-stabilized adduct **84** which then fragments to give methyl radicals and sulfinic acid **85**, Scheme 24.



Scheme 24: Reaction of DMSO with hydroxyl radicals

As expected the electron rich $\cdot\text{Me}$ radical reacted at the nitrono moiety forming a stable nitroxyl radical adduct **86** (Scheme 25) as judged from the characteristic EPR spectrum of a triplet of doublets, Figure 23.



Scheme 25: Reaction with methyl radicals

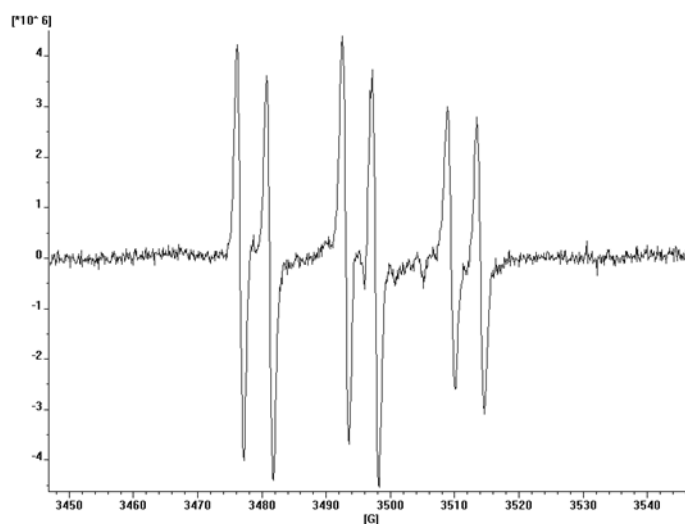
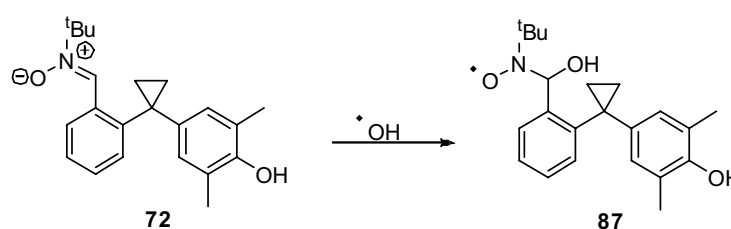


Figure 23: $g = 2.0056$, $A_N = 16.32 \text{ G}$ (t), $A_H^\beta = 4.57 \text{ G}$ (d); Reagents and conditions: 3.3 mM nitrono, 0.33 mM H_2O_2 , 0.33 mM Fe(II)SO_4 , 1:2 DMSO- H_2O

The reaction conditions had to be optimised as using Fenton conditions with high concentrations of hydrogen peroxide afforded both the methyl and hydroxyl radical adducts. As Fenton conditions produce hydroxyl radicals instantaneously high concentrations of hydrogen peroxide affords high concentrations of hydroxyl radicals which increases the chance of the radical reacting with the spin trap before it reacts with the DMSO in solution to produce the methyl radical.⁷⁵ Meaning two adducts are formed giving a complicated spectrum.

The spin trap was then reacted with $\cdot\text{OH}$ radicals, produced via Fenton conditions in DMF. The hydroxyl radical reacts at the nitron moiety producing the radical adduct **87**, Scheme 26 which gives an EPR signal of a triplet of doublets, Figure 24. The H^{β} hyperfine coupling is significantly smaller than those in the methyl radical adduct **86**, 1.85 G vs 4.57 G, and these hyperfine couplings are therefore distinctive for the two adducts.



Scheme 26: Reaction with hydroxyl radicals

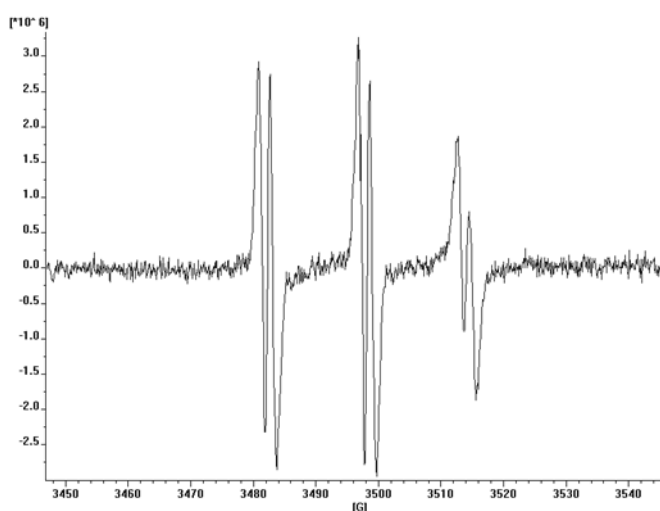
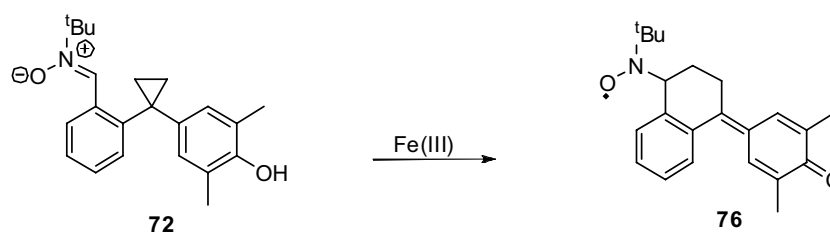


Figure 24: $g = 2.0059$, $A_N = 15.93$ G (t), $A_{H^{\beta}} = 1.85$ G (d); Reagents and conditions: 3.3 mM nitron, 0.33 mM H_2O_2 , 0.33 mM Fe(II)SO_4 , 1:2 DMF- H_2O

The hydroxyl radical adduct's EPR signal diminished over time due to decomposition revealing a more complex underlying signal of a more stable radical adduct which increased over time, Figure 25. It was thought that the by-product of the Fenton reaction, Fe(III) was acting as an oxidant reacting at the phenolic moiety producing the tricyclic nitroxyl radical adduct **76**.



Scheme 27: Reaction with Fe(III)Cl₃

As expected when the spin trap was treated with iron(III)chloride an identical spectrum was produced. The spectra was more complex due to the additional couplings to the γ and/or δ hydrogen atoms.

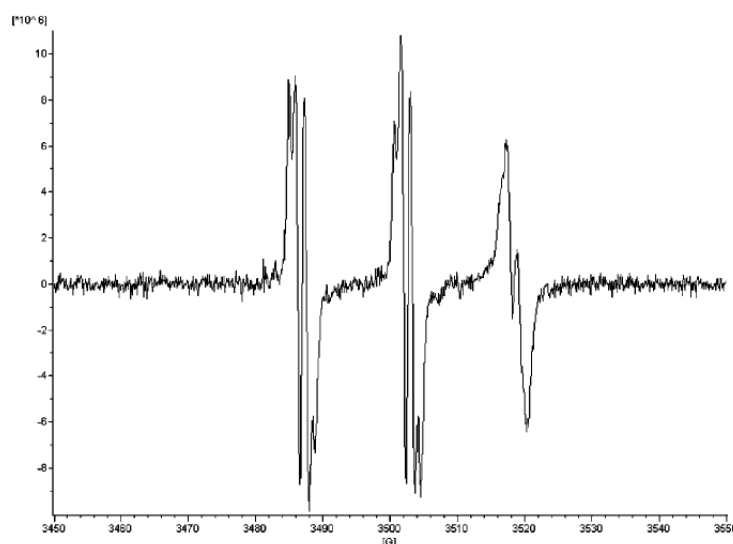
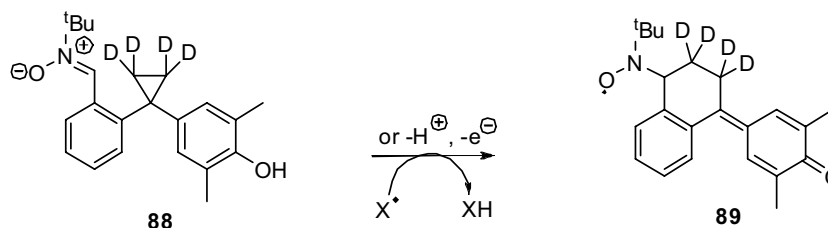


Figure 25: $g = 2.0055$, $A_N = 15.70 \text{ G (t)}$, $A_H^\beta = 1.42 \text{ G (d)}$, $A_H^{\gamma/\delta} = 1.05 \text{ and } 0.99 \text{ G (dd)}$; Reagents and conditions: 3.3 mM nitron, 0.33 mM FeCl₃, 1:2 DMF-H₂O

As before conditions had to be optimised in order to obtain a decent spectrum with sufficient signal to noise, when 2 eq of iron(III) ions were used it resulted in quenching of the nitroxyl radical adduct and EPR silence.

To confirm the assignment of the tricyclic EPR spectrum the tetra-deutero derivative **88** had to be prepared, again by another group member, Stuart Caldwell.



Scheme 28: Reaction of tetra-deutero spin trap with Fe(III)Cl

The tetra-deuterated derivative **88** was then treated with iron(III)chloride to give the tricyclic radical adduct **89**. This resulted in a simplified spectrum, Figure 26, which confirmed the *beta*-hydrogen hyperfine coupling in nitroxide **76** and aided the assignment of the γ and/or δ hydrogen couplings.

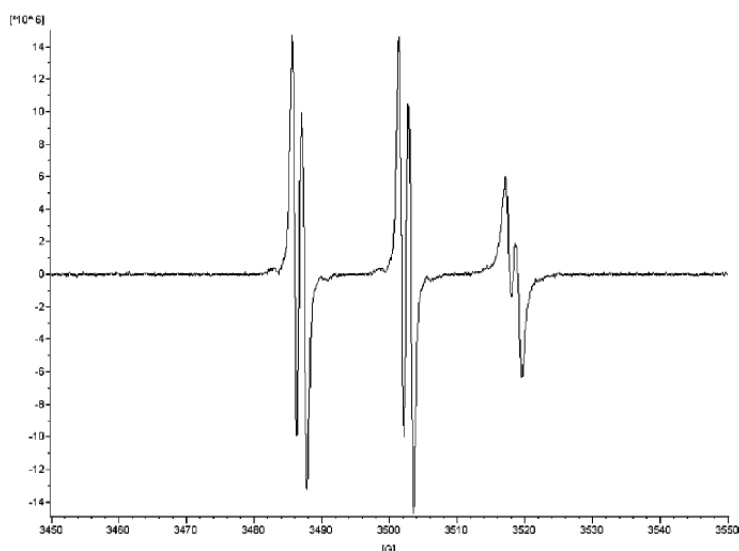


Figure 26: $g = 2.0055$, $A_N = 15.70$ G (t), $A_H^\beta = 1.42$ G (d); Reagents and conditions: 3.3 mM nitroxide, 0.33 mM Fe(III)Cl, 1:2 DMF-H₂O

The coupling of the two γ and/or δ hydrogen atoms observed are approximately 1 G, and are consistent with literature for cyclohexyl nitroxide.⁷⁶

6 Synthesis and Evaluation of a Mitochondrial Targeted Spin

6.1 Background

Another nitron spin trap designed and synthesized to investigate mitochondria and ROS was the mitochondria-targeted spin trap **90** (MitoSpin). MitoSpin **90** was specifically designed with a view to further improve upon the currently available spin traps. Although the dual sensor **72** was designed to produce EPR spectra which were more differentiating it is not targeted to mitochondria, the main source of ROS. Furthermore as an acyclic nitron spin trap it has a similar reactivity and decomposition profile to existing acyclic nitron spin traps.

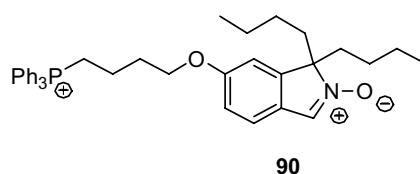


Figure 27: MitoSpin

The two most commonly used and widely available nitron spin traps are shown below, Figure 28, α -phenyl-*tert*-butylnitron (PBN) **49** and 5,5-dimethylpyrrolone-*N*-oxide (DMPO) **51**.

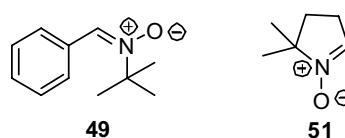
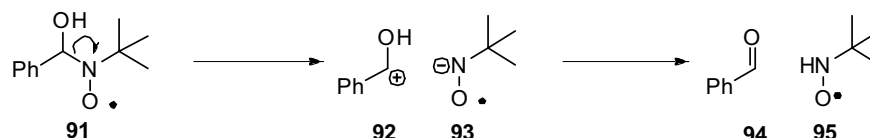


Figure 28 : Common spin traps

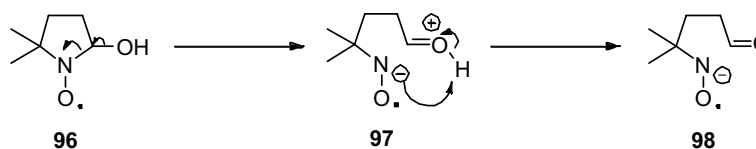
These spin traps are good, but there are a few problems associated with them. The first issue is the stability of the radical adducts formed via their reaction with ROS. The hydroxyl radical adduct of PBN **49** has a half-life <1 min and the peroxy and hydroperoxy radical adducts fragment so rapidly they are almost impossible to detect.^{77,78} DMPO has better stability than PBN with the hydroxyl adduct having a half-life of around 55 min¹⁴. There two main ways by which spin trap radical adducts decompose: ionic cleavage of the C-N bond or

disproportionation. When the hydroxyl radical adduct **91** of PBN **49** undergoes cleavage of the C-N bond it produces two distinct products **92** and **93**⁷⁹. Therefore, this reaction is entropically favoured and thought to be the main degradation pathway for PBN **49** and acyclic nitrones. The reaction occurs via a variety of similar mechanisms depending on pH. The general mechanism is shown below Scheme 29.



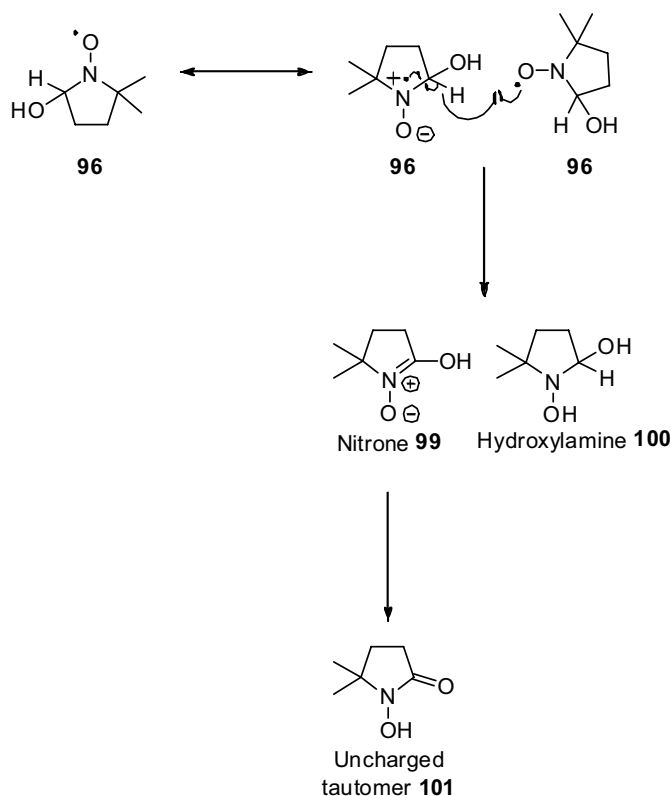
Scheme 29: Fragmentation of hydroxyl adduct via cleavage of the C-N bond for PBN

DMPO **51** is a cyclic spin trap and therefore the ring discourages C-N cleavage of its radical adducts such as the hydroxyl adduct DMPO-OH **96**, as the reaction will afford only one product **97** and is therefore not entropically favoured. It is postulated that this is one reason for the increased stability. The initially formed radical **97** would be expected to rearrange to give the nitroxyl radical **98**.



Scheme 30: Mechanism for β C-N cleavage for DMPO

Disproportionation by β H-abstraction, Scheme 31, is another method by which radical adducts decompose⁸⁰. It occurs when two radical adducts **96** react with each other one being oxidised the other reduced affording a nitronium **99** and a hydroxylamine **100**. The nitronium can rearrange to form the uncharged tautomer **101**. This process is thought to be the major route for decomposition of hydroxyl spin adducts for cyclic spin traps.



—

Scheme 31: Decomposition by β -H abstraction

Many spin traps have low reaction rate with superoxide radicals, and the spin adducts are generally short lived. The rate constant for SOD catalysed disproportionation of superoxide is $10^9 \text{ M}^{-1}\text{s}^{-1}$ whereas the rate constant for a nitron reacting with superoxide is normally $<100 \text{ M}^{-1}\text{s}^{-1}$ which, is substantially slower²⁵. Therefore, a second major issue with nitrones is that they have a low affinity for oxygen-centred radicals¹⁴. This is due to poor HOMO-SOMO interactions. Nitrones are electron poor and have a low energy highest occupied molecular orbital (HOMO) and a low energy lowest unoccupied molecular orbital (LUMO). The singly occupied molecular orbital (SOMO) of radicals can interact with either HOMO or LUMO's to form bonds, but interaction is best when the two interacting orbitals are close in energy. Electron poor oxygen-centred radicals have low energy SOMOs that will interact best with high energy HOMOs, while electron-rich carbon centred radicals have high energy SOMOs that interact best with low energy LUMOs. Therefore nitrones react faster with carbon-centred radicals than with oxygen-centred radicals. The combination of these two factors makes trapping of the superoxide radical more difficult. Thus sometimes the rate of decay is greater than the rate of reaction meaning that no adduct is

observed. There are various spin traps in the literature (e.g. **54**, **52** and **103**) that have also tried to improve upon these issues, Figure 29.

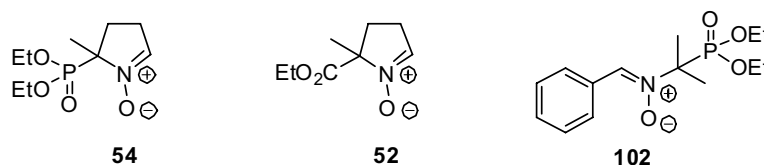


Figure 29: Spin-traps with electron withdrawing substituents.

There have been some significant improvements to spin traps regarding reactivity and half life of radical adducts since PBN **49** and DMPO **51** were first developed. Tordo *et al* first showed that addition of an electron withdrawing group at the C-5 position led to longer-lived superoxide adducts of the 5-diethoxyphosphoryl-5-methyl-1-pyrroline N-oxide **54** (DEPMPO)⁵⁰. This was further substantiated by the synthesis of and **52** (EMPO)⁴⁷ which has an ester moiety as the electron-withdrawing group at the C-5 position. They also went on to show that the principle was also true for acyclic spin traps with increased half lives were reported when the phosphoryl analogue of PBN **49**, N-benzylidene-1-diethoxyphosphoryl-1-methylethylamine N-oxide **102** (PPN)⁸¹, trapped oxygen centred radicals. Further work has showed that other electron-withdrawing groups have the same effect with trifluoromethyl⁸² and amide⁸³ substituents also increasing half life times for adducts compared to DMPO and PBN.

Following on from some of these findings MitoSPIN was designed to try and overcome these problems associated with spin traps, Figure 30.

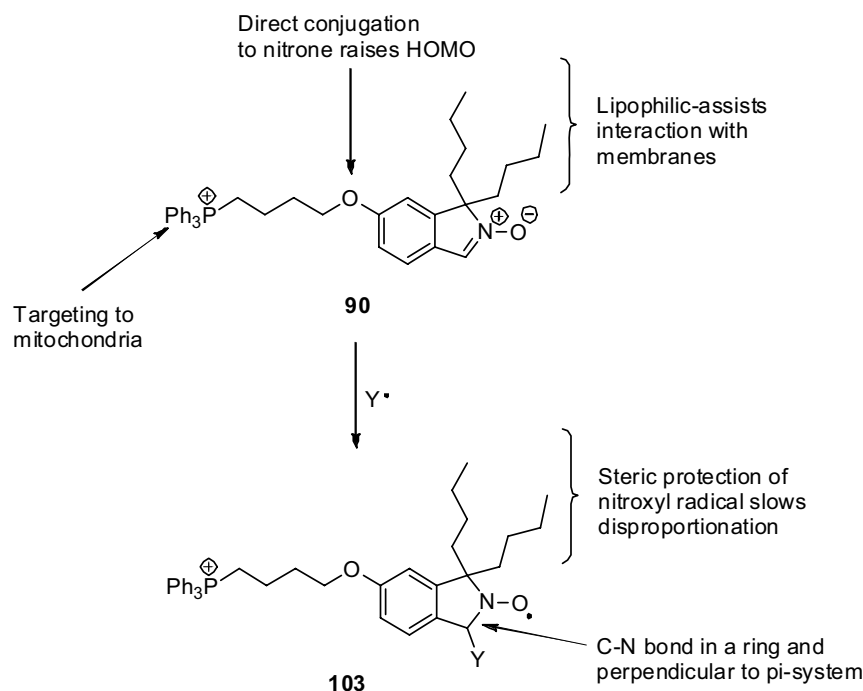


Figure 30: MitoSpin - special features

The *para*-alkoxy group increases the electron density of the nitroxide, due to the conjugation of a lone pair on the oxygen atom of the methoxy group with the aromatic system. This raises the HOMO of the nitroxide allowing for better HOMO-SOMO interactions increasing the nitroxide's affinity for oxygen-centred radicals. The butyl groups should then sterically hinder the nitroxyl radical adduct **103**, formed after reaction with a radical (Y^\bullet), elongating the half-life of the adduct by hindering the disproportionation reaction, Scheme 31.

Furthermore, the spin trap is cyclic which should hinder the fragmentation of radical adducts via ionic cleavage of the carbon-nitrogen bond. This is further reinforced by the aromatic ring as the C-N bond is perpendicular to the pi-system (Figure 31), this means that electron donation from the pi-system cannot assist ionic cleavage and the fused bicyclic nature of the nitroxide means that cleavage of the C-N bond does not give rise to as many rotatable bonds as a similar fragmentation of DMPO.

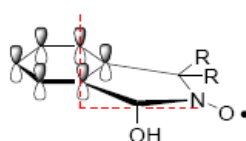


Figure 31

A fourth design feature is the lipophilic triphenylphosphonium cation, which targets the spin-trap to the mitochondria. Targeting of small molecules via the TPP cation is well presided.⁸³ This technique, of using a conjugated TPP cation has been used by Murphy and Smith to target a variety antioxidants to the mitochondria⁸⁴, Figure 32.

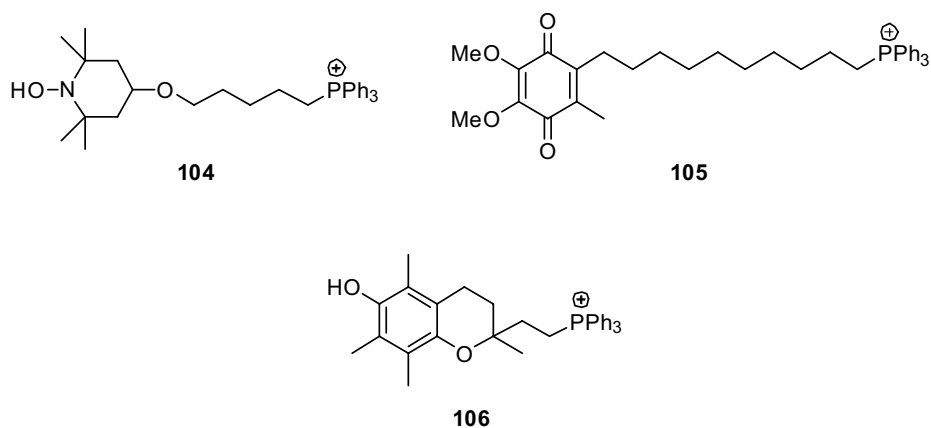


Figure 32: Mitochondrial targeted antioxidants

His group has successfully targeted a variety of antioxidants to the mitochondria and showed their uptake and their ability to react with ROS. They have prepared mitochondria-targeted TEMPO⁸⁵ **104**, ubiquinol⁸⁶ **105**, vitamin E⁸⁷ **106**, and a peroxidase⁸³ and superoxide dismutase⁸³ and have used these to further understand the production of radicals inside the mitochondria. The TPP accumulates in the mitochondria by electrophoresis, Figure 33.

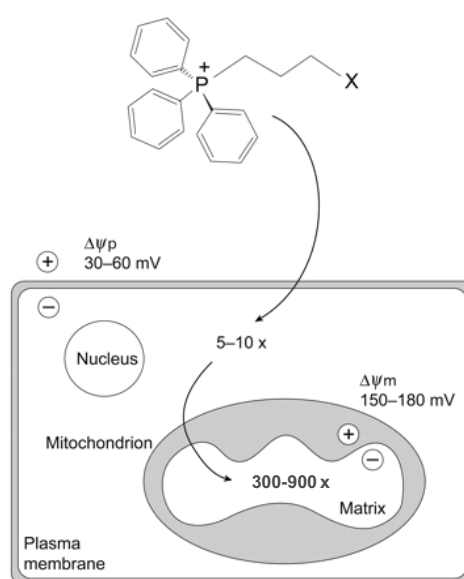


Figure 33: Targeting to the Mitochondrion⁸⁸

As discussed in the introduction, due to the proton motive force, mitochondria have a large membrane potential of approximately -180 mV (negative on the inside) across the membrane between the inner membrane space and the matrix. This means the cation would accumulate almost 1000 fold within the matrix. There is also membrane potential of -30 mV (negative on the inside) across the plasma membrane, which already draws cations from the intracellular space across the plasma membrane into the cytosol. The degree of accumulation can be calculated using the Nernst equation, Figure 34, which shows the relationship between membrane potential and cation ratio.

$$\Delta\Psi = 61.5 \log_{10} \left(\frac{\text{Cation}_{\text{in}}}{\text{Cation}_{\text{out}}} \right)$$

Figure 34: Nernst Equation

Furthermore the cation is shielded by the lipophilic phenyl groups. This prevents repulsion of the charge by the membranes and results in activation energy for movement through membranes to be lower than other cations.

In fact spin traps, which also incorporate the mitochondrial targeting TPP moiety, have already been reported in the literature, Figure 35. So far there have been DEPMPO **107**⁶⁰ and PBN **108**⁶⁰ derivatives as well as mitoBMPO **109**⁶⁰.

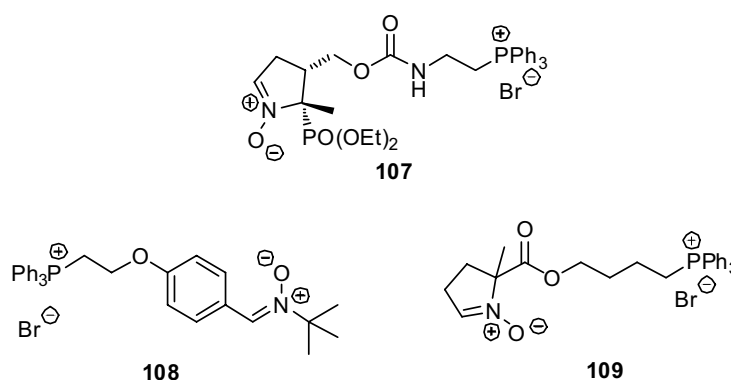


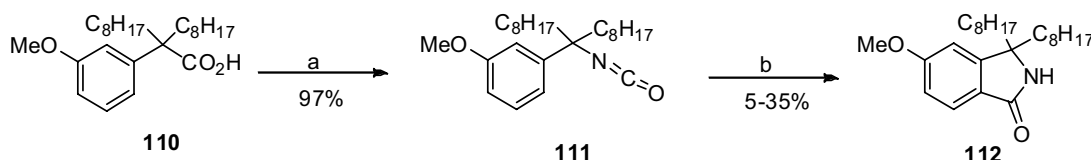
Figure 35: Mitochondria targeted spin traps

6.2 Synthesis

Synthesis of the bicyclic core of MitoSpin, via formation of an isoindolone proved to be synthetically challenging. There had been a number attempts within the

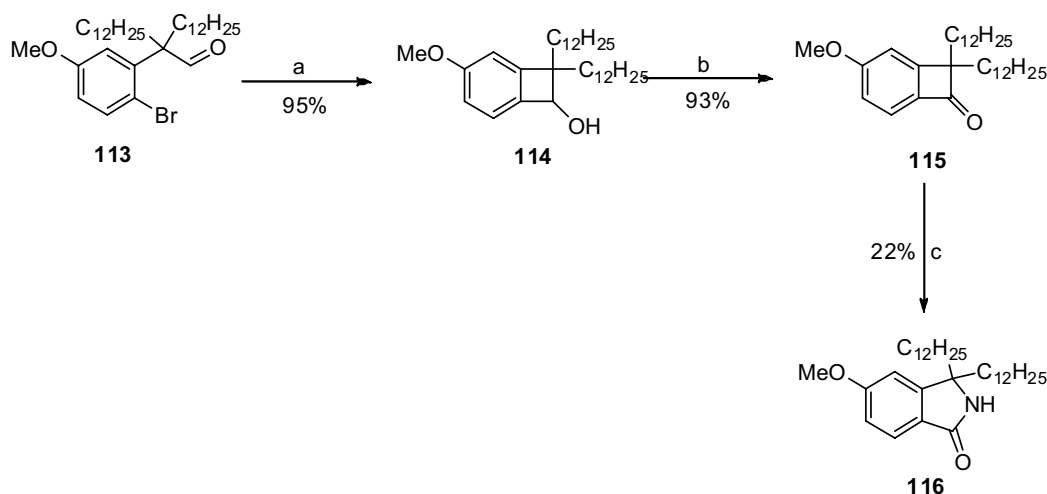
Hartley group to form the isodolone with longer alkyl chains before I took up the project.

The first approach, carried out by Alison Hay, followed a route for the formation of an isoindoline reported by Fevig⁸⁹, Scheme 32. Acid **109** is converted into the isocyanate **110** and cyclised with Lewis acid.



Scheme 32: Reagents and conditions: a) 1 eq. DPPA, 1 eq. NEt₃, Tol; b) 2.1 eq. FeCl₃, DCE

The isoindoline **112** is afforded via an isocyanate intermediate **111** followed by reaction with the Lewis acids FeCl₃. Although the desired isoindolone **112** was isolated the yield was very low, max 35%, therefore another route was attempted. The second synthetic route attempted by Alison Hay was via a cyclobutanone intermediate, Scheme 33.

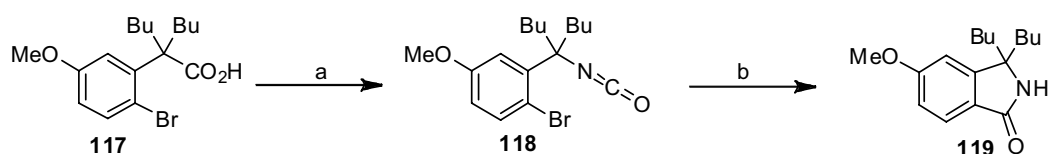


Scheme 33: Reagents and conditions: a) 1 eq. ^tBuLi, THF, -78°C; b) cat. TPAP, NMO; c) NH₂OSO₃H, AcOH

Isoindolone **116** was formed by reacting the aryl bromide **113** with BuLi to give an aryllithium which underwent a 4-*exo-trig* cyclisation to afford the cyclobutanone **115**. This was subsequently oxidised to the cyclobutanone **115**. The

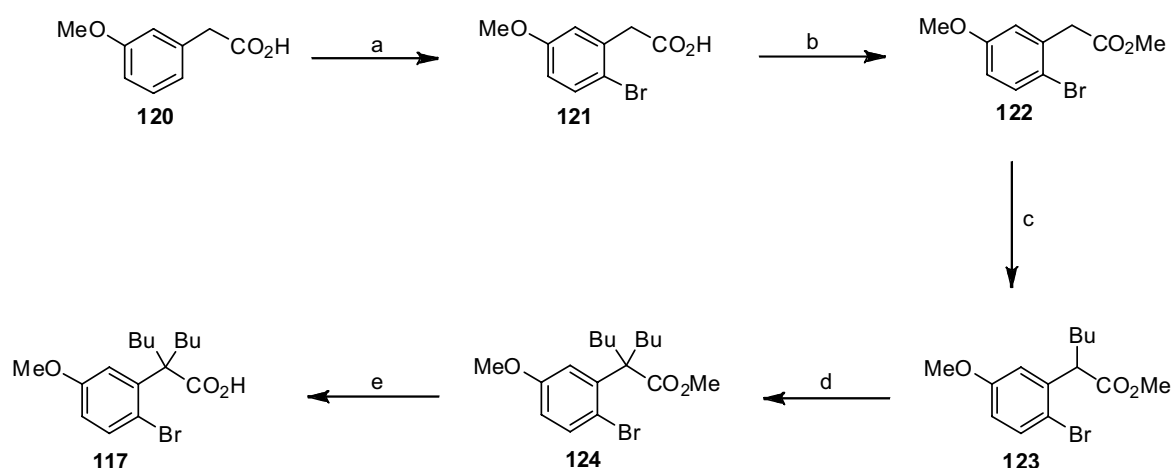
4-membered ring was then expanded utilising the Beckman rearrangement to afford the isoindolone **116**. However, the ring expansion proceeded in low yield.

It was then thought that ring could be introduced via a Parham type cyclisation with lithium halogen exchange followed by attack at the isocyanate, Scheme 34. The Parham cyclisation hinges upon aromatic lithiation followed by subsequent reaction with an internal electrophile⁹⁰. In this case the electrophile is the isocyanate moiety. This would be the first example of a cyclisation via the isocyanate being used to access an isoindolone.



Scheme 34: Reagents and conditions: a) 1 eq. DPPA, 1 eq. NEt₃, Tol; b) 1 eq. ^tBuLi, THF, -78°C

The synthesis begins with the formation of the dialkylated acid **117**, Scheme 35. The synthesis of spin trap begins with (3-Methoxyphenyl)acetic acid, **120**. The first two steps involve bromination to give the carboxylic acid **121** followed by esterification using acid as a catalyst to yield ester **122**. These two steps are interchangeable and produce similar yields when the order is reversed. The ester was then doubly alkylated to afford ester **124** over two steps. The butylations were accomplished using freshly prepared lithium diisopropylamide to form the enolate intermediate before alkylating with iodobutane.



Scheme 35: Reagents and conditions: a) 1 eq. Br₂, CHCl₃; 100% b) MeOH, cat. H₂SO₄; 98% c) i) 1.5 eq. LDA, THF, -78°C; ii) 1.5 eq. ⁿBuI, THF, -78°C; 91% d) i) 1.5 eq. LDA, THF, -78°C; ii) 1.5 eq. ⁿBuI, THF, -78°C; 93% e) KOH, DMSO, 100°C 84%

The saponification of the doubly alkylated ester **124** to the carboxylic acid **117** proved to be problematic with standard procedures for hydrolysis simply giving the starting material; LiOH, KOH, KOOH and ^tBuOOH were tried in MeOH, THF and Et₂O at room temperature and at reflux with no avail.

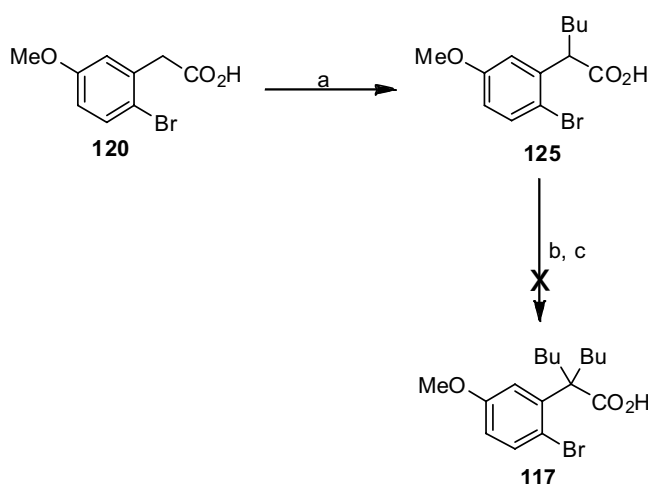
It was thought that the reaction was not occurring due to the steric bulk of the bulk alkyl groups preventing nucleophilic attack on the carbonyl group. As a result conversion from the ester to the carboxylic acid was attempted via a S_N2 type dealkylation using lithium iodide, Figure 36.

Entry	Reaction Conditions	Time	Yield
1	Lil, Py 125 °C	72 h	33 %
2	Lil, DMF, 125 °C	12 h	25 %
3	Lil, Py, mw, 125°C, 100 psi	30 min [*]	65% SM: 35% product**
4	Lil, Py, mw, 90°C, 100 psi	30 min [*]	0%
5	Lil, Py, mw, 120°C, 0 psi	120 min	60%
6	Lil, Py, mw, 125°C, 0 psi	60 min	70%

Figure 36: S_N2 type Dealkylation (* under pressure, ** yield calculated from NMR)

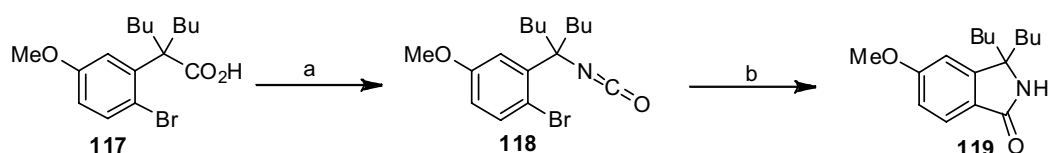
The reaction was initially carried out at 125 °C (entries 1 and 2) with the best yield being observed when the reaction was carried out in pyridine and heated to reflux for 3 d, which is not ideal. Therefore, the reaction was then carried out in a microwave to try and reduce reaction times (entries 3-6). Primarily the microwave reactions were attempted under pressure however at elevated temperature the pressure became too high which cut the power. At lower temperatures no reaction was observed. Therefore reactions in the microwave were then carried out higher at atmospheric pressure with the optimum yield of 70% occurring after 60 min at 125°C. However, when the reaction was carried out on a larger scale, 1 g instead of the 0.1 g, the reaction was very unpredictable and either gave yields of 70-80% or produced a black tar with no product of start material recovered. As the reaction was unpredictable other routes to the carboxylic acid were explored. The first route was to form the acid without esterification, Scheme 36. The dienolate was prepared from carboxylic

acid **120** and reacted with butyl iodide to give the monoalkylated product **126**, but a similar procedure failed to then give the dialkylated product **117**.



Scheme 36 : Reagents and conditions: a) i) 2 eq. LDA, THF, -78°C ; ii) 2 eq. $^n\text{BuLi}$, THF, -78°C ; 98%
 b) i) 2 eq. LDA, THF, -78°C ; ii) 2 eq. $^n\text{BuLi}$, THF, -78°C c) i) 2.5 eq. LDA, THF, -78°C ; ii) 2.5 eq. $^n\text{BuLi}$, THF, -78°C

Since, this route was not successful the hydrolysis was retried at a higher temperature. The reaction was carried out with KOH in DMSO at 100°C which afforded the carboxylic acid with a 70% yield which could be reproduced on larger scale.

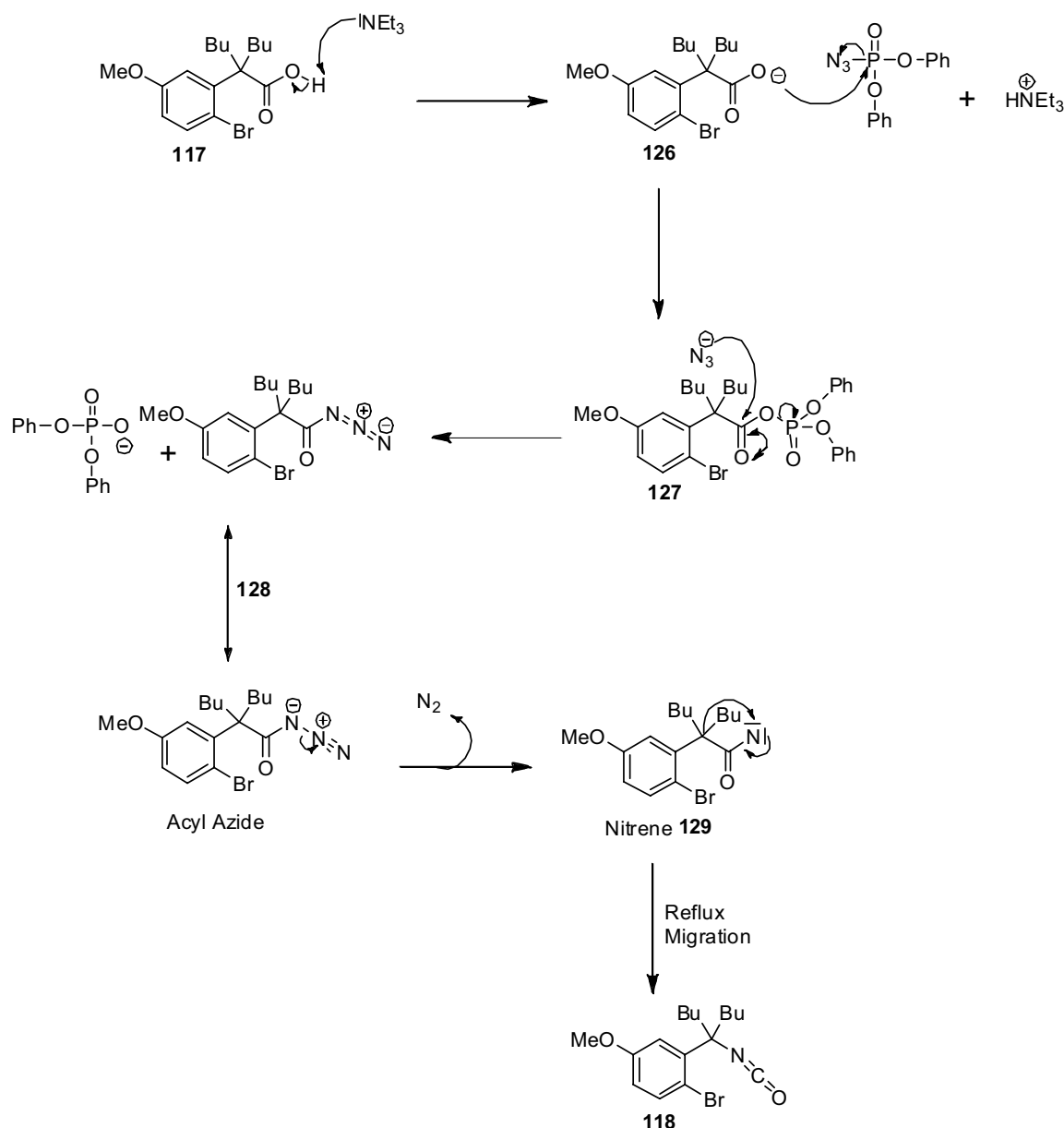


Scheme 37: Reagents and conditions: a) i) 1 eq. NEt_3 , 1 eq. DPPA, Tol. 0°C , ii) Reflux; 97% b) 2 eq. $^t\text{BuLi}$, THF, -78°C to RT, 93%

Once there was a successful and reproducible route to the dialkylated carboxylic acid **117** it was converted to the isocyanate **118** via the Curtius rearrangement with diphenylphosphoryl azide (DPPA). The isocyanate was then treated with $^t\text{BuLi}$ which resulted in lithium-halogen exchange followed by attack at the carbon atom of the isocyanate leading to cyclisation affording the isoindolone **119**.

The Curtius rearrangement involves a two stage reaction, the formation of an acyl azide **128** at 0°C followed by conversion to the isocyanate **118** with loss of

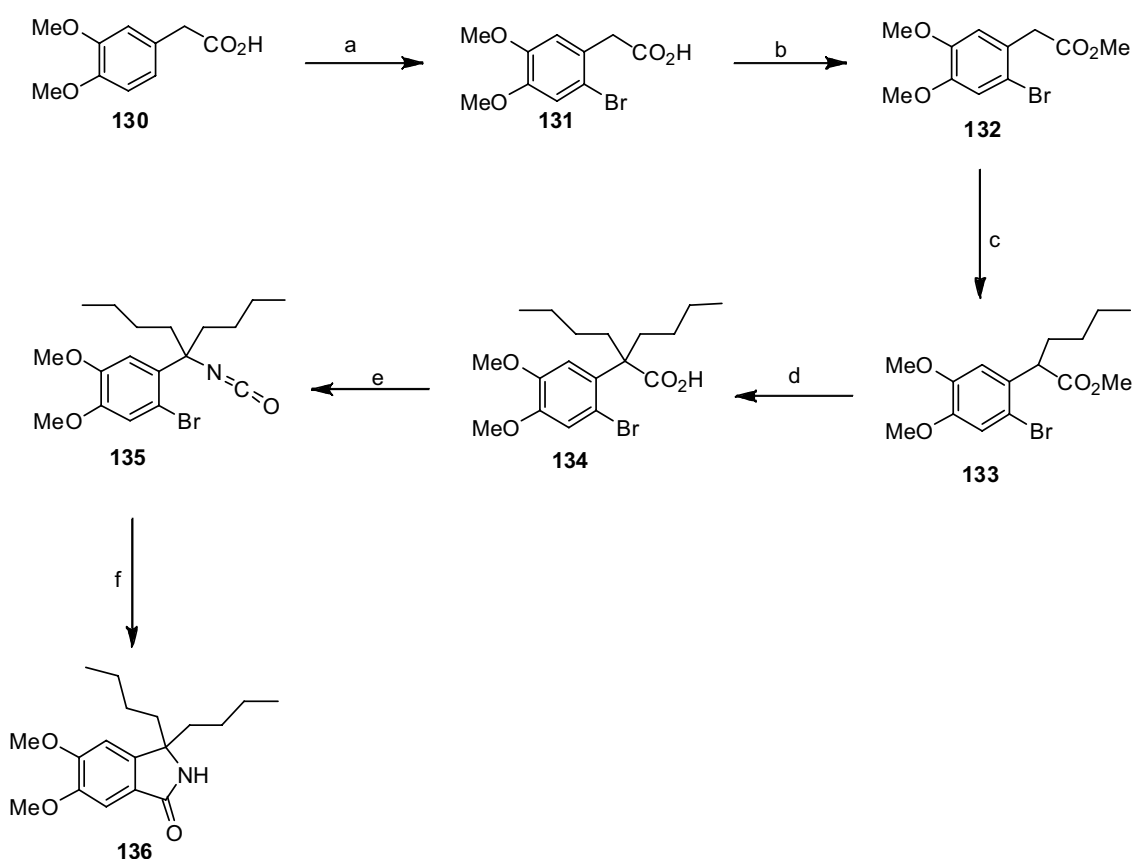
nitrogen at reflux. The mechanism is outlined in Scheme 38. Nucleophilic attack of DPPA by the carboxylate **126**, formed from the deprotonation of carboxylic acid **117**, affords the activated carboxylic acid derivative **127** with the release of an azide anion. The azide anion then displaces the phosphoryl leaving group to give the acyl azide **128**. Heating to reflux then causes the loss of nitrogen gas to form the nitrene **129** which rearranges to give the desired isocyanate **118**.



Scheme 38: Mechanism of the Curtius rearrangement

As the reaction occurred on the first attempt we wanted to see if the cyclisation would occur on a similar substrate. Therefore the dimethoxy analogue was synthesized as shown in Scheme 39.

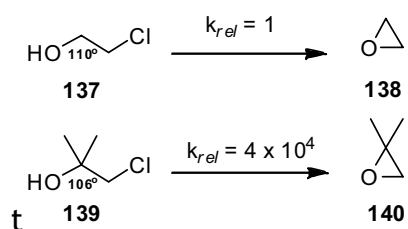
The synthesis of the dimethoxy derivate **136** was carried as for MitoSpin. The synthesis began with bromination of acid **130** followed by esterification to give aryl bromide **131** in excellent yield over two steps. The ester was then doubly alkylated using the standard alkylating conditions with moderate yields to afford ester **133**. The ester contained an unknown impurity with a ratio of 2:1 desired product: undesired side product. The mixture was inseparable by column chromatography or using kugle r hr distillation and therefore was carried on to the next stage without purification. The impure material was hydrolysed using KOH to give carboxylic acid **134** which was then converted into the isocyanate **135** via the Curtius rearrangement using DPPA. The isocyanate **135** was treated with BuLi in order to carry out the cyclisation which afforded the amide **136** in a moderate yield.



Scheme 39 : Reagents and Conditions: a) 1 eq. Br₂, CHCl₃; 98% b) MeOH, cat. H₂SO₄; 97% c) 1.5 eq. LDA, 1.5 eq. BuI, THF, -78°C to RT; 93% d) i) 1.5 eq. LDA, 1.5 eq. BuI, THF, -78°C to RT; ii) KOH, DMSO, Reflux; 22% e) 1.1 eq. DPPA, 1.1 eq. NEt₃, toluene, 0 °C to reflux, 58% f) tBuLi, THF, -78°C to RT, 58%

It was thought that the cyclisation was mainly occurring due to the Thorpe-Ingold effect. The Thorpe-Ingold effect is a phenomenon that was first reported

in 1915⁹¹ when it was observed that when geminal substituents were present ring forming reactions occurred at much faster rates.



Scheme 40: Formation of epoxides

In the formation of small rings, such as epoxides Scheme 40, it is thought this mainly occurs due to the lower C-C-C bond angle bringing the two ends of the ring closer together. Inclusion of geminal methyl groups lowers the angle by approximately 4°. The lowered size is closer to that of the final ring structure, 60°.

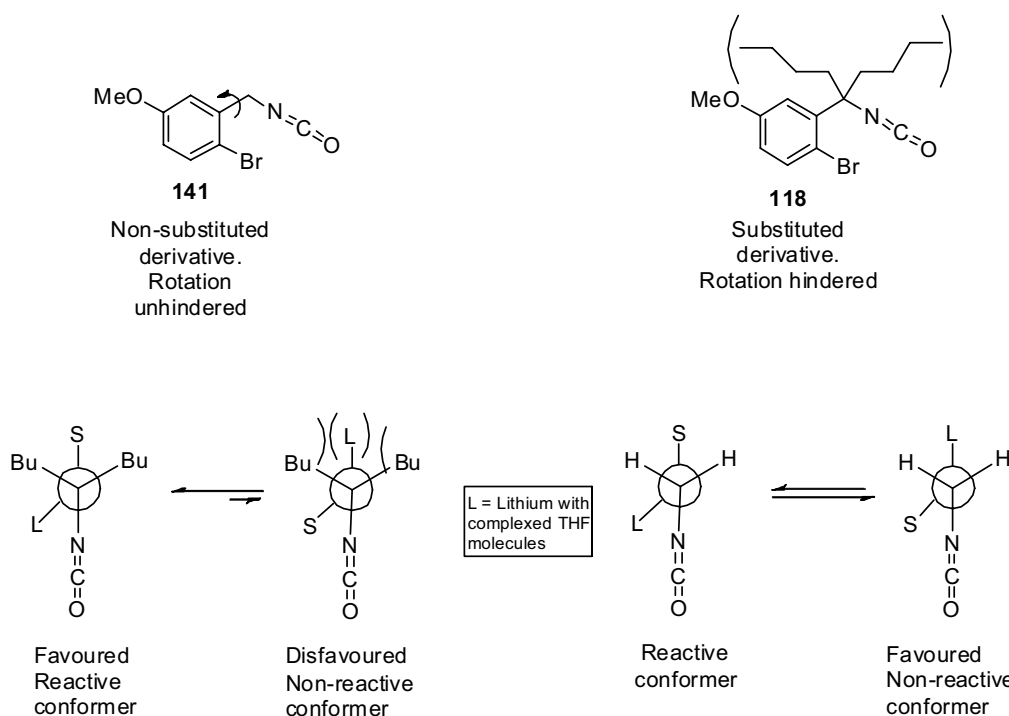
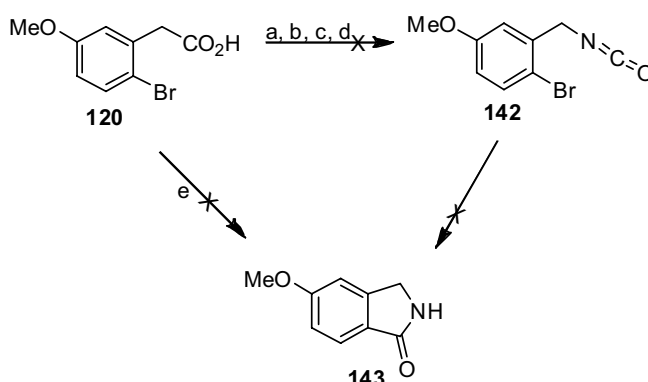


Figure 37

However for larger rings it is thought to occur due to restricted rotation due to increasing steric hindrance on inclusion of geminal alkyl groups, Figure 37. In non-substituted starting materials there are many conformations that can be formed as there is high flexibility. On formation of a ring this flexibility is lost and therefore there is a large drop in entropy between the lowest energy conformer and the transition state which results in an unfavourable ΔG^\ddagger . When

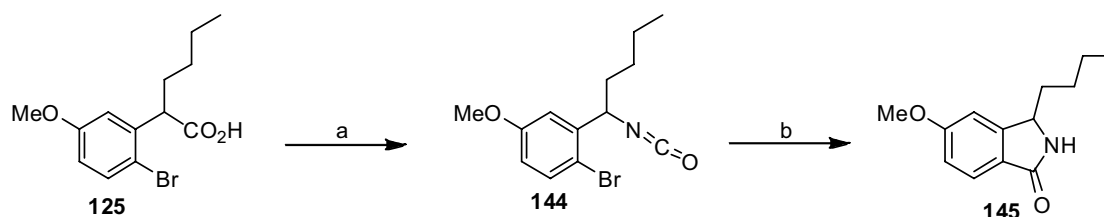
the starting material contains geminal substituents the entropy is already low as the groups limit the number of possible conformers and in some cases the lowest energy conformer is much closer in energy to the transition state meaning due to a less negative ΔS^\ddagger resulting in a lower ΔG^\ddagger so reaction is much faster.

In order to substantiate whether this was indeed the case attempts were made to synthesize then cyclise the non-alkylated and mon-alkylated isocyanates, Schemes 41 and 42. Synthesis of the non-alkylated derivative **142** proved to be very difficult with the high temperature required for the migration from the carbon atom to the nitrogen atom during the Curtius rearrangement, Scheme 38, causing the decomposition of the isocyanate **142**. After a number of attempts to synthesize the isocyanate **142** and even attempting the cyclisation in situ without isolation and therefore attempts to make the non-alkylated derivative **143** were abandoned.



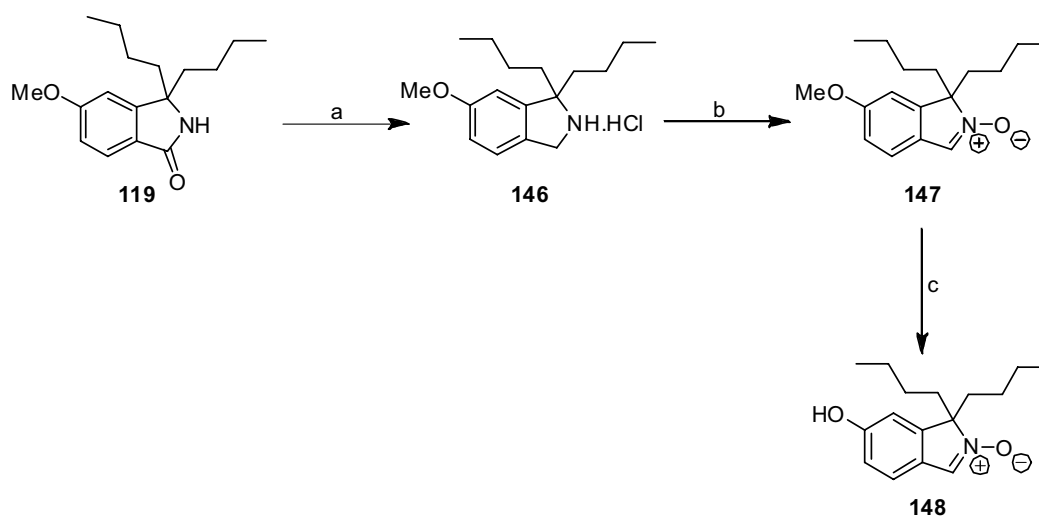
Scheme 41: Reagents and conditions a) 1.1 eq. DPPA, 1.1 eq. NEt₃, toluene, 0 °C to reflux; b) 1.1 eq. DPPA, 1.1 eq. NEt₃, toluene, 0 °C to 60 °C; c) 1.1 eq. DPPA, 1.1 eq. NEt₃, DCM, 0 °C to 40 °C; d) 1.1 eq. DPPA, 1.1 eq. NEt₃, THF, 0 °C to reflux; e) i) 1.1 eq. DPPA, 1.1 eq. NEt₃, THF, 0 °C to reflux; ii) ^tBuLi, THF, -78 °C to RT

The synthesis of the monoalkylated isocyanate **144** was much more straight forward with the Curtius rearrangement affording the isocyanate **144** with a moderate yield. The cyclization was then carried out as for the dialkylated derivative affording the isoindoline in a poor yield after notably more rigorous purification. The yield of the monoalkylated version is significantly lower than that of the dialkylated analogues which indicated that the Thorpe-Ingold effect may in fact be encouraging the formation of the isoindole. Although without testing of the non-alkylated version a firm conclusion cannot be reached.



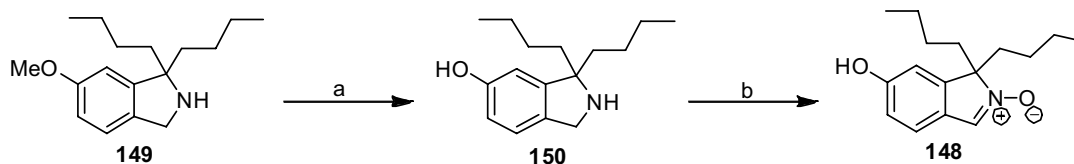
Scheme 42: Reagents and Conditions a) 1.1 eq. DPPA, 1.1 eq. NEt_3 , toluene, 0°C to reflux, 43% b) tBuLi , THF, -78°C to RT, 22%

Having formed the isoindoline **119**, it was then reduced to the amine **146** using borohydride. THF complex. The amine was then converted into a non-targeted version of the spin trap **147** to allow preliminary investigations of the EPR reactions. The non-targeted nitron was then treated with HBr to give the phenol **148**.



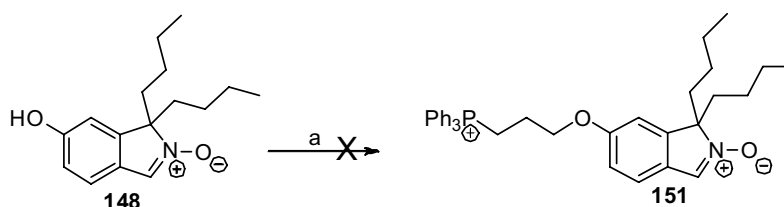
Scheme 43: Reagents and conditions: a) i) 2.5 eq. $\text{BH}_3 \cdot \text{THF}$, THF, 0°C ii) Reflux 99% iii) Ethereal HCl b) i) 1 eq. NaHCO_3 ii) 3 eq. H_2O_2 (aq), 0.1 eq. Na_2WO_4 , MeOH 34% c) 78% HBr, Reflux 55%

In later syntheses of the phenol **148**, the reaction was carried out by converting the amine **149** into the phenol **150** with BBr_3 , then oxidation to afford the nitron which proceeded with a higher yield, Scheme 44.



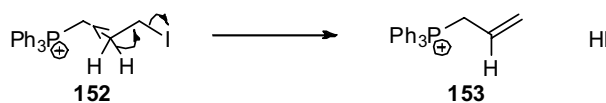
Scheme 44: Reagents and conditions: a) 3.5 eq. BBr_3 , DCM; 93% b) 3 eq. H_2O_2 (aq), 0.1 eq. Na_2WO_4 , MeOH, 61%

Having formed the phenol there was only one synthetic step left, conjugation of the phosphonium salt to add the mitochondrial targeting moiety. Originally, attempts were made to attach a 3-carbon chain using (3-iodopropyl) triphenylphosphonium iodide **152** which was synthesised from diiodopropane⁹². Alkylation was attempted using a variety of solvents and bases. However, the reaction would not occur with no product being observed and starting material being recovered.



Scheme 45: Reagents and conditions: 1.1 eq. (3-iodopropyl)triphenylphosphonium iodide, 1 eq. Cs_2CO_3 , MeOH

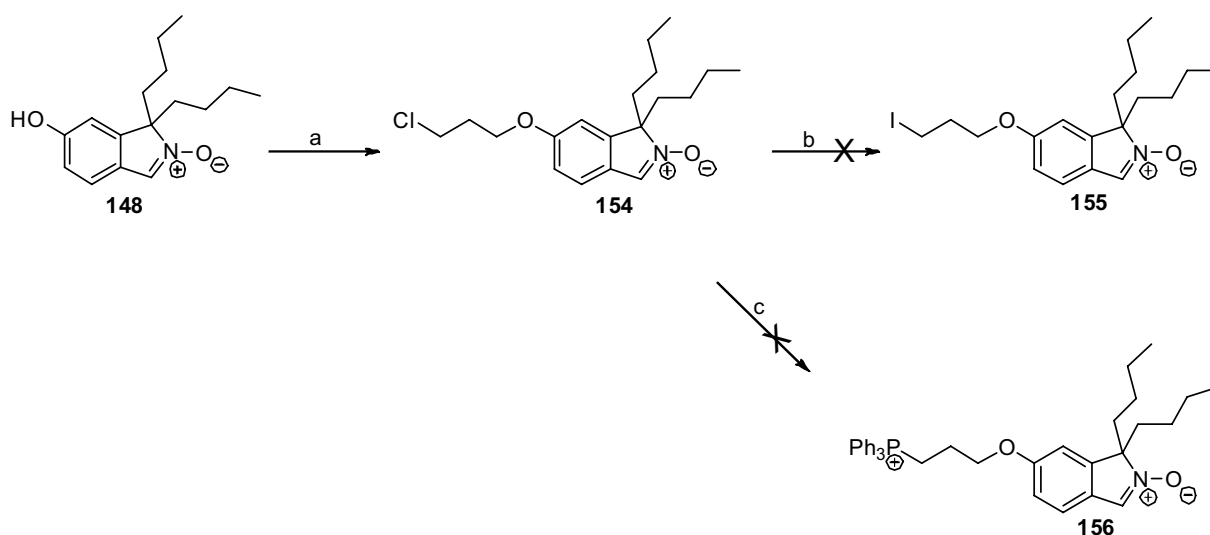
Inspection of NMR spectra from attempts to attach the 3 carbon chain showed the presence of an alkene **153**. The alkene **153** was formed by elimination of the iodide, Scheme 46. The electron withdrawing phosphonium salt would encourage the elimination as it makes the protons β to it more acidic, Scheme 46. This was further substantiated by the literature as all examples contained chains longer than three carbons. In most cases the four carbon chain was used, with the extra carbon distance lowering the amount of elimination.



Scheme 46: Phosphonium induced elimination of iodide

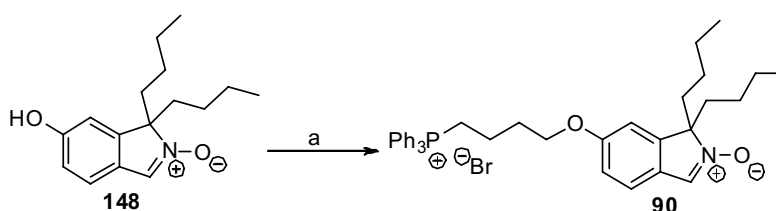
Therefore another route was attempted, Scheme 45. A dihalide was reacted with the phenoxide to afford the chloride **154**. Attempts to convert the chloride **154**

to the phosphonium salt **156** did not succeed. Therefore the Finkelstein reaction was carried out to try and convert the chloride into the iodide **155** in the hope that the phosphonium salt could be reached more successfully due to the iodide being a better leaving group. However, the reaction afforded a complex mixture, and this route was abandoned.



Scheme 47: Reagents and conditions: a) 1.1 eq. 1-bromo-3-chloropropane, 1 eq. Cs_2CO_3 , MeOH; 14% b) 1 eq. NaI, Acetone, Reflux; c) 1.5 eq. PPh_3 , PhMe, Reflux

Next alkylation was attempted using the 4 carbon derivative **90** which afforded the desired mitochondrial spin trap. Reaction was carried out with both the commercially available (4-bromobutyl)triphenylphosphonium bromide and the iodo analogue in an attempt to improve the yield, however the yield was lower with the iodo derivative and some eliminated product was observed.



Scheme 48: Reagents and conditions: a) 1.5 eq. (4-bromobutyl)triphenylphosphonium bromide, 1.1 eq. Cs_2CO_3 , MeOH, Reflux, 24%

6.3 Uptake in Mitochondria

Having synthesised the desired target its uptake into mitochondria was then tested using an ion-selective electrode in collaboration with Prof. Murphy and his group in MRC Dunn labs in Cambridge. The ion-selective electrode is used to measure the concentration of triphenylphosphonium cations (TPP) in a solution. The graph is shown below, Figure 38.

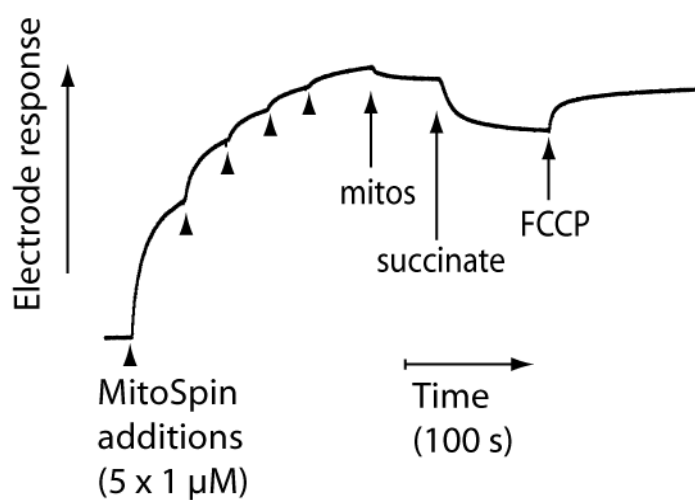


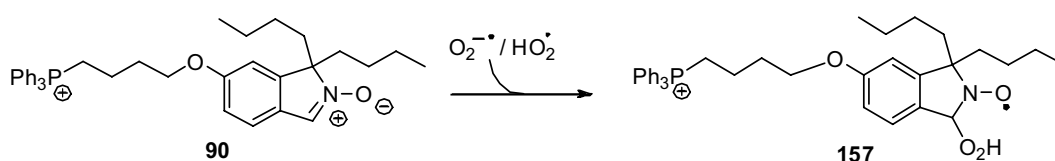
Figure 38: Uptake of MitoSpin by energized mitochondria. An electrode sensitive to the TPP moiety of MitoSpin was inserted into 3 mL KCl buffer supplemented with 4 mg/mL rotenone with stirring at 37°C and five consecutive additions of MitoSpin increasing the concentration by 1 mM each time were used to calibrate the response of the ion-selective electrode (arrowheads). The addition of rat liver mitochondria (mitos; 1 mg protein/mL), succinate (10 mM), and FCCP (1 mM) are indicated.

The graph shows the incremental increase of MitoSpin concentration to a plateau, this is followed by the introduction of homogenised rat liver mitochondria which have been treated with rotenone which inhibits complex I of the electron transport chain and this means that the mitochondria at introduction do not have a membrane potential therefore MitoSPIN stays in the bulk solution. There is a small decrease in the concentration of MitoSPIN due to the lipophilicity of the molecule causing non-selective binding to the mitochondrial membrane. After the introduction of mitochondria, succinate, a substrate for complex II of the electron transport chain, was added. The presence of succinate initiates the electron transport chain and produces a membrane potential. The increased membrane potential results in the influx of

MitoSpin into the mitochondria and out of solution resulting in a decrease in the concentration of MitoSpin in the bulk solution and a dip in the graph. Carbonylcyanide p-(trifluoromethoxy)phenylhydrazone (FCCP) a known mitochondrial uncoupler was then added to the solution this caused the mitochondrial membrane potential to decrease and efflux of MitoSPIN out of the mitochondria and into the solution. Therefore MitoSPIN is taken up into mitochondria when the membrane potential is high. Having tested MitoSPINs uptake into mitochondria its properties as a spin trap were tested.

6.4 Spin trapping of superoxide radicals

The spin trap was subjected to superoxide to try to form the superoxide radical adduct on reaction with superoxide with little success. Various methods and reagents were used and results are as outlined below.



Scheme 49: Reagents and conditions: xanthine oxidase grade III, acetaldehyde, H_2O/DMF

Initial attempts to react with superoxide were carried out using potassium superoxide and 18-crown-6, however no signal was observed. The high concentration of superoxide means there would be a higher rate of dismutation and probably meant the superoxide was been quenched before it could react with the nitroxide. The superoxide radical was then produced using the enzyme xanthine oxidase. Xanthine oxidase is known to be a source of superoxide *in vivo*; it produces superoxide as a side product from the catalytic conversion of xanthine to uric acid as discussed in Chapter 1 p 7. Originally xanthine was used as the substrate but due to poor solubility the reaction afford no superoxide radical adduct therefore acetaldehyde was used as the substrate. Production of superoxide was confirmed from the observation of cytochrome C reduction.

Conc MitoSpin	Enzyme	Substrate	Solvent	Reduction Cyt C
10mM	Xanthine Oxidase Grade I	Xanthine	1:2 DMF:PBS	NO
10mM	Xanthine Oxidase Grade I	Xanthine	1:2 DMF:H ₂ O	NO
10mM	Xanthine Oxidase Grade I	Xanthine	1:9 DMF:H ₂ O	NO
10mM	Xanthine Oxidase Grade III	Xanthine	1:3 DMF: H ₂ O	YES
10mM	Xanthine Oxidase Grade III	Acetaldehyde	1:3 DMF: H ₂ O	YES
20mM	Xanthine Oxidase Grade III	Acetaldehyde	1:3 DMF: H ₂ O	YES

Figure 39: Enzymatic conditions attempted

However, despite many alterations to the reaction conditions, Figure 39, only a very weak adduct signal is observed Figure 40, which cannot be unambiguously assigned to be the superoxide adduct. It is thought that this is due to a combination of poor reactivity towards superoxide and low stability of radical adduct. Though disappointing, this is not surprising considering the reactivity of most cyclic spin traps. Indeed a similar spin trap TMINO showed no signal for superoxide⁹³.

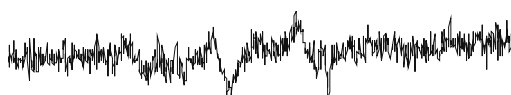
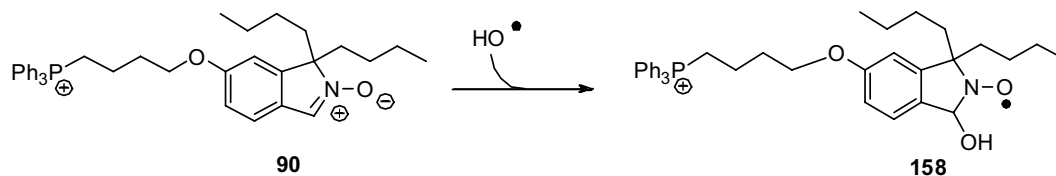


Figure 40: EPR spectrum of superoxide adduct

6.5 Spin trapping of hydroxyl radicals

As discussed in the introduction hydroxyl radicals should react well with the nitrene **90** to afford the hydroxyl adduct **158**. Hydroxyl radicals are most commonly produced *in vitro* by the Fenton reaction using iron(II) ions and hydrogen peroxide as described in chapter 6 p 39. A second method to produce hydroxyl radicals is by the hydrolysis of hydrogen peroxide using UV light. Both methods were used.



Scheme 50: Proposed reaction of MitoSpin with hydroxyl radicals

Reaction of MitoSpin **90** in the presence high concentrations of hydrogen peroxide, > 0.33 mM, or Fe(II) result in the spectrum shown in Figure 41.

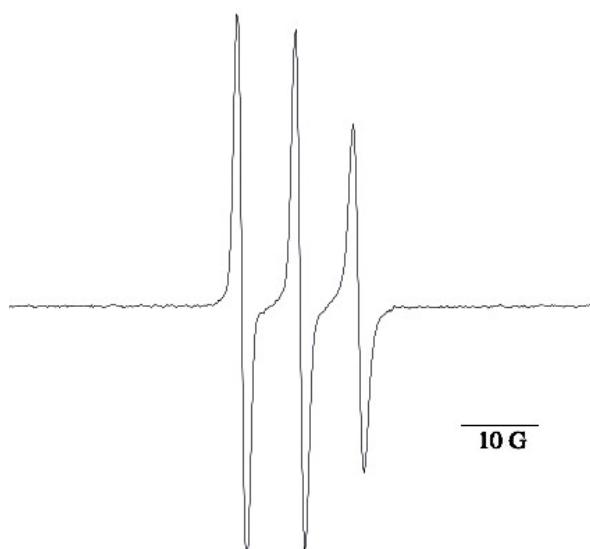


Figure 41: $g = 2.00108$, $A_N = 7.60$ G; Reagents and conditions: 3.3 mM nitron, 0.33 mM H_2O_2 , 0.33 mM $Fe(II)SO_4$, 1:2 DMSO- H_2O or 3.3 mM nitron, 0.33 mM H_2O_2 , 1:2 DMSO- H_2O , UV

The spectra is inconsistent with those normally attributed to hydroxyl adducts as the nitrogen hyperfine splitting is 7 G rather than 14 G and there is no hyperfine coupling to a β -hydrogen. The same spectrum was formed with lower concentrations of H_2O_2 and when UV was used to produce the hydroxyl radical. It was also observed when trying to form the carbon-centred radical adducts using Fe(II) and H_2O_2 . The signal was persistent lasting over 72 h in solution. However it was rapidly reduced with the known antioxidants, glutathione and ascorbic acid. Therefore further analysis was carried out.

6.6 Analysis by HPLC and ESI-MS

Subsequent investigation of the reaction via HPLC showed the presence of a new peak, which was isolated and analysis by mass spectrometry gave a mass of MitoSpin +16 amu, suggesting the addition of an oxygen atom, Figure 42. The compound is proposed to be hydroxamic acid **159** formed by the oxidation of the hydroxyl adduct **158**.

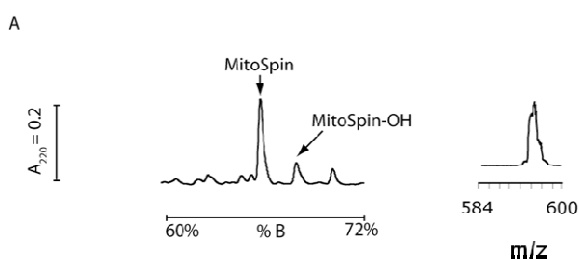
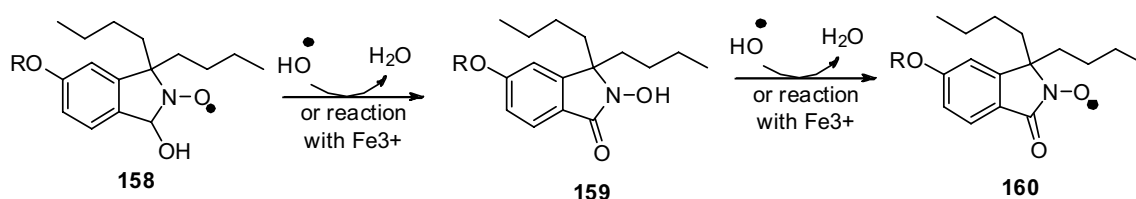


Figure 42: Reagents and conditions: Reagents and conditions: 3.3 mM nitron, 0.33 mM H₂O₂, 0.33 mM Fe(II)SO₄, DMSO-H₂O

Furthermore, it was thought that the radical species detected by EPR spectroscopy was an oxidised version **160** of a common decomposition product **159**. The EPR signal is similar to that observed for oxidised version of the decomposition product **102** of DMPO, which also gives a triplet with a splitting around 7 G⁹⁴. The decomposition product **160** forms from the hydroxyl adduct via a double oxidation which either occur via reaction with Fe(III) when Fenton conditions are used or other \cdot OH radicals, Scheme 51, as disproportionation would be unlikely due to the steric bulk.



Scheme 51: Formation of decomposition product observed by EPR

Although the EPR signal is persistent as it is rapidly reduced by antioxidants it would not be useful for detection of hydroxyl radicals *in vivo*. However, the oxidised product **159** potentially could be detected via mass spectrometry after reaction with radicals *in vivo* and so give a measure of oxidative stress. To check whether this would be possible MitoSpin **90** was incubated with homogenised rat

liver mitochondria under a variety conditions by Jan Trnka from the Murphy research group at the MRC in Cambridge.

First MitoSPIN was incubated with unstressed mitochondria which should not produce an excess of free radicals. The fractions that occur at the same retention time in the HPLC trace as the peak previously observed for the oxidation product **159** afforded no peak in ESI-MS, Figure 43.

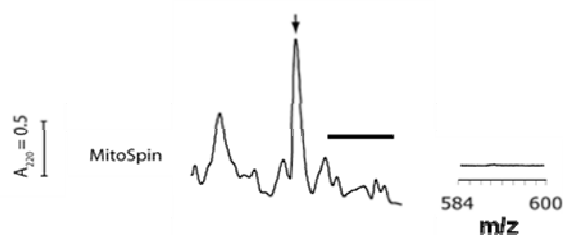


Figure 43: HPLC Spectrum and MS after incubation of MitoSPIN with unstressed rat liver mitochondria after 24 h

MitoSpin was then incubated with mitochondria treated with cumeme hydroperoxide which induces oxidative stress increasing the volume of hydroxyl radicals produced. After 24 h the extracts were separated by HPLC as before and the fraction from the region of the trace where the Mitospinamic acid **159** should appear were collected and analysed by ESI-MS. The ESI-MS showed the presence of MitoSpinamic acid **159** showing that the oxidation could be detected, Figure 44.

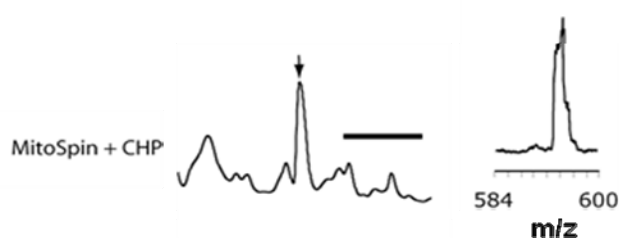


Figure 44: HPLC Spectrum and MS after 24 h incubation of MitoSPIN with rat liver mitochondria and cumene hydrogen peroxide, to induce oxidative stress

A control reaction was also carried out where mitochondria and substrates were incubated and the extracts separated by HPLC, fractions were collected and ESI-MS run. No peak was observed, Figure 45.

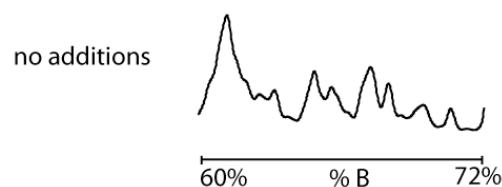


Figure 45: Mitochondria incubated for 24 h only with substrates for ETC.

The use of ESI-MS instead of EPR spectrometry has some advantages. The inclusion of the TPP cation provides an advantage for the detection by ESI-MS. The fixed positive charge allows for very sensitive detection as the entirety of the compound is a singly charged species. Indeed the incorporation of fixed positive charges such as TPP has been used extensively to improve detection sensitivity in mass spectrometry.⁹⁵ When using EPR spectrometry the concentration of radical adducts needs to be reasonable high in order to produce a good spectrum from radical adducts due to the efficiency of trapping the moderate stability of the adducts and the sensitivity of the EPR machine. Typically we use 3.3 mM spin trap. If a similar concentration is used in cell cultures it would lead to up to a 3 M solution within in the mitochondria. Though a lower loading should be possible, the small volume of mitochondrial relative to the cell as a whole means that the concentration of the spin trap within the mitochondria may have to be significantly higher than 3 mM to get a good EPR signal. Furthermore as the triphenylphosponium cation is cone shaped high concentrations within the mitochondria would lead to membrane rupture and resulting in apoptosis. ESI-MS has higher sensitivity and the oxidised product **159** is likely to be stable so detection using lower concentrations of spin trap should be possible. MitoSpin could therefore be used as a probe for the detection of ROS by ESI-MS

7 MS probe for H₂O₂

As a result of the findings in the evaluation of MitoSpin and its potential to be used as a mass spectrometry probe for the detection of hydrogen peroxide in mitochondria was designed.

7.1 Background

Mass spectrometry has been used very frequently to help investigate biological systems whether it is investigation of the metabolism of a drug or the pathway for the synthesis of a natural product. Both of these techniques use the isotopes and their mass difference to identify metabolites and intermediates respectively. Mass spectrometry has also been used in the investigation of oxidative stress, it has been used to identify levels of antioxidants within plants⁹⁶ and it has also been used to quantify biomarkers of oxidative stress when investigating the role of oxidative stress in disease⁹⁷.

Our aim was to make a probe that specifically detected hydrogen peroxide in mitochondria. Our target was MitoB **161** which contains the mitochondrial targeting triphenylphosphonium moiety and a boronate ester which should react with hydrogen peroxide, to give the phenol **162**. The change from boronate to phenol, Figure 46, would result in a significant change in mass allowing the probe **161** and oxidation product **162** to be distinguished by ESI-MS.

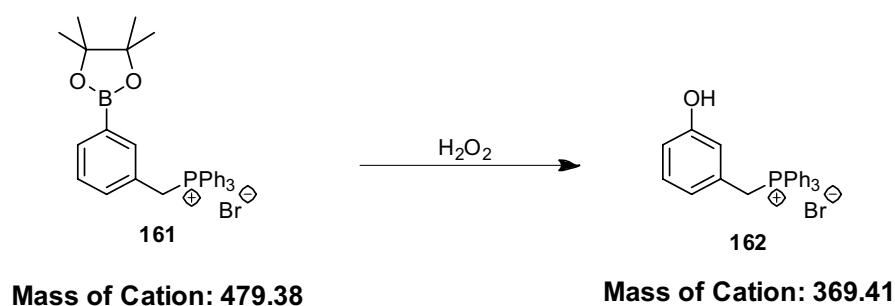
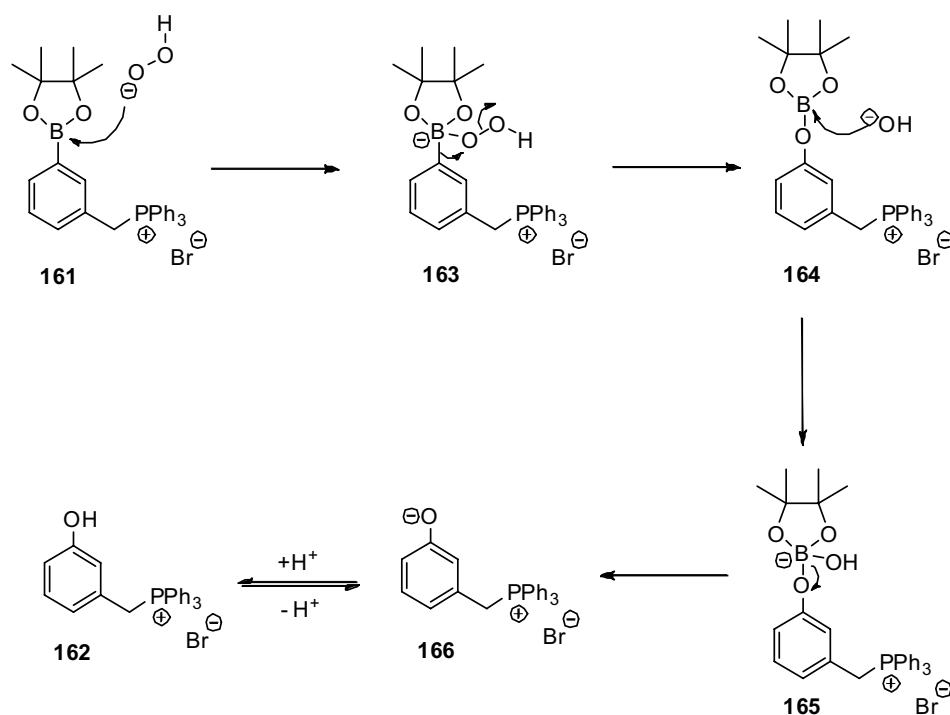


Figure 46

Conversion of boronates to phenols with hydrogen peroxide is a well known reaction and is commonly used as a synthetic route to the synthesis of phenols⁹⁸. It has also recently been utilised as a linker in solid phase synthesis⁹⁹.

The reaction of the boronate ester with hydrogen peroxide, Scheme 52, involves four mechanistic steps: attack on the boron by hydro peroxide ions, migration of the aryl group from the boron atom to the oxygen atom with the release of hydroxide, hydroxide attack and finally cleavage of the B-O bond to afford the phenoxide **166**, which is then protonated to give the phenol **162**.



Scheme 52: Reaction of MitoB with hydrogen peroxide

This reaction has been previously reported in the literature for the study of H_2O_2 in biological systems using fluorescence. Chang *et al* have synthesised a range of masked fluorescent compounds **167-169**. These di-boronate compounds react with hydrogen peroxide affording fluorescent compounds, Figure 47.

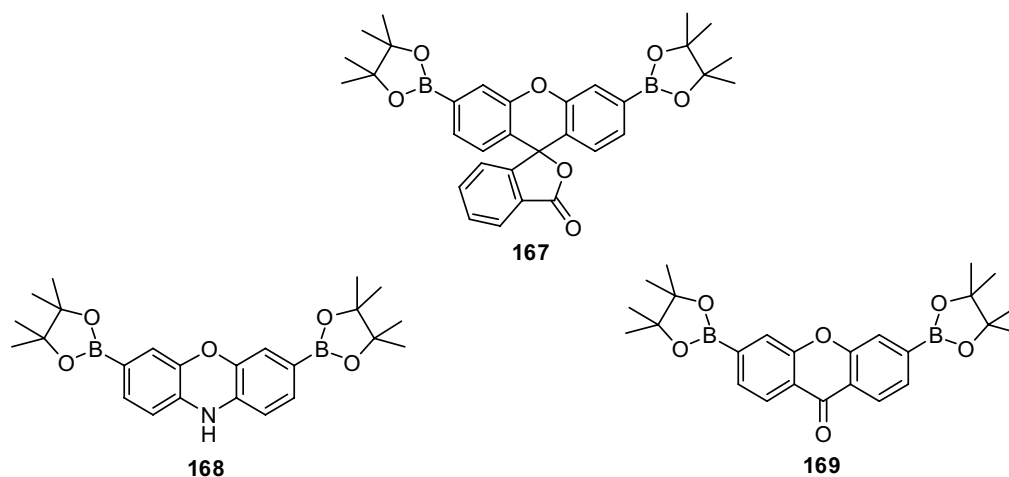
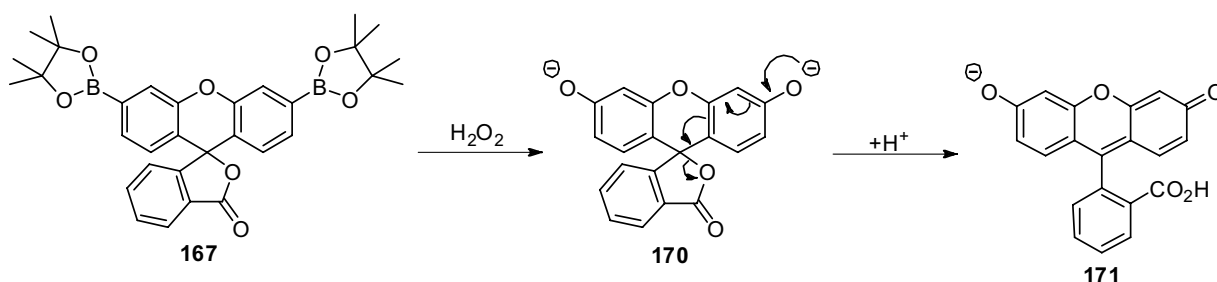


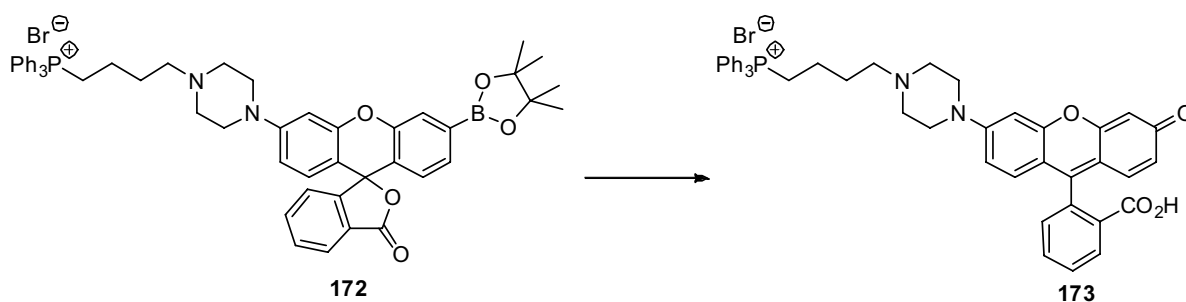
Figure 47: Hydrogen peroxide selective probes

All of these fluorescent probes have been found to react selectively with hydrogen peroxide, they can function within HEK cells and are cell permeable. Peroxyfluor-1 **167** is converted to green fluorescein **171** on reaction with hydrogen peroxide, Scheme 53.



Scheme 53: Hydrogen peroxide activated fluorescent probe

The group has also more recently reported a mitochondrial targeted version mitochondria peroxy yellow 1 (MitoPY1) **172**, Scheme 54, which is structurally similar to peroxyfluor-1 and reacts by a comparable mechanism to afford the fluorescent product **173**. Chang has shown that MitoPY1 **172** is taken up into mitochondria where it reacts with the hydrogen peroxide produced. They have also demonstrated increased fluorescence is observed in stressed mitochondria versus non stressed mitochondria.

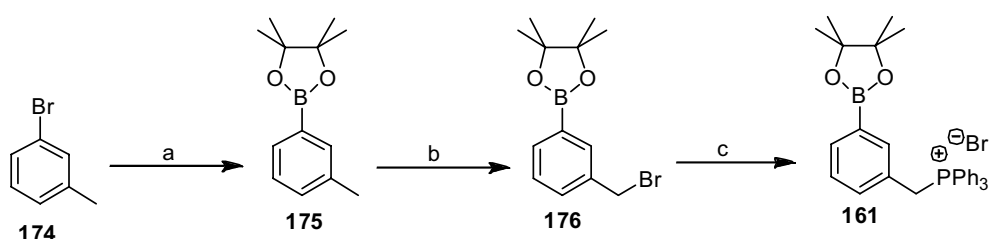


Scheme 54: Mitochondrial targeted derivative

As the reaction was well documented and there is literature precedent within biological systems this made us confident the reaction would proceed as expected. The combination of mitochondria-targeting and the higher pH of the mitochondria means that the MitoB will react only with the hydrogen peroxide in the mitochondrial matrix. The hydrogen peroxide in the mitochondria is produced by dismutation of superoxide therefore production of the phenol is directly proportional to the level of superoxide produced and the amount of oxidative stress that occurs.

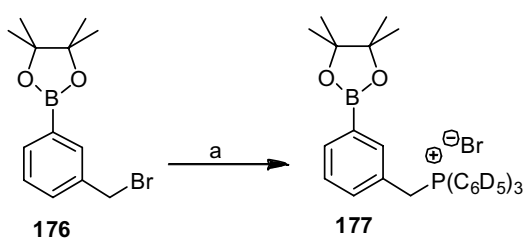
7.2 Synthesis of MitoB

In order to carry out any experiments, MitoB **161** first had to be synthesized, Scheme 55. Synthesis of Mito B began with 1-bromo-3-methylbenzene **174** which underwent lithium halogen exchange, when treated with *tert*-butyllithium, and was then reacted with 2-isopropoxy-4,4,5,5-tetramethyl-1,3,2-dioxaborolane to introduce the boronate moiety affording the boronate **175** in good yield. The boronate was then converted to bromide **176** via radical bromination at the benzylic position with NBS. The phosphonium salt was then introduced by S_N2 displacement of the bromide affording MitoB **161**.



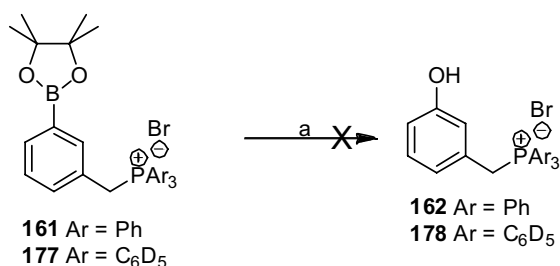
Scheme 55: Reagents and conditions: a) i) 1 eq. ^tBuLi, THF; ii) 1 eq. 2-isopropoxy-4,4,5,5-tetramethyl-1,3,2-dioxaborolane; 94% b) 1.1 eq. NBS, 0.1 eq benzoyl peroxide, CCl₄, 54% c) 1.1 eq. PPh₃, PhMe, Reflux, 38%

A deuterated version of MitoB **177** was also synthesized for the use as an internal standard to correct for variability in extraction and detection by HPLC-ESI-MS¹⁰⁰ whereby biological samples are spiked with known quantities of deuterated standards prior to extraction and analysis. The deuterated version **177** was synthesised in the same way as MitoB with triphenylphosphine being replaced by deuterated triphenylphosphine.



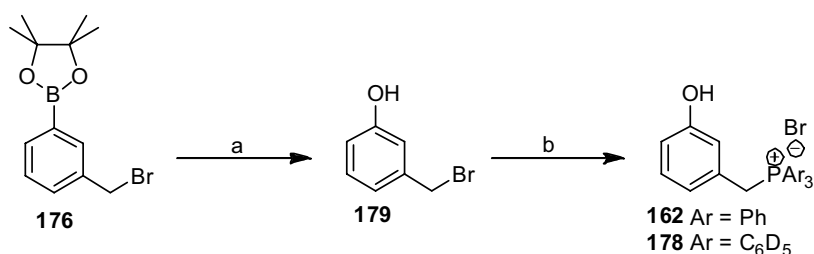
Scheme 56: Reagents and conditions: a) 1.1 eq. PPh₃-d₁₅, PhMe, Reflux 81%

The concentration of the product produced would also need to be determined accurately. In order to help with this the phenol product **162** of the proposed reaction between boronate **161** and hydrogen peroxide, together with its deuterated analogue **178** were prepared. Initial attempts to synthesize the phenol **162** mimicked the reaction which should occur *in vivo*, using hydrogen peroxide, sodium bicarbonate in a mixture of methanol and water.



Scheme 57: Reagents and conditions: a) H_2O_2 , NaHCO_3 , $\text{MeOH}/\text{H}_2\text{O}$

Although the phenol **162** was produced its hydrophilicity made it difficult to extract from the aqueous layer meaning that it could not be separated from the inorganic materials. Some of the product did crystallise out of the solution, but this was not a viable route to the phenol **162**. As a result the product was synthesised in two steps from the benzylic bromide **176** Scheme 58. The bromide **176** was prepared as in the original synthesis of Mito B **161** and was converted to the phenol **179** using hydrogen peroxide under basic conditions and then the phosphonium salt was prepared by substitution of the bromide as before affording the target phenols **162** and **178**.



Scheme 58: Reagents and conditions: a) H_2O_2 , NaHCO_3 , $\text{MeOH}/\text{H}_2\text{O}$ b) 1.1 eq. PPh_3 or $\text{PPh}_3\text{-d}_{15}$, PhMe , Reflux **163** = 56% over two steps, **179** = 67% over two steps..

Having synthesized both the deuterated and non-deuterated versions of the boronate ester and the phenol the compounds were sent to Prof Murphy's lab in Cambridge for testing.

It will be used by the Murphy group to study oxidative stress, testing the mitochondrial free radical theory of aging. The probe will be fed to *Drosophila* on two different diets. One group will be fed normally and the other will be on a calorie restricted diet. The level of phenol will be measured at the end of the experiment and this will allow for the quantification of oxidative stress in the mitochondria of flies. As mentioned in the introduction calorie restriction leads to prolonged lifetimes and this is thought to be due to lower metabolism which would lead to less radical production in mitochondria. Therefore, this experiment will directly test the mitochondrial free radical theory of aging. The experimental results should show whether calorie restriction does in fact lead to lower production of hydrogen peroxide in mitochondria and so the lowered levels of oxidative damage, explaining the reason for elongated life span.

Combined with research tools previously discussed, i.e. the dual sensor and MitoSpin we have illustrated ways to identify and quantify and ameliorate ROS. However, none of the compounds can prevent or reduce the production of ROS, they merely scavenge and/or report on the ROS being produced. This leads on to the next family of compounds which were specifically designed to moderate the production of ROS.

8 Mitochondrial moderators

As discussed previously, high membrane potential across the mitochondrial inner membrane is believed to be responsible for the reduction of the oxygen to superoxide, which disproportionate to give hydrogen peroxide and leads to other ROS and the oxidative stress responsible for ageing. We wished to make compounds that would allow chemical biological testing of this mitochondrial free radical theory of ageing by reducing the membrane potential in response to excess ROS. Ideally such compounds would be targeted to mitochondria, so as to avoid off-target effects, and in theory would be effective in any cell line or organism. The first stage was to develop compounds that combined a ROS trigger with a molecule that would reduce the membrane potential, i.e. an uncoupler.

8.1 Background

As discussed in chapter 1 the electron transport chain pumps protons out of the matrix into the intermembrane space as it transports electrons down the chain. By driving the protons into the intermembrane space a pH and a charge gradient is created across the membrane. The protons can pass back into the matrix through ATP synthase driving ATP production. There are many chemical compounds which have been used to abolish the potential across the membrane, for example rotenone, which inhibits the ETC and FCCP, which is an uncoupler. We used both of these compounds were used to evaluate the mitochondrial uptake of MitoSpin, chapter 7. Uncouplers transport protons across the mitochondrial membrane by-passing ATP synthase, allowing electron transport to proceed without the production of ATP i.e. uncoupling the two processes. As the protons are shuttled across the mitochondrial membrane into the matrix of the uncoupled mitochondrion removal of the membrane potential is observed. For a molecule to function as an uncoupler it must possess two key attributes. It must have a dissociable proton with a suitable pKa that permits the molecule to exist in both a protonated and unprotonated form at physiological pH. Secondly it must be hydrophobic enough to allow the molecule to diffuse freely between the mitochondrial membrane in both its charged and uncharged forms

Another commonly used uncoupler is dinitrophenol **180** with a pKa of 4.1¹⁰¹ it can exist in both its protonated **180** and unprotonated **181** forms, Figure 48, at physiological pH and as a small molecule both forms can easily diffuse across the mitochondrial membrane.

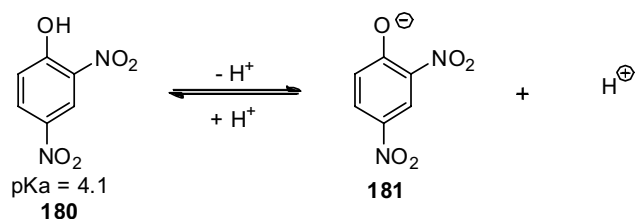


Figure 48: Dinitrophenol

Dinitrophenol uncouples the mitochondrial membrane, lowering the potential between the mitochondrial matrix and the inter membrane space, Figure 49. In the intermembrane space where the pH is lower (pH ~7) and there is an abundance of protons DNP is in the protonated form. When it diffuses into the mitochondrial matrix where the pH is higher (pH = 8.3) it becomes deprotonated releasing the proton into the matrix before diffusing back into the intermembrane space where it becomes protonated again, Figure 49. This means that the protons are shuttled across the membrane to lower the potential.

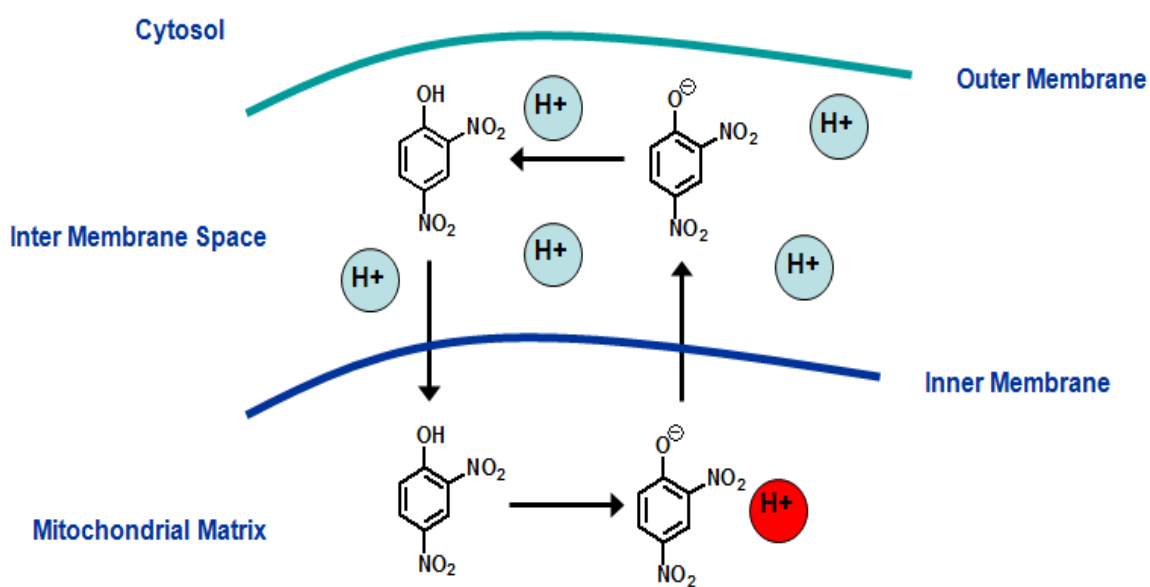
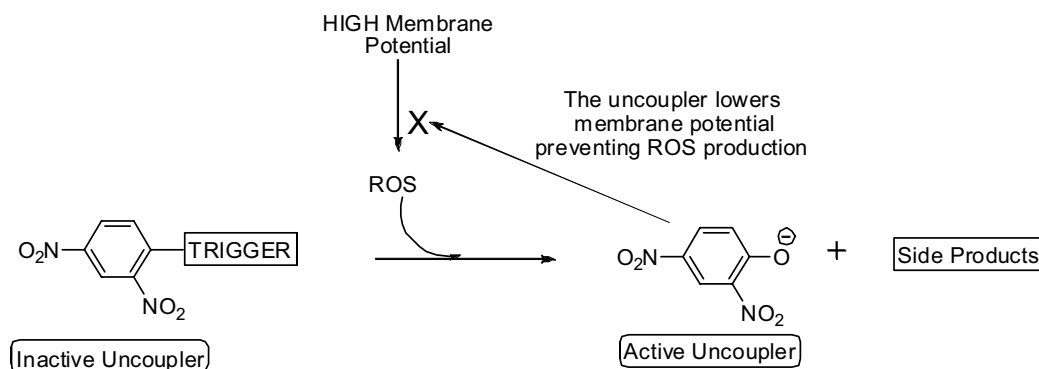


Figure 49: Mechanism of 2,4-dinitrophenol

Such compounds abolish the membrane potential regardless of whether the radical production is high or low and are always in their active form and therefore stop radical production but do not moderate it.

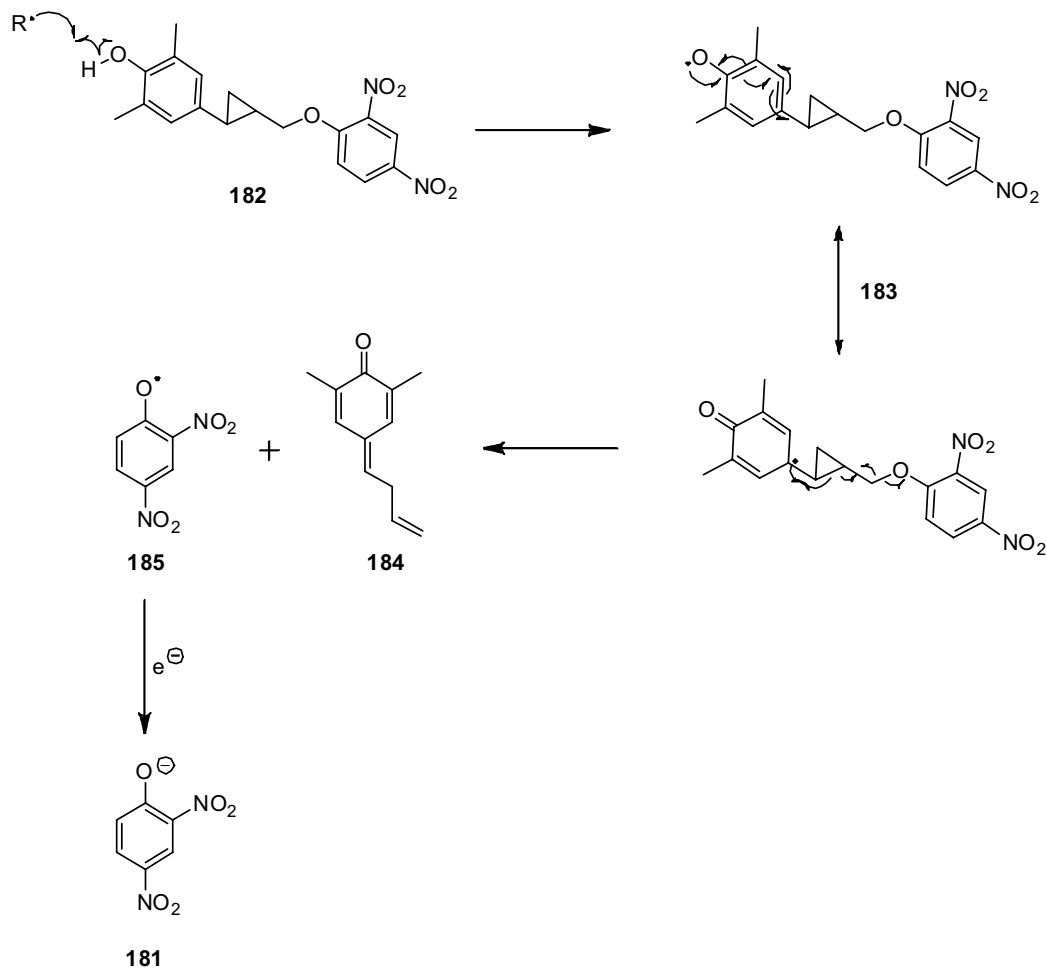
Therefore, a range of molecules which on reaction with radicals and ROS would fragment and release mitochondrial uncouplers, Scheme 59, for moderation of ROS were synthesized. The release of DNP should be a self-regulating system, DNP^- will only be released when it reacts with ROS which occurs at higher levels when membrane potential is high. DNP^- will lower the membrane potential, which should lower the production of ROS resulting in fewer reactions with the caged DNP molecules, leading to lowered release of DNP^- . The DNP should naturally diffuse out of the mitochondria.



Scheme 59: Reaction of moderator with hydrogen peroxide

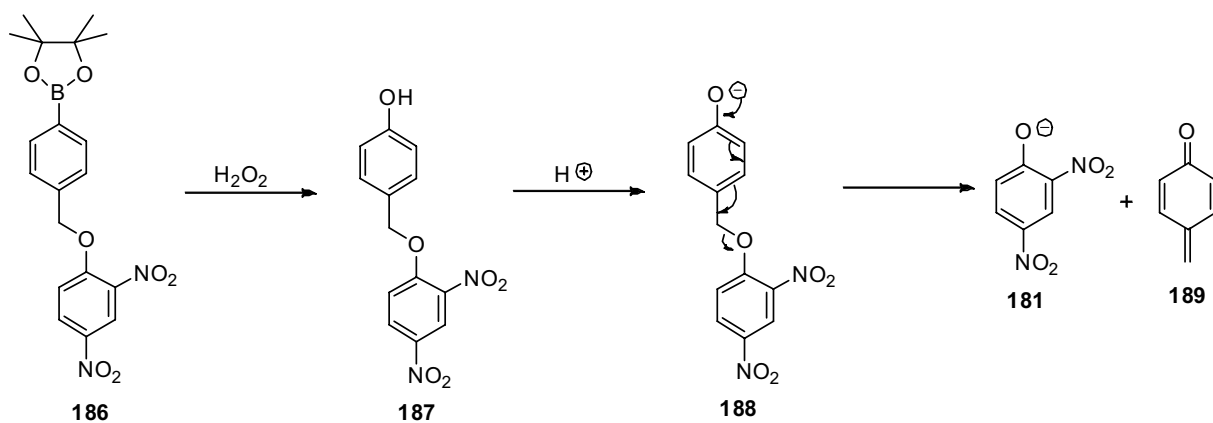
Two classes of molecules were synthesized as mitochondria moderators type A, which react with radicals and fragment to release an uncoupler (Scheme 60) and type B, which react with hydrogen peroxide and fragment to release an uncoupler (Scheme 61).

The type A compound **182** would react with radicals via hydrogen atom-abstraction to afford the phenoxyl radical **183** which would fragment with the collapse of the cyclopropane and release the radical **185** which would be the precursor to uncoupler **181** and would be rapidly reduced to the active uncoupler **181**.



Scheme 60: Reaction of type A moderator with radicals.

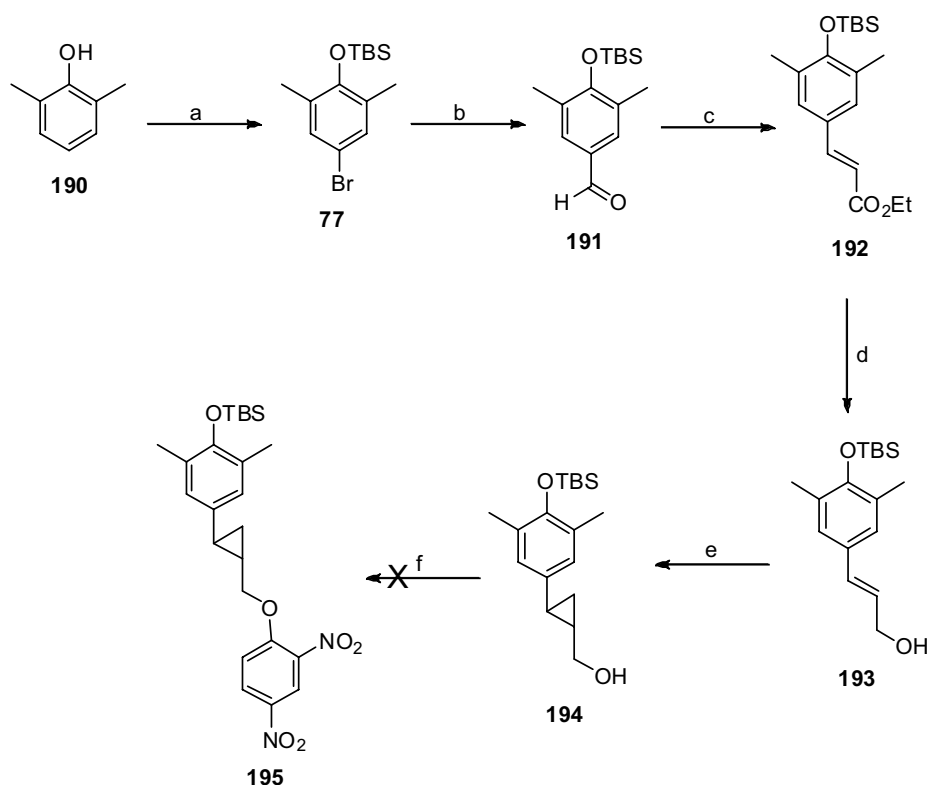
The type B compound **186** contains the boronate ester moiety, as with MitoB, which would react with hydrogen peroxide to form the phenol **187** which should fragment under basic conditions to afford the active uncoupler **181**.



Scheme 61: Reaction of type B moderator with radicals.

8.2 Synthesis of Type A compound

The synthesis of the cyclopropane-containing type A moderator began as shown in Scheme 62. The bromide **77** was prepared from the phenol **190** by treatment with bromine followed by protection of the phenol group with *tert*-butyldimethylsilyl (TBS) chloride. The bromide **77** was converted to the aldehyde **191** via lithium-halogen exchange followed by reaction with DMF. The aldehyde was then reacted with phosphonacetate using a Horner-Wadsworth-Emmons reaction affording the allylic ester **192**. The ester was then reduced to the allylic alcohol **193** using DIBAL. The alcohol was cyclopropanated using the modified Simmons-Smith reaction as reported for the dual sensor **72** affording the cyclopropanol. **194**. Initially, the cyclopropanation was attempted using zinc metal rather than diethylzinc. Although, it was easier to purify there were problems with forming the complex which resulted in a poor yield. Having formed the cyclopropanol the dinitrophenol moiety had to be introduced.

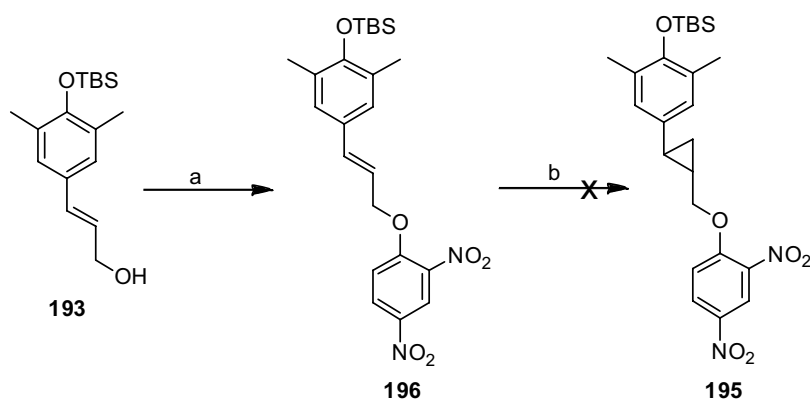


Scheme 62: Reagents and Conditions: a) i) 1 eq. Br, CHCl₃, ii) 1.1 eq. TBSCl, 2 eq. Imidazole, DCM; 94% b) i) 1 eq. ⁿBuLi, THF, -78°C, ii) 1 eq. DMF; 78% c) 1.2 eq. LiCl, 1.1 eq. DBU, 1.2 eq. phosphonacetate, MeCN; 78% d) 2 eq. DIBAL, DCM; 37% e) 5 eq. Et₂Zn, 10 eq. CH₂ I₂, DCM 42% f) 1.5eq PPh₃, 1.5 eq. DIAD, DCM

To conjugate the dinitrophenol moiety the first method attempted was to use the Mitsunobu reaction, however, there was attack at the cyclopropane instead.

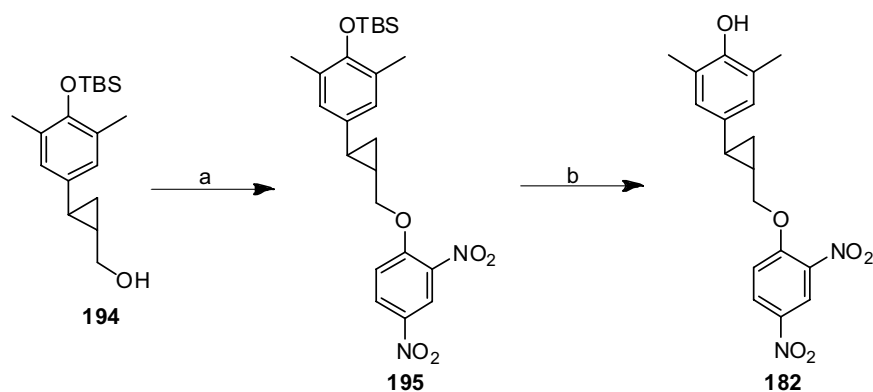
Another synthetic route was attempted, this time coupling the allylic alcohol to dinitrophenol and then carrying out the cyclopropanation, Scheme 63.

The Mitsunobu reaction with the allylic alcohol afforded the desired product in poor yield and therefore the S_NAr nucleophilic addition of alcohol with dinitrofluorobenzene was attempted. Having successfully attached the di-nitro phenol moiety the next step was to form the cyclopropane. However all attempts to carry out this reaction afforded a complex mixture which contained neither starting material nor product.



Scheme 63: Reagents and conditions: a) 1.5eq PPh_3 , 1.5 eq. DIAD, 1.5 eq. DNP, DCM 15% or 1 eq. 2,4-dinitrofluorobenzene, cat NEt_3 b) 5 eq. Et_2Zn , 10 eq. CH_2I_2 , DCM

Having discovered that nucleophilic aromatic substitution with 2,4-dinitrofluorobenzene could be used to attach the DNP moiety the previous synthetic route was reinvestigated, Scheme 64.



Scheme 64: Reagents and conditions: a) 1 eq. 2,4-dinitrofluorobenzene, cat NEt₃, Et₂O; b) 1 eq. TBAF, DCM

Reaction of the alcohol **194** with 2,4-dinitrofluorobenzene afforded the conjugated product **195** as an inseparable mixture of product, DNP **181** and 2,4-dinitrofluorobenzene. After many attempts to separate the mixture was used without further purification and the mixture treated with TBAF to carry out the deprotection which afforded the desired product **182** and the di-conjugated side product **197** (18% yield), Figure 50, due to the excess fluoro-DNP in the mixture.

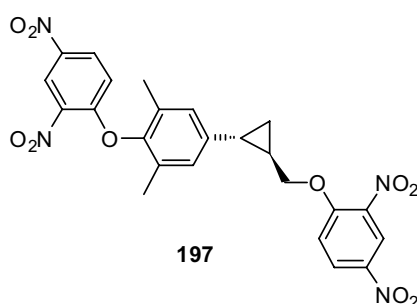
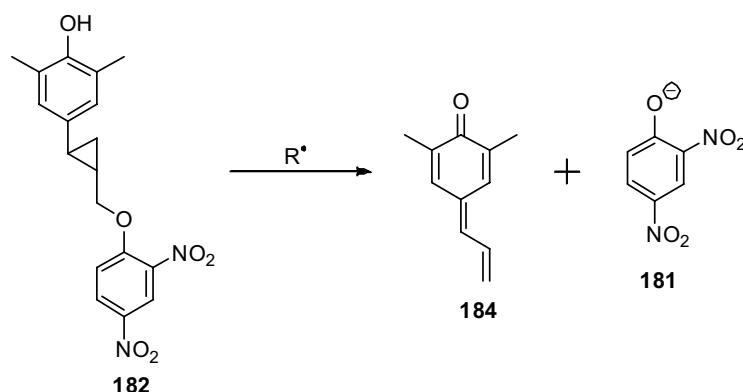


Figure 50: Di-conjugated side product

8.3 Reaction of type A moderator with radicals.

Having successfully isolated the desired product it was treated with a variety of radical species to see if it would react as hypothesised. The first radical species it was subjected to was superoxide.

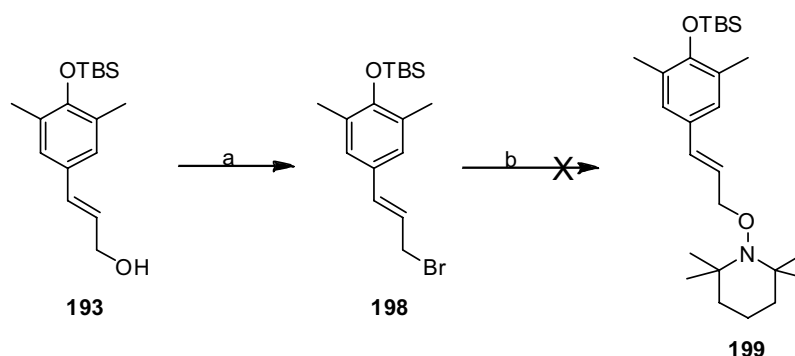


Scheme 65: **A:** 1 eq. KO_2 , 1 eq. 18-crown-6, 1:1 MeOH:H₂O, **B:** 1 eq. H₂O₂, 1 eq. Fe(II)SO₄ DMF-H₂O (1:2) **D** 1 eq. H₂O₂ UV, DMF-H₂O (2:1)

A 25 mM solution of the product in MeOH-H₂O (2:1) was mixed with 18-crown-6 and potassium superoxide and the reaction mixture observed by UV and by NMR. However no change was noticed. The cyclopropane was then treated with hydroxyl radicals produced via two methods; either by reaction of hydrogen peroxide with Fe(II) or by irradiation of hydrogen peroxide with UV light. In both cases no reaction and fragmentation was observed. The inability to produce dinitrophenol in retrospect is not surprising as release of a DNP radical is unfavourable. The O-H bond dissociation energy (BDE) of DNP is much greater than that of phenol due to the electron withdrawing groups destabilizing the phenoxyl radical. For comparison the BDE of phenol is about 20 kJmol⁻¹ less than para-nitrophenol.¹⁰²

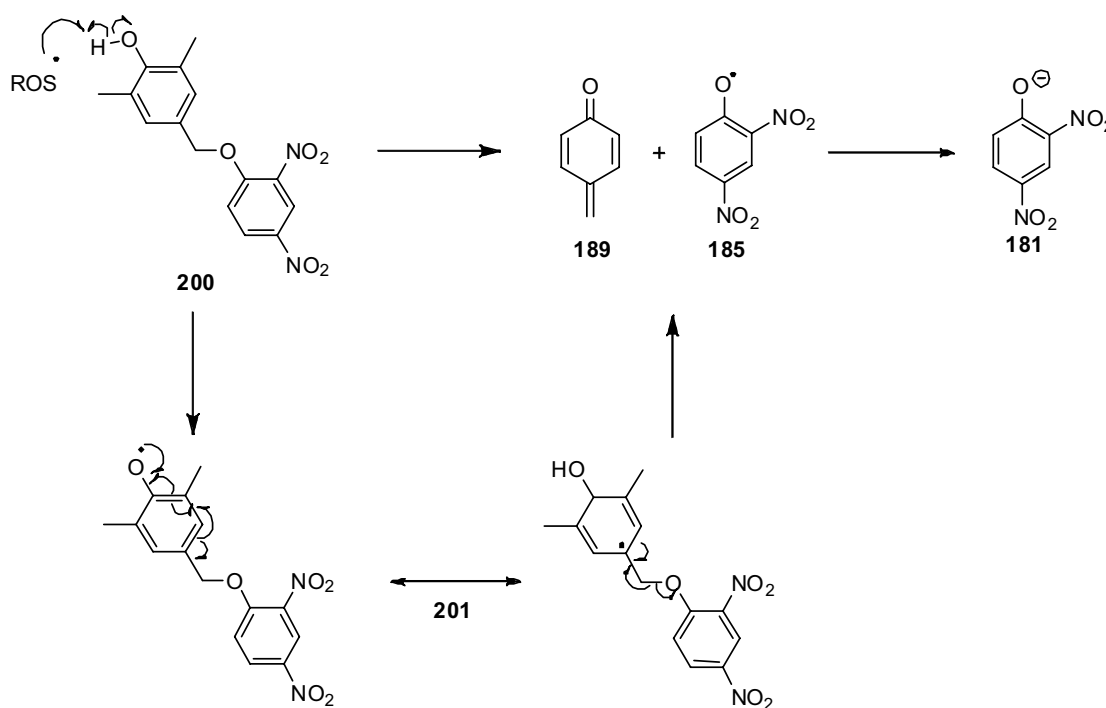
In order to test whether it was due to release of an unfavourable radical that fragmentation did not occur attempts were made to synthesize a derivative which would release TEMPO on fragmentation. TEMPO is a well known stable radical which has often been used to study and ameliorate oxidative stress. TEMPO is a well known for its antioxidant properties and ability to ameliorate oxidative stress by reducing superoxide and hydroxyl radicals, so a compound which released TEMPO during high levels of oxidative stress would increase the level of this antioxidant would be increased when it is most needed. Synthesis of a caged TEMPO version of the cyclopropanated derivative was therefore attempted, Scheme 66. The allylic alcohol **193** was converted into the bromide **198** using carbon tetrabromide and triphenylphosphine. Although the bromide **198** could be isolated as an almost pure compound it could not be completely purified due to decomposition. Attempt to generate a Grignard reagent from the

bromide and to react with TEMPO gave decomposition and the route was abandoned.



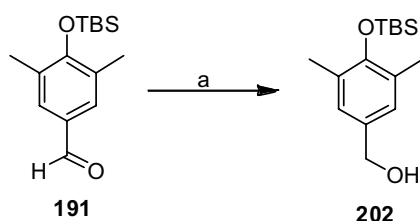
Scheme 66: Reagents and conditions: a) 1 eq. PPh₃, 1 eq. CBr₄, DCM, 42% b) 5 eq. Mg, 1 eq. TEMPO

At the same time as the cyclopropanated membrane-potential moderator **182** was prepared a more simple derivative was being synthesized, which would react with ROS as shown in Scheme 67. When mitochondria have a high membrane potential there is believed to be an increase in the concentration of ROS produced by the electron transport chain. It was proposed that the ROS would react with the phenol **200** via hydrogen atom abstraction or by proton loss and single electron transfer causing fragmentation and the release of dinitrophenoxyl radical **185**.



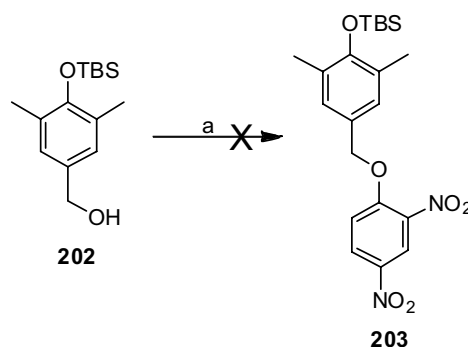
Scheme 67: Reaction of Ben-DNP with ROS

The synthesis of the phenol **202** began with the synthesis of the benzylic alcohol as shown in Scheme 69. The alcohol **204** was formed by reduction of the aldehyde **192** prepared during the synthesis of cyclopropanated mitochondrial moderator **183**.



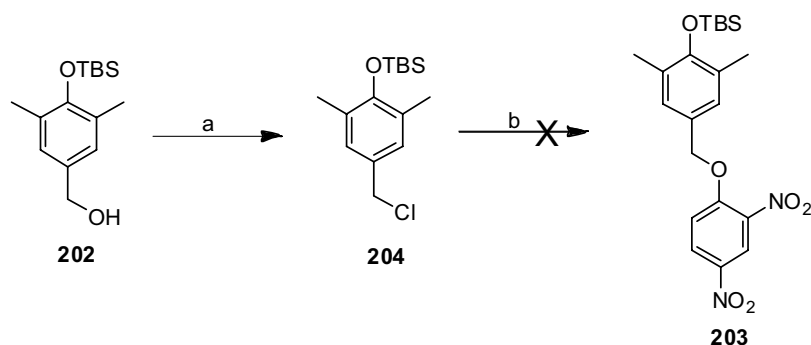
Scheme 68: Reagents and Conditions: a) 1.1 eq. NaBH₄, MeOH; 95%

The alcohol **202** then had to be conjugated to the dinitrophenoxy moiety, Scheme 70. Introduction of the DNP moiety proved to be problematic. The original synthetic strategy involving coupling the benzylic alcohol **202** to 2,4-dinitrophenol using the Mitsunobu reaction, which was unsuccessful affording only the triphenylphosphine-DIAD intermediate complex and starting material, despite a range of conditions being attempted.



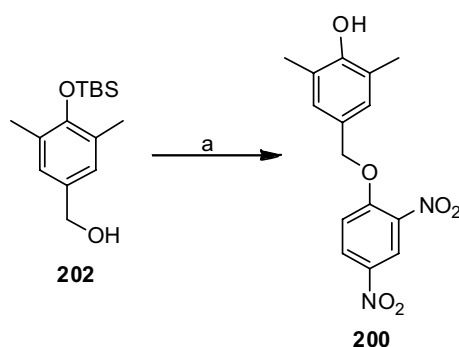
Scheme 69: Reagents and conditions: a) 1.5eq PPh₃, 1.5 eq. DIAD, DCM

A second approach involved conversion of the benzylic alcohol **202** into a good leaving group then substitution with dinitrophenoxide. Treatment of alcohol **202** with tosyl chloride gave the unstable benzylic chloride **204**. Substitution with 2,4-dinitrophenoxide was attempted but no product was observed.



Scheme 70: Reagents and Conditions: a) 1.1 eq. TsCl, 1.1 eq. NEt₃, 0.2 eq. DMAP; 64% b) 1.1 eq. 2,4-dinitrophenol, 1 eq. Cs₂CO₃, DMF

At this time the S_NAr reaction had been successful for the attachment of the dinitrophenoxyl functionality to the cyclopropanated derivative **182**, so this strategy was attempted for the preparation of phenol, Scheme 72. Aromatic nucleophilic substitution of the fluoride of dinitrofluorobenzene afforded the conjugated product **203**. However, it could not be separated and had to be purified via column chromatography, which led to deprotection affording the desired alcohol **200** as a mixture with DNP **180**. Attempts to recrystallize led to increased levels of DNP as the final target was decomposing in solution even in the absence of base.



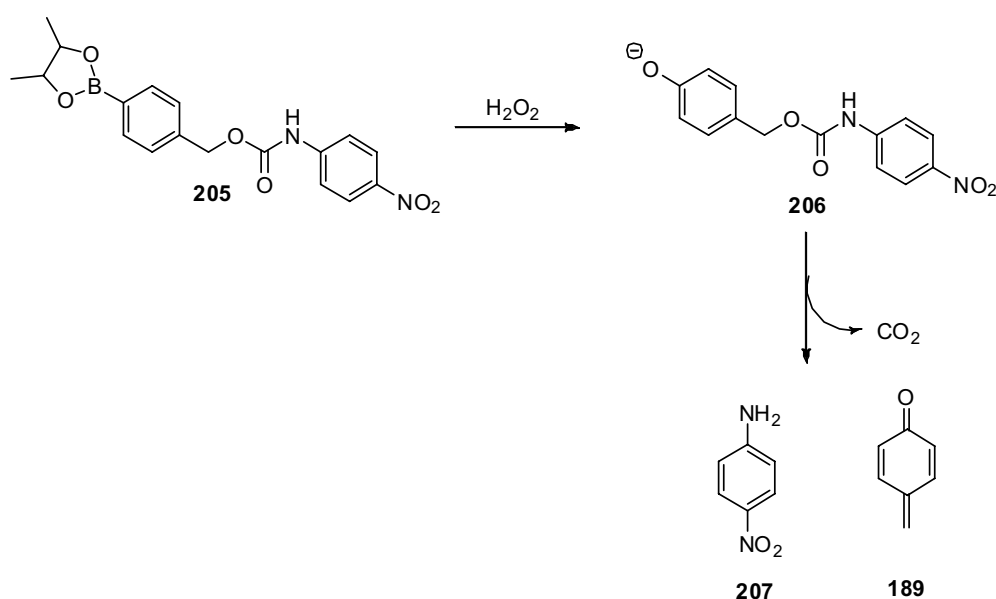
Scheme 71: Reagents and Conditions: a) 1.2 eq. 2,4-dinitrofluorobenzene, cat. NEt₃.

Although phenol **202** decomposed spontaneously and would not be useful as a moderator of membrane potential it is in fact the intermediate expected to be produced by a Type B probe reacting with hydrogen peroxide. Therefore its instability gave us confidence that when type B probes reacted with H₂O₂ and were converted into the phenols the compounds would fragment releasing DNP.

8.4 Synthesis of Type B - hydrogen peroxide stimulated selective uncoupling molecule.

The next synthetic target was a Type B derivative which would fragment upon reaction with hydrogen peroxide to give DNP⁻ **181**. From the results discussed in previous sections, i.e. the reactivity of the boronate functional group in Mito B and the decomposition of the type A moderator **200** we were reasonably confident that the type B probe would react with hydrogen peroxide as hypothesised, Scheme 61.

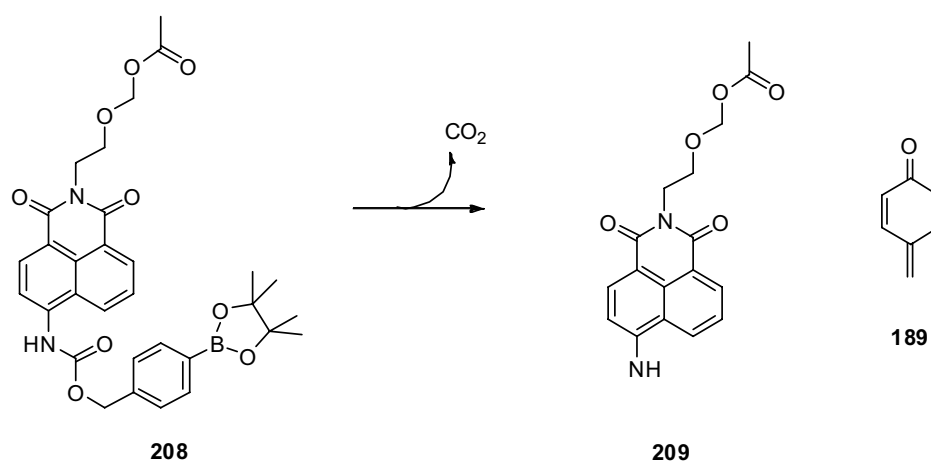
This reaction of boronate and fragmentation and release of an active molecule is also preceded in the literature. Chu and Lo synthesised a series of compounds for the detection of H₂O₂. Boronate **205** reacted with hydrogen peroxide to release a small coloured compound **207** and this mechanism was exploited for indication and quantification of H₂O₂ production within cells¹⁰³, Scheme 72



Scheme 72: Chu and Lo's H₂O₂ sensitive probe

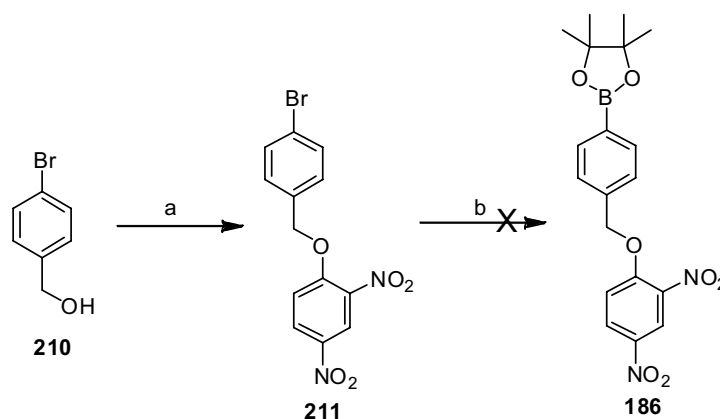
The Chang group have reported a similar hydrogen peroxide sensitive probe, peroxy lucifer 1 **208**, which reacts by the same two step mechanism, Scheme 73¹⁰⁴. This probe, however, is ratiometric i.e. there is an observable signal before and after reaction with hydrogen peroxide. The parent compound peroxy lucifer 1 **208** is blue-fluorescent (emission maximum 475 nm) however upon reaction with hydrogen peroxide the green-fluorescent aniline **209** is formed

(emission maximum 540 nm). The ratio of F_{540}/F_{475} can be measured in each experiment.



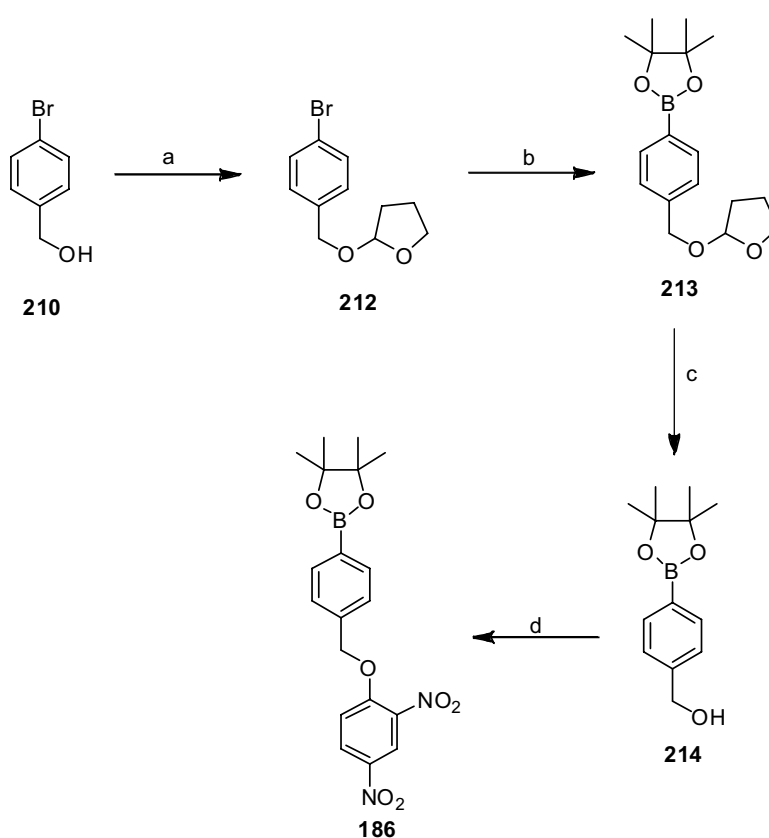
Scheme 73: Chang's H_2O_2 sensitive probe

The first attempt to synthesize a type B moderator of membrane potential **186** consisted of two steps, conjugation with the dinitrophenoxy moiety by the $\text{S}_{\text{N}}\text{Ar}$ reaction to form the bromide **211** followed by the introduction of the boronate ester using palladium catalysis to give the boronate **186**. Although the first step proceeded with excellent yield the formation of the boronate could not be achieved. Lithium-halogen exchange could not be used with the aryl bromide **211** due to the incompatibility of the nitro groups with organolithium reagents. Therefore an alternative route had to be utilised for the synthesis of the target compound, Scheme 74.



Scheme 74: Reagents and conditions: a) 1 eq. 2,4-dinitrofluorobenzene, cat NEt_3 64% ; b) 1 eq. bis(pinacolato)diboron, cat. $\text{PdCl}_2(\text{dppf})$,

The second route began with the protection of the benzylic alcohol **210** with a tetrahydrofuranyl group to afford the acetal **212**. This was followed by introduction of the boronate using standard conditions as reported for MitoB to produce boronate ester **213**. The THF protecting group was then removed to give the benzylic alcohol **214** using aluminium trichloride in ethanol which was used in preference to standard deprotection using acid due to the sensitivity of the boronate ester. Having formed the benzylic alcohol **214** it was then coupled with 2,4-dinitrofluorebenzene using the standard S_NAr method with to give the desired boronate **186**. Having successfully synthesised the boronate ester **186** its reactivity with hydrogen peroxide had to be tested.



Scheme 75: Reagents and conditions: a) 1.1 eq. 2,3-DHF, cat. TsOH, DCM; 95% b) i) 1 eq. BuLi, THF, -78°C, ii) 1.1 eq. 2-Isopropyl-4,4,5,5-tetramethyl-1,3,2-dioxaborolane; 95% c) 3 eq. AlCl₃, EtOH; 81% d) 1 eq. 2,4-dinitrofluorobenzene, cat NEt₃ 21%

8.5 Reaction of Boronate with Hydrogen Peroxide

Preliminary studies with hydrogen peroxide were carried out in collaboration with Professor Nick Price at the University of Glasgow. Production of DNP on reaction with hydrogen peroxide was measured using UV spectroscopy, measuring the absorption at 410 nm of the absorption peaks for DNP where the

starting material did not absorb. The reaction was carried out using *pseudo* first order conditions with the boronate in a large excess.

We had chosen to measure the production of DNP^- by UV spectrometry as DNP^- gave a very distinctive absorption spectrum. The spectrum of 0.2 mM DNP^- in a solution of DMF and aqueous NaHCO_3 buffer is shown in Figure 51. Furthermore, we had chosen to monitor the production of DNP^- at 410 nm, an absorbance maxima for DNP^- .

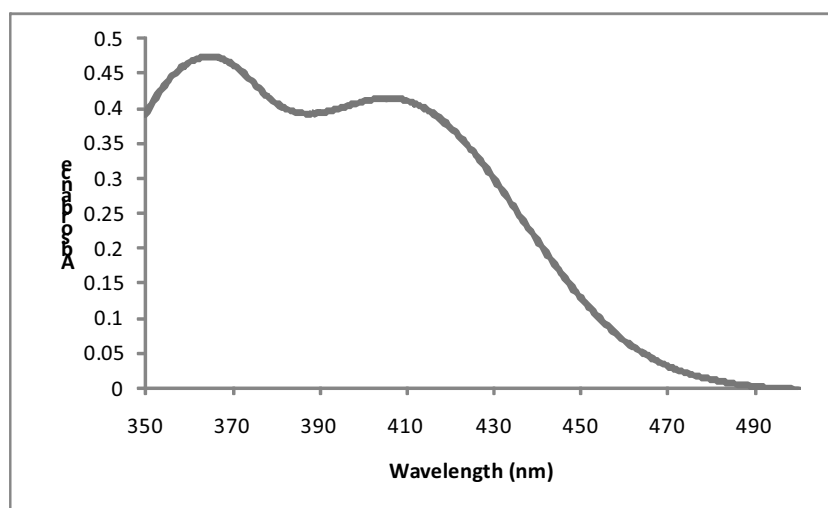


Figure 51: UV spectrum of 0.2 mM solution of DNP in DMF/ NaHCO_3 , buffer (aq). 3:2 [0.2 mL 1 mM solution DNP in DMF + 0.4 mL 0.14 M NaHCO_3 buffer (aq) + 0.4 mL DMF]

However, to confirm that it was possible to monitor the absorption at 410 nm we first had to make sure that Boronate DNP did not absorb in this region. Therefore an absorption spectrum of 0.2 mM Boronate DNP in DMF/ NaHCO_3 , buffer (aq) 3:2 was obtained, Figure 52, and showed that Boronate DNP did not absorb at 410 nm.

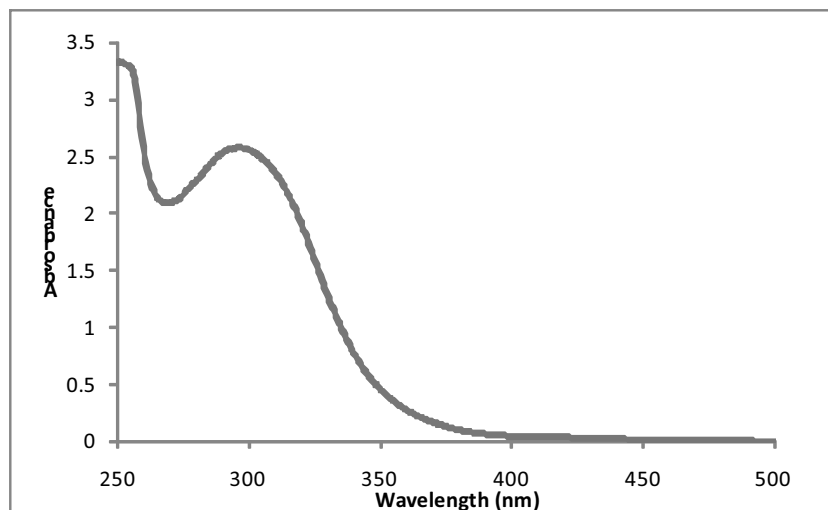


Figure 52: UV spectrum of 0.2 mM solution of Boronate DNP in DMF/NaHCO₃, buffer (aq). 3:2 [0.2 mL 1 mM solution Boronate DNP + 0.4 mL 0.14 M NaHCO₃ buffer (aq) + 0.4 mL DMF]

After confirming that the production of DNP⁻ could be monitored at 410 nm the reaction of Boronate DNP with hydrogen peroxide was carried out.

It is believed that the reaction would be second order and have the rate equation:

$$\frac{d[\text{DNP}^-]}{dt} = k_2^{\text{DNP}} [\text{H}_2\text{O}_2] [\text{Boronate DNP}]$$

A second order rate constant is difficult to calculate directly as it would require the observation of the concentration of both the Boronate DNP and the hydrogen peroxide. However, if one reagent is used in excess you can create *pseudo*-first order conditions as the concentration of the reagent in excess would essentially remain constant. This would result in the *pseudo*-first order rate equation:

$$\frac{d[\text{DNP}^-]}{dt} \approx k_1^{\text{DNP}} [\text{H}_2\text{O}_2]$$

Utilising this approximation the concentration of hydrogen peroxide could be used to calculate the *pseudo*-first order rate constant k_1^{DNP} . Furthermore dividing this value by the concentration of Boronate DNP used a reasonable estimation of the second order rate constant k_2^{DNP} could be obtained.

A 200 μM solution of Boronate DNP in 1:1 mixture of DMF and aqueous sodium bicarbonate buffer (0.14 M) at pH 8.3 the approximate pH of the mitochondrial matrix, was treated with 24.3 μM of hydrogen peroxide and the absorption measured over 2000 s, Figure 53. The spectrum clearly shows the increase in concentration of DNP over the 2000 s. The *pseudo*-first order rate constant was $2.26 \times 10^{-3} \text{ s}^{-1}$ and the second order rate constant was $11.3 (\pm 0.5) \text{ M}^{-1}\text{s}^{-1}$. Considering the absorption of t 20 μM DNP^- in the same buffer system is 0.4097, this gives a 68% yield of DNP^- with respect to hydrogen peroxide used. Subsequently another member of the Hartley group has repeated this reaction under more rigorous conditions and found a $10.8 \text{ M}^{-1}\text{s}^{-1}$ second order reaction rate constant and a 60 % conversion with respect to hydrogen peroxide.

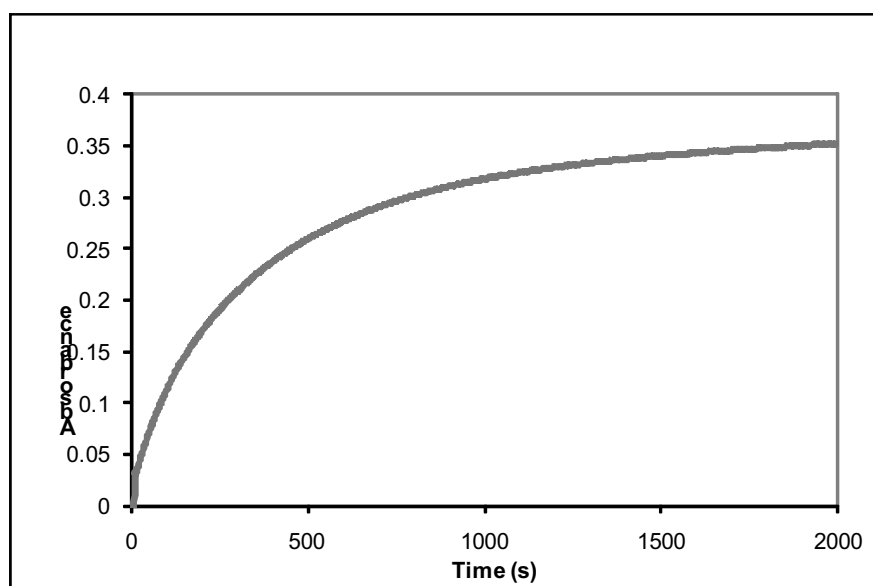
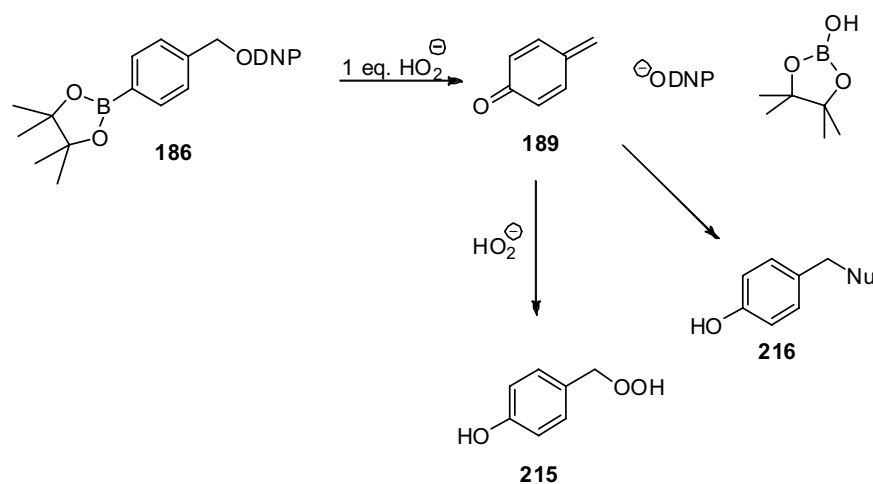


Figure 53: Spectrum of reaction of Boronate-DNP, Reagents and conditions: 200 μM Boronate, 24.3 μM H_2O_2 in 140 mM NaHCO_3 buffer/DMF

It is thought incomplete conversion is caused by the preferential reaction of the hydrogen peroxide rather than water with the side product formed, quinone methide **189**, Scheme 77. If this were the case two equivalents of hydrogen peroxide would be used to produce one molecule of DNP^- . However, we observed 60% conversion rather than 50% conversion which could be attributed to pKa of the benzylic peroxide being higher than that of hydrogen peroxide or that some of the quinone methide **189** goes on to react with other nucleophiles in solution.



Scheme 76: Reaction of quinone methide with nucleophiles

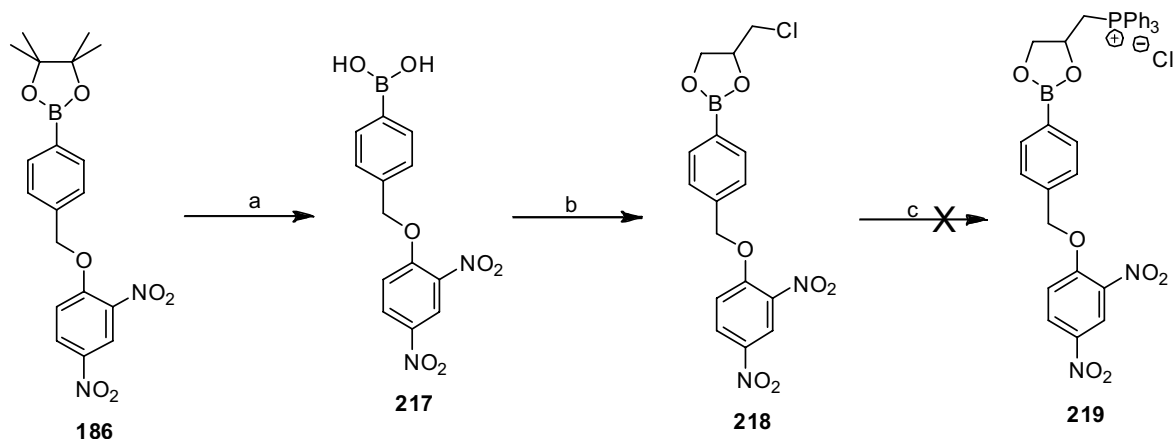
The next step was to try and target the boronate to the mitochondrion, using the triphenylphosphonium cation. The majority of the boronate would then accumulate in stressed mitochondria due to the elevated membrane potential resulting in the release of the DNP and moderation of ROS production, where and when it was required.

8.6 Attempts to synthesize a Mitochondrial targeted version

The easiest way to introduce the triphenylphosphonium cation, it was thought, would be by transesterification of the boronate ester **186** to afford the targeted analogue **219**. There were two synthetic routes to the desired boronate **219**; the first route attempted is outlined in Scheme 78. The route would involve exchange of diols to give the chloride **218** followed by the introduction of the phosphonium salt.

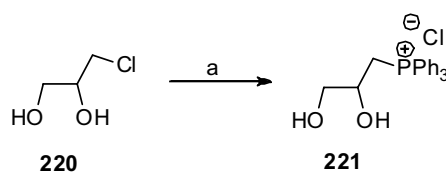
The boronic acid **217** first had to be synthesized. The boronic acid **217** was initially afforded using $\text{HCl}_{(\text{aq})}$. However, the reaction was poor yielding and the product difficult to purify so subsequent production of the boronic acid **217** from the ester **186** utilised periodate to cleave the pinacol when it was released in aqueous media. Condensation of the boronic acid and diol proved to be problematic under the majority of conditions, with various solvents and dehydration methods, returning starting material and affording no product. However, eventually the chloride boronate ester **218** was successfully synthesized using DCM as the solvent and magnesium sulfate as the dehydrating

agent. The final step was to substitute the chloride for the phosphonium cation, attempts to do this were carried out as per MitoB, but no product was observed. Reaction of the primary alkyl chloride is more demanding than the reaction between a benzylic bromide and triphenylphosphine both because the leaving group is poorer and there are no electronic features assisting reaction.



Scheme 77: Reagents and conditions: a) i) 3 eq. NaIO₄, THF/H₂O, ii) 1 N HCl; 60% b) 2 eq. MgSO₄, DCM; 39% c) 1.5 eq. PPh₃, PhMe, reflux

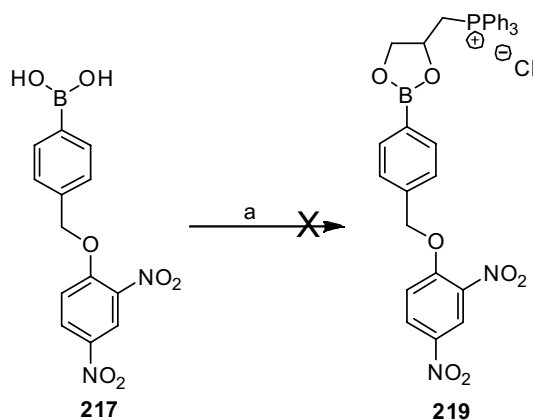
As the attempts to introduce the phosphonium salt proved unsuccessful, the second synthetic pathway was attempted. In this route the phosphonium group was introduced before the exchange of diol moieties. The first step was synthesis of the phosphonium salt **221**, Scheme 79. The phosphonium cation was again introduced by displacement of a halide but in this case no solvent was needed and triphenylphosphine was heated under reflux in excess diol **220**. The resulting salt **221** was then separated by a series of washes with ether.



Scheme 78: Reagents and conditions: a) 0.1 eq. PPh₃, reflux; 76%

Having formed the phosphonium diol **221**, attempts were then made to couple it to the boronic acid synthesized previously in Scheme 77. Several attempts were made to form the boronate ester **219** however as yet no material has been

successfully isolated with starting material being returned in all cases (Scheme 79).

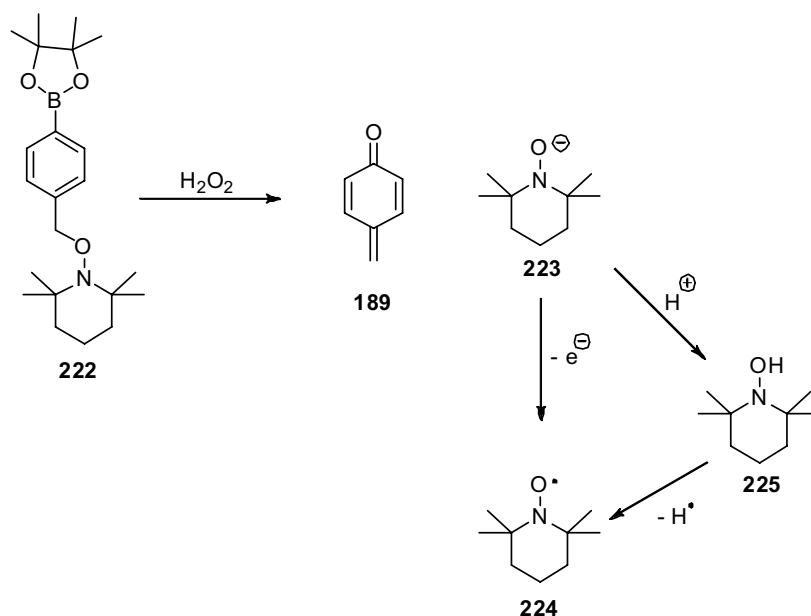


Scheme 79: Reagents and conditions: 2 eq. MgSO₄/molc.sieves, 1 eq./1.5 eq/2 eq. Diol **221**, DCM/THF/MeCN/DMF, RT - 100°C

Time in the laboratory ran out before further attempts to form the mitochondria-targeted analogue could be carried out. However, since then work on this area has been carried on by another member of the Hartley group. It has now been concluded that introduction of the triphenylphosphonium cation directly through the boronate ester would not be the best approach as boronate esters may be hydrolysed *in vivo* to boronic acids with the loss of the targeting group

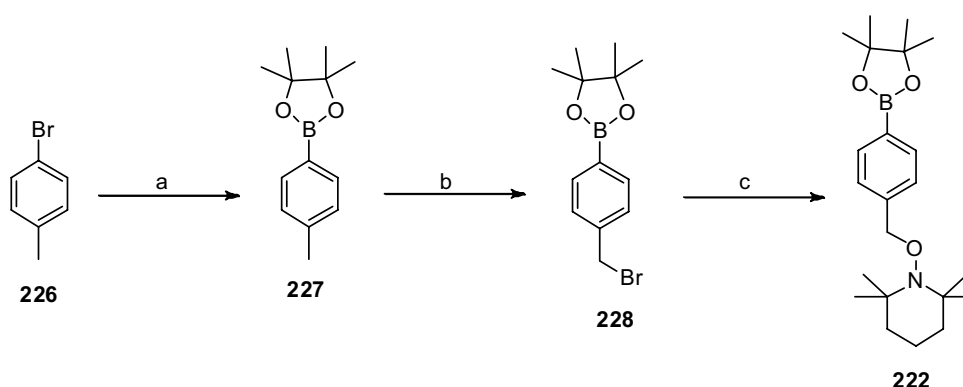
8.7 Synthesis of a TEMPO derivative.

As with the cyclopropanated moderators of membrane potential, synthesis of a TEMPO-derivative **222** was planned. However, in this case fragmentation would lead to release of the TEMPO anion **223** which would then be rapidly oxidized to the radical species **224** (Scheme 80).



Scheme 80: Reaction of Boronate TEMPO with H₂O₂

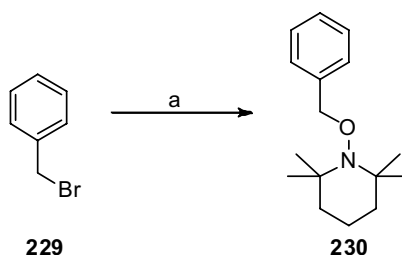
A key intermediate in the synthesis was the formation of the benzyl bromide **228**, which is a regioisomer of the *meta*-benzylic bromide **176** as reported in the synthesis of MitoB, Chapter 8. Therefore the first two synthetic steps were carried out under the same conditions as previously reported giving first boronate **227** then benzylic bromide **228**. The benzyl bromide **228** was then converted to the Grignard reagent, using Magnesium, and reacted with TEMPO to afford the target compound **222**.



Scheme 81: Reagents and conditions: a) i) 1 eq. BuLi, THF, -78°C, ii) 1 eq. 2-isopropoxy-4,4,5,5-tetramethyl-1,3,2-dioxaborolane; 90% b) 1.1 eq. NBS, 0.1 eq benzoyl peroxide, CCl₄; 57% c) 5 eq. Mg, 1 eq. TEMPO, Et₂O 45%

The Grignard reaction was initially tried on benzylbromide as proof of principle, which successfully afforded the conjugated product **230**. As the benzylbromide is very reactive the reaction proceeded very easily. However, when the same

conditions were reapplied to the boronate derivative the reaction proved to be more difficult. Extra care had to be taken to ensure the reaction was completely dry and the Mg treated with iodine before reaction.



Scheme 82: Reagents and conditions: 2.5 eq. Mg, 1 eq. TEMPO, Et₂O, 0 °C 38%

8.8 Reaction of the TEMPO derivative with Hydrogen Peroxide

Preliminary investigations as to whether the TEMPO derivative **222** would release TEMPO upon reaction with hydrogen peroxide were carried out. The conditions used were similar to those reported for the type B probe **186**, but in this case *pseudo*-first order conditions were achieved by having an excess of hydrogen peroxide rather than an excess of the boronate, in case the hydrogen peroxide was also used to oxidise the hydroxylamine anion released. Furthermore, the reaction could not be monitored by UV spectroscopy as the extinction coefficient for the main absorption maximum for TEMPO is very low¹⁰⁵. Therefore, the reaction was monitored using EPR spectroscopy.

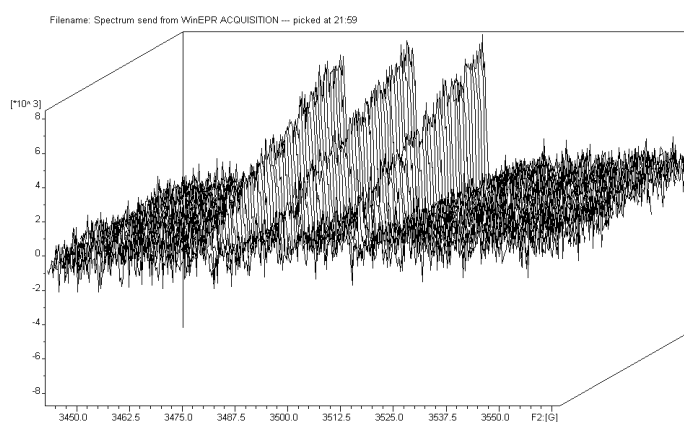


Figure 54: EPR after 30 min from reaction of **224** with hydrogen peroxide

The first reaction was carried out over 30 min with 243 μM hydrogen peroxide being added to a 50 μM solution of boronate in a 1:1 mixture of DMF and 0.14 M $\text{NaHCO}_3(\text{aq})$, and acquiring a spectrum every 30 seconds. This afforded the 2 D plot shown, Figure 54.

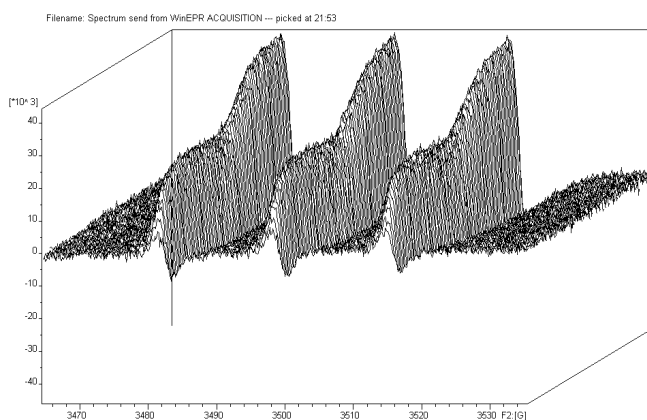


Figure 55: EPR over 120 min from reaction with Hydrogen Peroxide.

The plot shows that reaction with hydrogen peroxide does in fact result in the production of TEMPO. However, after calibration with known quantities of TEMPO it transpired that only 15 % of the possible TEMPO production had been detected. Therefore, the reaction was repeated and spectra acquired for 120 min to afford the plot shown in Figure 55.

This reaction gave interesting results. The concentration of TEMPO steadily increased over 30 min before reaching a plateau which remained for a further 30 min before beginning to steadily increase again over the following 30 min.

The reason for this reaction profile is unknown and optimization of conditions is certainly necessary. It was thought that it may be caused by the oxidation of the hydroxylamine anion to the radical being dependent on oxygen. Attempts were made to either remove all oxygen from the reaction or to saturate the solution with oxygen to investigate this theory. However, a mixture of time constraints and limited laboratory equipment meant that this work could not be completed. The reaction will need further investigation and optimization but the probe has been synthesized and the results so far are promising.

9 Mitochondria-targeted, light-activated uncoupler

Another project which involved the synthesis of a small molecule to study the role of mitochondria in biology was the preparation of a photocleavable bioagent which would release an uncoupler upon irradiation, Figure 56.

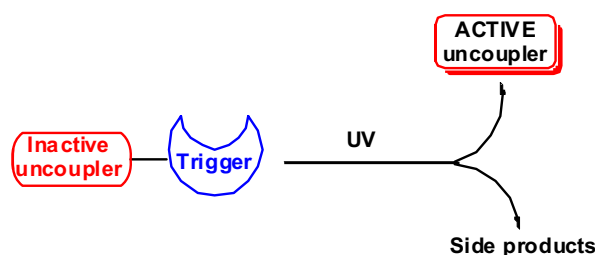
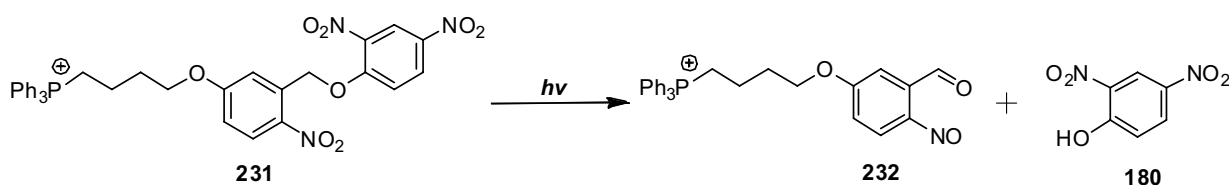


Figure 56

All of the probes reported in the preceding chapters act in response to an elevated production of ROS and the results are therefore controlled by the biological processes. Release of the uncoupler by irradiation allows the researcher to have spatial and temporal control of where and when the uncoupler is released. This approach allows for the design of experiments to investigate the effect of an individual mitochondrion or small group of mitochondria on a process, e.g. calcium release in smooth muscle cells

9.1 Background

The synthetic target is illustrated in scheme 83 and should respond to UV irradiation by releasing DNP 180.



Scheme 83: Reaction of light-activated probe with UV light.

The molecule 231 will also be targeted to mitochondria by the triphenyl phosphonium cation as previously described.

The *o*-nitrobenzyl moiety is the most commonly used photolabile linker employed to cage bioactive compounds for the study of biological systems¹⁰⁶. The linker was originally intended for use in organic synthesis. The first reported use to cage biological molecules was the synthesis of caged ATP **233** in 1978¹⁰⁷, Figure 57. Since then a number of bioactive molecules have been caged from amino acids, DNA and RNA to alcohols and phenols, with over 40 commercially available. These caged compounds are mainly used for the study of proteins and their production.

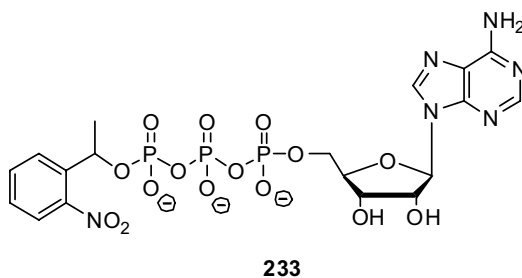
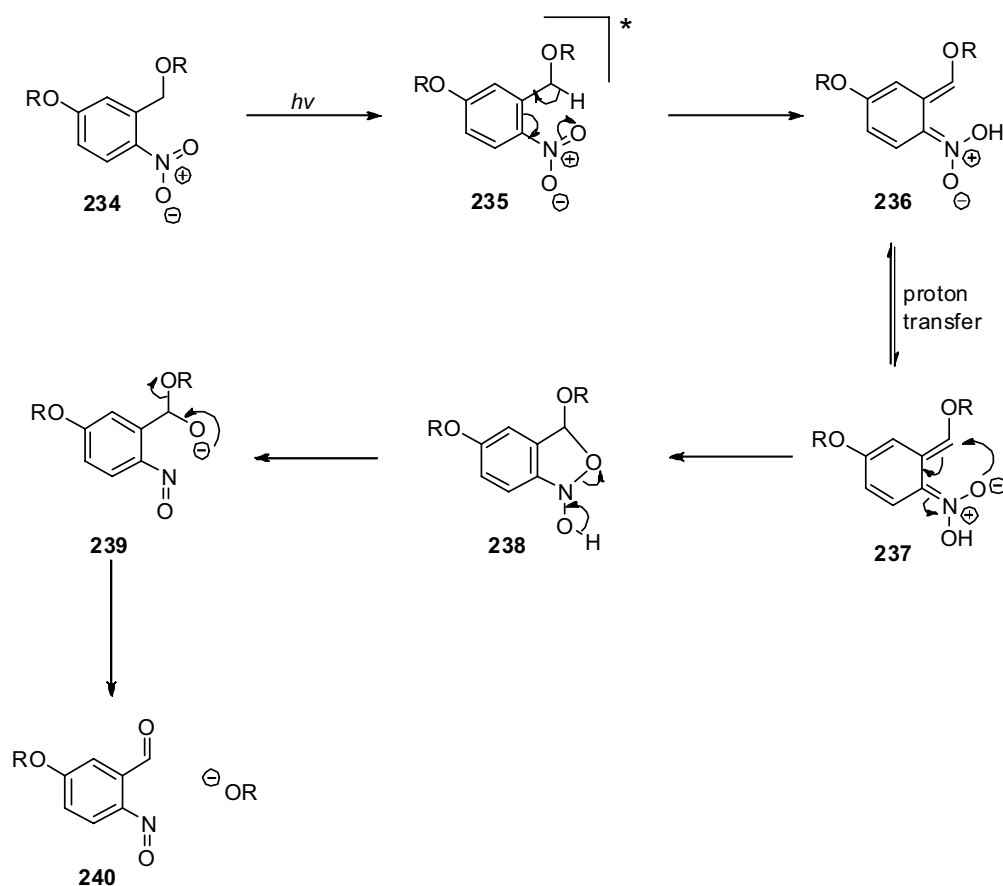


Figure 57: caged ATP

The linker fragments¹⁰⁸ upon irradiation as shown in Scheme 84.

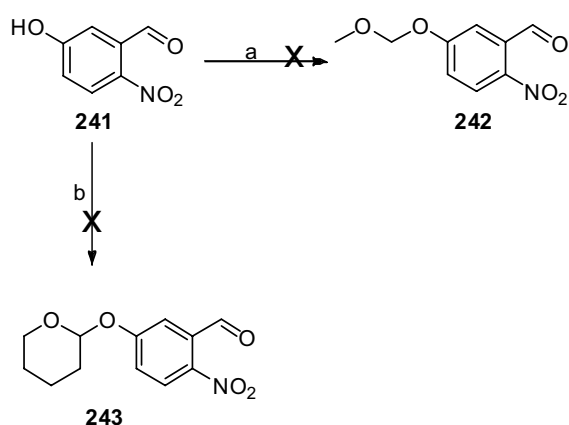


Scheme 84: Mechanism for fragmentation

Irradiation with UV light induces activation to the triplet state **235** which results in a 1,5-sigmatropic rearrangement to afford **236** which upon proton transfer cyclises to restore aromaticity affording acetyl **238**. Acetyl ring then opens forming a nitroso group and a hemiacetal **239**. The hemiacetal then fragments to release the biologically active molecule with formation of the aldehyde side product **240**.

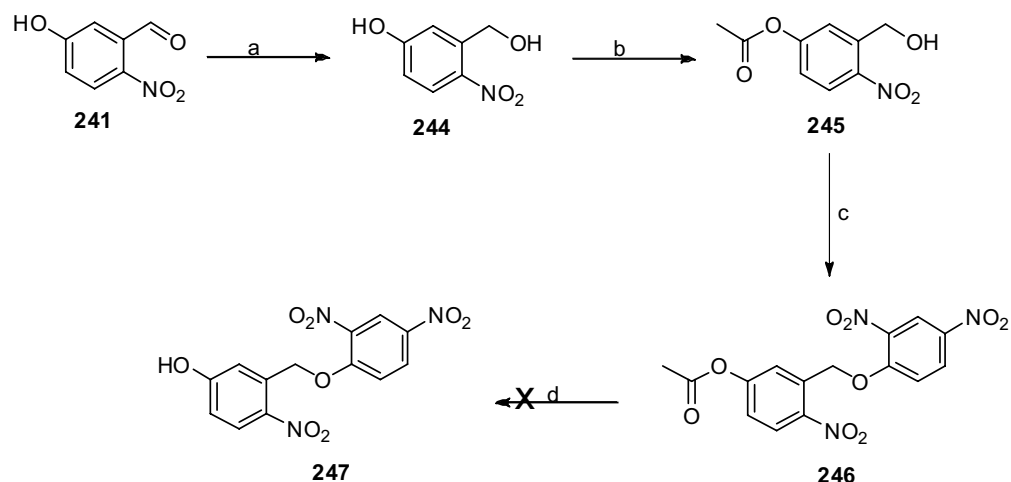
9.2 Synthesis of the light-activated uncoupler

The initial synthetic route attempted for the synthesis of probe **231** involved the conjugation of the DNP moiety followed by alkylation with (4-bromobutyl)triphenylphosphonium bromide, to introduce the triphenyl phosphonium group in the last step to avoid the problematic preparation of phosphonim salts experienced in the synthesis of MitoSpin. The phenolic hydroxyl group of 5-hydroxy-2-nitrobenzaldehyde first had to be protected, Scheme 85.



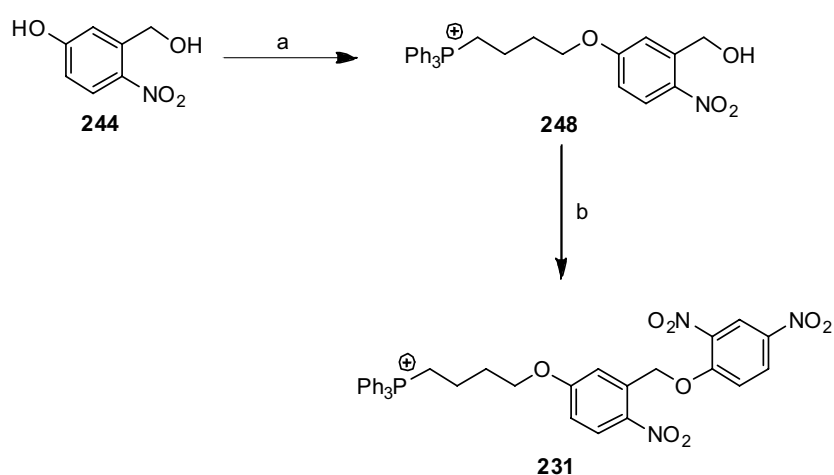
Scheme 85: Reagents and conditions: a) MOMCl, b) 1.1 eq. 2,3-DHP, cat. TsOH, DCM;

Attempts to protect the phenolic hydroxyl group as an acetal, either as a MOM **242** or THP **243** were unsuccessful. Both reactions afforded a complex mixture with no starting material or product observed. The next strategy was to protect the phenol motif as an acetate ester **245**, Scheme 86.



Scheme 86: Reagents and conditions: a) 1.1 eq. NaBH₄, MeOH; 99% b) i) 1.5 eq. KOH, H₂O, ii) 1.2 eq. Acetic anhydride 78% c) 1 eq. 2,4-dinitrofluorobenzene, cat NEt₃; 10% d) HCl, MeOH

The aldehyde **241** was first reduced to give benzyl alcohol **244** then the phenol selectively protected using acetic anhydride to afford the acetate **245**. The dinitrophenyl motif was then attached using 2,4-dinitrofluorobenzene as previously reported. The conjugated product **246** was produced in poor yield and had poor solubility which meant the deprotection to afford the phenol was unsuccessful. Therefore, an alternative synthetic pathway was carried out with introduction of the triphenylphosphonium group before the dinitrophenoxyl moiety despite the potential problems with purification.



Scheme 87: Reagents and conditions: a) 1.5 eq. (4-bromobutyl)triphenylphosphonium bromide, 1.1 eq. Cs₂CO₃, MeOH, Reflux; 51% b) 1 eq. 2,4-dinitrofluorobenzene, cat NEt₃ 42%

The phenolic hydroxyl group was selectively alkylated under alkaline conditions with (4-bromobutyl)triphenylphosphonium bromide to afford the phosphonium salt **248** as a dark red gum. The dinitrophenyl motif was then introduced by nucleophilic aromatic substitution of the fluoride from 2,4-dinitrofluorobenzene affording the target compound **231** in moderate 22% yield over two steps.

The probe was then tested by Prof. John McCarron and Dr Susan Chalmers at the University of Strathclyde. Smooth muscle cells were treated with the photoactivatable probe **231** (200 nM) together with a fluorescent marker tetramethylrhodamine ethyl ester (TMRE⁺, 10 nM). TMRE⁺ is a lipophilic cation and accumulates in mitochondria when there is a membrane-potential across the mitochondrial inner membrane. The mitochondria appeared as small fluorescent regions under the microscope and one illuminated region within a 10 mm diameter circle was irradiated at 355 nm for 0.1 s; irradiation caused loss of the fluorescence at that position indicating loss of membrane potential. Proper controls ruled out photobleaching and further studies have shown that switching of a single mitochondrion or small group of mitochondria in this way has a profound effect on the calcium-wave spreading through the smooth muscle during contraction.

10 Conclusions and future work

10.1 Conclusions

This thesis outlines a number of chemical tools which were designed for the study of oxidative stress and ageing. The dual sensor spin trap **72** reacted by two different mechanisms to produce radical adducts which were detected by EPR spectroscopy. The unique EPR signals observed provided distinction between oxygen-centred, carbon-centred and redox active metal ions.

A novel mitochondria-targeted spin trap, MitoSpin **90** was prepared utilising a novel method to construct the isoindolone core, a Parham type cyclisation. Although MitoSpin did not react sufficiently with superoxide radicals, reaction with hydroxyl radicals gave a distinctive EPR signal. In collaboration with Mike Murphy and Jan Trnka at MRC in Cambridge the oxidised product formed on reaction with hydroxyl adduct in the stressed mitochondria was detected by ESI-MS which alluded to a potential use as a ESI-MS probe for hydroxyl radicals. We also proved that MitoSpin accumulates within mitochondria with a membrane potential.

In addition a series of mitochondrial moderators were prepared. The type A moderators, which should release a mitochondrial uncoupler on reaction with radicals, were synthesized. Nevertheless, the moderator **200** proved to be unstable and the cyclopropanated derivative **182** did not release the uncoupler as expected.

However, Boronate DNP, **186** a type B moderator, which is activated upon reaction with hydrogen peroxide, was also prepared. Boronate DNP **186** reacted with hydrogen peroxide and afforded DNP^- with a second order rate constant of approximately $11 \text{ M}^{-1}\text{s}^{-1}$.

Finally a mitochondria-targeted, light activated probe **231** was synthesized. Subsequently Prof McCarron and Dr Chalmers at the University of Strathclyde have proved its ability to uncouple individual mitochondria within smooth muscle cells.

We have successfully prepared probes which detect and identify and ameliorate oxidative stress by scavenging ROS as well as probes which ameliorate oxidative stress by inhibiting the production of ROS.

10.2 Future Work

The use of ESI-MS probes for the study of oxidative stress shows a lot of promise therefore it would be advantageous to prepare MS probes which are selective for different ROS or react with other oxidation products.

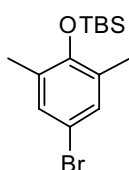
Furthermore, the results from the reaction of Boronate DNP and Boronate TEMPO with hydrogen peroxide are encouraging. It would be ideal if the preparation of the mitochondria-target versions is completed so the reactions with hydrogen peroxide could be studied *in vivo*.

Finally, we have only carried out preliminary investigations into the use of a light-activated probe. Therefore the uses of the light-activated probe warrant further exploration.

11 Experimental

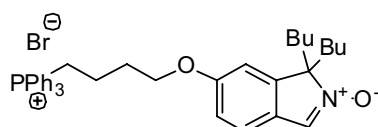
All reactions were carried out under an inert atmosphere unless otherwise stated, all glassware was either oven-dried or flame dried. All reagents were purchased from commercial suppliers and used without further purification. Column chromatography was carried out using Fisher Matrex TM silica gel (mesh size 35-70 μm). Thin layer chromatography was performed on aluminium backed silica gel plates of the same type used for chromatography and were visualised using UV light. ^1H , ^{13}C NMR spectra were obtained on a Bruker DPX/400 spectrometer operating at 400, 100 and MHz respectively. All coupling constants are measured in Hz. DEPT was used to assign the signals in the ^{13}C NMR spectra as C, CH, CH_2 or CH_3 . Infra-red (IR) spectra were obtained on a Shimadzu FTIR-8400S spectrometer using attenuated total reflectance (ATR) so that the IR spectrum of the compound (solid or liquid) could be directly detected (thin layer) without any sample preparation. Mass spectra were obtained employing electron impact ionisation on a Jeol M-Station, Dual Sector, High Resolution, Mass Spectrometer, unless otherwise stated. Solutions were added via syringe. THF was freshly distilled from sodium benzophenone. Dichloromethane was distilled from CaH_2 prior to use or tetrahydrofuran, dichloromethane, were dried where necessary using a solvent drying system, PuresolvTM, in which solvent is pushed from its storage container under low nitrogen pressure through two stainless steel columns containing activated alumina and copper. Acetone was dried over 4Å molecular sieves. MeOH and EtOH were distilled from Mg and stored over molecular sieves. Triethylamine was dried by distillation over calcium hydride and stored over potassium hydroxide. Reagents were obtained from commercial suppliers and used without further purification unless otherwise stated.

(4-Bromo-2,6-dimethylphenoxy)-*tert*-butyldimethylsilane 77



Following the procedure of Caldwell et al¹⁰⁹: Bromine (7.5 mL, 147 mmol) was added slowly to a solution of 2,6-dimethylphenol **190** (18.0 g, 147 mmol) in chloroform (450 mL). The solution was stirred at RT for 1h then washed with sat. Na₂O₃(aq). The organic layer was dried over MgSO₄ and concentrated *in vacuo*. The residue was dissolved in DCM (450 mL) then imidazole (20.0 g, 295 mmol) and TBSCl (23.3 g, 155 mmol) were added. The resulting cloudy solution was stirred overnight at RT then concentrated under vacuum. The residue was passed through a plug of silica eluting with hexane to give the bromide **77** as an oil (43.5 g, 94%). ¹HNMR, δ_H (CDCl₃, 400 MHz): 7.09 (2H, s, H-3 and H-5), 2.18 (6H, s, Me), 1.03 (9H, s, ^tBu), 0.19 (6H, s, Me₂Si). ¹³CNMR, δ_C (CDCl₃, 100 MHz): 151.33 (C), 131.19 (CH), 130.79 (C), 113.32 (C), 26.05 (CH₃), 17.62 (CH₃), - 2.96 (CH₃). IR (Thin Layer, cm⁻¹): 2957-2858 (C-H), 1472 (Ar). LRMS (EI) *m/z*: 316 [M⁺ (⁸¹Br), 29%], 314 [M⁺ (⁷⁹Br), 29], 259 [M⁺ (⁸¹Br) - ^tBu⁺, 91], 257 [M⁺ (⁷⁹Br) - ^tBu⁺, 92], 178 (M⁺ - CH₂=CMe₂ and HBr, 100). HRMS: 316.0687 and 314.0698. C₂₁H₂₉O₂⁸¹BrSi requires (M+), 316.0681; C₂₁H₂₉O₂⁷⁹BrSi requires (M+), 314.0702. Data is consistent with literature.¹¹⁰

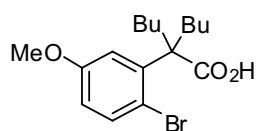
[4-(3',3'-Dibutyl-2'-oxy-3'H-isoindol-5'-yloxy)butyl]triphenylphosphonium bromide **90**



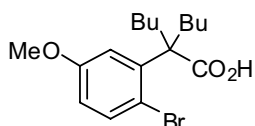
A stirred solution of nitrone **148** (500 mg, 1.9 mmol), cesium carbonate (686 mg, 2.10 mmol) and 4-bromobutyltriphenylphosphonium bromide (1.83 g, 3.83 mmol) in dry MeOH (15 mL) were heated to reflux for 48 h. The mixture was then partitioned between H₂O (20 mL) and EtOAc (20 mL) and the aqueous phase was extracted with EtOAc (2 x 20 mL). The combined organic extracts were dried over MgSO₄ and concentrated *in vacuo* to give a yellow solid foam. Recrystallization from EtOAc-hexane gave the nitrone as an amorphous solid (298 mg, 24%). Mp: decomposes at 84 °C. δ_H (CDCl₃, 400 MHz): 7.92-7.87 (6H, m, Ph), 7.80-7.77 (3H, m, Ph), 7.70-7.66 (6H, m, Ph), 7.64 (1H, s, CH=NO), 7.22 (1H, d, *J* = 8.4 Hz, H-7'), 6.85 (1H, dd, *J* = 8.4, 2.0, Hz H-6'), 6.73 (1H, d, *J* = 2.0 Hz, H-

4'), 4.19 (2H, t, $J = 5.8$ Hz, CH₂O), 4.06-4.03 (2H, m, CH₂), 2.35-2.25 (2H, m, 2 x CHCH^xH^y), 2.13-2.05 (2H, m, 2 x CHCH^xH^y), 1.96-1.63 (4H, m, 2 x CH₂), 1.25-1.14 (4H, m, 2 x CH₂), 0.99-0.82 (2H, m, CH₂), 0.75 (6H, t $J = 6.4$ Hz, 2 x CH₃), 0.61-0.48 (2H, m, CH₂). δ_c (CDCl₃, 100 MHz): 159.30 (C), 144.48 (C), 135.10 (CH), 133.82 (d, $J = 9.9$ Hz, CH), 133.58 (CH), 130.55 (d, $J = 12.6$ Hz, CH), 126.82 (C), 120.89 (CH), 118.84 (d, $J = 85.8$ Hz, C) 114.24 (CH), 108.41 (CH), 84.18 (C), 67.19 (CH₂), 37.21 (CH₂), 29.562 (d, $J = 16.6$ Hz), 24.83 (CH₂), 22.51 (CH₂), 22.05 (CH₂), 19.52 (CH₂), 13.90 (CH₃). IR (KBr, cm⁻¹): 3051 (C-H), 2929-2858 (C-H), 1683 (Ar), 1611 (Ar) 1586 (Ar), 1526 (Ar). LRMS (FAB/NOBA): 578 [M⁺ (phosphonium cation), 100]. HRMS: 578.3188. C₃₈H₄₅NO₂P requires 578.3188.

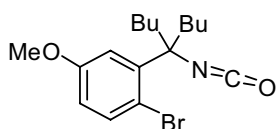
2-(2'-Bromo-5'-methoxyphenyl)-2-butylhexanoic acid 117



5 M KOH_(aq) (25 mL) was added to a stirred solution of ester **124** (10.0 g, 27.0 mmol) in DMSO (150 mL) and the resulting mixture heated to reflux overnight open to the atmosphere. The reaction was allowed to cool, was acidified with 5 M HCl_(aq) and extracted with EtOAc (3 x 200 mL). The combined organic extracts were washed with brine, dried over MgSO₄ and concentrated *in vacuo* to afford the carboxylic acid **117** as an off-white solid (8.08 g, 84%). A small portion was recrystallized from DCM to give needles. Mp: 163-165 °C. δ_H (CDCl₃, 400 MHz): 7.46 (1H, d, $J = 8.6$ Hz, H-3'), 6.91 (1H, d, $J = 3.0$ Hz, H-6'), 6.66 (1H, $J = 8.6$ Hz, 3.0 Hz, H-4'), 3.80 (3H, s, CH₃O), 2.24-2.16 (2H, m, C(CH^xH^y)₂), 1.99-1.92 (2H, m, C(CH^xH^y)₂), 1.33-1.25 (6H, m, 3x CH₂), 0.99-0.92 (2H, m, CH₂), 0.88 (6H, t, $J = 7.2$ Hz, 2 x CH₃). δ_c (CDCl₃, 100 MHz): 181.71 (C), 158.39 (C), 142.34 (C), 135.02 (CH), 116.99 (CH), 114.48 (C), 112.18 (CH), 55.46 (CH₃), 54.54 (C), 32.94 (CH₂), 26.09 (CH₂), 23.12 (CH₂), 14.03 (CH₃). IR (KBr, cm⁻¹): 3010-2955 (C-H), 2610 (acid O-H), 1703 (C=O), 1597 (Ar), 1570 (Ar). LRMS (EI⁺), m/z : 358 [M⁺ (⁸¹Br), 2%], 370 [M⁺ (⁷⁹Br), 2], 291 (M⁺ - ⁷⁹Br, 100), 85 (35). HRMS: 356.0987 and 358.0976. C₁₇H₂₅⁷⁹BrO₃ requires (M⁺) 356.0987 and C₁₇H₂₅⁸¹BrO₃ requires (M⁺) 358.0969.

2-(2'-Bromo-5'-methoxyphenyl)-2-butylhexanoic acid 117

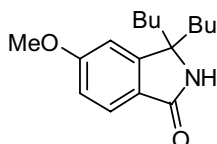
The ester **124** (100 mg, 0.27 mmol) and anhydrous Lil (1.35 mmol) were dissolved in anhydrous Pyridine (1 mL) then placed in a microwave reactor equipped with stirrer bar. The reactor was fitted with condenser and left open to the atmosphere then heated to 125 oC under a maximum microwave power of 250 W for 1 h at which time NMR analysis showed the reaction to be complete. The reaction mixture was washed with 20% conc. HCl solution (10 mL) and extracted into CHCl₃ (3 x 10mL). The organic layers were combined dried over magnesium sulphate then concentrated *in vacuo* to give a dark brown slurry. Upon addition of hexane the slurry separated into a brown solution and an off-white solid. The solid was isolated and found to be carboxylic acid **117** (67 mg, 70 %). Data as above.

1-Bromo-2-(5'-isocyanatonon-5'-yl)-4-methoxybenzene 118

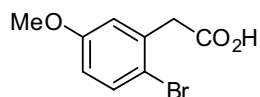
Triethylamine (9.2 mL, 66 mmol) was added to a stirred solution of carboxylic acid **117** (21.5 g, 60.2 mmol) in dry toluene (250 mL) at 0 °C under argon. Diphenylphosphoryl azide (14.3 mL, 66 mmol) was then added and the resulting mixture allowed to stir for 15 min before heating to reflux for 18 h. The reaction was then quenched with saturated ammonium chloride solution (200 mL) and the mixture extracted with Et₂O (3 x 200 mL). The combined organics were washed with brine (200 mL), dried over MgSO₄ and concentrated *in vacuo* to give a brown oil. Flash chromatography on silica gel eluting with hexane-EtOAc (4:1) gave the isocyanate **118** as an oil (20.8 g, 97%). *R_f* [SiO₂, hexane-Et₂O (4:1)]: 0.78 δ_H (CDCl₃, 400 MHz): 7.47 (1H, d, *J* = 8.8 Hz, H-3), 7.25 (1H, d, *J* = 2.8 Hz, H-6), 6.67 (1H, dd, *J* = 8.8, 2.8 Hz, H-4), 3.82 (3H, s, CH₃O), 2.74-2.66 (2H, m, C(CH^xH^y)₂), 1.90-1.83 (2H, m, C(CH^xH^y)₂), 1.43-1.22 (6H, m, 3 x CH₂), 1.00-0.84

(2H, m, CH₂), 0.70 (6H, t, $J = 7.6$ Hz, 2 x CH₃). δ_C (CDCl₃, 100 MHz): 158.73 (C), 141.33 (C), 136.18 (CH), 121.85 (C), 117.39 (CH), 113.54 (CH), 109.42 (C), 70.73 (C), 55.48 (CH₃), 40.81 (CH₂), 26.56 (CH₂), 22.71 (CH₂), 14.05 (CH₃). IR (Thin film, cm⁻¹) 3010-2850 (C-H), 2261 (N=C=O), 1592 (Ar), 1569 (Ar). MS, (EI⁺), m/z : 355 [M⁺ (⁸¹Br), 36%], 353 [M⁺ (⁷⁹Br), 36], 298 [M⁺ (⁸¹Br) - Bu⁺, 100], 296 [M⁺ (⁷⁹Br) - Bu⁺, 100], 242 [M⁺ (⁸¹Br) - Bu⁺ and C₄H₈, 60], 240 [M⁺ (⁷⁹Br) - Bu⁺ and C₄H₈, 61], 201 [(C₈H₈⁸¹BrO)⁺, 39], 199 [(C₈H₈⁷⁹BrO)⁺, 36], 174 (81). HMRS: 353.0990 and 355.0972. C₁₇H₂₄⁷⁹BrNO₂ requires (M⁺) 353.0990 and C₁₇H₂₄⁷⁹BrNO₂ requires (M⁺) 355.3970.

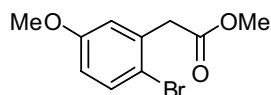
3,3-Dibutyl-2,3-dihydro-5-methoxyisoindol-1-one 119



^tBuLi (24 ml, 1 M in cyclohexane, titrated using 1,3-Diphenyl acetone-*p*-tosylhydrazone, 24 mmol) was added dropwise to a stirred solution of the isocyanate **118** (4.00 g, 11.8 mmol) in dry THF (100 mL) at -78 °C under argon. The resulting mixture was allowed to warm to RT and stirred overnight before ice cold water (100 mL) was added. The mixture was extracted with EtOAc (100 mL) and the organic layer was washed with brine (100 mL), dried over MgSO₄ and concentrated *in vacuo* to afford amide **119** as an amorphous solid (3.02 g, 93%). Mp: 96-97 °C. δ_H , (CDCl₃, 400 MHz): 7.71 (1H, d, $J = 8.4$ Hz, H-7), 6.93 (1H, dd, $J = 8.4, 2.2$ Hz, H-6), 6.75 (1H, d, $J = 2.2$ Hz, H-4), 5.88 (1H, s, NH), 3.87 (3H, s, CH₃O), 1.88-1.72 (4H, m, 2 x CH₂), 1.25-1.14 (6H, m, 3 x CH₂), 0.84-0.77 (8H, m, CH₂, 2 x CH₃). δ_C (CDCl₃, 100 MHz): 170.56 (C), 163.16 (C), 153.23 (C), 125.17 (CH), 125.06 (C), 113.85 (CH), 106.50 (CH), 64.80 (C), 55.75 (CH₃), 39.24 (CH₂), 25.62 (CH₂), 22.90 (CH₂), 14.01 (CH₃). IR (KBr, cm⁻¹) 3286 (N-H), 2955-2850 (C-H), 1693 (C=O), 1661 (Ar), 1606 (Ar) 1488 (Ar). LRMS (EI⁺), m/z : 275 (M⁺, 1.5%), 218 (M⁺ - Bu⁺, 100%). HRMS: 275.1885. C₁₇H₂₅O₂N requires (M⁺) 275.1885.

(2'-Bromo-5'-methoxyphenyl)acetic acid 121

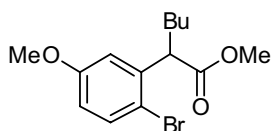
Bromine (8.3 mL, 162 mmol) was added drop-wise to a solution of 3-methoxyphenylacetic acid **120** (25.7 g, 154 mmol) in CHCl₃ (100 mL). The resulting mixture was allowed to stir overnight at RT and then poured into 20% aqueous sodium thiosulfate solution (300 mL). The layers were separated and the aqueous layer was extracted with CHCl₃ (200 mL). The combined organics were washed with 20% aqueous sodium thiosulfate solution (200 mL), dried over MgSO₄ and concentrated *in vacuo* to give the aryl bromide **121** as an off-white solid (37.9 g, 100%), a small portion was recrystallized from EtOAc-hexane to give plates. Mp 108-109 °C. δ_{H} (CDCl₃, 400 MHz): 7.46 (1H, d, J = 8.8 Hz, H-3'), 6.85 (1H, d, J = 3.0 Hz, H-6'), 6.74 (1H, dd, J = 8.8, 3.0 Hz, H-4'), 3.80 (2H, s, CH₂CO₂H), 3.78 (3H, s, OMe). δ_{C} (CDCl₃, 100 MHz): 176.50 (C), 158.95 (C), 134.27 (C), 133.40 (CH), 117.29 (CH), 115.46 (C), 114.84 (CH), 55.51 (CH₃), 41.49 (CH₂). IR (KBr cm⁻¹): 2949-2856 (C-H), 1692 (C=O), 1594 (Ar), 1571 (Ar). LRMS (EI⁺), m/z : 246 [M⁺ (⁸¹Br), 28%], 244 [M⁺ (⁷⁹Br), 28%], 201 [M⁺ (⁸¹Br) - [•]CO₂H, 20%], 199 [M⁺ (⁷⁹Br) - [•]CO₂H, 20%], 165 (M⁺ - [•]Br, 100%). HMRS: 243.9734. C₉H₉BrO₃ requires (M⁺) 243.9735. ¹H and ¹³C NMR matches literature¹¹⁰.

Methyl (2'-bromo-5'-methoxyphenyl)acetate 122

Concentrated sulfuric acid (6 drops) was added to a solution of the carboxylic acid **121** (37.9 g, 155 mmol) in methanol (150 mL). The resulting mixture was stirred at RT overnight. The reaction was concentrated *in vacuo* to approximately 20 mL and the mixture taken up in EtOAc (100 mL) and washed with 1 M NaOH_(aq) (50 mL), then with brine (100 mL). The organics were dried over MgSO₄ and concentrated *in vacuo* to give ester **122** (37.6 g, 98%) as a yellow oil, which crystallized on standing to give prisms. Mp: 38-40 °C δ_{H} (CDCl₃, 400

MHz): 7.43 (1H, d, $J = 8.8$ Hz, H-3'), 6.84 (1H, d, $J = 3.0$ Hz, H-6'), 6.70 (1H, dd, $J = 8.8, 3.0$ Hz H-4'), 3.77 (3H, s, CH₃O), 3.74 (2H, s, ArCH₂), 3.71 (3H, s, CH₃O). δ_c (CDCl₃, 100 MHz): 170.98 (C), 158.99 (C), 135.04 (C), 133.38 (CH), 117.22 (CH), 115.44 (C), 114.64 (CH), 55.53 (CH₃), 52.29, (CH₃), 41.73 (CH₂) IR (thin film, cm⁻¹) 3007 (Ar-H), 2952 (C-H), 1743 (C=O). LRMS (EI⁺), m/z : 260 [M⁺ (⁸¹Br), 16%], 258 [M⁺ (⁷⁹Br), 16], 179 (M⁺ - ⁷⁹Br, 100%). HMRS: 257.9892 and 259.9871. C₁₀H₁₁⁷⁹BrO₃ requires (M⁺) 257.9892, and C₁₀H₁₁⁸¹BrO₃ requires (M⁺) 259.9872. Data is consistent with literature.¹¹¹

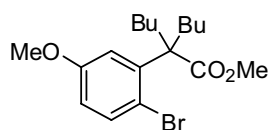
Methyl 2-(2'-bromo-5'-methoxyphenyl)hexanoate 123



n-BuLi (43 mL, 2.5M in hexane, 109 mmol) was added dropwise to a stirred solution of diisopropylamine (15 mL, 109 mmol) in dry THF (150 mL) at -78 °C under argon ensuring that the internal temperature remained below -60 °C. The resulting solution was allowed to stir for 15 min and a solution of methyl ester 122 (25 g, 99 mmol) in dry THF (200 mL) was added drop-wise ensuring that the internal temperature remained below -60 °C. The reaction mixture was allowed to stir for 15 min and then butyl iodide (12.0 mL, 109 mmol) was added drop-wise. The mixture was allowed to warm to RT and stirred overnight. The reaction was quenched by the addition of ice cold H₂O and extracted with Et₂O. The organic layer was washed with H₂O, dried over MgSO₄, and concentrated *in vacuo* to give a brown oil. The oil was purified using flash chromatography on silica gel eluting with hexane followed by hexane-Et₂O (3:2) to afford the ester 123 as a yellow oil (20.7 g, 91%). R_f [SiO₂, hexane-Et₂O (3:2)]: 0.63. δ_H (CDCl₃, 400 MHz): 7.43 (1H, d, $J = 8.8$ Hz, H-3'), 6.93 (1H, d, $J = 3.1$ Hz, H-6'), 6.67 (1H, dd, $J = 8.8, 3.1$ Hz H-4'), 4.09 (1H, t, $J = 7.5$ CHBu), 3.77 (3H, s, CH₃O), 3.65 (3H, s, CH₃O), 2.07-1.98 (1H, m, CHCH^XH^Y), 1.78-1.70 (1H, m, CHCH^XH^Y), 1.36-1.21 (4H, m, CH₂CH₂CH₃), 0.82 (3H, t, $J = 6.9$ Hz, CH₂CH₃). δ_c (CDCl₃, 100 MHz): 174.04 (C), 159.21 (C), 139.87 (C), 133.46 (CH), 115.28 (CH), 114.34 (C), 114.34 (CH), 55.50 (CH₃), 52.13 (CH₃) 49.99 (CH), 33.16 (CH₂), 29.62 (CH₂), 22.58 (CH₂),

13.98 (CH₃). IR (thin film, cm⁻¹) 3010-2800 (C-H), 1737 (C=O), 1595 (Ar), 1572 (Ar). LRMS (EI⁺), *m/z*: 316 [M⁺ (⁸¹Br), 49%], 314 [M⁺ (⁷⁹Br), 49%], 257 [M⁺ (⁸¹Br) - ^tBu, 12%], 314 [M⁺ (⁷⁹Br) - ^tBu, 12%], 235 [M⁺ - ^tBr, 100]. HMRS: 314.0518 and 316.047. C₁₄H₁₉⁷⁹BrO₃ requires (M⁺) 314.0518, and C₁₄H₁₉⁸¹BrO₃ requires (M⁺) 316.0499

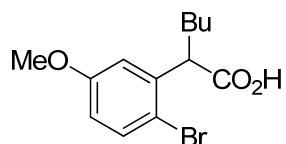
Methyl 2-(2'-bromo-5'-methoxyphenyl)-2-butylhexanoate 124



n-BuLi (39 mL, 2.5 M in hexane, 99 mmol) was added dropwise to a stirred solution of diisopropylamine (14 mL, 99 mmol) in dry THF (150 mL) at -78 °C under argon ensuring that the internal temperature remained below -60 °C. The resulting solution was allowed to stir for 15 min and a solution of ester **123** (28.4 g, 90.1 mmol) in dry THF (200 mL) was added drop-wise ensuring that the internal temperature remained below -60 °C. The reaction mixture was allowed to stir for 15 min and then butyl iodide (11 mL, 99 mmol) was added drop-wise. The mixture was allowed to warm to RT and stirred overnight. The reaction was quenched by the addition of ice cold H₂O and extracted with Et₂O. The organic layer was washed with H₂O, dried over MgSO₄, and concentrated *in vacuo* to give a brown oil. Flash chromatography on silica gel eluting with hexane followed by hexane-Et₂O (3:2) afforded the ester **124** as a yellow oil which crystallized on standing and was washed with hexane to give the ester as a an amorphous solid (22.9 g, 93%). Mp: 53-54 °C. R_f [SiO₂, hexane-Et₂O (3:2)]: 0.65. δ_H (CDCl₃, 400 MHz): 7.45 (1H, d, *J* = 8.7 Hz, H-3'), 6.91 (1H, d, *J* = 3.0 Hz, H-6'), 6.65 (1H, dd, *J* = 8.7, 3.0 Hz, H-4'), 3.81 (3H, s, CH₃O), 3.67 (3H, s, CH₃O), 2.20-2.12 [2H, m, C(CH^xH^y)₂], 1.99-1.92 [2H, m, C(CH^xH^y)₂], 1.32-1.24 (4H, m, 2 x CH₂), 1.11-1.05 (2H, m, CH₂), 0.96-0.90 (8H, m, CH₂, 2 x CH₃). δ_C (CDCl₃, 100 MHz): 175.94 (C), 158.36 (C), 142.97 (C), 134.90 (CH), 116.87 (CH), 114.33 (C), 111.94 (CH), 55.41 (CH₃), 54.48 (C) 52.15 (CH₃) 33.26 (CH₂), 26.15 (CH₂), 23.11 (CH₂), 14.01 (CH₃). IR (thin layer, cm⁻¹) 3010-2800 (C-H), 1732 (C=O), 1596 (Ar). LRMS (EI⁺), *m/z*: 372 [M⁺ (⁸¹Br), 3%], 370 [M⁺ (⁷⁹Br), 3], 291 (M⁺ - ^tBr, 100). HRMS: 372.1125 and

370.1143. $C_{18}H_{27}^{81}BrO_3$ requires (M^{++}) 372.1125 and $C_{18}H_{27}^{79}BrO_3$ requires (M^{++}) 370.1144.

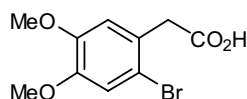
2-(2'-Bromo-5'-methoxyphenyl)-hexanoic acid 125



n BuLi (2.5 mL, 2.5 M in hexanes, 4.1 mmol) was added to a stirred solution of diisopropylamine (0.60 mL, 4.3 mmol) in dry THF (7 mL) under argon which had been cooled to -78 °C ensuring the temperature did not rise above -60 °C. The solution was stirred for 15 min before a solution of (2'-bromo-5'-methoxyphenyl)acetic acid 121 (500 mg, 2.0 mmol) in THF (4 mL) was added dropwise again ensuring the temperature did not rise above -60 °C. The resulting mixture was allowed to stir for 15 min before iodobutane (0.6 mL, 4.1 mmol) was added dropwise. The reaction mixture was allowed to warm to RT under argon overnight. The mixture was then quenched with ice-cold water (20 mL) and washed with Et_2O (2 x 20 mL). The aqueous phase was acidified with 1 M $HCl_{(aq)}$ and extracted with Et_2O (3 x 20 mL). The organic extracts were combined, washed with brine, dried over $MgSO_4$ then concentrated *in vacuo* to afford a light brown oil. The oil was filtered through silica eluting with hexane followed by EtOAc. The EtOAc fractions were concentrated *in vacuo* to give the acid 125 (602 mg, 98 %) as a white powder, a small portion was recrystallized from EtOAc-hexane to give prisms Mp: $63-65$ °C. δ_H ($CDCl_3$, 400 MHz): 7.46 (1H, d, $J = 8.8$ Hz, H-3'), 6.94 (1H, d, $J = 3.2$ Hz, H-6'), 6.70 (1H, dd, $J = 8.8, 3.2$ Hz, H-4'), 4.15 (1H, t, $J = 7.6$ Hz, CH), 3.78 (3H, s, OCH_3), 2.07-2.01 (1H, m, $CHCH^xH^y$), 1.79-1.74 (1H, m, $CHCH^xH^y$), 1.33-1.21 (4H, m, 2 x CH_2), 0.88 (3H, t, $J = 6.8$ Hz, CH_2CH_3). δ_C ($CDCl_3$, 400 MHz): 179.44 (C), 159.13 (C), 139.07 (C), 133.46 (CH), 115.46 (C), 114.60 (CH), 114.38 (CH), 55.49 (CH_3), 49.85 (CH), 32.68 (CH_2), 29.42 (CH_2), 22.48 (CH_2), 13.88 (CH_3). IR (ATR, cm^{-1}): 2964 (C-H), 2941 (C-H), 2870 (C-H), 2652 (CO_2H), 1699 (C=O), 1599 (Ar), 1572 (Ar), 1471 (Ar). LRMS (EI^+), m/z : 302 [M^{++} (^{81}Br), 98 %], 300 [M^{++} (^{79}Br), 98], 246 [M^{++} (^{81}Br) - $\cdot Bu$, 22], 244 [M^{++} (^{79}Br) - $\cdot Bu$, 22], 201 [M^{++} (^{81}Br) - $\cdot Bu$, - CO_2H 100], 199 [M^{++} (^{79}Br) -

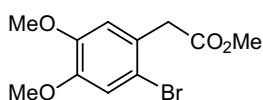
$^{\bullet}\text{Bu}$, - CO_2H 100]. HMRS: 300.0361 and 302.0343. $\text{C}_{13}\text{H}_{17}^{79}\text{BrO}_3$ requires ($\text{M}^{+\bullet}$) 300.0361, and $\text{C}_{13}\text{H}_{17}^{81}\text{BrO}_3$ requires ($\text{M}^{+\bullet}$) 302.0342.

(2-Bromo-4,5-dimethoxyphenyl)acetic acid **131**



Bromine (1.4 mL, 28 mmol) was added dropwise to a stirred solution of 4,5-dimethoxyphenyl) acetic acid **130** (5.00 g, 25.5 mmol) in chloroform (100 mL). The resulting mixture was stirred overnight, open to the atmosphere. The mixture was then quenched with sat. aqueous $\text{Na}_2\text{S}_2\text{O}_3$ (100 mL) and allowed to stir for 10 min. The aqueous phase was washed with chloroform (2 x 200 mL) and the organic layers were combined, dried over MgSO_4 and concentrated *in vacuo* to give the aryl bromide **131** as a solid (6.88 g, 98%). Mp: 114-116 °C, (prisms from hexane-EtOAc) (Lit¹¹² mp, 113-115 °C). δ_{H} , (CDCl_3 , 400 MHz): 7.02 (1H, s, H-3 or H-6), 6.79 (1H, s, H-3 or H-6), 3.87 (3H, s, OCH_3), 3.86 (3H, s, OCH_3), 3.77 (2H, s CH_2). δ_{C} (CDCl_3 , 100 MHz): 177.06 (C), 149.11 (C), 148.54 (C), 125.31 (C), 115.58 (CH), 115.19 (C), 134.02 (CH), 56.28 (CH_3), 56.21 (CH_3), 40.98 (CH_2). IR (ATR, cm^{-1}): 2987 - 2837 (O-H + C-H), 1695 (C=O), 1607 (Ar), 1508 (Ar) LRMS (EI^+), m/z : 276 [$\text{M}^{+\bullet}$ (^{81}Br), 68%], 274 [$\text{M}^{+\bullet}$ (^{79}Br), 68], 231 [$\text{M}^{+\bullet}$ (^{81}Br) - $\cdot\text{CO}_2\text{H}$, 100], 229 [$\text{M}^{+\bullet}$ (^{79}Br) - $\cdot\text{CO}_2\text{H}$, 100], 195 ($\text{M}^{+\bullet}$ - $\cdot\text{Br}$, 38). HRMS: 273.9837 and 275.9832. $\text{C}_{10}\text{H}_{11}^{79}\text{BrO}_4$ requires ($\text{M}^{+\bullet}$) 273.9841, and $\text{C}_{10}\text{H}_{11}^{81}\text{BrO}_4$ requires ($\text{M}^{+\bullet}$) 275.9821. Mp and ^1H NMR data is consistent with literature.¹¹²

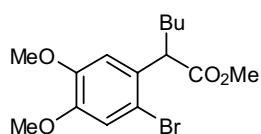
Methyl (2'-bromo-4',5'-dimethoxyphenyl)acetate **132**



Concentrated sulfuric acid (5 drops) was added to a solution of the carboxylic acid **131** (6.80 g, 24.8 mmol) in methanol (70 mL). The resulting mixture was

allowed to stir at RT overnight and then the reaction quenched with sat. Aqueous NaHCO₃ (100 mL). The mixture was extracted with diethyl ether (3 x 200 mL) and the organic layers combined, dried over MgSO₄ and concentrated *in vacuo* to give the ester **132** (6.95 g, 97 %) as a prism. Mp: 66-68 °C. δ_{H} , (CDCl₃, 400 MHz): 7.04 (1H, s, H-3' or H-6'), 6.80 (1H, s, H-3' or H-6'), 3.87 (3H, s, CH₃), 3.86 (3H, s, CH₃), 3.69 (3H, s, CH₃), 3.68 (2H, s, CH₂). δ_{C} (CDCl₃, 100 MHz): 171.37 (C), 148.90 (C), 148.48 (C), 126.03 (C), 115.56 (CH), 115.04 (C), 113.95 (CH), 56.26 (CH₃), 56.16 (CH₃), 52.26 (CH₃), 41.06 (CH₂). IR (ATR, cm⁻¹): 3010 - 2839 (C-H), 1722 (C=O), 1604 (Ar), 1510 (Ar). LRMS (EI⁺), *m/z*: 290 [M⁺ (⁸¹Br), 51%], 288 [M⁺ (⁷⁹Br), 51], 231 [M⁺ (⁸¹Br) - ¹⁴C=O, 100], 229 [M⁺ (⁷⁹Br) - ¹⁴C=O, 100], 209 (M⁺ - ⁷⁹Br, 97). HRMS: 288.005 and 289.9987. C₁₁H₁₃⁷⁹BrO₄ requires (M⁺) 287.9997, and C₁₁H₁₃⁸¹BrO₄ requires (M⁺) 289.9978. ¹H NMR data similar to literature where NMR was run at 300 Hz¹¹²

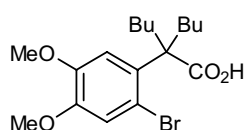
Methyl 2-(2'-bromo-4',5'-dimethoxy-phenyl)hexanoate **133**



ⁿBuLi (59.0 mL, 2.5 M in hexanes, 150 mmol) to a stirred solution of dry diisopropylamine (21.7 mL, 160 mmol) in dry THF (200 mL) under argon which had been cooled to -78 °C and the resulting mixture was stirred for 15 min. Methyl (2'-bromo-4',5'-dimethoxyphenyl)acetate **132** (28.0 g, 90 mmol) in THF (300 mL) was then added ensuring the temperature did not rise above -60 °C. The resulting mixture was allowed to stir for 15 min before iodobutane (16.5 mL, 150 mmol) was added dropwise. The reaction mixture was allowed to warm to RT overnight before quenching with H₂O (500 mL). The resulting mixture was extracted with Et₂O (3 x 300 mL) and the organic extracts combined, dried over MgSO₄ and concentrated *in vacuo* to afford a brown oil. The oil was filtered through silica gel eluting with hexane followed by EtOAc. The ethyl acetate fractions were concentrated *in vacuo* to give **133** as a yellow oil (33.0 g, 98%). δ_{H} (CDCl₃, 400 MHz): 7.00 (1H, s, H-3' or H-6'), 6.84 (1H, s, H-3' or H-6'), 4.00 (1H, t, *J* = 7.6, CH), 3.79 (3H, s, OCH₃), 3.77 (3H, s, OCH₃), 3.59 (3H, s, OCH₃), 1.98-1.91 (1H, m, CHCH^{*x*}H^{*y*}), 1.69-1.60 (1H, m, CHCH^{*x*}H^{*y*}), 1.29-1.22 (3H, m, 2 x CH₂),

0.89-0.53 (4H, m, CH₃, CH₂). ¹³CNMR, δ_C (CDCl₃, 100 MHz): 174.22 (C), 148.62 (C), 148.47 (C), 130.60 (C), 115.27 (CH), 114.54 (C), 110.78 (CH), 55.72 (CH₃), 51.85 (CH₃), 47.54 (CH), 33.07 (CH₂), 29.70 (CH₂), 22.58 (CH₂), 13.80 (CH₃). IR (KBr, cm⁻¹): 2956 (C-H), 2871 (C-H) 1736 (C=O), 1603 (Ar), 1509 (Ar). LRMS (EI⁺), *m/z*: 346 [M⁺ (⁸¹Br), 31%], 344 [M⁺ (⁷⁹Br), 31], 265 [M⁺ - ·Br, 100]. HRMS: 346.0604 and 344.0623. C₁₅H₂₁⁸¹BrO requires (M⁺) 346.0603 and C₁₅H₂₁⁷⁹BrO₄ requires (M⁺) 344.0623.

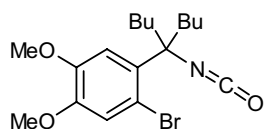
2-(2-Bromo-4,5-dimethoxy-phenyl)-2-butyl-hexanoic acid 134



A stirred solution of monoalkylated ester **133** (33.0 g, 90.0 mmol) was cooled to -78 °C. LDA, freshly prepared as before using ⁿBuLi (57.6 mL, 0.14 mol) and dry diisopropylamine (21.6 mL, 0.15 mol) in dry THF (200 mL) was added dropwise by cannulation and the mixture was allowed to stir for 15 min. Iodobutane (16.4 mL) was added dropwise then the resulting mixture was allowed to warm to RT and was stirred overnight. The reaction was quenched with water (500 mL) and the resultant mixture extracted with Et₂O (3 x 300 mL). The organic extracts were combined washed with brine (200 mL), dried over MgSO₄ and concentrated *in vacuo* to give a dark brown oil. The oil was filtered through silica gel eluting with hexane followed by EtOAc. The EtOAc fractions were combined and concentrated *in vacuo* to give a dark brown oil. The resulting oil contained a 2:1 mixture of dialkylated ester and an unknown impurity which was inseparable by column chromatography or kugle röhre distillation. The impure ester (13.0 g) was dissolved in DMSO (150 mL) and then 7 N KOH (75 mL) was added. The resulting mixture was heated stirred under reflux overnight. The mixture was allowed to cool and then acidified with 5 M HCl_(aq), washed with brine, dried over MgSO₄ and concentrated *in vacuo* to afford the carboxylic acid **134** as an off-white solid (6.9 g, 22%). Mp: 118-121°C (prisms EtOAc). δ_H (CDCl₃, 400 MHz): 7.08 (1H, s, H-3' or H-6'), 6.87 (1H, s, H-3' or H-6'), 3.92 (3H, s, OCH₃), 3.88 (3H, s, OCH₃), 2.26-2.18 (2H, m, 2 x CHCH^xH^y), 2.03-1.95 (2H, m, 2 x CHCH^xH^y), 1.40-1.33 (4H, m, 2

x CH₂), 1.22-1.16 (2H, m, CH₂), 1.33-0.99 (2H, m, CH₂), 0.75 (6H, t, *J* = 7.2 Hz, 2 x CH₃CH₂). δ_C (CDCl₃, 100 MHz): 181.93 (C), 147.99 (C), 147.48 (C), 133.39 (C), 117.41 (CH), 114.19 (C), 112.73 (CH), 56.24 (CH₃), 56.04 (CH₃), 54.24 (C), 33.30 (CH₂), 26.19 (CH₂), 23.15 (CH₂), 14.04 (CH₃). IR (KBr, cm⁻¹): 3185 (O-H Stretch), 2951-2868 (C-H Stretch), 1719 (C=O Stretch), 1494 (C=C Aromatic Stretch), 1465 (C=C Aromatic Stretch). LRMS (EI⁺), *m/z*: 388 [M⁺ (⁸¹Br), 5%], 386 [M⁺ (⁷⁹Br), 5%], 307 (M⁺ - ⁷⁹Br, 100). HRMS: 386.1095 and 388.1071. C₁₈H₂₇⁸¹BrO₄ requires (M⁺) 386.1093 and C₁₈H₂₇⁷⁹BrO₄ requires (M⁺) 388.1072.

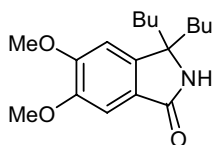
1-Bromo-4,5-dimethoxy-2-(5'-isocyanatonon-5'yl)benzene 135



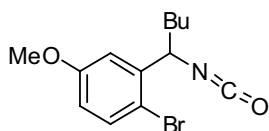
A stirred solution of acid **134** (500 mg, 1.3 mmol) in toluene (2 mL) was cooled to below 0 °C using a salt-ice bath. Triethylamine (0.20 mL, 1.4 mmol) was added dropwise followed by diphenylphosphoryl azide (0.22 mL, 1.4 mmol). The reaction mixture was then allowed to stir for 5 min before warming to RT. The mixture was then heated to reflux for 48 h. The reaction mixture was allowed to cool, was washed with ice-cold saturated aqueous sodium hydrogen carbonate solution (10 mL) followed by ice-cold brine (10 mL). The aqueous phases were washed with chloroform (2 x 10 mL). The organic layers were combined, dried over magnesium sulphate, and concentrated *in vacuo* to afford a dark brown oil. Column chromatography, on silica gel, eluting with EtOAc-hexane (1:19) gave isocyanate **135** (Rf. 0.70) as an oil (222 mg, 58 %). δ_H (CDCl₃, 400 MHz): 7.13 (1H, s, H-3 or H-6), 6.95 (1H, s, H-3 or H-6), 3.83 (3H, s, OCH₃), 3.80 (3H, s, OCH₃), 2.65-2.57 (2H, m, 2x CHCH^xH^y), 1.82-1.74 (2H, m, 2 x CHCH^xH^y), 1.30-1.18 (6H, m, 6H from CH₂), 0.91-0.85 (2H, m, 4H from CH₂), 0.77 (6H, t, *J* = 7.0 Hz). δ_C (CDCl₃, 100 MHz): 147.03 (C), 146.59 (C), 131.34 (C), 120.88 (C), 117.00 (CH), 112.67 (CH), 107.84 (C), 69.54 (C), 55.15 (CH₃), 54.99 (CH₃), 43.30 (CH₂), 25.48 (CH₂), 21.58 (CH₂), 12.94 (CH₃). IR (NaCl, cm⁻¹): 2958 (C-H), 2931 (C-H), 2169 (C-H), 2268 (C=N=O), 1591 (Ar), 1569 (Ar), 1464 (Ar). LRMS, (EI⁺), *m/z*: 385 [M⁺ (⁸¹Br), 28 %], 383 [M⁺ (⁷⁹Br), 28], 329 [M⁺ (⁸¹Br) - CH₂=CHCH₂CH₃, 100], 327 [M⁺

(^{79}Br) - - $\text{CH}_2=\text{CHCH}_2\text{CH}_3$, 100], 273 [M^{++} (^{81}Br) - 2 x $\text{CH}_2=\text{CHCH}_2\text{CH}_3$, 55], 271 [M^{++} (^{79}Br) - 2 x $\text{CH}_2=\text{CHCH}_2\text{CH}_3$, 56]. HMRS: 385.1078 and 383.1094. $\text{C}_{18}\text{H}_{26}^{81}\text{BrNO}_3$ requires (M^{++}) 385.1076 and $\text{C}_{18}\text{H}_{26}^{79}\text{BrNO}_3$ requires (M^{++}) 383.1096.

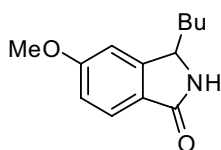
3,3-Dibutyl-2,3-dihydro-5,6-dimethoxy-isoindol-1-one 136



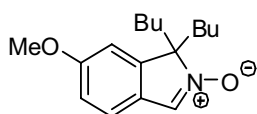
A stirred solution of isocyanate **135** (50 mg, 0.13 mmol) in dry THF (2 mL) under argon was cooled to -78°C then $^t\text{BuLi}$ (0.17 mL, 1 M in hexanes, 0.26 mmol) was added dropwise. The reaction mixture turned bright yellow immediately. The solution was allowed to warm to RT and was stirred overnight. The reaction was slowly quenched by adding ice-cold water (10 mL), the yellow solution became colourless, and was then extracted into chloroform (2 x 10 mL). The organic extracts were combined, washed with brine (10 mL), dried over magnesium sulphate and concentrated *in vacuo* to afford the lactam **136** as a solid (21.2 mg, 58%). δ_{H} (CDCl_3 , 400 MHz): 7.20 (1H, s, H-4 or H-7), 6.62 (1H, s, H-4 or H-7), 3.89 (3H, s, OCH_3), 3.87 (3H, s, OCH_3), 1.79-1.65 (4H, m, 4H from 2 x CH_2), 1.20-1.11 (6H, m, 6H from 4 x CH_2), 0.82-0.69 (8H, m, 2H from 2 x CH_2 , 6H from 2 x CH_3). δ_{C} (CDCl_3 , 100 MHz): 169.68 (C), 151.95 (C), 148.37 (C), 413.40 (C), 123.30 (C), 104.16 (CH), 102.13 (CH), 63.58 (C), 55.27 (CH_3), 55.16 (CH_3), 38.04 (CH_2), 24.53 (CH_2), 21.78 (CH_2), 12.89 (CH_3). IR (KBr, cm^{-1}): 3214 (N-H Stretch) 2910-2858 (C-H Stretch), 1682 (C=O Stretch), 1613 (C=C aromatic Stretch), 1497 (C=C aromatic Stretch). MS, (EI^+), m/z : 305 [M^{++} , 18%], 248 [M^{++} - Bu^{\bullet} , 100], 206 [M^{++} - Bu^{\bullet} , $\text{CH}_2=\text{CH}_2\text{CH}_3$, 12], 190 [M^{++} - 2 x BuH , 13]. HRMS: 305.1991. $\text{C}_{18}\text{H}_{27}\text{NO}_3$ requires (M^{++}) 305.1991.

1-Bromo-2-(1-isocyanatopentyl)-4-methoxy- 144

The carboxylic acid **125** (0.50 g, 1.7 mmol) was dissolved in dry toluene (2 mL) under argon and the solution cooled to below 0 °C using a salt-ice bath. Triethylamine (0.20 mL, 1.8 mmol) was added dropwise followed by diphenylphosphoryl azide (0.29 mL, 1.8 mmol). The reaction mixture was allowed to stir for 5 min before warming to RT. The mixture was then heated at reflux for 24 h. The reaction mixture was allowed to cool, then washed with ice-cold saturated aqueous sodium hydrogen carbonate solution (10 mL) followed by ice-cold brine (10 mL). The aqueous phases were washed with chloroform (2 x 10 mL) and the organic layers were combined, dried over magnesium sulfate, then concentrated *in vacuo* to afford a dark brown oil. Column chromatography, on silica gel, eluting with EtOAc-hexane (1:19) gave the isocyanate **144** as an oil (215 mg, 43 %). R_F [hexane:EtOAc(19:1)]. 0.71. δ_H (CDCl₃, 400 MHz): 7.41 (1H, d, J = 8.8 Hz, H-6), 7.02 (1H, d, J = 3.0 Hz, H-3), 6.72 (1H, dd, J = 8.8, 3.0 Hz, H-5), 5.02 (1H, dd, J = 9.1, 4.1 Hz, CH), 3.82 (3H, s, OCH₃), 1.87-1.80 (1H, m, CHCH^xH^y), 1.74-1.64 (1H, m, CHCH^xH^y), 1.47-1.32 (4H, m, 2 x CH₂), 0.93 (3H, t, J =7.2 Hz, CH₃). δ_C (CDCl₃, 100 MHz): 158.34 (C), 140.49 (C), 132.50 (CH), 122.16 (C), 113.85 (CH), 112.01 (CH), 110.94 (C), 57.47 (CH), 54.49 (CH₃), 36.83 (CH₂), 27.33 (CH₂), 21.07 (CH₂), 12.91 (CH₃). IR (KBr, cm⁻¹): 3003-2860 (C-H Stretch), 2259 (N=C=O stretch), 1596 (C=C aromatic Stretch), 1573 (C=C Aromatic Stretch) MS, (EI⁺), m/z : 299 [M^{++} (⁸¹Br), 94], 297 [M^{++} (⁷⁹Br), 94], 242 [M^{++} (⁸¹Br) - Bu[•] 100], 240 [M^{++} (⁷⁹Br)- Bu[•] 100], 162 [M^{++} - CH₂=CHCH₂CH₃ and Br[•] 95]. HMRS: 297.0365 and 299.0344. C₁₃H₁₆O₂N⁷⁹Br requires (M^{++}) 297.0364 and C₁₃H₁₆O₂N⁸¹Br requires (M^{++}) 299.0345.

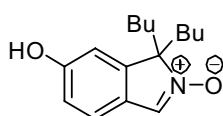
3-Butyl-2,3-dihydro-5-methoxyisoindol-1-one 145

A stirred solution of isocyanate **144** (100 mg, 0.30 mmol) in dry THF (2 mL) under argon was cooled to -78°C then $t\text{BuLi}$ (0.56 mL, 1.7 M in hexanes, 0.7 mmol) was added dropwise. The reaction mixture turned bright red immediately. The solution was allowed to warm to RT overnight, then slowly quenched by the dropwise addition of ice-cold water (10 mL). The red solution became colourless, and was extracted with CHCl_3 (2 x 10 mL). The organic extracts were combined, washed with brine (10 mL), dried over MgSO_4 and concentrated *in vacuo* to afford a brown oil. Column chromatography, on silica gel, eluting with EtOAc-hexane (1:9) afforded the isoindolone **145** as a light brown oil (16.1 mg, 22%). $^1\text{H NMR}$, δ_{H} (CDCl_3 , 400 MHz): 7.68 (1H, d, $J=8.7$, H-7), 6.92 (1H, dd, $J=8.7, 2.9$ Hz, H-6), 6.81 (1H, d, $J=2.9$ Hz, H-4), 4.47 (1H, dd, $J=7.6, 4.4$ Hz, H-3), 3.71 (3H, s, OCH_3), 1.89-1.83 (1H, m, $\text{CHCH}^{\text{x}}\text{H}^{\text{y}}$), 1.60-1.50 (1H, m, $\text{CHCH}^{\text{x}}\text{H}^{\text{y}}$), 1.41-1.15 (4H, m, 2 x CH_2), 0.82 (3H, t, $J=7.4$ Hz). $^{13}\text{C NMR}$, δ_{C} (CDCl_3 , 100 MHz): 171.01 (C), 163.07 (C), 150.12 (C), 125.19 (CH), 123.89 (C), 114.50 (CH), 107.37 (CH), 56.63 (CH), 56.63 (CH_3), 34.43 (CH_2), 27.61 (CH_2), 22.64 (CH_2), 13.93 (CH_3). IR (KBr, cm^{-1}): 3241 (N-H Stretch), 2960-2858 (C-H Stretch), 1683 (C=O Stretch), 1607 (C=C aromatic Stretch), 1489 (C=C Aromatic Stretch). MS, (EI^+), m/z : 219 ($\text{M}^{+\bullet}$, 14%), 162 ($\text{M}^{+\bullet} - \text{Bu}^{\bullet}$, 100).

1,1-Dibutyl-6-methoxy-1-H-isoindole-2-oxide 147

The hydrochloride salt **146** (500 mg, 1.68 mmol) was dissolved in MeOH (5 mL) then NaOH (70.5 mg, 1.68 mmol), Na₂WO₄ (58.0 mg, 0.17 mmol) and 30% H₂O₂ in H₂O (0.57 mL, 5.04 mmol) were added. The resulting mixture was then allowed to stir at RT under argon for 3 days. The reaction was then quenched with 20% Na₂S₂O₃ in brine (10 mL) and extracted into EtOAc (3 x 10 mL). The organic extracts were combined dried over MgSO₄ and concentrated to give an orange oil. Column chromatography, on silica gel, eluting with EtOAc-hexane (3:7) gave the nitron **147** as a pale orange solid (157 mg, 34%). δ_{H} , (CDCl₃, 400 MHz): 7.67 (1H, s, H-3), 7.25 (1H, d, $J = 8.4$ Hz, H-4), 6.88 (1H, dd, $J = 8.4, 1.6$ Hz, H-5), 6.75 (1H, d, $J = 1.6$ Hz, H-7), 3.87 (3H, s, OCH₃), 2.14-2.07 (2H, m, 2 x CHCH^xH^y), 1.87-1.79 (2H, m, 2 x CHCH^xH^y), 1.30-1.11 (4H, m, 2 x CH₂), 1.02-0.91 (2H, m, CH₂), 0.77 (6H, t, $J = 7.2$, CH₃), 0.64-0.58 (2H, m, CH₂). δ_{C} (CDCl₃, 100 MHz): 159.98 (C), 144.48 (C), 133.56 (C), 126.85 (C), 120.82 (CH), 112.98 (CH), 108.28 (CH), 84.10 (C), 55.62 (CH₃), 37.20 (CH₂), 24.77 (CH₂), 22.48 (CH₂), 13.82 (CH₃). IR (KBr, cm⁻¹): 3100-2800 (C-H), 1588 (Ar), 1525 (Ar). MS (EI⁺), m/z : 275 (M⁺, 18%), 258 (M⁺ - [•]OH, 82), 219 (M⁺ - C₄H₈, 100), 202 (M⁺ - C₄H₈ and [•]OH, 41), 176 [M⁺ - C₄H₈ and [•]Pr, 96], 160 (M⁺ - C₄H₈, C₃H₆ and [•]OH, 32). HRMS: 275.1885. C₁₇H₂₅O₂N requires (M⁺) 275.1885.

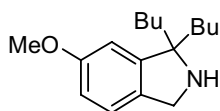
3,3-Dibutyl-2-oxy-3H-isoindol-5-ol **148**



Sodium tungstate (1.00 g, 3.0 mmol) and hydrogen peroxide (2.1 mL, 90 mmol) were added to a stirred solution of amine **150** (1.50 g, 6.1 mmol) in dry methanol (20 mL) and the resulting mixture allowed to stir at RT for 72 h. The reaction mixture was then quenched with 20% aqueous sodium sulfite solution and extracted with DCM (3 x 50 mL). The combined organic extracts were washed with brine, dried over MgSO₄ and concentrated *in vacuo* to give an orange foam. The foam was triturated with EtOAc to give an off-white solid **148** (980 mg, 61%). A small portion was recrystallized from hexane-EtOAc to give prisms. Mp: 193-195 °C δ_{H} (CDCl₃, 400 MHz): 9.53 (1H, s, OH), 7.70 (1H, s, H-1),

7.34 (1H, d, $J = 8.4$ Hz, H-7), 6.86 (1H, dd, $J = 8.4, 2.0$, H-6), 6.74 (1H, d, $J = 2.0$ Hz, H-4), 2.09-2.02 (2H, m, 2 x CHCH^xH^y), 1.82-1.75 (2H, m, 2 x CHCH^xH^y), 1.18-0.99 (4H, m, 2 x CH₂), 0.93-0.81 (2H, m, CH₂), 0.71 (6H, t, $J = 6.4$ Hz, 2 x CH₃), 0.60-0.48 (2H, m, CH₂). δ_c (CD₃OD, 400 MHz): 160.82 (C), 146.81 (C), 139.29 (CH), 125.71 (C), 123.72 (CH), 116.73 (CH), 110.07 (CH), 85.11 (C), 37.69 (CH₂), 25.88 (CH₂), 23.38 (CH₂), 14.14 (CH₃). IR (KBr, cm⁻¹): 3439 (OH), 2954-2857 (C-H), 1587 (Ar), 1537 (Ar). LRMS (EI⁺), m/z : 261 (M⁺, 10%), 244 (M⁺ - [•]OH, 23), 216 (M⁺ - H₂O and HCN, 58), 205 (M⁺ - C₄H₈, 69%), 188 (M⁺ - [•]OH and C₄H₈, 37), 162 (M⁺ - C₄H₈ and [•]Pr, 100), 146 (M⁺ - [•]Bu and BuH, 32). HRMS: 261.1729. C₁₆H₂₃NO₂ requires (M⁺) 261.1729.

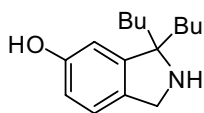
1,1-Dibutyl-2,3-dihydro-6-methoxy-1*H*-isoindole 149



Borane-THF complex was added over 20 min to a stirred solution of amide **119** (3.50 g, 12.7 mmol) in dry THF (50 mL) at 0 °C under argon and the mixture allowed to stir for 1 h. After this time the mixture was heated to reflux for 48 h. The reaction was then quenched by the slow addition of ice cold H₂O (100 mL). 1M NaOH_(aq) (50 mL) was added and the mixture extracted with Et₂O (2 x 100 mL). The combined organic extracts were washed with brine (100 mL), dried over MgSO₄ and then concentrated *in vacuo* to give an oil **149** (3.30 g, 99%). δ_H (CDCl₃, 400 MHz): 7.16 (1H, d, $J = 8.4$ Hz, H-4), 6.77 (1H, dd, $J = 8.4, 2.4$ Hz, H-5), 6.61 (1H, d, $J = 2.4$ Hz, H-7), 4.14 (2H, s, CH₂NH), 3.82 (3H, s, OCH₃), 2.05-1.65 (4H, m, 2 x CH₂), 1.26-1.23 (6H, m, 3 x CH₂), 1.10-1.04 (2H, m, CH₂), 0.89 (6H, t, $J = 7.2$ Hz, CH₃). The amine **149** was dissolved in Et₂O (20 mL) and ethereal HCl added affording the salt **146** as a white precipitate. Mp: decomposed at 210 °C. δ_H (CDCl₃, 400 MHz): 10.19 (2H, s, NH₂), 7.17 (1H, d, $J = 8.4$ Hz, H-4), 6.88 (1H, dd, $J = 8.4, 2.2$ Hz, H-5), 6.59 (1H, d, $J = 2.2$ Hz, H-7), 4.60 (2H, s, CH₂), 3.82 (3H, s, OCH₃), 2.13-1.96 (4H, m, 2 x CH₂), 1.57-1.48 (2H, m, CH₂), 1.42-1.23 (6H, m, 3 x CH₂), 0.91 (6H, t, $J = 7.2$ Hz, CH₃). δ_c (CDCl₃, 400 MHz): 160.27 (C), 143.38 (C), 125.75 (C), 123.90 (CH), 114.35 (CH), 108.18 (CH), 75.66 (C), 55.66 (CH₃), 48.51 (CH₂), 37.30 (CH₂), 25.63 (CH₂), 22.71 (CH₂), 13.95 (CH₃). IR (KBr, cm⁻¹): 3010-2800 (C-H), 2717 (C-H), 1621 (Ar), 1588 (Ar). MS,

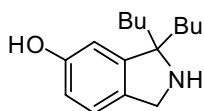
(Cl⁺), *m/z*: 262 [M+H⁺ (amine), 82%], 218 [M+H⁺ (amine) - BuH, 24], 79 (100%). HRMS: 262.2171. C₁₇H₂₈ON requires [M+H⁺ (amine)] 262.2171.

3,3-Dibutyl-2,3-dihydro-1*H*-isoindol-5-ol 150



BBr₃ (54 mL of a 1 M solution in DCM 54mmol) was added drop-wise to a solution amine **149** (4.00 g, 15.3 mmol) in dry DCM (100 mL) at 0 °C under argon. The reaction mixture was then allowed to warm to RT for 72 h. After this time the reaction was quenched with ice-cold water. The mixture was basified with 1 M NaOH_(aq) and extracted with DCM (3 x 100 mL). The combined organics were washed with brine, dried over MgSO₄ and concentrated *in vacuo* to give phenol **150** as an amorphous solid (3.52 g, 93%). Mp: 110-111 °C. δ_H (CD₃OD, 400 MHz): 7.21 (1H, d, *J* = 8.3 Hz, H-7), 6.84 (1H, dd, *J* = 8.3, 2.2 Hz, H-6), 6.65 (1H, d, *J* = 2.2 Hz, H-4), 4.46 (2H, s, CH₂NH), 2.09-2.02 (2H, m, 2 x CHCH^xH^y), 1.93-1.85 (2H, m, 2 x CHCH^xH^y), 1.45-1.32 (6H, m, 3 x CH₂), 1.26-1.16 (2H, m, CH₂), 0.88 (6H, t, *J* = 7.1 Hz, CH₃). δ_C (CD₃OD, 400 MHz): 159.77 (C), 143.88 (C), 125.17 (C), 125.07 (CH), 117.64 (CH), 110.37 (CH), 76.62 (C), 49.68 (CH₂), 37.45 (CH₂), 26.56 (CH₂), 23.82 (CH₂), 14.20 (CH₃). IR (KBr, cm⁻¹): 3433 (O-H), 3310 (N-H), 2955-2931 (C-H), 2858 (C-H), 1612 (Ar), 1481 (Ar), 1465 (Ar). LRMS (Cl⁺), *m/z*: 248 [M+H⁺ (amine), 100%], 190 [M+H⁺ (amine) - BuH, 25]. HRMS: 248.2014 C₁₆H₂₆NO requires [M+H⁺ (amine)] 248.2014.

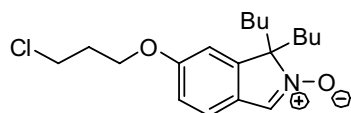
3,3-Dibutyl-2,3-dihydro-1*H*-isoindol-5-ol 150



The hydrochloride salt **148** (100 mg, 0.34 mmol) was dissolved in 78% HBr (2mL) and the resulting mixture heated to reflux and stirred overnight. The reaction mixture was allowed to cool then basified with 1 N KOH and extracted into

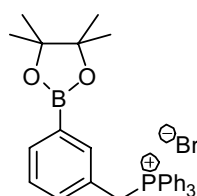
EtOAc (3 x 50 mL). The organic extracts were dried over MgSO₄ and concentrated *in vacuo* to afford phenol **150** as a yellow solid. (45.7 mg, 55%). Data as above.

1,1-Dibutyl-6-(3chloropropoxy)-1*H*-isoindole-2-oxide **154**



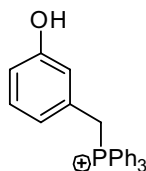
Phenol **148** (100 mg, 0.38 mmol) was taken up in anhydrous DMF (5 mL) then anhydrous CsCO₃ (124 mg, 0.38 mmol) was added followed by the 1,3-bromochloropropane (0.1 mL, 0.8 mmol) under argon. The stirred reaction mixture was then heated to 120 °C and stirred at this temperature under argon for 2 d. After this time the reaction was cooled and partitioned between H₂O (20 mL) and DCM (20 mL). The organic layer was washed three times with H₂O (20 mL) followed by brine (20 mL) before drying over MgSO₄ and concentrating *in vacuo* to give a brown oil. Column chromatography, on silica gel, eluting with MeOH:DCM (1:19-1:4) gave alkyl chloride **154** as an oil. (17 mg, 14 %). δ_{H} (CDCl₃, 400 MHz): 7.37 (1H, s, H-1'), 7.11 (1H, d, *J* = 8.4 Hz, H-4'), 6.82 (1H, dd, *J* = 8.4, 2.0, Hz H-5'), 6.69 (1H, d, *J* = 2.0 Hz, H-7'), 4.09 (2H, t, *J* = 6.0 Hz, CH₂O), 3.71 (2H, t, *J* = 6.4 Hz, CH₂Cl), 2.22-2.19 (2H, m, CH₂), 2.03-1.98 (2H, m, CH₂), 1.78-1.73 (2H, m, CH₂), 1.18-1.24 (4H, m, 2 x CH₂), 0.82-0.74 (4H, m, 2 x CH₂), 0.71 (6H, t *J* = 6.4 Hz, 2 x CH₃), 0.60-0.48 (2H, m, CH₂ LRMS, (Cl⁺), *m/z*: : 340 [M+H (³⁷Cl), 10%], 338 [M+H (³⁵Cl), 28%], 222 [M+H (³⁷Cl)-H₂O, 43%], 220 [M+H (³⁵Cl) - H₂O, 100%].

[3-(4',4',5',5'-Tetramethyl-1',3',2'-dioxaborolan-2'-yl)benzyl]triphenyl phosphonium bromide **161**



A solution of bromide **178** (500 mg, 1.7 mmol) and PPh₃ (446 mg, 1.7 mmol) were heated under reflux in dry toluene (5 mL) under argon for 36 h. The white precipitate formed was filtered off and recrystallised from EtOAc-hexane yielding the phosphonium salt **161** as an amorphous solid (360 mg, 38%). Mp: 220 °C (decomposes). δ_{H} (CD₃OD, 400 MHz): 7.93-7.90 (3H, m, 3 × *p*-H of PPh₃), 7.76-7.63 (13H, m, H-6 and 6 × *o*-H and 6 × *m*-H of PPh₃), 7.31 (1H, s, H-2), 7.27 (1H, t, *J* = 7.6 Hz, H-5), 7.17 (1H, d, *J* = 7.6 Hz, H-4), 4.92 (2H, d, *J* = 14.9 Hz, CH₂P), 1.30 (12H, s, 2 × Me₂C). δ_{C} (CD₃OD, 100 MHz): 138.71 (CH), 136.46 (CH, d, *J* = 3.0 Hz), 135.85 (CH), 135.41 (CH, d, *J* = 9.7 Hz), 134.91 (CH, *J* = 5.6 Hz), 131.34 (CH, d, *J* = 12.2 Hz), 129.54 (CH), 128.09 (C, d, *J* = 8.1 Hz), 119.06 (C, d, *J* = 85.7 Hz), 85.26 (C), 30.72 (CH₂, *J* = 48.5 Hz), 25.18 (CH₃). IR (ATR, cm⁻¹): 2970 (C-H), 2859 (C-H), 2839 (C-H), 2778 (C-H), 1435 (PPh₃). LRMS (FAB/NOBA): 479 [M⁺ (phosphonium cation), 100%]. HRMS: 479.2307. C₃₁H₃₃O₂PB requires [M⁺ (phosphonium cation)] 479.2317.

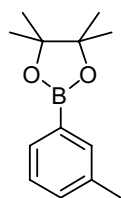
(3-Hydroxybenzyl)triphenylphosphonium bromide **162**



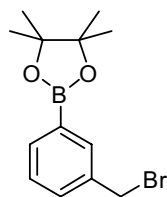
Aqueous hydrogen peroxide (1.7 mL, 50% w/w, 0.84 mmol) was added to a stirred solution of the benzylic bromide **176** (50 mg, 0.17 mmol) in a 1:2 mixture of saturated aqueous NaHCO₃ and MeOH (5 mL). The resulting mixture was stirred for 2 h then diluted with H₂O (5 mL) and extracted into Et₂O (5 mL). The organic layer was dried over MgSO₄ and concentrated *in vacuo* to afford the phenol **179** as an oil. Due to the instability of the phenol it was carried on without further purification. The bromide was dissolved in PhMe (3 mL) and Ph₃P (45 mg, 0.17 mmol) added. The reaction mixture was then heated to reflux and allowed to stir overnight. The precipitate formed was filtered off and recrystallised from EtOH to give (3-hydroxybenzyl)triphenylphosphonium bromide **162** (53 mg, 56 %) as an amorphous solid. Mp: 290-291 °C (decomposes). δ_{H} (CD₃OD, 400 MHz): 7.94-7.90 (3H, m, 3 × *p*-H of PPh₃), 7.77-

7.64 (12H, m, 6 × *o*-H and 6 × *m*-H of PPh₃), 7.05 (1H, t, *J* = 7.6 Hz, H-5), 6.76 (1H, d, *J* = 7.6 Hz, H-4), 6.45 (1H, d, *J* = 7.6 Hz, H-6), 6.44 (1H, s, H-2), 4.83 (2H, d, *J* = 15.2 Hz, CH₂P). δ_C (CD₃OD, 100 MHz): 159.20 (C), 136.41 (CH, d, *J* = 3.2 Hz), 135.39 (CH, d, *J* = 10.0 Hz), 131.31 (CH, d, *J* = 12.1 Hz), 131.12 (CH), 129.91 (C), 123.03 (CH, d, *J* = 6.1 Hz), 119.31 (C, d, *J* = 86.5 Hz), 119.08 (CH, d, *J* = 5.0 Hz), 116.74 (CH, d, *J* = 4.2 Hz), 30.72 (CH₂, *J* = 48.3 Hz) IR (ATR, cm⁻¹): 3078 (OH), 2884 (C-H), 2859 (C-H), 2787 (C-H), 1610 (Ar), 1587 (Ar), 1483 (PPh₃). LRMS (FAB/NOBA): 369 [M⁺ (phosphonium cation), 100%]. HRMS: 369.1404. C₂₅H₂₂OP requires [M⁺ (phosphonium cation)] 369.1408. ¹H NMR data in broad agreement with those reported for the compound in CDCl₃.¹¹²

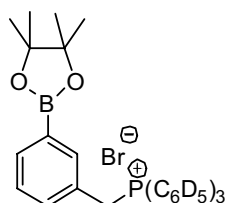
2-(3'-Methylphenyl)-4,4,5,5-tetramethyl-1,3,2-dioxaborolane **175**



^tBuLi (21.0 mL of a 1.7 M solution in hexanes, 35.1 mmol) was added dropwise to a stirred solution of bromide **174** (3.00 g, 17.5 mmol) in dry THF (40 mL) under argon at -78 °C. After 15 min, the boronate (11.9 mL, 58.3 mmol) was added dropwise. The solution was allowed to stir for 1 h before quenching with ice-cold H₂O (20 mL). The mixture was extracted with EtOAc (30 mL) and the organic layer washed with brine (30 mL), dried over MgSO₄ and concentrated *in vacuo* at 60 °C for 3 h affording the boronic ester **175** as an oil (3.59 g, 94%). δ_H (CDCl₃, 400 MHz): 7.64-7.60 (2H, m, ArH), 7.28-7.27 (2H, m, ArH), 2.36 (3H, s, CH₃Ar), 1.35 (12H, 2 × Me₂C). δ_C (CDCl₃, 100 MHz): 137.18 (C), 135.50 (CH), 132.18 (CH), 131.96 (CH), 127.84 (CH), 83.80 (C), 25.00 (CH₃), 21.42 (CH₃). IR (ATR, cm⁻¹): 2982 (C-H), 2924 (C-H), 1605 (Ar), 1582 (Ar). MS, (Cl⁺), *m/z*: 219 (M+H⁺, 100%). HRMS: 219.1553. C₁₃H₂₀O₂B requires (M+H⁺) 219.1559. ¹H and ¹³C NMR in good agreement with literature.¹¹³

2-[3'-(Bromomethyl)phenyl]-4,4,5,5-tetramethyl-1,3,2-dioxaborolane 176

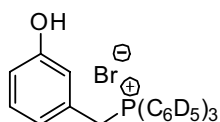
NBS (1.71 g, 9.6 mmol) and benzoyl peroxide (40 mg, 0.2 mmol) were added to a stirred solution of the boronic ester **175** (2.00 g, 9.2 mmol) in CCl₄ (25 mL). The resulting mixture was heated under reflux overnight. The mixture was allowed to cool and then concentrated *in vacuo*. The resulting oil was dissolved in DCM (100 mL) and washed with H₂O (100 mL). The organic layer was dried over MgSO₄ and concentrated to dryness and the yellow solid recrystallised from hexane affording the bromide **176** as prisms (1.47 g, 54%) Mp: 89-92 °C. δ_{H} (CDCl₃, 400 MHz): 7.82 (1H, s, H-2'), 7.74 (1H, d, $J = 7.5$ Hz, H-6'), 7.50 (1H, d, $J = 7.5$ Hz, H-4'), 7.36 (1H, t, $J = 7.5$ Hz, H-5'), 4.50 (2H, s, CH₂Br), 1.35 (12H, s, 2 × Me₂C). δ_{C} (CDCl₃, 100 MHz): 137.24 (C), 135.32 (CH), 134.92 (CH), 132.10 (CH), 128.40 (CH), 84.09 (C), 33.63 (CH₂), 25.00 (CH₃). IR (ATR, cm⁻¹): 2978 (C-H), 1602 (Ar). MS, (Cl⁺), m/z : 299 [M+H⁺ (⁸¹Br), 26%], 297 [M+H⁺ (⁷⁹Br), 26], 219 (53), 217 (57), 89 (100). HRMS: 297.0665 and 299.0634. C₁₃H₁₉O₂⁷⁹BrB requires (M+H⁺) 297.0664 and C₁₃H₁₉O₂⁸¹BrB requires (M+H⁺) 299.0645. Compound mentioned in literature¹¹⁴, but no spectral data provided.

[3-(4',4',5',5'-Tetramethyl-1',3',2'-dioxaborolan-2'-yl)benzyl]tris(penta deuterophenyl) phosphonium bromide 177

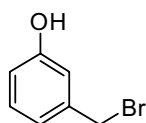
A solution of bromide **176** (500 mg, 1.7 mmol) and triphenylphosphine-d₁₅ (446 mg, 1.7 mmol) were heated under reflux in dry toluene (3 mL) under argon for

24 h. The white precipitate formed was filtered off and then recrystallised from EtOAc-hexane yielding the phosphonium salt **177** as an amorphous solid (790 mg, 81%). Mp: 220 °C (decomposes). δ_{H} (CD₃OD, 400 MHz): 7.69 (1H, d, $J = 7.6$ Hz, H-6), 7.29 (1H, s, H-2), 7.26 (1H, t, $J = 7.6$ Hz, H-5), 7.16 (1H, d, $J = 7.6$ Hz, H-4), 4.75 (2H, d, $J = 15.2$ Hz, CH₂P), 1.29 (12H, s, 2 × Me₂C). δ_{C} (CD₃OD, 100 MHz): 138.78 (CH, d, $J = 5.0$ Hz), 135.79 (CH, d, $J = 3.1$ Hz), 136.20-134.55 (m), 131.09-130.71 (m), 129.54 (CH, d, $J = 3.2$ Hz), 128.18 (C, d, $J = 9.1$ Hz), 117.51 (C, d, $J = 86.6$ Hz), 85.31 (C), 30.81 (CH₂, $J = 47.3$ Hz), 25.25 (CH₃). IR (ATR, cm⁻¹): 2974 (C-H), 2868 (C-H), 2839 (C-H), 2777 (C-H), 1433 (PPh₃). LRMS (FAB/NOBA): 494 [M⁺ (phosphonium cation), 100%]. HRMS: 494.3247. C₃₁H₃₃O₂PB requires [M⁺ (phosphonium cation)] 494.3253.

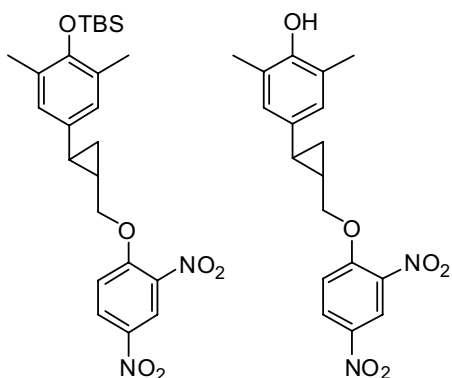
(3-Hydroxybenzyl)tris(pentadeuterophenyl)phosphonium bromide **178**



In the same way except using triphenylphosphine-d₁₅ instead of Ph₃P, the benzylic bromide **176** (50 mg, 0.17 mmol) gave (3-hydroxybenzyl)tris(pentadeuterophenyl)phosphonium **178** (65 mg, 67%) as prisms after recrystallisation from EtOH. Mp: 295-296 °C (decomposes). δ_{H} (CD₃OD, 400 MHz): 7.03 (1H, t, $J = 7.6$ Hz, H-5), 6.74 (1H, d, $J = 7.6$ Hz, H-4), 6.44 (1H, d, $J = 7.6$ Hz, H-6), 6.42 (1H, s, H-2), 4.81 (2H, d, $J = 15.2$ Hz, CH₂P). δ_{C} (DMSO, 100 MHz): 157.53 (C, d, 3.3 Hz), 135.0-134.3 (m), 133.9-133.3 (m), 130.3-129.3 (m), 129.04 (CH, d, $J = 8.6$ Hz), 121.37 (CH, d, $J = 5.5$ Hz), 117.81 (CH, d, $J = 5.5$ Hz), 117.74 (C, d, $J = 85.5$ Hz), 115.30 (CH), 28.15 (CH₂, $J = 48.3$ Hz). IR (ATR, cm⁻¹): 3078 (OH), 2887 (C-H), 2858 (C-H), 2787 (C-H), 1616 (Ar), 1587 (Ar), 1483 (PPh₃). LRMS (FAB/NOBA): 384 [M⁺ (phosphonium cation), 100%]. HRMS: 384.2354. C₂₅H₇D₁₅OP requires [M⁺ (phosphonium cation)] 384.2350.

3-(Bromomethyl)phenol 179

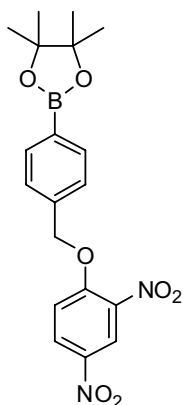
For synthesis of **179** see experimental for **162** (3-hydroxybenzyl)triphenyl phosphonium bromide

2,6-Dimethyl-4-[2'-(2'',4''-dinitrophenoxymethyl)cyclopropyl]- phenol 182 and 1-{2'-[4''-(*tert*-Butyldimethylsilyloxy)-3'',5''-dimethylphenyl] cyclopropyl-1'-yl}methoxy-2,4,dinitrobenzene 195

The alcohol (200 mg, 0.65 mmol) was dissolved in dry Et₂O (1 mL) under argon and 2,4-dinitrofluorobenzene (79 μL, 0.66 mmol) added to the resulting solution and the mixture stirred at RT overnight. The reaction mixture was then concentrated *in vacuo* affording crude silyl protected compound as an inseparable mixture with 2,4-dinitrofluorobenzene. ¹H NMR, data for TBS ether **195** δ_H (CDCl₃, 400 MHz): 8.75 (1H, d, *J*= 2.8 Hz, H-3), 8.25 (1H, dd, *J*= 9.2, 2.8 Hz, H-5), 7.21 (1H, d, *J*= 9.2 Hz, H-6), 6.71 (2H, s, H-2'' and H-6''), 4.32-4.19 (2H, m, CH₂O), 2.16 (6H, s, 2 x MeAr), 1.94-1.89 (1H, m CH), 1.56-1.50 (1H, m, CH), 1.10-1.01 (2H, m), 0.96 (9H, s, ^tBu), 0.16 (6H, s, 6H, Me₂Si). The yellow oil was dissolved in DCM (1 mL) and TBAF (650 μL, 1 M soln. in DCM, 0.65 mmol) added before allowing to stir overnight. The reaction was diluted with DCM (10

mL) washed with H₂O (10 mL), dried over MgSO₄ and concentrated under vacuum. Column chromatography, on silica gel, eluting with EtOAc-hexane (3:10) affording the phenol **182** as a pale yellow oil (58 mg, 25%). (*R*_F = 0.25) ¹H NMR data for phenol δ_H (CDCl₃, 400 MHz): 8.85 (1H, d, *J* = 2.8 Hz, H-3''), 8.25 (1H, dd, *J* = 9.3, 2.8 Hz, H-5''), 6.85 (2H, s), 6.72 (1H, d, *J* = 9.3 Hz, H-6'') 3.67-3.59 (2H, m, CH₂O), 2.08 (6H, s, 2 x MeAr), 1.83-1.78 (1H, m, CH), 1.49-1.40 (1H, m, CH), 0.97 (2H, dd, *J* = 6.9, 7.3 Hz, CH₂). δ_C (CDCl₃, 100 MHz): 155.81 (C), 147.40 (C), 141.35 (C), 140.96 (C), 138.29 (C), 130.26 (C), 129.15 (CH), 127.01 (CH), 122.45 (CH), 115.82 (CH), 66.48 (CH₂), 25.54 (CH), 20.86 (CH), 16.16 (CH₃), 13.93 (CH₂). IR (ATR, cm⁻¹): 3103-2992 (CH), 1602 (Ar), 1533 (Ar). LRMS (Cl⁺), *m/z*: 359 [M+H⁺, 59%], 341 [M+H⁺ - H₂O, 100], 329 [M+H⁺ - CH₂=O, 38], 175 [M+H⁺ - DNP]. HRMS: 359.1245. C₁₈H₁₉O₆N₂ (M+H) requires 359.1243.

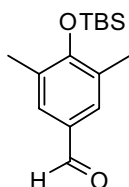
2-[4'-(2'',4''-Dinitrophenoxymethyl)phenyl]-4,4,5,5-tetramethyl-1,3,2-dioxaborolane **186**



Benzylic alcohol **214** (200 mg, 0.854 mmol) was mixed with 2,4-dinitrofluorobenzene (0.11 mL, 0.41 mmol) and 2 drops of anhydrous NEt₃ added. The reaction mixture was allowed to stir at RT overnight then the solution concentrated *in vacuo* the resulting slurry triturated with Et₂O and the pale yellow solid was filtered and recrystallized from EtOAc-hexane to afford Boronate DNP **186**. (72 mg, 21%). Mp: 141-143°C, prisms. δ_H (CDCl₃, 400 MHz): 8.76 (1H, d, *J* = 2.7 Hz, H-3''), 8.36 (1H, dd, *J* = 2.7, 9.2 Hz, H-5''), 7.84 (2H, d, *J* = 8.3 Hz, H-2' and H-6'), 7.43 (2H, d, *J* = 8.3 Hz, H-3' and H-5'), 7.20 (1H, d, *J* = 9.2 Hz, H-6''), 5.39 (2H, s, ArCH₂), 1.34 (12H, s, 4 x Me). δ_C (CDCl₃, 100 MHz): 156.31 (C), 140.28 (C), 139.22 (C), 137.04 (C), 135.43 (CH), 129.09 (CH),

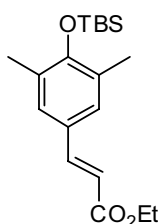
126.24 (CH), 121.98, (CH), 115.14 (CH), 84.09 (C), 72.05 (CH₂), 24.94 (CH₃). IR (thin layer, cm⁻¹): 3120 (C-H), 3080 (C-H), 2992 (C-H), 2982 (C-H), 1604 (Ar), 1522 (NO₂), 1356 (NO₂), LRMS (Cl⁺), *m/z*: 401 [M+H⁺, 12%], 273 [16], 233 [50], 219 [100]. HRMS: 401.1519. C₁₉H₂₂N₂O₇B (M+H⁺) requires 401.1520.

4-(*tert*-Butyldimethylsilyloxy)-3,5-dimethylbenzaldehyde **191**



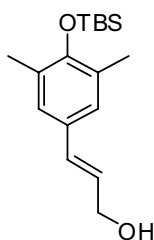
Adapting the procedure of Caldwell¹⁰⁹: a stirred solution of bromide **77** (1.00 g, 3.2 mmol) in dry THF (10 mL) under argon was cooled to -78°C and ⁿBuLi (1.3 mL, 2.5 M in hexanes, 3.2 mmol) was added dropwise and the resulting mixture stirred for 20 min before the dropwise addition of DMF (0.25 mL, 3.2 mmol). After stirring for 1 h the reaction mixture was poured onto ice-cold water and the aqueous phase washed with DCM (3 x 20 mL). The organic layers were combined, dried over MgSO₄ and concentrated under vacuum to give aldehyde **191** as a yellow oil. (0.838 g, 78 %). δ_H (CDCl₃, 400 MHz): 10.01 (1H, s, CHO), 7.65 (2H, s, H-2 and H-6), 2.39 (6H, s, CH₃Ar), 1.19 (9H, s, ^tBu), 0.39 (6H, s, Me₂Si). ¹³CNMR, δ_C (CDCl₃, 100 MHz): 191.44 (CH), 158.14 (C), 130.85 (CH), 129.53 (C), 128.67 (C), 26.16 (CH₃), 18.85 (C), 17.84 (CH₃), -2.74(CH₃). IR (KBr, cm⁻¹): 2931 (C-H), 2859 (C-H), 2718 (C-H), 1695 (C=O), 1598 (Ar), 1474 (Ar). MS, (Cl⁺), *m/z*: 275 [M+H, 100%], 218 [M+H -CH=O, 9%]. HRMS: 265.1625. C₁₅H₂₅OSi requires (M+H) 265.1624.

Ethyl (*E*)-3-[4'-(*tert*-butyldimethylsilyloxy)-3',5'-dimethylphenyl] acrylate **192**



Lithium Chloride (69 mg, 2.3 mmol) was added to dry MeCN (1 mL) and stirred under argon for 15 min until dissolved. DBU (0.34 mL, 2.2 mmol) and triethyl phosphonoacetate (0.45 mL, 2.3 mmol) were then added dropwise followed by aldehyde **191** (500 mg, 1.9 mmol) and the reaction mixture allowed to stir overnight. After this time the reaction was concentrated *in vacuo*, and the residue taken up in EtOAc, then washed with H₂O. The organic layer was dried over MgSO₄ and concentrated to give the α,β -unsaturated ester **192** (478 mg, 78%). Mp: 47-51°C, (prisms from hexane). δ_{H} (CDCl₃, 400 MHz): 7.49 (1H, d, J = 14.0 Hz, CH=CHCO₂Et), 7.06 (2H, s, H-2' and H-6'), 6.23 (1H, d, J = 14.0 Hz, CH=CHCO₂Et), 4.15 (2H, q, J = 6.4 Hz, CH₂CH₃), 2.12 (6H, s, 2 x MeAr), 1.23 (3H, t, J = 6.4 Hz, CH₂CH₃), 0.94 (9H, s, ^tBu), 0.11 (6H, s, Me₂Si). δ_{C} (CDCl₃, 100 MHz): 167.56 (C), 154.55 (C), 144.78 (CH), 129.27 (C), 129.00 (CH), 127.62 (C), 115.82 (CH), 60.36 (CH₂), 26.16 (CH₃), 18.89 (C), 17.94 (CH₃), 14.37 (CH₃), - 2.77 (CH₃). IR (NaCl, cm⁻¹): 2930-2718 (C-H), 1691 (C=O), 1598 (Ar), 1473 (Ar). MS, (EI⁺), m/z : 334 [M⁺, 41%], 289 [M⁺ - OCH₂CH₃, 10], 277 [M⁺ - ^tBu, 100]. HRMS: 334.1962. C₁₉H₃₀O₃Si, requires (M⁺) 334.1964.

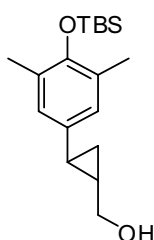
(E)-3-[4'-(tert-Butyldimethylsilyloxy)-3',5'-dimethylphenyl]prop-2-en-1-ol 193



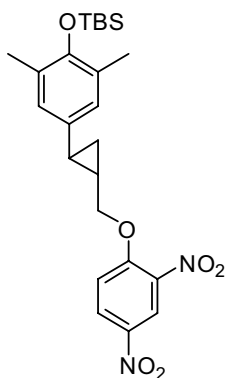
DIBAL (1.3 mL, 1.3 mmol) was added dropwise to a stirred solution of ester **192** (200 mg, 0.6 mmol) in dry DCM (5 mL), under argon, cooled to 0 °C the solution was allowed to warm to RT and stirred overnight. After this time the reaction was filtered through cellite and concentrated *in vacuo* to give a yellow oil. Column chromatography, on silica gel, eluting with EtOAc-hexane (1:19) afforded allylic alcohol **193** as an oil (64 mg, 37 %). δ_{H} (CDCl₃, 400 MHz): 7.02 (2H, s, H-2' and H-6'), 6.49 (1H, d, J = 16.0 Hz, H-3), 6.22 (1H, dt, J = 16.0, 6.0 Hz, H-2), 4.28 (2H, d, J = 6.0 Hz, CH₂), 2.20 (6H, s, 2 x MeAr), 1.02 (9H, s, ^tBu),

0.19 (6H, s, Me₂Si). δ_C (CDCl₃, 100 MHz): 152.24 (C), 131.50 (CH), 129.73 (C), 128.87 (C), 127.12 (CH), 126.31 (CH), 64.20 (CH₂), 26.23 (CH₃), 18.90 (C), 17.98 (CH₃), - 2.82 (CH₃). IR (NaCl, cm⁻¹): 3339 (O-H), 2930 (C-H), 2858 (C-H), 1654 (C=C), 1601 (Ar), 1484 (Ar). MS, (EI⁺), *m/z*: 292 [M⁺, 88%], 235 [M⁺ - ^tBu, 100], 217 [M⁺ - ^tBu, -H₂O, 34], 191 [42]. HRMS: 292.1856. C₁₇H₂₈O₂Si, requires (M⁺) 292.1859.

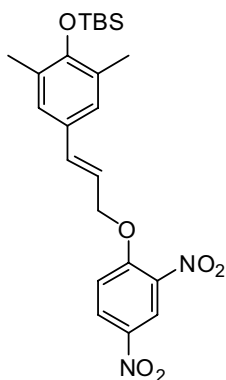
{2-[4'-(*tert*-Butyldimethylsilyloxy)-3',5'-dimethylphenyl]cycloprop-1-yl} methanol 194



CH₂I₂ (0.28 mL, 3.42 mmol) and Et₂Zn (1.71 mL, 1 M in hexanes, 1.71 mmol) were added dropwise to a stirred solution of alkene **193** (100 mg, 0.34 mmol) in dry DCM (1 mL) under argon. The resulting solution was allowed to stir at RT for 1 h before quenching with H₂O (10 mL). The aqueous layer was washed with DCM (2 x 10 mL) and the organic layers combined, dried over MgSO₄ and concentrated *in vacuo* to give a brown oil. Column chromatography, on neutral alumina, eluting with EtOAc- hexane (1:4) afforded cyclopropane **194** as an oil (44 mg, 42%). (R_F = 0.22). δ_H (CDCl₃, 400 MHz): 6.67 (2H, s, H-2' and H-6'), 3.63-3.50 (2H, m, CH₂OH), 2.16 (6H, s, 2 x MeAr), 1.72-1.66 (1H, m CH), 1.40-1.35 (1H, m, CH₂), 1.02 (9H, s, ^tBu), 0.75-0.71 (2H, m) 0.16 (6H, s, 6H, 2 x Me). ¹³CNMR, δ_C (CDCl₃, 100 MHz): 150.25 (C), 134.69 (C), 128.54 (C), 126.28 (CH), 66.98 (CH₂), 26.90 (CH₃), 24.93 (CH), 20.71 (CH), 18.86 (C), 17.96 (CH₃), 13.46 (CH₂), - 2.84 (CH₃). IR (thin layer, cm⁻¹): 3423 (O-H), 2929 (C-H), 1655 (Ar), 1473 (Ar). MS, (CI⁺), *m/z*: 307 [M+H⁺, 64%], 289 [M+H⁺ - H₂O, 100]. HRMS: 307.2095. C₁₈H₃₁O₂Si requires (M+H⁺) 307.2093.

1-{2'-[4''-(*tert*-Butyldimethylsilyloxy)-3'',5''-dimethylphenyl] cyclopropyl-1'-yl} methoxy-2,4,dinitrobenzene 195

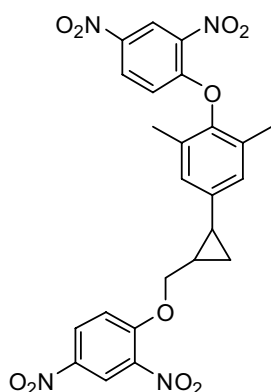
For the experimental of **195** please refer to the synthesis of 2,6-Dimethyl-4-[2'-(2'',4''-dinitrophenoxymethyl)cyclopropyl]- phenol **182**.

(*E*)-1-[4'-(*tert*-Butyldimethylsilyloxy)-3'-5'-dimethylphenyl]-3-(2'',4''-dinitrophenoxy)propene 196

Diisopropyl azo dicarboxylate (DIAD) (0.10 mL, 0.41 mmol) was added dropwise to a cooled stirred solution of the allylic alcohol **193** (100 mg, 0.34 mmol), 2,4-dinitrophenol (75 mg, 0.41 mmol) and PPh₃ (107 mg, 0.41 mmol) in dry DCM (2 mL) under argon. The reaction mixture was heated to reflux overnight. The resulting solution was then cooled and the reaction quenched with water (10 mL) and diluted with DCM (10 mL). The layers were separated and the organic layer was washed with H₂O (2 x 10 mL), dried over MgSO₄ and concentrated *in vacuo* to give a yellow oil. Phosphine impurities were precipitated using Et₂O and

the remaining yellow oil purified by column chromatography, on silica gel, eluting EtOAc-hexane (1:4) to afford ether **196** as yellow needles (24 mg, 15%). δ_{H} (CDCl_3 , 400 MHz): 8.85, (1H, d, $J = 2.8$ Hz, H-3''), 8.36 (1H, dd, $J = 9.3, 2.8$ Hz, H-5''), 7.26 (1H, d, $J = 9.3$ Hz, H-6''), 6.97 (2H, s, H-2 and H-6), 6.55 (1H, d, $J = 16.1$ Hz, ArCH=), 6.12 (1H, dt, $J = 16.1, 6.0$ Hz, =CHCH₂), 4.88 (2H, d, $J = 6.0$ Hz, =CHCH₂), 2.31 (6H, s, 2 x MeAr), 1.13 (9H, s, ^tBu), 0.30 (6H, s, Me₂Si). δ_{C} (CDCl_3 , 100 MHz): -2.81 (CH₃), 17.96 (CH₃), 18.90 (C), 26.20 (CH₃), 71.64 (CH₂), 114.99 (CH), 118.72 (CH), 122.08 (CH), 127.48 (CH), 128.53 (C), 129.06 (C), 129.12 (CH), 135.58 (CH), 139.19 (C), 153.03 (C), 155.63 (C). IR (ATR, cm^{-1}): 2961-2857 (C-H), 1609 (Ar), 1526 (NO₂), 1340 (NO₂), 1232 (C-O), 1256 (SiMe_n), 1070 (O-Si). LRMS, (EI⁺), m/z : 458 [M^{+} , 19%], 275 [M^{+} - DNP, 100%].

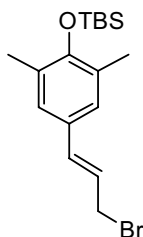
2,4-Dinitrophenoxy-1-{2'-[4''-(2''',4'''-dinitrophenoxy)-3'',5''-dimethylphenyl]cycloprop-1'ylmethoxy}benzene 197



The doubly coupled product **197** was synthesized as a side product of the synthesis of 2,6-Dimethyl-4-[2'--(2'',4''-dinitrophenoxymethyl)cyclopropyl]-phenol **182** and was isolated as a yellow oil from the same reaction following chromatography. (18%) δ_{H} (CDCl_3 , 400 MHz): 8.84 (1H, d, $J = 2.4$ Hz, H-3 or H-3'''), 8.74 (1H, d, $J = 2.4$ Hz, H-3 or H-3'''), 8.43 (1H, dd, $J = 9.1, 2.4$ Hz, H-5 or H-5'''), 8.26 (1H, dd, $J = 9.1, 2.4$ Hz, H-5 or H-5'''), 7.23 (1H, d, $J = 9.1$ Hz, H-6 or H-6'''), 6.92 (2H, s, H-2'' and H-6''), 6.74 (1H, d, $J = 9.1$ Hz, H-6 or H-6'''), 4.40 (1H, dd, $J = 9.9, 6.1$ Hz, CH^XCH^YOAr), 4.20 (1H, dd, $J = 9.9, 7.1$ Hz, CH^XCH^YOAr), 2.09 (6H, s), 2.05- 2.03 (1H, m), 1.67-1.59 (1H, m), 1.19-1.14 (2H,

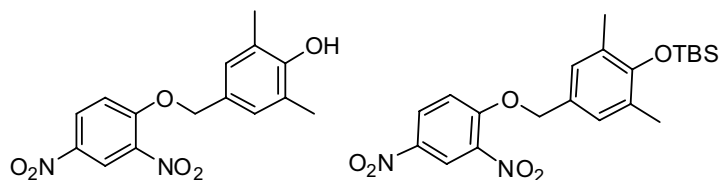
m). IR (ATR, cm^{-1}): 3109 (C-H), 2928 (C-H), 2872 (C-H), 1604 (Ar), 1526 (Ar), 1475 (Ar). No M^+ or $\text{M}+\text{H}$ peak observed in MS, using EI, CI or FAB.

[4'-(3-Bromoprop-1(E)-en-1-yl)-2',6'-dimethyl-phenoxy]-tertbutyldimethyl silane 198



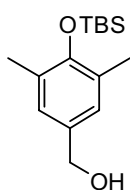
The allylic alcohol **193** (100 mg, 0.34 mmol) and PPh_3 (90 mg, 0.34 mmol) was dissolved in DCM (2 mL) and CBr_4 (112 mg, 0.34 mmol) was added portionwise, an exotherm was observed. The resulting solution was stirred for 1 h before concentrating in *vacuo* to give a brown oil. Column chromatography, on neutral alumina, eluting with EtOAc-hexane (1:19) to afforded the allylic bromide **198** as an oil (50.7 mg, 42%). δ_{H} (CDCl_3 , 400 MHz): 7.01 (2H, s, H-3' and H-5'), 6.21 (1H, d, $J = 16.0$ Hz, $\text{CH}=\text{CHAr}$), 5.86 (1H, dt, $J = 16.0, 6.3$ Hz, $=\text{CHCH}_2$), 3.79 (1H, d, $J = 6.3$ Hz, $=\text{CHCH}_2$), 1.93 (6H, s, 2 x Me), 0.76 (9H, s, ^tBu), 0.08 (6H, s, Me_2Si). δ_{C} (CDCl_3 , 100 MHz):154.14 (C), 132.30 (CH), 129.54 (C), 127.48 (CH), 126.99 (C), 124.00 (CH), 65.39 (CH_2), 26.09 (CH_3), 18.76 (C), 17.85 (CH_3), -2.95 (CH_3). IR (NaCl, cm^{-1}): 2945 (C-H), 2828 (C-H), 1668 (C=C), 1609 (Ar), 1491 (Ar), 1090 (SiMe_n), 1004 (Si-O). LRMS (EI^+) m/z : 276.2 ($\text{M}^{+\bullet} - ^\bullet\text{Br}$, 62%), 263 (75%) 207 (100%).

4-(2,4-Dinitrophenoxymethyl)-2,6-dimethyl phenol 200 and 4-[4'-(tert-butyl dimethylsilyloxy)-3',5'-dimethylbenzyloxy]-1,3-dinitrobenzene 203



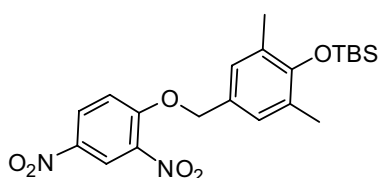
Adapting the procedure of Whalley¹¹⁵, the benzyl alcohol (200 mg, 0.76 mmol) was mixed with 2,4-dinitrofluorobenzene (0.10 mL, 0.76 mmol) and 2 drops of anhydrous NEt_3 were added. The reaction mixture was stirred at RT overnight then diluted with Et_2O (10 mL) and washed with H_2O (3 x 10 mL). The organic layer was dried over MgSO_4 and concentrated *in vacuo* to give a 1:1 mixture of ether and 2,4-dinitrophenol. ^1H NMR, data for ether **203** δ_{H} (CDCl_3 , 400 MHz): 8.58 (1H, d, H-2, $J = 2.7$ Hz), 8.21 (1H, dd, $J = 9.5, 2.7$ Hz, H-6), 7.07 (1H, d, $J = 9.5$ Hz, H-5) 6.86 (2H, s, H-2' and H-6'), 5.06 (2H, s, CH_2O), 2.04 (6H, s, 2 x Me), 0.86 (9H, s, ^tBu), 0.06 (6H, s, 2 x Me). Column chromatography, on silica gel, eluting with EtOAc-hexane (1:4) afforded a mixture of deprotected phenol and 2,4-dinitrophenol. Attempts to purify using hexane-EtOAc resulted in an increased concentration of dinitrophenol due to instability of the product. No further attempt to purify were carried out. ^1H NMR, data for phenol **200** δ_{H} (CDCl_3 , 400 MHz): 8.89 (1H, d, $J = 2.7$ Hz, H-3), 8.36 (1H, dd, $J = 9.5, 2.7$ Hz, H-5'), 7.40 (1H, d, $J = 9.5$ Hz, H-6'), 6.79 (2H, s, H-3 and H-5), 4.87 (2H, s, CH_2O), 2.19 (6H, s, 2 x Me). δ_{C} (CDCl_3 , 100 MHz): 170.10 (C) 153.57 (C), 150.16 (C), 141.20 (C), 138.09 (CH), 136.09 (CH) 133.77 (C), 130.99 (C), 129.87 (CH), 127.46 (CH), 127.36 (C), 126.44 (CH), 125.03 (CH), 122.20 (CH), 116.00 (CH), 52.01 (CH_2), 7.50 IR (ATR, cm^{-1}): 3099-2992 (C-H), 1602 (Ar), 1533 (NO_2), 1340 (NO_2), 1236 (C-O).

[4-(*tert*-Butyldimethylsilyloxy)-3,5-dimethylphenyl]methanol **202**



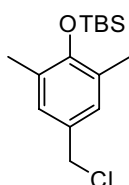
Sodium borohydride (0.86 g, 22.8 mmol) was added portionwise to a stirred solution of aldehyde **191** (5.00 g, 20.7 mmol) in MeOH (70 mL). The reaction mixture was allowed to stir for 3 h then the reaction was quenched with ice-cold water (20 mL) and the solution concentrated *in vacuo* to approximately 20 mL. The mixture was extracted with Et₂O (2x 100 mL) and the organic layers combined, dried over MgSO₄ and concentrated *in vacuo* to give alcohol **202** as an oil (5.80 g, 95%). δ_{H} (CDCl₃, 400 MHz): 7.02 (2H, s, H-2 and H-6), 4.59 (2H, d, J = 5.6 Hz, CH₂), 2.25 (6H, s, 2 x CH₃Ar), 1.60 (1H, t, J = 5.6 Hz, OH), 1.06 (9H, s, ^tBu), 0.23 (6H, s, Me₂Si). ¹³CNMR, δ_{C} (CDCl₃, 100 MHz): 151.84 (C), 133.58 (C), 128.89 (C), 127.97 (CH), 65.36 (CH₂), 26.23 (CH₃), 18.88 (C), 17.94 (CH₃), - 2.82 (CH₃). IR (thin layer cm⁻¹): 3331 (OH), 2930 (CH), 2886 (CH), 2858 (CH), 1609 (Ar), 1483 (Ar), 1152 (SiMe_n), 1032 (C-O), 1007 (Si-O). LRMS (EI⁺), m/z : 266 [M⁺, 44%], 209 [M⁺ - ^tBu⁺, 100], 169 [25]. HRMS: 266.1704. C₁₅H₂₆O₂Si requires (M⁺) 266.1702.

4-[4'-(*tert*-butyldimethylsilyloxy)-3',5'-dimethylbenzyloxy]-1,3-dinitrobenzene **203**



For synthesis of **203** see experimental for 4-[4'-(*tert*-butyldimethylsilyloxy)-3',5'-dimethylbenzyloxy]-1,3-dinitrobenzene **200**

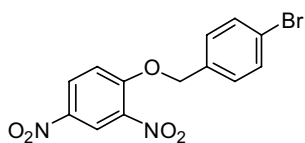
4-(*tert*-Butyldimethylsilanoxy)-3,5-dimethylbenzylchloride **204**



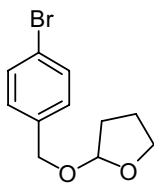
The benzyl alcohol **202** (500 mg, 1.87 mmol) was dissolved in dry DCM (5 mL) under argon. NEt₃ (0.31 mL, 2.25 mmol) was added slowly followed by TsCl (429 mg, 2.25 mmol) and DMAP (138 mg, 1.13 mmol). The reaction mixture was stirred for 1 h at RT. The reaction mixture diluted with DCM (15 mL) and washed with

H₂O (3 x 10 mL). The organic phase was dried over MgSO₄ and concentrated *in vacuo* to afford the chloride **204** (345 mg, 64%). δ_{H} (CDCl₃, 400 MHz): 6.99 (2H, s, H-2, H-6), 4.49 (2H, s, CH₂Cl), 2.19 (6H, s 2 x MeAr), 1.02 (9H, s, ^tBu), 0.18 (6H, s, Me₂Si). ¹³CNMR, δ_{C} (CDCl₃, 100 MHz): 152.35 (C), 139.21 (C), 128.46 (C), 128.76 (CH), 46.57 (CH₂), 26.08 (CH₃), 18.75 (C), 16.97 (CH₃), - 2.90 (CH₃). IR (thin layer cm⁻¹): 2927-2858 (CH), 1609 (Ar), 1491 (Ar). LRMS (EI⁺) *m/z*: 250.2 [M⁺-Cl, 100%], 207.2 (53%).

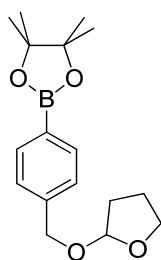
1-(4-Bromobenzyloxy)-2,4-dinitrobenzene **211**



2,4-Dinitrofluorobenzene (50 μ L, 0.54 mmol) and 2 drops of anhydrous NEt₃ were added to a stirred solution of benzyl alcohol **210** (100 mg, 0.54 mmol) in anhydrous Et₂O (1 mL). The reaction mixture was allowed to stir at RT overnight then the solution was concentrated *in vacuo* and the resulting slurry triturated with Et₂O. The pale yellow solid was collected by filtration washing with Et₂O to afford the ether **211** as fine needles (189 mg, 64%). Mp: 158-161°C, needles δ_{H} (CD₃Cl, 400 MHz): 8.78 (1H, d, *J* = 2.8 Hz - H-3), 8.42 (1H, dd, *J* = 9.2, 2.8 Hz, H-5), 7.56 (2H, d, *J* = 8.4 Hz, H-2' and H-6'), 7.34 (2H, d, *J* = 8.4 Hz, H-3' and H-5'), 7.23 (1H, d, *J* = 9.2 Hz, H-6), 5.312 (2H, s, CH₂). δ_{C} (CDCl₃, 100 MHz): 156.01 (C), 140.52 (C), 139.63 (C), 133.01 (C), 132.23 (CH), 129.08 (CH), 128.71 (CH), 123.00 (C), 122.06 (CH), 114.82 (CH), 77.35 (CH₂). IR (ATR, cm⁻¹): 2920 (C-H), 2853 (C-H), 1607 (Ar), 1591 (Ar), 1532 (NO₂), 1485 (Ar). LRMS (EI⁺): 188 [M⁺, (⁸¹Br), 52 %], 185 [M⁺, (⁷⁹Br), 52], 107 (100). HRMS: 187.9667 and 185.9684. C₇H₇⁸¹BrO requires M⁺, 187.9660 and C₇H₇⁷⁹BrO requires M⁺, 185.9680. Mp is consistent with literature.¹¹⁶

2-(4'-bromobenzoyloxy)tetrahydrofuran 212

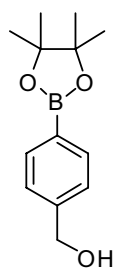
4-bromobenzylalcohol **210** (5.00 g, 26.7 mmol), 2,3-dihydrofuran (2.4 mL, 32.1 mmol) and *para*-toluenesulfonic acid (20 mg) were dissolved in dry DCM (50 mL) and the resulting solution stirred for 1 h. After this time the reaction was washed with H₂O (2 x 50 mL) and sat. NaHCO_{3(aq)} (50 mL) and the organic phase dried over MgSO₄ and concentrated *in vacuo* to afford the protected alcohol **212** as an oil (6.59 g, 95%). ¹HNMR, δ_H (CDCl₃, 400 MHz): 7.44 (2H, d, *J* = 8.3 Hz, H-3' and H-5'), 7.20 (2H, d, *J* = 8.3 Hz, H-2' and H-6'), 5.20 (1H, dd, *J* = 3.7, 2.6 Hz, H-2), 4.62 (1H, d, *J* = 12.4 Hz ArCH^XH^Y), 4.40 (1H, d, *J* = 12.4 Hz ArCH^XH^Y), 3.98-3.81 (2H, m, 2x H-5), 2.06-1.80 (4H, m, 2 x H-3 and 2 x H-4). δ_C (CDCl₃, 100 MHz): 137.46 (C), 131.47 (CH-Ar), 129.50 (CH-Ar), 121.36 (C), 103.21 (CH), 68.04 (CH₂), 67.15 (CH₂), 32.39 (CH₂), 23.49 (CH₂). IR (ATR, cm⁻¹): 2883 (C-H), 1593 (Ar), 1487 (Ar). LRMS (EI⁺), *m/z*: 258 [M⁺ (⁸¹Br), 5%], 256 [M⁺ (⁷⁹Br), 5], 185 [M⁺ (⁸¹Br) - THF, 13], 183 [M⁺ (⁷⁹Br) - THF, 13], 169 [M⁺ (⁸¹Br) - OTHF, 25], 167 [M⁺ (⁷⁹Br) - OTHF, 25], 71 [100]. HRMS: 258.0079 and 256.0099. C₁₁H₁₃⁸¹BrO₂ requires M⁺, 258.0078 and C₁₁H₁₃⁷⁹BrO₂ requires M⁺, 256.0099.

2-[4'-(4'',4'',5'',5''-Tetramethyl[1'',3'',2'']dioxaborolan-2-yl)-benzyloxy]tetrahydrofuran 213

A stirred solution of the bromide **212** (1.00 g, 3.7 mmol) in dry THF (10 mL) under argon was cooled to -78°C and ^tBuLi (2.2 mL, 1.68 M in hexanes 3.7 mmol)

was added dropwise and the mixture allowed to stir for 15 min. After this time 2-Isopropyl-4,4,5,5-tetramethyl-[1,3,2]dioxaborolane (2.5 mL, 12.2 mmol) was added dropwise and the resulting solution allowed to stir for 2 h. The reaction was quenched with H₂O (100 mL) and the compound extracted with DCM (3 x 100 mL). The organic layers were combined, washed with brine (100 mL), dried over MgSO₄ and concentrated *in vacuo* at 60 °C for 3 h to afford boronate **213** as an oil (1.07 g, 95%). δ_{H} (CDCl₃, 400 MHz): 7.77 (2H, d, $J = 8.2$ Hz, H-3' and H-5'), 7.34 (2H, d, $J = 8.0$ Hz, H-2' and H-6'), 5.19 (1H, dd, $J = 1.7, 4.5$ Hz, H-2'), 4.61 (1H, d, $J = 13.6$ Hz ArCH^XH^Y), 4.42 (1H, d, $J = 13.6$ Hz ArCH^XH^Y), 3.94-3.83 (2H, m, 2 x H-5), 1.95-1.78 (4H, m, 2 x H-3 and 2 x H-4), 1.33 (12H, s, 4 x Me). δ_{C} (CDCl₃, 100 MHz): 141.65 (C), 134.92 (CH-Ar), 127.05 (CH-Ar), 103.17 (CH), 83.83 (C), 68.69 (CH₂), 67.11 (CH₂), 32.40 (CH₂), 24.91 (CH₃), 23.50 (CH₂). IR (thin layer, cm⁻¹): 2979 (C-H), 1614 (Ar), 1517 (Ar), 1360 (B-O), 1271 (B-C), 1088 (C-O). LRMS (EI⁺): 304 (M⁺, 4%), 217 (75), 83 (100). HRMS: 304.1842. C₁₇H₂₅¹¹BO₄ requires M⁺, 304.1846.

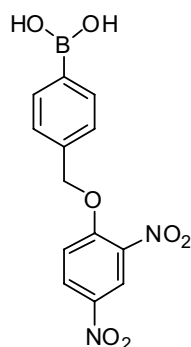
[4-(4,4,5,5-Tetramethyl[1,3,2]dioxaborolan-2-yl)phenyl]methanol **214**



The protected benzyl alcohol **213** (500 mg, 15.8 mmol) was dissolved in dry EtOH (5 mL) and aluminium trichloride (20 mg, 1.6 mmol) was added. The solution was allowed to stir overnight before being concentrated to give a grey oil. The oil was dissolved in Et₂O and undissolved solid was removed by filtration. The filtrate was then concentrated *in vacuo* to afford the unprotected alcohol **214** as a colourless oil (299 mg, 81%). δ_{H} (CDCl₃, 400 MHz): 7.81 (2H, d, $J = 7.9$ Hz, H-3 and H-5), 7.38 (2H, d, $J = 7.9$ Hz, H-2 and H-6), 4.72 (2H, s, ArCH₂), 1.36 (12H, s, 4 x Me). δ_{C} (CDCl₃, 100 MHz): 144.10 (C), 135.15 (CH-Ar), 126.19 (CH-Ar), 83.94 (C), 65.34 (CH₂), 24.97 (CH₃). IR (ATR, cm⁻¹): 3423 (OH),

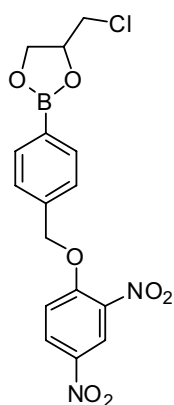
2932 (C-H), 1614 (Ar), 1517 (Ar). LRMS (EI⁺), *m/z*: 234 [M⁺, 62%], 219 [M⁺ - ·Me, 65%], 135 (100). HRMS: 234.1426. C₁₃H₁₉O₃B requires (M⁺) 234.1427. Data consistent with literature¹¹⁷.

4-(2'4'-Dinitrophenoxymethyl)phenylboronic acid **217**



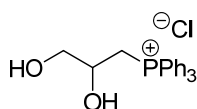
The boronic ester **186** (100 mg, 0.25 mmol) was dissolved in a THF-H₂O (4:1, 2.5 ml). NaIO₄ (160 mg, 0.75 mmol) was added and the mixture stirred for 1 h before 1M HCl_(aq) (0.1 mL) was added. The mixture was then extracted with EtOAc (20 mL) and the organic layer, dried over MgSO₄ concentrated *in vacuo* to give an off-white solid which was recrystallised from EtOAc affording the boronic acid **217** as an amorphous solid (48 mg, 60%). Mp: decomposes at 180-182°C. δ_H (DMSO, 400 MHz): 8.82 (1H, d, *J* = 2.8 Hz, H-3'), 8.55 (1H, dd, *J* = 9.3, 2.8 Hz, H-5'), 8.15 (2H, s, BO₂H), 7.85 (2H, d, *J* = 8.0 Hz, H-2 and H-6 or H-3 and H-5), 7.71 (1H, d, *J* = 9.3 Hz, H-6'), 7.45 (2H, d, *J* = 8.0 Hz, H-2 and H-6 or H-3 and H-5), 5.52 (2H, s, CH₂O). ¹³CNMR: δ_C (DMSO, 100 MHz): 155.49 (C), 139.76 (C), 138.76 (C), 136.93 (C), 134.14 (CH), 129.26 (CH), 126.45 (CH), 121.20 (CH), 116.09 (CH), 71.53 (CH₂) IR (ATR, cm⁻¹): 3580 (O-H), 3358 (O-H), 3097 (C-H), 1609 (Ar), 1520 (NO₂), 1340 (NO₂). LRMS (EI⁺), *m/z*: 318 (M⁺, 9%), 274 (M⁺ - HOB=O, 21%), 152 (45%), 136 (CH₃C₆H₄B(OH)₂⁺, 100%). HRMS: 318.0663. C₁₃H₁₁N₂O₇B requires (M⁺) 318.0659. HOCH₂C₆H₄B(OH)₂⁺.

4-(Chloromethyl)-2-[4'-(2'',4''-dinitrophenoxymethyl)phenyl]-1,3,2-dioxaborolane 218



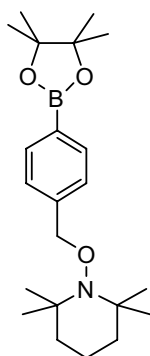
The boronic acid **217** (48 mg, 0.15 mmol) was dissolved in dry DCM (1 mL) then MgSO_4 (36 mg, 0.30 mmol) and 3-chloropropanediol (15 μL , 0.17 mmol) were added and the resulting solution stirred overnight under argon. The reaction mixture was filtered off and concentrated *in vacuo* to give a red solid. Column chromatography, on silica gel, eluting with EtOAc gave the boronic ester **218** as a clear glass (23 mg, 39%). δ_{H} (CDCl_3 , 400 MHz): 8.78 (1H, d, $J = 2.8$ Hz, H-3''), 8.39 (1H, dd, $J = 9.3, 2.8$ Hz, H-5''), 7.87 (2H, d, $J = 8.1$ Hz, H-3' and H-5' or H-2' and H-6'), 7.47 (2H, d, $J = 8.1$ Hz, H-3' and H-5' or H-2' and H-6'), 7.22 (1H, d, $J = 9.3$ Hz, H-6''), 5.40 (2H, s, CH_2Ar), 4.88-4.82 (1H, m, CH-O), 4.49 (1H, dd, $J = 9.5, 8.1$, Hz, $\text{OCH}^{\text{X}}\text{CH}^{\text{Y}}$), 4.28 (1H, dd, $J = 9.5, 6.0$ Hz, $\text{OCH}^{\text{X}}\text{CH}^{\text{Y}}$), 3.72-3.70 (2H, m, CH_2Cl). δ_{C} (CDCl_3 , 100 MHz): 156.95 (C), 139.86 (C), 138.06 (C), 135.73 (CH), 129.10 (CH), 126.38 (CH), 122.14 (CH), 114.93 (CH), 76.30 (CH), 72.01 (CH_2), 69.18 (CH_2), 46.46 (CH_2). IR (ATR, cm^{-1}): 3115 (C-H), 3077 (C-H), 1599 (Ar), 1520 (NO_2), 1342 (NO_2). LRMS (EI^+), m/z : 397 [$\text{M}^{+\bullet}$, (^{35}Cl) 4%] 392 [$\text{M}^{+\bullet}$, (^{35}Cl) 12%], 274, (BnOC₆H₃(NO₂)₂, 29), 212 (CH₃C₆H₄BO₂C₃H₅³⁷Cl, 25) 210 (CH₃C₆H₄BO₂C₃H₅³⁵Cl, 100). HRMS: 392.0590. C₁₆H₁₄N₂O₇¹¹B³⁵Cl ($\text{M}^{+\bullet}$) requires 392.0583.

(2,3-Dihydroxypropyl)triphenylphosphonium chloride 221



Triphenylphosphine (0.50 g, 1.9 mmol) was dissolved in 3-chloropropane-1,2-diol **220** (1.6 mL, 19.0 mmol) then heated to 80 °C for 48 h. The resulting black solution was diluted with Et₂O and a brown oil separated out. The solvent was decanted off and the remaining oil was dissolved in minimal DCM and a brown solid was precipitated with Et₂O decanting off the excess solvent. This procedure was repeated 3 times to afford the phosphonium salt **221** as a pale brown solid. (538 mg, 76%). δ_{H} (CD₃Cl, 400 MHz): 7.79 - 7.72 (m, 9H, 6 x *o*-H and 3 x *p*-H of Ph₃P), 7.60-7.63 (6H, m, 6 x *m*-H of Ph₃P), 4.00-3.92 (m, 2H, CHCH₂OH), 3.648 (2H, dd, *J* = 12.0, 64.4 Hz, CHCH₂P), 3.506-3.420 (1H, m, CHCH₂OH). δ_{C} (MeOD, 100 MHz): 135.86 (CH), 135.11 (CH, d, *J* = 10.1 Hz), 131.12 (CH, d, *J* = 13.1 Hz), 121.03 (C, d, *J* = 87.6 Hz), 67.98 (CH, d, *J* = 7.1 Hz), 67.37 (CH₂, d, *J* = 16.1 Hz), 28.26 (CH₂, d, *J* = 55.4 Hz). IR (ATR, cm⁻¹): 3223 (OH), 2886 (C-H), 1485 (Ar), 1433 (P-Ph). MS, (FAB/NOBA), *m/z*: 337 [M⁺(phosphonium cation), 100%]. HRMS: 337.1360. C₂₁H₂₂O₂P requires [M⁺(phosphonium cation)] 337.1357.

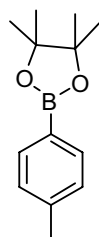
2,2,6,6-tetramethyl-1-[4'-(4'',4'',5'',5''-tetramethyl-1'',3'',2''-dioxaborolan-2-yl)benzyloxy]piperidine **222**



Magnesium turnings (55 mg, 2.3 mmol) and crystals of iodine were warmed in a degassed flask until the flask was filled with iodine vapours then dry Et₂O (0.5 mL) was added followed by the dropwise addition of the aryl bromide **228** (100 mg, 0.46 mmol) in dry Et₂O (0.5 mL). The slurry was stirred and warmed slightly until there was evidence of gas evolution. TEMPO (72 mg, 0.46 mmol) in dry Et₂O

(mL) was then added dropwise and the mixture allowed to stir overnight. The reaction mixture was then quenched with H₂O (5 mL), washed with brine (5 mL), dried over MgSO₄ and concentrated *in vacuo* to afford a pale orange oil. Column chromatography, on silica gel, eluting with EtOAc-hexane (1:19) afforded Boronate TEMPO **222** as prisms (77 mg, 45 %). Mp: 58-60 °C. δ_{H} (CDCl₃, 400 MHz): 7.79 (2H, d, $J = 7.6$ Hz, H-2' and H-6' or H-3' and H-5'), 7.36 (2H, d, $J = 7.6$ Hz, H-2' and H-6' or H-3' and H-5'), 4.84 (2H, s, CH₂O), 1.54-1.48 (6H, m, 3 x CH₂), 1.34 (12H, s, 4 x Me), 1.24 (6H, s, 2 x Me_AMe_B), 1.14 (6H, s, 2 x Me_AMe_B). ¹³CNMR: δ_{C} (CDCl₃, 100 MHz): 140.23 (C), 133.44 (CH), 125.36 (CH), 82.40 (C), 77.43 (CH₂), 58.71 (C), 38.40 (CH₂), 31.78 (CH₃), 22.55 (CH₃), 18.98 (CH₃), 15.82 (CH₂). IR (ATR, cm⁻¹): 2974 (C-H), 2942 (C-H), 2909 (C-H), 1614 (Ar), 1321 (B-O), 1138 (B-C), 1074 (C-O), 608 (C-Br). LRMS (Cl⁺), m/z : 374 (M+H⁺, 80%), 140 (53%), 89 (100%). HRMS: 374.2861. C₂₂H₃₇O₃NB requires (M+H⁺) 374.2871.

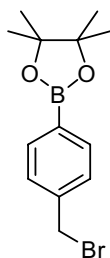
2-(4'-Methylphenyl)-4,4,5,5-tetramethyl-1,3,2-dioxaborolane **227**



The aryl bromide **226** (3.00 g, 17.5 mmol) was dissolved in dry THF (40 mL) under argon and the resulting solution cooled to -78 °C. ^tBuLi (21.0 mL, 1.7 M solution in hexanes, 35.1 mmol) was added dropwise and the reaction mixture allowed to stir for 15 min before boronate (11.9 mL, 58.3 mmol) was added dropwise. The solution was allowed to stir for 1 h at -78 °C before quenching with ice-cold H₂O (20 mL). The mixture was extracted with EtOAc (30 mL) and the organic layer washed with brine (30 mL), dried over MgSO₄ and concentrated *in vacuo* at 60 °C for 3 h affording the boronic ester **227** as an oil (3.45 g, 90%). δ_{H} (CDCl₃, 400 MHz): 7.94 (2H, d, $J = 7.9$ Hz, H-2' and H-6' or H-3' and H-5'), 7.17 (2H, d, $J = 1.9$ Hz, H-2' and H-6' or H-3' and H-5'), 2.40 (3H, s, MeAr), 1.37 (12H, s, 4 x Me). δ_{C} (CDCl₃, 100 MHz): 141.53 (C), 134.94 (CH), 128.65 (CH), 83.74 (C), 24.98 (CH₃), 21.86 (CH₃). IR (ATR, cm⁻¹): 2978-2926 (C-H), 1612 (Ar),

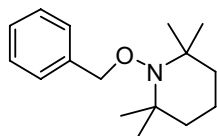
1385 (Ar) LRMS (Cl^+), m/z : 219 [$\text{M}+\text{H}^+$, 85 %], 89 [100%]. HRMS: 219.1551. $\text{C}_{13}\text{H}_{20}\text{O}_2\text{B}$ requires ($\text{M}+\text{H}$) 219.1556. Data is consistent with literature.¹¹⁸

2-[4'-(Bromomethyl)phenyl]-4,4,5,5-tetramethyl-1,3,2-dioxaborolane 228



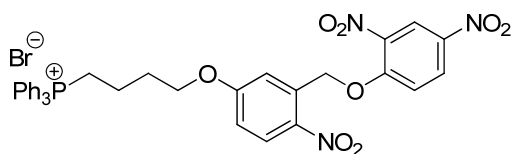
The boronic ester **227** (2.00 g, 9.2 mmol) was dissolved in CCl_4 (25 mL) and NBS (1.71 g, 9.6 mmol) and benzoyl peroxide (40 mg, 0.2 mmol) added. The resulting mixture was then heated to reflux and stirred overnight. The reaction mixture was allowed to cool and concentrated *in vacuo*. The resulting oil was dissolved in DCM (100 mL) and washed with H_2O (100 mL). The organic layer was dried over MgSO_4 and concentrated to dryness and the resulting yellow solid recrystallised from hexane affording the bromide **228** as a clear solid (1.55 g, 57%). Mp: 75-78 °C, (prisms hexane). δ_{H} (CDCl_3 , 400 MHz): 7.78 (2H, d, $J = 8.0$ Hz, H-2' and H-6' or H-3' and H-5'), 7.39 (2H, d, $J = 8.0$ Hz, H-2' and H-6' or H-3' and H-5'), 4.49 (2H, s, CH_2Br), 1.34 (12H, s, 4 x Me). δ_{C} (CDCl_3 , 100 MHz): 140.79 (C), 135.35 (CH), 128.43 (CH), 84.04 (C), 33.45 (CH_2), 24.98 (CH_3). IR (ATR, cm^{-1}): 2980 (C-H), 1605 (Ar), 1424 (Ar). LRMS (EI^+): 298 [M^{++} , (^{81}Br), 4 %], 296 [M^{++} , (^{79}Br), 4], 217 ($\text{M}^{++} - \text{Br}^{\bullet}$, 100). HRMS: 298.0549 and 296.0567. $\text{C}_{13}\text{H}_{18}^{11}\text{B}^{81}\text{BrO}_2$ requires M^{++} , 298.0563 and $\text{C}_{13}\text{H}_{18}^{11}\text{B}^{79}\text{BrO}_2$ requires M^{++} , 296.0583. Mp and ^{13}C NMR consistent with literature¹¹⁵

1'-Benzyloxy-2,2,6,6-tetramethylpiperidine 230



Benzyl bromide **229** (494 μL , 3.2 mmol) was added dropwise to a slurry of magnesium turnings (202 mg, 8.3 mmol) in dry Et_2O (10 mL) under argon and allowed to stir for 30 min. after this time a solution of TEMPO (100 mg, 3.2 mmol) in dry Et_2O (5 mL) was added dropwise and the reaction stirred for 2 h. The mixture was quenched with H_2O (20 mL) and the organic layer dried over MgSO_4 and concentrated *in vacuo* to give a colourless oil. Column chromatography, on silica gel, eluting with EtOAc-hexane (1:9) to give 1-Benzyloxy-2,2,6,6-tetramethyl-piperidine **230** as an oil (301 mg, 38 %). δ_{H} (CDCl_3 , 400 MHz): 7.38-7.32 (4H, m, Ar), 7.28-7.25 (1H, m, H-4'), 4.83 (2H, s, OCH_2), 1.59-1.48 (5H, m), 1.36-1.33 (1H, m), 1.26 (6H, s, 2 x Me), 1.15 (6H, s, 2 x Me). ^{13}C NMR, δ_{C} (CDCl_3 , 100 MHz): 138.43 (C), 128.36 (CH), 127.60 (CH), 127.44 (CH), 78.85 (CH_2), 60.14 (C), 39.84 (CH_2), 33.23 (CH_3), 20.44 (CH_3), 17.25 (CH_2). IR (ATR, cm^{-1}): 2974 (C-H), 2870 (C-H), 1497 (Ar). LRMS, (EI^+), m/z : 247 ($\text{M}^{+\bullet}$, 5%), 232 ($\text{M}^{+\bullet}$ - Me, 4%), 181 (10%), 156 ($\text{M}^{+\bullet}$ - PhCH_2 , 100%). HRMS: 2247.1935. $\text{C}_{16}\text{H}_{25}\text{ON}$, requires ($\text{M}^{+\bullet}$) 247.1936.

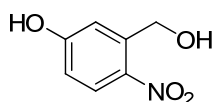
{4-[3-(2'',4''-Dinitrophenoxymethyl)-4'-nitrophenoxy]butyl triphenylphosphonium bromide 231



The benzyl alcohol **248** (100 mg, 0.18 mmol) was dissolved in anhydrous Et_2O (0.5 mL) and 2,4-dinitrofluorobenzene (23 μL , 0.86 mmol) and 1 drop of anhydrous NEt_3 added. The reaction mixture was allowed to stir at RT overnight then the solution was concentrated *in vacuo* the resulting slurry triturated with Et_2O . The yellow oil was dissolved in minimal DCM and then precipitated with Et_2O decanting off the excess solvent. This procedure was repeated 3 times then

the yellow oil dried *in vacuo* to give **231** as a pale yellow foam (49 mg, 42%). $^1\text{H NMR}$: δ_{H} (CD_3Cl , 400 MHz): 8.65 (1H, d, $J = 2.8$ Hz, H-2''), 8.41 (1H, d, $J = 9.2$, 2.8 Hz, H-5''), 8.04 (1H, d, $J = 9.2$ Hz, H-6''), 7.63-7.46 (15H, m, Ph_3P), 7.36 (1H, d, $J = 2.8$ Hz, H-2'), 7.27 (1H, d, $J = 9.6$ Hz, H-5'), 6.79 (1H, dd, $J = 2.8$, 9.6 Hz, H-6'), 5.55 (2H, s, CH_2Ar), 4.10 (2H, t, $J = 6.0$ Hz, $\text{CH}_2\text{CH}_2\text{O}$), 3.65-3.58 (2H, m, $\text{CH}_2\text{CH}_2\text{P}$), 2.04-2.00 (2H, m, $\text{CH}_2\text{CH}_2\text{P}$), 1.70-1.66 (2H, m, $\text{CH}_2\text{CH}_2\text{O}$). δ_{C} (CDCl_3 , 100 MHz): 163.94 (C), 156.15 (C), 140.70 (C), 139.26 (C), 138.56 (C), 135.28 (CH, d, $J = 3.0$ Hz), 133.79 (CH, d, $J = 11.0$ Hz), 130.65 (CH, d, $J = 13.1$ Hz), 130.01 (CH), 128.40 (CH), 122.52 (CH), 118.28 (C, d, $J = 85.5$ Hz), 115.52 (CH), 114.48 (CH), 114.00 (CH), 69.55 (CH_2), 68.15 (CH_2), 29.24 (CH_2 , d, $J = 17.1$ Hz), 22.29 (CH_2 , d, $J = 51.3$ Hz), 19.26 (CH_2). IR (ATR, cm^{-1}): 3059 (CH), 2941 (CH), 2874 (CH), 1606 (Ar), 1577 (Ar), 1506 (NO_2), 1438 (P-Ph). MS, (FAB/NOBA), m/z : 652 [M^+ (phosphonium cation), 72%], 86 (100). HRMS: 652.1842. $\text{C}_{35}\text{H}_{31}\text{O}_8\text{N}_3\text{P}$ requires [M^+ (phosphonium cation)] 652.1849.

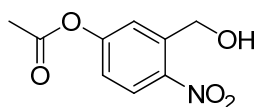
3-(Hydroxymethyl)-4-nitrophenol **244**



5-hydroxy-2-nitro-benzaldehyde **241** (1 g, 5.96 mmol) was dissolved in MeOH (20 mL) and stirred and cooled to 0°C using a ice bath. NaBH_4 (6.56 mg, 6.56 mmol) was added portionwise over 30 min. The reaction mixture was then allowed to stir for 1 hr before quenching with ice cold water H_2O (20 mL). The desired alcohol was extracted into Et_2O (2 x 100 mL) and the organic layers combined, dried over MgSO_4 and concentrated *in vacuo* to give alcohol **244** as an oil which crystallised on standing. (1.01 g, 99 %). Mp: $109\text{-}111^\circ\text{C}$, amorphous solid. δ_{H} (MeOD, 400 MHz): 7.89 (1H, d, $J = 9.2$ Hz, H-5), 7.27 (1H, s, H-2), 6.59 (1H, d, $J = 9.2$ Hz, H-6), 4.77 (2H, s, CH_2). δ_{C} (MeOD, 100 MHz): 164.49 (C), 143.27 (C), 139.99 (C), 128.87 (CH), 115.00 (CH), 114.82 (CH), 62.35 (CH_2). IR (ATR, cm^{-1}): 3381 (OH), 3121 (C-H), 3086 (C-H), 3010 (C-H), 2942 (C-H), 1628 (Ar), 1581 (Ar),

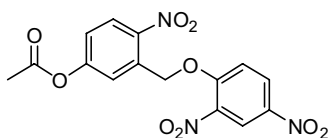
1537 (NO₂). MS, (EI⁺), *m/z*: 169 [M⁺, 15%], 123 [M⁺ - NO₂, 21%], 106 [100%], HRMS: 169.0379. C₇H₇O₄N requires [M⁺] 169.0375.

3-(Hydroxymethyl)-4-nitrophenyl acetate **245**



The phenol **244** (1.20 g, 7.09 mmol) was mixed with KOH (600 mg, 10.6 mmol) in H₂O (2.0 mL) then 3.6 g ice added. The solution was stirred for 30 min then acetic anhydride (0.8 mL, 8.5 mmol) added before neutralising with 1 M HCl_(aq). DCM(100 mL) was then added and the layer separated and the aqueous phase washed with DCM (2 x 100 mL). The organic extracts were combined washed with brine (100 mL), dried over MgSO₄ and concentrated *in vacuo* affording the alcohol **245** as a solid (1.17 g, 78%) which went dark red. Mp: 116-118°C, δ_H (CD₃Cl, 400 MHz): 8.20 (1H, d, *J* = 8.8 Hz, H-5), 7.49 (1H, d, 2.8 Hz, H-2), 7.14 (1H, dd, 2.8, 8.8 Hz, H-6), 4.97 (2H, s, CH₂OH), 2.304 (3H, s, CH₃CO₂Ar). δ_C (MeOD, 100 MHz): 170.21 (C), 156.27 (C), 145.37 (C), 142.14 (C), 127.49 (CH), 122.42 (CH), 122.14 (CH), 61.77 (CH₂), 20.87 (CH₃). IR (ATR, cm⁻¹): 2304 (OH), 2930 (C-H), 2845 (CH), 1759 (C=O), 1614 (Ar), 1584 (Ar), 1518 (NO₂), 1334 (NO₂), 1192 (C-O), 1178 (C-O) LRMS: (Cl⁺) 212 [M+H⁺ 100%], 194 [M+H⁺ -H₂O 38%]. HRMS: 212.0561. C₉H₁₀O₅N requires [M+H⁺] 212.0559.

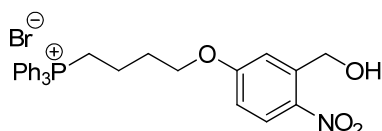
3-(2',4'-Dinitrophenoxymethyl)-4-nitrophenyl acetate **246**



To a stirred solution of benzylic alcohol **245** (100 mg, 0.47 mmol) in anhydrous Et₂O (1.0 mL) 2,4-dinitrofluorobenzene (44 μL, 0.47 mmol) and 1 drop of anhydrous NEt₃ were added. The reaction mixture was allowed to stir at RT overnight then the solution concentrated *in vacuo* and the resulting slurry triturated with Et₂O. The pale orange solid was collected by filtration washing

with Et₂O to afford the ether **246** as a pink solid (17 mg, 10 %). δ_{H} (CD₃Cl, 400 MHz): 8.96 (1H, d, J = 2.8 Hz, H-3'), 8.58 (1H, dd, J = 2.8, 9.2 Hz, H-5'), 8.39 (1H, d, J = 8.8 Hz, H-6'), 7.91 (1H, d, J = 2.4 Hz, H-2), 7.48 (1H, dd, J = 2.4, 8.8 Hz, H-6), 7.40 (1H, d, J = 8.8 Hz, H-5), 5.83 (2H, s, CH₂Ar), 2.445 (3H, s, CH₃CO₂Ar). δ_{C} (CDCl₃, 100 MHz): 173.85 (C), 160.33 (C), 159.65 (C), 149.21 (C), 144.94 (C), 143.16 (C), 138.86 (C), 135.32 (CH), 132.58 (CH), 128.07 (CH), 126.87 (CH), 121.56 (CH), 73.87 (CH₂), 26.12 (CH₃). IR (ATR, cm⁻¹): 3115 (C-H), 3082 (C-H), 2978 (C-H), 1769 (C=O), 1607 (Ar), 1518 (NO₂), 1342 (NO₂). LRMS (EI⁺) m/z : 377.05 334.3 [M⁺ - CH₃CO⁺, 8], 194.1 [M⁺ - ¹⁴DNP, 16], 152.1 [M⁺ - ¹⁴DNP and CH₂=C=O, 41], 91.1 (100).

{4-[3'-(Hydroxymethyl)-4'-nitrophenoxy]butyl}triphenylphosphonium bromide **248**



A stirred solution of phenol **244** (100 mg, 0.59 mmol), cesium carbonate (212 mg, 0.65 mmol) and 4-bromobutyltriphenylphosphonium bromide (425 mg, 0.89 mmol) in dry MeOH (1 mL) were heated to reflux under argon for 48 h. The mixture was then partitioned between H₂O (10 mL) and EtOAc (10 mL) and the aqueous phase was extracted with EtOAc (2 x 10 mL). The combined organic extracts were dried over MgSO₄ and concentrated *in vacuo* to give a maroon oil. The oil was dissolved in minimal DCM and precipitated with Et₂O, decanting off the excess solvent. This procedure was repeated 3 times then the maroon oil was dried *in vacuo* to give **248** as a dark red foam (170 mg, 51%). δ_{H} (MeOD, 400 MHz): 8.17 (1H, d, J = 9.2 Hz, H-5'), 7.93-7.75 (15H, m, Ph₃P), 7.37 (1H, d, J = 2.8 Hz, H-2'), 6.95 (1H, dd, J = 9.2, 2.8 Hz, H-6'), 5.00 (2H, s, CH₂OH), 4.22 (2H, t, J = 6.0 Hz, CH₂OAr), 3.541-3.490 (2H, m, CH₂P), 2.119-2.086 (2H, m, CH₂CH₂O), 196-1.92 (2H, m, CH₂CH₂P). δ_{C} (CDCl₃, 100 MHz): 163.24 (C), 142.80 (C), 140.50 (C), 135.25 (CH), 133.75 (CH, d, J = 10.1 Hz), 130.66 (CH, d, J = 12.1 Hz), 127.41 (CH), 118.14 (C, d, J = 85.5 Hz), 114.23 (CH), 113.58 (CH), 67.20 (CH₂), 68.26 (CH₂), 29.06 (CH₂), 22.27 (CH₂, d, J = 51.3 Hz), 19.26 (CH₂). IR

(ATR, cm^{-1}): 3317 (OH), 3059 (CH), 2941(CH), 2874 (CH), 1606 (Ar), 1577 (Ar), 1506 (NO_2), 1438 (P-Ph). MS, (FAB/NOBA), m/z : 486 [M^+ (phosphonium cations), 100%]. HRMS: 486.1837. $\text{C}_{29}\text{H}_{29}\text{O}_4\text{NP}$ requires [M^+ (phosphonium cations)] 486.1834.

13 References

- 1 *Mid-2007 Population Estimates*, Office for National Statistics, 2008 b) *National Population projections 2006-based*, Office for National Statistics, 2008
- 2 *2001 Population Report-Comparisons to 1981*, General Register Office for Scotland, 2001
- 3 Philp, I *A Recipe for Care – Not a Single Ingredient* Department of Health, London, 2007
- 4 *General Household Survey 2006*, Office for National Statistics ,2008
- 5 Harman, D; *J. Gerontol.* **1956** 11, 298–300.
- 6 Harman, D; *J Am Geriatr Soc.* **1972** 20(4):145-147.
- 7 Dalle-Donne, I.; Rossi, R.; Colombo, R.; Giustarini, D.; Milzani, A.; *Clinical Chemistry* **2006** 52(4) 601–623
- 8 a) Hulbert A. J.; Pamplona, R.; Buffenstein, R.; Buttemer W. A.; *Physiol Rev* **2007** 87 1175-1213, b) Harman, D; *Age* **1994** 17 119–146.
- 9 Keller, L.; Jemielity, S.; *Exp. Gerontol.* **2006** 41 553–556.
- 10 Herrero, A.; Barja G.; *Mechanisms of Ageing and Development* **1997** 98 95–111
- 11 Finkel, T.; Holbrook, N. J.; *Nature* **2000**, 408, 239-247
- 12 Sohal, R. S.; Weindruch, R.; *Science* **1996** 273 59–63
- 13 Taylor, R. W.; Turnbull, D. M.; *Nature Rev.* **2005** 6 389-392
- 14 Halliwell, B.; Gutteridge, J.M.C.; *Free Radicals in Biology and Medicine*, 3rd Ed., OUP, Oxford 1999
- 15 Martínez-Cayuela, M. *Biochimie* **1995**, 77, 147-161
- 16 McMurray, J.; Castellion, M. E. *Fundamentals of General Organic and Biological Chemistry*, 4th Ed., Pearson Education, Upper Saddle River, N. J., 2003
- 17 Smith, R. A. J.; Porteous, C. M.; Gane, A. M.; Murphy, M. P. *Proc. Natl. Acad. Sci.* **2003**, 100, 5407-5412
- 18 . Raha, S.; Robinson, B. H.; *Trends Biochem. Sci.* **2000** 25 502-508
- 19 a) Kudin, A. P.; Bimpong-Buta, N. Y.; Vielhaber, S.; Elger, C. E.; Kunz, W. S.; *J. Biol. Chem.* **2004** 279 4127–4135 b) Kussmaul, L.; Hirst, J.; *Proc. Natl. Acad. Sci. U.S.A.* **2006** 103 7607–7612 c) Liu, Y.; Fiskum, G.; Schubert, D.; *J. Neurochem.* **2002** 80 780–787
- 20 Murphy M. P.; *Biochem. J.* **2009** 417 1–13
- 21 a) Forman H. J.; Torres M.; *Am J Respir Crit Care Med* **2002** 166 S4–S8, b) Dahlgren C.; Karlsson A.; *Journal of Immunological Methods* **1999** 232 3–14

-
- 22 Valko, M.; Izakovic, M.; Mazur, M.; Rhodes, C. J.; Telser, J.; *Mol. Cell. Biochem.* **2004** 266 37-56
- 23 a) Lovstad, R. A.; *BioMetals* **2003** 16 435-439 b) Fridovich, I.; *J. Bio. Chem.* **1970** 245 4053-4057
- 24 Buttner, G.; *Arch. Biochem. Biophys.* **1993** 535
- 25 Rosen, G. M.; Britigan, B.E.; Halpern, H. J.; Pou, S.; *Free Radicals: Biology and Detection by Spin Trapping*. First Edition. 1999: Oxford University Press
- 26 Sutton, H. C.; Winterbourn, C. C.; *Free Rad. Biol. Med.* **1989** 6 53-60
- 27 Hutchinson F.; *Radiat Res* **1957** 7 473-83
- 28 Hüttermann, J.; Voit, K.; Oloff, H.; Köhnlein, W.; Gräslund, A.; Rupprecht, A.; *Faraday Discuss. Chem. Soc.* **1984** 78 135
- 29 Breen, A. P.; Murphy J. A.; *Free Rad. Biol. Med.* **1995** 181033
- 30 Valko, M.; Izakovic, M.; Mazur, M.; Rhodes, C. J.; Telser, J.; *Mol. Cell. Biochem.* **2004** 266 37-56
- 31 a) Valko, M.; Rhodes, C. J.; Moncol, M.; Izakovic, M.; Mazur, M.; *Chem. Bio. Int.* **2006** 160 1-40
b) Porter, N. A.; *Acc. Chem. Res.* **1986** 19 262-268.
- 32 Marnett, L. J.; *Mutation Research* **1999** 424 83-95
- 33 Berlett B. S.; Stadtman E. R.; *J. Bio. Chem.* **1997** 272 20313-20316
- 34 Uchida, K.; Kawakishi, S.; *J. Bio. Chem.*, **1994** 269, 2405-2410.
- 35 Halliwell, B.; Gutteridge, J. M. C.; *J. Lab Clin. Med.* **1992** 119 598-620
- 36 Whittaker J. W.; *Biochem. Soc. Trans.* **2003** 31 1318-1321
- 37 Parker, L.; Witt, E. H.; Tritschler, H. J.; *Free Rad. Biol. Med.*, **1995** 19 227-250
- 38 Moosmann, B.; Behl, C.; *Proc. Natl. Acad. Sci. USA* **1999**. 96 8867-8872
- 39 a) Graf, B. A.; Mullen, W.; Caldwell, S. T.; Hartley, R. C.; Duthie, G. G.; Lean, M. E. J.; Crozier, A.; Edwards, C. A.; *DMD* **2005**, 33, 1036-1043
- 40 Hartley, R. C.; Kennedy, M. W.; *Trends Ecol. Evol.* **2004** 19 353-354
- 41 Winkler, B. S.; Boulton, M. E.; Gottsch J. D.; Sternberg, P.; *Molecular Vision* **1999** 5, 32-42
- 42 Lundqvist, H.; Dahlgren, C.; *Free Rad. Bio. Med.* **1996** 20 785-792,
- 43 Soh, N.; *Anal Bioanal Chem* **2006** 386 532-543
- 44 Bartosz, G; *Clinica Chimica Acta* **2006** 368 53- 76
- 45 Myhrea, O.; Andersena, J. M.; Aarnesc, H.; Fonnum, F.; *Biochem. Pharmacol.* **2003** 65 1575-1582
- 46 Frejavalle, C.; Karoui, H.; Tuccio, B.; Le Moigne, H.; Culcasi, M.; Pietri, S.; Lauricella, R.; Tordo, P.; *J. Chem. Soc. Chem. Comm.* **1994** 15 1793-1794

-
- 47 Stolze, K.; Rohr-Udilova, N.; Rosenau, T.; Hofinger, A.; Kolarich, D.; Nohl H.; *Bioorg. Med. Chem.* **2006** 14 3368–3376
- 48 Stolze, K.; Rohr-Udilova, N.; Rosenau, T.; Hofinger, A.; Kolarich, D.; Nohl H.; *Bioorg. Med. Chem.* **2006** 14 3368–3376
- 49 Hay, A.; Burkitt, M. J.; Jones, C. M.; Hartley, R.C.; *Arch. Biochem. Biophys* **2005**, 336-346
- 50 Clement; J.-L.; Tordo, P.; *Electron Paramag. Reson.* 2007 **20** 29-49
- 51 Olive, G.; Mercier, A.; Le Moigne, A.; Rockenbauer, A.; Tordo. P.; *Free Rad. Biol. Chem.* **2000** 28 403-408
- 52 Stolze, K.; Rohr-Udilova, N.; Rosenau, T.; Stadtmuller, R.; Nohl H.; *Biochem Pharmacol* **2005**; 69 1351-1361.
- 53 Zeghdaoui, A.; Tuccio, B.; Finet, J-P.; Cerri, V.; Tordo, P.; *J. Chem. Soc. Perkin. Trans.* **1995** 12 2087-2089
- 54 a) Bernotas, R. C.; Adams, G.; Carr, A. A.; *Tetrahedron* **1996** 52 6519-6526 c) Fevig, T. L.; Bowen, S. M.; Janowick, D. A.; Jones, B. K.; Munson, H. R.; Ohlweiler, D. F.; Thomas, G. E.; *J. Med. Chem.* **1996** 39 4988-4996
- 55 a) Durand, G.; Polidori, A.; Ouari, O.; Tordo, P.; Geromel, V.; Rustin, P.; Pucci, B.; *J. Med. Chem.* **2003** 46 5230-5237 b) Durand, G.; Polidori, A.; Salles, J-P.; Pucci, B.; *Bioorg. Med. Chem. Lett.* **2003** 13 859-862
- 56 Han, Y.; Tuccio, B.; Lauricella, R.; Villamena, F. A.; *J. Org. Chem.* **2008** 73 7108–7117
- 57 Han, Y.; Liu, Y.; Rockenbauer, A.;Zweier, J. L.; Durand,G.; Villamena, F. A.; *J. Org. Chem.* **2009** 74 5369-5380
- 58 Hardy, M.; Ouari, O.; Charles, L.; Finet, J-P.; Iacazio, G.; Monnier, V.; Rockenbauer, A.; Tordo, P.; *J. Org. Chem.* **2005** 70 10426-10433
- 59 Gamliel, A.; Afri, M.; Frimer, A. A.; *Free Rad. Biol. Med* **2008** 44 1394-1405
- 60 Liu, Y. P.; Ji, Y. Q.; Song, Y. G.; Liu, K. J.; Liu, B.; Tiana, Q.; Liu, Y.; *Chem. Commun.,* **2005** 4943–4945
- 61 a) Hardy, M.; Chalier, F.; Ouari, O.; Finet, J. P.; Rockenbauer, A.; Kalyanaraman, B.; Tordo, P.; *Chem Commun* **2007**:1083–1085. b) Hardy, M.; Rockenbauer, A.; Vasquez-Vivar, J.; Felix, C.; Lopez, M.; Srinivasan, S.; Avadhani, N.; Tordo, P.; Kalyanaraman, B.; *Chem. Res. Toxicol.* **2007** 20 1053–1060. c) Xu, Y.; Kalyanaraman, B. *Free Radic Res* **2007** 41 1–7. d) Murphy, M. P.; Echtay, K. S.; Blaikie, F. H.; Asin-Cayuella, J.; Cocheme, H. M.; Green, K.; Buckingham, J. A.; Taylor, E. R.; Hurrell, F.; Hughes, G.; Miwa, S.; Cooper, C. E.; Svistunencko, D. A.; Smith, R. A.; Brand, M. D.; *J Biol Chem* **2003** 278:48534–48545.
- 62 Gomez-Mejiba, S. E.; Zhai, Z.; Akram, H.; Deterding, L. J.; Hensley, K.; Smith, N.; Towner, R. A.; Tomer, K. B.; Mason, R. P.; Dario C. Ramirez, D. C.; *Free Rad. Biol. Med.* **2009** 46 853–865
- 63 a) Floyd, R. A.; *Ageing Cell* **2006** 5 51–57 b) Floyd, R. A.; Kopke, R. D.; Choi C-H.; Foster, S. B.;

- Doblas, S.; Towner, R. A. *Free Rad. Biol. Med.* **2008** 45 1361–1374
- 64 Floyd, R. A.; *Proc. Soc. Exp. Biol. Med.* **1999** 222 236–245.
- 65 Yokoyama, M.; *Curr. Opin. Pharmacol.* **2004** 4 110–115.
- 66 a) Ramadan, M.; Gamal-Eldeen, A. M.; Abdel-Aziz, M.; El-Din Abuo-Rahma, G.; Abdel-Nabi, H.; Abdel-Hamid Nagib, A. H *Arch. Pharm. Chem. Life Sci.* **2006**, 339, 242–249
- 67 a) Henderson, D.; Bielefeld, E. C.; Harris, K. C.; Hu, B. H.; *Ear Hear.* **2006** 27:1–19; b) Kopke, R.; Bielefeld, E.; Liu, J.; Zheng, J.; Jackson, R.; Henderson, D.; Coleman, J. K. *Acta Otolaryngol.* **2005** 125 235–243;.
- 68 Shuaib, A.; Hussain, M. S.; *Eur Neurol* **2008**;59:4–14
- 69 Edenius, C.; Strid, S.; Borga, O.; Breitholtz-Emanuelsson, A.; Vallen, K. L.; Fransson, B. J.; *Stroke Cerebrovasc. Dis.* **2002** 11:34–42
- 70 Ley, J. J.; Prado, R.; Wei, J. Q.; Bishopric, N. H.; Becker, D. A.; Ginsberg, M. D.; *Biochem. Pharmacol.* **2008** 75 448–456
- 71 Sun, Y.; Jiang, J.; Zhang, Z.; Yu, P.; Wang, L.; Xu, C.; Liu, W.; Wang, Y.; *Bioorg. Med. Chem.* **2008** 16 8868–8874
- 72 Zuo, L.; Chen, Y-R.; Reyes, L. A.; Lee, H-L; Chen, C-L.; Villamena, F. A.; Zweier, J. L.; *JPET* **2009** 329:515–523
- 73 Margail, I.; Plotkine, M.; Lerouet, D.; *Free Rad. Biol. Med.* **2005** 39 429–443
- 74 Kotake, Y.; Sang, H.; Miyajima, T.; Wallis, G. L.; *Biochim. Biophys. Acta* **1998** 1448:77–84;
- 75 Rosen, G. M.; Britigan, B. E.; Halpern, H. J.; Pou, S.; *Free Radicals: Biology and Detection by Spin Trapping*. First Edition. 1999: Oxford University Press
- 76 Wajer, T. A. J. W.; Mackor, A.; de Boer, T. J.; *Recl. Trav. Chim. Pays-Bas* **1971** 90 568-576.
- 77 Villamena, F. A.; Zweier, J. L.; *Antioxid. Redox. Signal.* **2004** 6 619-629
- 78 Kotake Y.; Janzen E.G.; *J. Am. Chem. Soc.* **1991** 113 9503-9506
- 79 a) Janzen E. G.; Kryzman P. H; Lindsay D. A.; Haire D. L.; *J. Am. Chem. Soc.* **1990** 112 8279-8284 b) Villamena F. A.; Hadad C. M.; Zweier J. L.; *J. Am. Chem. Soc.* **2004** 126 1816-1829
- 80 a) Ouari O.; Polidori A.; Pucci B.; Tordo P.; Chalier F.; *J. Org. Chem* **1999** 64 3554-3556 b) Durand G.; Polidori A.; Salles J. P; Prost M.; Durand P.; Pucci B.; *Bio Med. Chem. Let.* **2003** 13 2673-2676 c) Durand G.; Ouari O.; Polidori A.; Pucci B.; Tordo P.; Polidori A.; Geromel V.; Rustin P.; *J. Med. Chem.* **2003** 46 5230-5237
- 81 Zeghdaoui, A.; Tuccio, B.; Finet, J. P.; Cerri V.; Tordo, P.; *J. Chem.Soc., Perkin Trans. 2* **1995** 2087-2089
- 82 Khramtsov, V. V.; Reznikov, V. A.; Berliner, L. J.; Litkin, A. K.; Grigor'ev, I. A.; Clanton, T. L.; *Free Rad. Biol. Med.* **2001** 30 1099-1107

-
- 83 Villamena, F. A.; Rockenbauer, A.; Gallucci, J.; Velayutham, M.; Hadad, C. M.; Zweier, J. L.; *J. Org. Chem.* **2004** 69 7994-8004
- 84 Murphy, M. P.; Smith R. A. J.; *Annu. Rev. Pharmacol. Toxicol.* **2007** 47 15.1-15.28
- 85 Trnka, J.; Blaikie, F.H.; Smith, R. A. J.; Murphy, M. P.; *Free Radical Biology & Medicine* **2008** 44 1406–1419
- 86 Kelso, G.F.; Porteous, C.M.; Coulter, C.V.; Hughes, G.; Porteous, W.K.; *J. Biol. Chem.* **2001** 276 4588–96
- 87 Smith, R. A. J.; Porteous, C. M.; Coulter, C. V.; Murphy, M. P.; *Eur. J. Biochem.* **1999** 263 709–716
- 88 Smith, R. A. J.; Porteous, C. M.; Gane, A. M.; Murphy, M. P. *Proc. Natl. Acad. Sci.* **2003**, 100, 5407-5412
- 89 Fevig, T. L.; Bowen, S. M.; Janowick, D. A.; Jones, B. K.; Munson, H. R.; Ohlweiler, D. F.; Thomas; *J. Med. Chem.* **1996** 39 4988-4996
- 90 Parham, W. E.; Jones, L.D.; Sayed, Y.; *J. Org. Chem.* **1975** 40 2394-2399
- 91 Beesley, R. M.; Ingold, C. K.; Thorpe, J. F.; *J. Chem. Soc.* **1915** 107 1080.
- 92 Lin, T-K; Hughes, G.; Muratovska. A; Blaikie, F. H.; Brookes, P. S.; Darlet-Usmar, V.; Smith, R. A. J.; Murphy, M. P.; *J. Bio. Chem.* **2002** 277 17048-17056
- 93 Bottle, S. E.; Micallef, A. S.; *Org. Biomol. Chem.* **2003** 1 2581-2584
- 94 Rosen, G. M.; Britigan, B.E.; Halpern, H. J.; Pou, S.; *Free Radicals: Biology and Detection by Spin Trapping*. First Edition. 1999: Oxford University Press
- 95 a) Barry, S. J.; Carr, R. M.; Lane, S.J.; Leaven, W. J.; Manning, C. O.; Monte, S.; Waterhouse, I.; *Rapid Commun Mass Spectrom* **2003** 17 484-497 b) Woo, H.K.; Go, E. P.; Hoang, L.; Trauger, S. A.; Bowen, B.; Siuzdak, G.; Northen, T. R.; *Rapid Commun Mass Spectrom* **2009** 23 1849-1855
- 96 Calerdon, A. I.; Wright, B. J.; Hurst, W. J.; Van Breemen, R. B.; *J. Agric. Food Chem.* **2009**, 57, 5693–5699
- 97 a) Mangal, D.; Vudathala, D.; Park, J-H.; Lee, S. H.; Penning, T.M.; Blair, I. A.; *Chem. Res. Toxicol.* **2009** 22 788–797
- 98 Duggan, P. J.; Tyndall, E. M.; *J. Chem. Soc., Perkin Trans. 1* **2002** 1325-1339,
- 99 Carboni, B.; Pourbaix, C.; Carreaux, F.; Deleuze H.; Maillard, B.; *Tetrahedron Lett.* **1999** 40 7979-7983
- 100 Li, Y.; Zhang, H; Fawcett, J. P.; Tucker, I. G. *Rapid Commun Mass Spectrometry* **2007** 21 1958-1964
- 101 Tehan, B.G.; Lloyd, E.J.; Wong, M.G.; Pitt, W. R.; Montana, J.G.; Manallack, D.T.; Ganacia, E.; *Quant. Struct.-Act. Relat.* **2002** 21 457-472

-
- 102 Lu, Y-R.; *Handbook of Bond Dissociation Energies*. CRC Press 2002 p182-184
- 103 Lo L-C.; Chu C-Y.; *Chem. Comm.* **2003** 2728–2729
- 104 Srikun, D.; Miller, E.W.; Domaille, D. W.; Chang, C. J.; *J. Am.Chem. Soc.* **2008** 130 4596-4597
- 105 Zhang, Z.; Chen, P.; Murakami, T. N.; Zakeeruddin, S. M.; Grätzel M.; *Adv. Funct. Mater.* **2008** 18 341–346
- 106 Pelliccioli, A. P.; Wirz, J.; *Photochem. Photobiol. Sci.* **2002** 1 441–458
- 107 Kaplan, J. H.; Forbush, B.; and Hoffman, J. F.; *Biochemistry* 1978 **17** 1929–1935.
- 108 Biley, F.; Schaper, K.; Gerner, H.; *Photochem. Photobiol.* **2008** 84 162-172
- 109 Caldwell, S. T.; Quin, C.; Edge, R.; Hartley, R. C.; *Org. Lett.* **2007** 9 3499-3502
- 110 Jeong, J. H.; Weinreb, S. M.; *Org. Lett.* **2006** 8 2309-2312
- 111 Reinhard, A.; von Angerer, S.; Wiegrebe, W.; *Arch. Pharm.* **1988** 321 481-486.
- 112 Dawson, M. I.; Hobbs, P. D.; Kuhlman, K.; Fung, V. A.; Helmes, C. T.; Chao, W.-R.; *J. Med. Chem.* **2003** 23, 1013-1002
- 113 Ishiyama, T.; Takagi, T.; Ishida.; Miyaura, N.; Anastasi, N. R., Hartwig, J. F.; *J. Am. Chem.Soc.***2002** 124 390-391
- 114 Howard, O. M. Z.; Fang Dong, H.; Oppenheim, J. J.; Insaf, S.; Santhosh, K. C.; Paul G.; Cushman M.; *Bioorg. & Med. Chem. Lett.* **2001** 11(1) 59-62
115. Whalley, W. B.; *Org. Syn.* **1950** 463 2241-2243
- 116 Gitis, A., Ivanova, O. J.; *Org.Chem USSR. (English Translation)* **1965** 1 1458
- 117 de Filippis, A.; Morin, C.; Thimon, C.; *Synth. Comm.* **2002** 32(17) 2669-2676.
- 118 Cameron, K. S.; Pincock, A. L.; Pincock, J. A.; Thompson, A.; *J. Org. Chem.* **2004** 69 4954-4960